JAGIELLONIAN UNIVERSITY
IN KRAKÓW

Faculty of Biology

Institute of Zoology and Biomedical Research

Circadian and periprandial rhythms of the rat Dorsomedial Hypothalamus under high-fat diet

Anna Sanetra

Doctoral dissertation
conducted under the supervision of
prof. dr hab. Marian H. Lewandowski
and dr Katarzyna Palus-Chramiec
at the Department of Neurophysiology and Chronobiology
of the Institute of Zoology and Biomedical Research

Kraków 2023

Reviewers

Prof. dr hab. Jan Konopacki

Department of Neurobiology, University of Łódź

&

Prof. dr hab. Krzysztof Tokarski

Department of Physiology, Maj Institute of Pharmacology Polish Academy of Sciences

&

Prof. dr hab. Jolanta B. Zawilska

Department of Pharmacodynamics, Medical University of Łódź

Acknowledgements

I wish to thank, first and foremost, my supervisor Prof. Dr hab. Marian H. Lewandowski, who welcomed me to his lab 8 years ago, and has continued to allow me to develop scientifically as part of his team to this day. I am forever grateful for everything I have been able to learn in the Department of Neurophysiology and Chronobiology, where I had the opportunity to be taught by amazing electrophysiologists and great people: Dr Katarzyna Palus-Chramiec, Dr hab. Łukasz Chrobok and Dr Jagoda Jęczmień-Łazur.

Thank you Kasia for your time and patience, when I was making my first, very small baby steps in the lab, and for all the pieces of advice at the later stages.

Thank you Łukasz, for your readiness to help no matter how far away you are at the time, and for always keeping me inspired.

Thank you Jagoda, for pushing me towards decision making and developing independence.

List of publications

Publications included in the thesis (in order of publication and appearance in the thesis):

2022 *Electrophysiological complexity in the rat dorsomedial hypothalamus and its susceptibility to daily rhythms and high-fat diet*
Sanetra, A. M., Palus-Chramiec, K., Chrobok, L., Lewandowski, M. H.
European Journal of Neuroscience, 56(4), 4363-4377. IF: 3.698.
https://doi.org/10.1111/ejn.15759

2022 *High-Fat-Diet-Evoked Disruption of the Rat Dorsomedial Hypothalamic Clock Can Be Prevented by Restricted Nighttime Feeding*
Sanetra, A. M., Palus-Chramiec, K., Chrobok, L., Jeczmien-Lazur, J. S., Gawron, E., Klich, J. D., Pradel, K., Lewandowski, M. H.
Nutrients, 14(23), 5034. IF: 6.706.
https://doi.org/10.3390/nu14235034

2023 *Proglucagon signalling in the rat Dorsomedial Hypothalamus – Physiology and high-fat diet-mediated alterations*
Sanetra, A. M., Palus-Chramiec, K., Chrobok, L., Jeczmien-Lazur, J. S., Klich, J. D., Lewandowski, M. H.
Molecular and Cellular Neuroscience, published online. IF: 4.626.
https://doi.org/10.1016/j.mcn.2023.103873

Other publications:

2021 *Role of heme-oxygenase-1 in biology of cardiomyocytes derived from human induced pluripotent stem cells*
Jez, M., Martyniak, A., Andrysiak, K., Mucha, O., Szade, K., Kania, A., Chrobok, L., Palus-Chramiec, K., **Sanetra, A. M.**, Lewandowski M. H., Pospiech E., Stepniewski J., Dulak, J.
Cells, 10(3), 522. IF: 7.666.
https://doi.org/10.3390/cells10030522

2021 *Modulation of the Rat Intergeniculate Leaflet of the Thalamus Network by Norepinephrine*
Sanetra, A. M., Palus-Chramiec, K., & Lewandowski, M. H.
Neuroscience, 469, 1-16. IF: 3.708.
https://doi.org/10.1016/j.neuroscience.2021.06.027

2021 *Intrinsic circadian timekeeping properties of the thalamic lateral geniculate nucleus*
Chrobok, L., Pradel, K., Janik, M. E., **Sanetra, A. M.**, Bubka, M., Myung, J., ... & Lewandowski, M. H.

Journal of Neuroscience Research, 99(12), 3306-3324. IF: 4.433.
https://doi.org/10.1002/jnr.24973

2022 *Daily changes in neuronal activities of the dorsal motor nucleus of the vagus under standard and high-fat diet*
Chrobok, L., Klich, J. D., Jeczmien-Lazur, J. S., Pradel, K., Palus-Chramiec, K., **Sanetra, A. M.**, ... & Lewandowski, M. H.
Journal of Physiology, 600(4), 733-749. IF: 6.228.
https://doi.org/10.1113/JP281596

2022 *Rhythmic neuronal activities of the rat nucleus of the solitary tract are impaired by high-fat diet–implications for daily control of satiety*
Chrobok, L., Klich, J. D., **Sanetra, A. M.**, Jeczmien-Lazur, J. S., Pradel, K., Palus-Chramiec, K., ... & Lewandowski, M. H.
Journal of Physiology, 600(4), 751-767. IF: 6.228.
https://doi.org/10.1113/JP281838

2022 *Day/night changes in the dorsomedial hypothalamus firing responses to ghrelin are modulated by high-fat diet*
Palus-Chramiec, K., **Sanetra, A. M.**, & Lewandowski, M. H.
Neuroscience, 494, 167-177. IF: 3.708.
https://doi.org/10.1016/j.neuroscience.2022.05.004

2023 *Metabolic cues impact non-oscillatory intergeniculate leaflet and ventral lateral geniculate nucleus: standard vs high-fat diet comparative study.*
Jeczmien-Lazur, J. S., **Sanetra, A. M.**, Pradel, K., Izowit, G., Chrobok, L., Palus-Chramiec, K., ... & Lewandowski, M. H.
Journal of Physiology, 601(5), 979–1016. IF: 6.228.
https://doi.org/10.1113/JP283757

Conference attendances

2017 **13th International Congress of the Polish Neuroscience Society, Warsaw, Poland**
Poster: *The effect of norepinephrine on the rat intergeniculate leaflet neurons – an in vitro electrophysiological study*
Sanetra, A., Palus, K., Chrobok, L., Lewandowski, M. H.

2018 **Neuronus IBRO Neuroscience Forum, Krakow, Poland**
Poster: *Norepinephrine affects activity of the rat intergeniculate leaflet neurons of the thalamus*
Sanetra, A., Palus, K., Chrobok, L., Lewandowski, M. H.

2018 **XI Electrophysiological Conference, Warsaw, Poland**

Oral presentation: *The effect of norepinephrine on the rat intergeniculate leaflet neurons*
Sanetra, A., Palus-Chramiec, K., Chrobok, L., Lewandowski, M. H.

2019 **XVI European Biological Rhythms Society Congress, Lyon, France**

- Poster: *Circadian rhythm of glucagon-like peptide 2 immunoreactivity in the rat Dorsomedial Hypothalamus*
  Sanetra, A. M., Palus-Chramiec, K., Chrobok, L., Jeczmien-Lazur, J., Klich, J., Lewandowski, M. H.
- Poster: *Carbachol modulates intergeniculate leaflet neuronal network of the rat*
  Palus-Chramiec, K., **Sanetra, A. M.**, Lewandowski, M. H.
- Poster: *Circadian pattern of glucagon-like peptides expression in the locus coeruleus of the rat-immunofluorescent study*
  Palus-Chramiec, K., **Sanetra, A. M.**, Cyrano, E., Chrobok, L., Jeczmien-Lazur, J., Klich, J., Lewandowski, M. H.
- Poster: *Circadian control of the dorsal motor nucleus of the vagus in rat by orexin and glucagon-like peptide-1*
  Klich, J., Chrobok, L., Jeczmien-Lazur, J. S., Palus-Chramiec, K., **Sanetra, A.**, Lewandowski, M. H.

2020 **12th FENS Forum of Neuroscience, Glasgow, UK (online)**

- Poster: *Disruption of circadian rhythmicity in food intake and c-Fos immunoreactivity in the Dorsomedial Hypothalamus and Nucleus of the Solitary Tract under high-fat diet in rats*
  Sanetra, A. M., Chrobok, L., Palus-Chramiec, K., Jeczmien-Lazur, J., Klich, J., Zmuda, A., Lewandowski, M. H.
- Poster: *The effect of ghrelin on the Dorsomedial Hypothalamus of rat – ex-vivo studies*
  Palus-Chramiec, K., **Sanetra, A. M.**, Lewandowski, M. H.
- Poster: *Daily changes in electrophysiology and responsiveness to metabolic cues in the development of obesity - study of the rat dorsal vagal complex*
  Klich, J., Chrobok, L., Jeczmien-Lazur, J. S., Palus-Chramiec, K., **Sanetra, A. M.**, Lewandowski, M. H.

2020 **Neuronus IBRO Neuroscience Forum, Krakow, Poland (online)**
Poster: *The effect of high-fat diet on the circadian rhythm of food intake and c-FOS immunoreactivity in the rat Dorsomedial Hypothalamus*
Sanetra, A. M., Palus-Chramiec, K., Chrobok, L., Jeczmien-Lazur, J., Klich, J., Zmuda, A., Lewandowski, M. H.

2021 **FENS Regional Meeting, Krakow, Poland (online)**

- Poster: *Disruption of the circadian clock in the Rat Dorsomedial Hypothalamus under high-fat diet*

Sanetra, A. M., Palus-Chramiec, K., Chrobok, L., Jeczmien-Lazur, J. S., Pradel, K., Klich, J. D., Lewandowski, M. H.

- Poster: *Cholinergic system play a modulatory role in neuronal network of the intergeniculate leaflet nucleus of the rat*
  Palus-Chramiec, K., **Sanetra, A. M.**, Lewandowski, M. H.

2021 **XXVIII Congress of the Polish Physiological Society, Gdansk, Poland (online)**

Poster: *Changes in the responsiveness of the rat Dorsomedial Hypothalamus to different metabolic conditions under high-fat diet*
Sanetra, A. M., Palus-Chramiec, K., Chrobok, L., Jeczmien-Lazur, J. S., Klich, J. D., Lewandowski, M. H.

2022 **XVII European Biological Rhythms Society Congress, Zurich, Switzerland**

Poster: *Disruption of Dorsomedial Hypothalamic rhythms under high-fat diet can be prevented by restricted nighttime feeding*
Sanetra, A. M., Palus-Chramiec, K., Chrobok, L., Jeczmien-Lazur, J. S., Gawron, E., Klich, J. D., Pradel, K., Lewandowski, M. H.

Financial resources

The Ph.D. candidate was funded from the project "ATUT PhD Programme in Biology". The project is co-financed by the European Union under the European Social Fund – Operational Programme Knowledge Education Development Axis III Higher Education for Economy and Development, Action 3.2 PhD Programme.

The studies underlying this dissertation were supported by:

2017 - 2021 **National Science Centre;** grant OPUS13 - 2017/25/B/NZ4/01433
Feeding time. Multidimensional studies on the impact of satiety signals on circadian timing system in the development of obesity
Grant executor

2020 – 2021 **Faculty of Biology of the Jagiellonian University in Krakow;** minigrant N18/MNS/000033
Wpływ diety wysokotłuszczowej na okołodobowy rytm pobierania pokarmu u szczura / The effect of high-fat diet on the circadian rhythm of food intake in rats
Principal investigator

2022 – 2023 **Faculty of Biology of the Jagiellonian University in Krakow;** minigrant U1U/W18/NO/28.16
Wpływ diety wysokotłuszczowej na okołodobowy rytm aktywności neuronalnej w grzbietowo-przyśrodkowym jądrze podwzgórza u szczura. Zależność od rytmiki pobierania pokarmu / The effect of high-fat diet on the circadian activity pattern of the rat Dorsomedial Hypothalamus. Dependence on the rhythm in the feeding behaviour
Principal investigator

Contents

Streszczenie

Otyłość i choroby współistniejące są przyczyną śmierci ponad 4 milionów ludzi w skali roku. Pomimo znacznego postępu terapeutycznego, częstość występowania przypadków nadwagi oraz otyłości stale rośnie, szczególnie w miejskich rejonach krajów wysoko rozwiniętych. Jest to związane z obecnością i rozwojem sprzyjającego otyłości środowiska (ang. *obesogenic environment*), na które składa się wysoce przetworzony oraz kaloryczny pokarm, połączony z obniżoną aktywnością fizyczną. Z tego względu w badaniach naukowych, otyłość wywołana dietą (ang. *diet-induced obesity* - DIO) stała się najczęściej wykorzystywanym modelem zwierzęcym, dzięki któremu możliwe jest zbadanie nie tylko jej konsekwencji, ale również mechanizmów leżących u podstaw różnych aspektów tej choroby. Badając efekty DIO u gryzoni wykazano, że otyłość wpływa dwukierunkowo na rytmikę okołodobową zarówno poprzez zmianę zachowania zwierząt, jak i procesy molekularne.

Wśród okołodobowych zegarów (oscylatorów) zależnych od pokarmu, które zlokalizowane są w ośrodkowym układzie nerwowym, otyłość wywołana dietą w szczególnie silny sposób wpływa na grzbietowo-przyśrodkowe jądro podwzgórza (ang. *Dorsomedial Hypothalamus* - DMH). Jest to struktura wrażliwa na sygnały głodu i sytości, regulująca pobieranie pokarmu w zależności od stanu metabolicznego zwierzęcia. DMH jest również niezwykle podatne na ograniczone czasowo (restrykcyjne) podawanie pokarmu, które wzmacnia jego właściwości oscylacyjne oraz przesuwa akrofazę aktywności struktury, umożliwiając przewidywanie pojawienia się pokarmu.

Wynikami mojej pracy doktorskiej potwierdziłam hipotezę, że dieta wysokotłuszczowa (ang. *high-fat diet* – HFD) powoduje zmiany w fizjologii DMH jeszcze przed rozwinięciem się otyłości co sugeruje, że uszkodzenie funkcjonowania tej struktury może pośredniczyć w rozwoju tej choroby. Przy użyciu metod elektrofizjologicznych oraz immunohistochemicznych, zaobserwowałam występowanie rytmicznie zmieniającej się aktywności tej struktury, oraz endogenny (niezależny od czynników zewnętrznych) charakter tego rytmu. Karmienie szczurów HFD spowodowało zaburzenie rytmiki okołodobowej aktywności komórek DMH, aczkolwiek efekt ten zależny był od rozregulowanego wzorca spożywanego pokarmu. Restrykcyjne podawanie pokarmu, ograniczone do czasu trwania fazy ciemnej (okresu aktywności zwierząt) zapobiegło tej desynchronizacji. W związku z tym, zbadałam wrażliwość neuronów DMH na różne stany metaboliczne (głód/sytość) zarówno u zwierząt karmionych regularnie, umożliwiając im przewidywanie posiłku, oraz takich, które nie miały możliwości przewidzenia pojawienia się pokarmu. W tym sposób pokazałam, że

sytość aktywuje różne subregiony DMH w zależności od tego czy jest ona zaplanowana. Wyniki te, wraz z obserwacją mnogich różnic elektrofizjologicznych pomiędzy trzema oddzielnymi częściami DMH, podkreślają funkcjonalną złożoność tej struktury.

W części farmakologicznej pracy zbadałam w DMH sygnalizację za pośrednictwem peptydów z rodziny pochodnych proglukagonu (ang. *proglucagon-derived peptides* – PGDP). Pomimo szerokiego zastosowania agonistów receptora dla glukagonopodobnego peptydu 1 (ang. *glucagon-like peptide 1 receptor* - GLP1R) w terapii otyłości, niewiele wiadomo o mechanizmie ich działania w obrębie podwzgórza. Amplituda odpowiedzi po podaniu PGDP pozytywnie korelowała z poziomem spontanicznej aktywności neuronów DMH. Zależność ta ulegała jednak zaburzeniu po podaniu diety wysokotłuszczowej. Dodatkowo, HFD zwiększyła liczbę komórek odpowiadających na agonistę GLP1R – eksendynę 4 (ang. *exendin-4* – Exn4), poprzez wzmocnienie aktywności synaptycznej po podaniu substancji. Nie tylko wrażliwość komórek DMH na PGDP, ale też ilość peptydu obecnego w strukturze była zaburzona przez HFD. Widoczne to było poprzez zanik dynamicznych zmian w immunoreaktywności GLP1 w zależności od stanu metabolicznego organizmu. Różnice we wpływie stosowanych diet nie były natomiast obserwowane, gdy zwierzęta karmione były w sposób restrykcyjny.

Przedstawione wyniki jednoznacznie potwierdzają silne powiązanie otyłości z zaburzeniem pracy zegara biologicznego, pokazując jego wczesne patologiczne zmiany na poziomie aktywności pojedynczych neuronów budujących ośrodkowy oscylator pokarmowy. Jednym z głównych powodów tych zmian jest nieregularne przyjmowanie pokarmu, który jest bardzo silnym synchronizatorem zegara biologicznego. Aspekt chronobiologiczny, w tym szczególnie chronoodżywianie (ang. *chrononutrition*), powinien być przedmiotem dalszych intensywnych badań poszukujących skutecznej terapii otyłości. Tylko bowiem prawidłowo funkcjonujący zegar biologiczny, jako jeden z istotnych elementów tzw. zdrowia metabolicznego, może spowolnić pandemię nadwagi i otyłości, konsekwencją których jest wiele chorób cywilizacyjnych.

Abstract

Obesity and successive comorbidities are estimated to kill over 4 million people per year. Despite considerable advancement in treatment methods, the prevalence of overweight and obesity continues to rise, affecting especially more developed, urban areas. This occurs due to an emergence of the obesogenic environment, composed of highly processed, calorie-dense food and reduced physical activity. In view of this, diet-induced obesity (DIO) has become the most commonly used rodent obesity model, not only to study its consequences, but also the mechanisms underlying various aspects of the disease. Using DIO mice and rats, obesity has been shown to bidirectionally interact with circadian rhythms, on both behavioural and molecular levels, via disrupted feeding and locomotor activity rhythm, as well as misaligned light- and food-entrained oscillators.

Amongst the feeding-responsive central circadian clocks, the Dorsomedial Hypothalamus (DMH) appears the most affected by DIO. The DMH is sensitive to both hunger and satiety signalling molecules, in turn regulating food intake. It is also extremely susceptible to feeding restriction, which potently enhances its oscillatory properties and adjusts the phase of the oscillation so as to enable meal anticipation.

The results of my work confirm a hypothesis, that the DMH is affected by high-fat diet (HFD) even before obesity onset, suggesting that this disruption might partake in the development of the disease. Using electrophysiology and immunohistochemistry I observed the existence of the day/night rhythms in the neuronal activity of the structure, as well as their endogenous (independent of the external cues) nature. HFD-feeding disrupted the rhythmicity of the DMH cells, however this effect was successfully prevented by restricted nighttime feeding, highlighting that this alteration is evoked by the irregular feeding pattern. In view of this, I studied DMH sensitivity to different metabolic states (fasted/fed) with and without regularly scheduled mealtimes. Distinct DMH subdivisions were activated by satiety, depending on whether or not it had been anticipated, which together with an observation of multiple electrophysiological differences between distinct DMH subdivisions, underlines its internal complexity.

In the pharmacological part of the thesis, I studied satiety signalling via the family of the proglucagon-derived peptides (PGDP), since despite the appreciation of the therapeutic potential of the glucagon-like peptide 1 receptor (GLP1R) agonists, not much is known about their mechanism of action upon the hypothalamus. The responsiveness to the PGDP was shown to depend on the level of the spontaneous neuronal activity, but this correlation was abolished

by HFD. Moreover, HFD increased the fraction of cells stimulated by the GLP1R agonist exendin-4 (Exn4), by enhancing the Exn4-evoked level of synaptic activity in the structure. Not only neuronal sensitivity, but also the amount of the PGDP in the structure was affected, with HFD attenuating the metabolic state-dependent changes in the GLP1 immunoreactivity. Differences were not observed when animals had been fed in a restricted manner.

Presented data confirm the presence of a strong connection between obesity and circadian clock disruption, with a desynchronisation of the neuronal oscillatory function occurring even after a short period of HFD-feeding. One of the main reasons for this pathology is an irregular pattern of food intake, which is an important circadian clock synchroniser. The chronobiological aspect of obesity treatment, especially chrononutrition, needs to be given more future consideration, because only a well synchronised circadian timing system, as one of the crucial parts of metabolic health, can slow down the pandemic of overweight and obesity, and their detrimental comorbidities.

Abbreviations

BAT	brown adipose tissue
BMI	body-mass index
CART	cocaine and amphetamine regulated transcript
CD	control diet
cDMH	compact DMH
dDMH	dorsal DMH
DIO	diet-induced obesity
DMH	Dorsomedial Hypothalamus
Exn4	exendin-4
FAA	food-anticipatory activity
FEO	food-entrainable oscillator
GABA	gamma-aminobutyric acid
GLP1/2	glucagon-like peptide 1/2
GLP1/2R	GLP1/2 receptor
HFD	high-fat diet
Lepr	leptin receptor
MEA	multi-electrode array
NF	night-feeding
NMDA	N-methyl-d-aspartic acid
NPY	neuropeptide Y
NTS	Nucleus of the Solitary Tract
OXM	oxyntomodulin
PC	prohormone convertase
PGDP	proglucagon-derived peptides
PPG	proglucagon
PSC	postsynaptic current
RF	restricted feeding
SCN	Suprachiasmatic Nucleus
TRF	time-restricted feeding
vDMH	ventral DMH
ZT	Zeitgeber time

1. Introduction

1.1. State of art

1.1.1. Obesity – epidemiological basis for model selection

Obesity has been recognised a pandemic since 1997 (WHO, 2000), however so far various attempts have been unsuccessful at holding it back. According to the 2017 Global Nutrition Report more than 2 billion adults worldwide are overweight, and half a billion obese. On top of that, 41 million children are also affected by excessive body weight, and the numbers for both adults and children keep rising (Hawkes & Fanzo, 2017).

Regional differences in the prevalence of the disease are evident. Strikingly, within the WHO European Region almost 60% of adult population are overweight and close to 25% obese (WHO, 2022), and these proportions are even higher in North America and Oceania (Hawkes & Fanzo, 2017). Generally, higher rate of occurrence, as well as growth speed, are recorded in high-income, developed countries, although this trend seems to be changing in the recent years, showing a rapid increase in overweight and obesity cases now also in the middle- and low-income countries (Ng *et al.*, 2014, Ford *et al.*, 2017). This shift is paralleled by developmental changes, including economic growth, urbanisation, and industrialisation, which create the "obesogenic" environment, composed of easy access to calorie-dense, processed food, decreased physical activity due to mechanised transport, and hormonal alterations, stemming from environmental pollution by endocrine disruptors (Hruby & Hu, 2015, Ford *et al.*, 2017, WHO, 2022). As far as the last one is only recently gaining more interest, an imbalance in the amount of calories ingested and spent has been commonly considered the basis for malnutrition. In particular, modern trends in feeding, such as foods high in fat (Miller *et al.*, 1994), lack of dietary diversity, low intake of fruits and vegetables (He *et al.*, 2004, Sagbo *et al.*, 2018), high amount of sweetened, fizzy drinks (Ganle *et al.*, 2019) and alcohol (Yoon *et al.*, 2016) consumption, have been concluded to potently stimulate weight gain.

In view of this, high-fat diet (HFD)-fed mice and rats have become the most frequently used rodent model of obesity (Winzell & Ahrén, 2004). Obesity induction by environmental, rather than genetic factors, better reflects the trends observed for human population, modelling not only the disease itself, but also processes occurring during its development, allowing for the study of the mechanisms responsible. This was crucial for the studies described in the thesis, as the focus here were changes arising before the onset of obesity.

1.1.2. Reciprocal influence of obesity and circadian misalignment

High body-mass index (BMI), the most common determinant in the diagnosis of malnutrition, has been recognised a risk factor for a variety of diseases, ranging from the two leading causes of death globally – cardiovascular disease and cancer (Zalesin *et al.,* 2008, Lauby-Secretan *et al.,* 2016, Ritchie *et al.,* 2018), down to type II diabetes mellitus (Chan *et al.,* 1994, Colditz *et al.,* 1995), respiratory disorders, including asthma (Camargo *et al.,* 1999, Thomson *et al.,* 2003, Aaron *et al.,* 2004, Canoy *et al.,* 2004), non-alcoholic fatty liver disease (Hamaguchi *et al.,* 2005), osteoarthritis (Felson *et al.,* 1992, Hart & Spector, 1993, Cicuttini *et al.,* 1996) and even psychological problems such as depression (Luppino *et al.,* 2010). Links to sleep disturbances have also been observed, both in the sleep duration (Taheri, 2006) and quality (Vgontzas *et al.,* 1998, Resta *et al.,* 2003, Xiao *et al.,* 2016, Moreno-Vecino *et al.,* 2017), however the relationship between obesity and sleep appears bidirectional.

On one hand, obesity correlates positively with the metrics of sleep disordered breathing (Davidson & Patel, 2008) and bariatric surgery is effective at improving sleep quality in the cases when sleep problems are related to respiratory alterations (Dixon *et al.,* 2001, Quintas-Neves *et al.,* 2016). Moreover, an enhanced release of proinflammatory cytokines during a low-grade systemic inflammation occurring under obesity (Wellen *et al.,* 2005) has been shown to influence sleep duration as well as pattern (Opp *et al.,* 1992, Vgontzas *et al.,* 1997, Gamaldo *et al.,* 2012). Obesity can also worsen sleep via gastrointestinal symptoms (Eslick & Talley, 2016), vitamin D deficiency (Muscogiuri *et al.,* 2010, McCarty *et al.,* 2013, Bertisch *et al.,* 2015), restless leg syndrome (Mallon *et al.,* 2008, Gao *et al.,* 2009, Schlesinger *et al.,* 2009), and emotional stress (Vgontzas *et al.,* 2008).

Studies on HFD-fed rodents have revealed impaired circadian rhythms in locomotor activity and feeding behaviour, clock gene expression in the liver, spleen and adipose tissue, rhythmically changing levels of circulating markers of glucose and lipid metabolism, as well as production of some hypothalamic neuropeptides (Ando *et al.,* 2005, Kohsaka *et al.,* 2007, Hsieh *et al.,* 2010, Pendergast *et al.,* 2013).

On the other hand, an even larger body of evidence points to the contribution of circadian rhythms' alterations in obesity development. First of all, the fact that vast majority of hormones (reviewed in Gamble *et al.,* 2014), and therefore many metabolites, (Dallmann *et al.,* 2012, Chua *et al.,* 2013) undergo circadian regulation strongly argues for the importance of such rhythmicity for metabolic health. Moreover, these rhythms can be disturbed by sleep deprivation (Davies *et al.,* 2014), which also decreases glucose tolerance and thyrotropin

concentration (Spiegel *et al.,* 1999), and elevates ghrelin - the main food intake stimulant (Taheri *et al.,* 2004). Shift-workers, representative of the chronically sleep-deprived group (Sanches *et al.,* 2015) are more susceptible to excessive weight gain (Di Lorenzo *et al.,* 2003, Karlsson *et al.,* 2001, 2003, Suwazono *et al.,* 2008), with the severity highly dependent on the shift-work duration (Van Amelsvoort *et al.,* 1999).

Disrupted circadian rhythms, in the form of misaligned circadian and behavioural cycles, cause desynchrony between central and peripheral circadian clocks (Damiola *et al.,* 2000, Stokkan *et al.,* 2001) influencing both circadian phase- and meal-related changes in the endocrine function (Scheer *et al.,* 2009, Morris *et al.,* 2015). Evidently, shift work results in a an alteration of circadian rhythmicity in feeding behaviour (Shaw *et al.,* 2019, Kosmadopoulos *et al.,* 2020), which serves as a plausible explanation for the disordered molecular rhythms responsive to food intake. Timing of the meals is indeed crucial for metabolic health, with data presenting late evening food intake and nighttime snacking deleterious to glucose responsiveness (Barrington & Beresford, 2019) and body weight (Ruiz-Lozano *et al.,* 2016, McHill *et al.,* 2017, Centofanti *et al.,* 2018).

A relatively new approach to healthy feeding involves intermittent fasting, such as time-restricted feeding (TRF), which consists of a defined, about several-hour long time window of calorie intake, followed by fasting for the remainder of the day. Such a schedule has to be kept long-term, with the feeding time window occurring at the same time every day. TRF has been shown to be effective at decreasing total daily meal size and body weight, and improving sleep (LeCheminant *et al.,* 2013, Gill & Panda, 2015) in humans. Studies on laboratory animals also indicate increased longevity (Acosta-Rodríguez *et al.,* 2022), attenuated levels of inflammation, cholesterol, glucose and insulin, and even possible prevention of metabolic diseases including obesity (Hatori *et al.,* 2012, Sherman *et al.,* 2012, Chaix *et al.,* 2014, Zarrinpar *et al.,* 2014).

Altogether, these data provide a very strong case for an involvement of disrupted circadian rhythmicity in the mechanism responsible for the development, as well as detrimental consequences of obesity.

1.1.3. Intrinsic and entrainable properties of the circadian rhythms

Circadian rhythms are manifested on multiple scales, from clock gene expression (Reddy *et al.,* 1984, Tei *et al.,* 1997), through the activity of individual cells (Welsh *et al.,* 1995, Herzog *et al.,* 1998) and tissues (Yamazaki *et al.,* 2000, Storch *et al.,* 2002), resulting in an orchestrated activity of various tissues performing distinct tasks, necessary for the behavioural rhythmicity

of an entire organism. Once believed to be a result of an activity pattern purely restricted to the hypothalamic Suprachiasmatic Nucleus (SCN), named the master circadian clock or the main rhythm generator, today many other endogenous oscillators have been found both in the brain (Abe *et al.,* 2002, Zhao & Rusak, 2005, Granados-Fuentes *et al.,* 2006, Guilding *et al.,* 2009, Myung *et al.,* 2018, Chrobok *et al.,* 2020, 2021a, 2021b, Northeast *et al.,* 2020), and on the periphery (Yamazaki *et al.,* 2000, Sadacca *et al.,* 2011), with the SCN serving as the synchroniser (pacemaker) keeping all the other clocks attuned. This synchronisation is so important, that SCN lesions cause complete arrhythmicity of the behaviour (Stephan & Zucker, 1972), and its implantation restores the rhythm in SCN-lesioned animals, with the period of the SCN donor (Drucker-Colín *et al.,* 1984, Ralph *et al.,* 1990).

Intrinsic nature of the circadian oscillations enables animals to anticipate environmental changes occurring within the 24 h cycle. Rather than simply responding to the cyclic day/night transitions, organisms can start preparing for the next phase in advance. This is a clear evolutionary advantage, since these rhythms have been recorded in all biological kingdoms (Edgar *et al.,* 2012), ranging from prokaryotes (Johnson *et al.,* 2008), protists (Jakobsen & Strom, 2004) and fungi (Grobbelaar *et al.,* 1986, Baker *et al.,* 2012) up to plants (De Mairan, 1729, Harmer, 2009) and of course animals (Aschoff, 1960, Chabot & Taylor, 1992, Frisch *et al.,* 1994, Tei *et al.,* 1997).

However, despite the beneficially endogenous nature of the circadian oscillations, the intrinsic clock must also be able to adapt, or entrain, to any changes in the temporal pattern of the environmental rhythms. The SCN does so by receiving visual information from the melanopsin retinal ganglion cells located in the retina (Hendrickson *et al.,* 1972, Moore & Lenn, 1972, Provencio *et al.,* 2000, Gooley *et al.,* 2001, Hattar *et al.,* 2002, Panda *et al.,* 2002, Ruby *et al.,* 2002) informing the clock about altered lighting conditions, which can be used to shift the phase of the SCN oscillation (Shigeyoshi *et al.,* 1997), and subsequently adjust animals' locomotor activity (Daan & Pittendrigh, 1976).

Light has been considered the most important and potent zeitgeber (*ger. time giver*), regulating not only circadian, but also seasonal rhythms (Arendt & Broadway, 1987). Historically, it was indeed the best predictor of the rhythmical changes in the environment, informative of food availability and predator danger for animals, and of course serving as a direct food source for plants and photosynthesising bacteria and algae. Nowadays, wide usage of artificial light, especially at night, has been interacting with all living organisms' circadian clocks, negatively influencing both wildlife (Gaston *et al.,* 2017, Sanders *et al.,* 2021) and humans (West *et al.,* 2011, Chang *et al.,* 2015).

However, light is not the only misused zeitgeber, with an altered function as a circadian synchroniser. Constant easy access to food, especially the low-quality and calorie-dense ready meals, eaten at various times of the day, results in diminished rhythms of the peripheral clocks sensitive to food intake, such as the liver (Greenwell *et al.,* 2019), causing hepatic lipid accumulation, systemic inflammation and rhythm alteration also in other peripheral tissues (Ni *et al.,* 2019, Manella *et al.,* 2021). On the contrary, when feeding regularly, such as under TRF, food may serve as a strong zeitgeber, keeping the circadian clocks synchronised.

Majority of laboratory studies examining TRF focus on its potential negative health implications, when feeding is restricted to the inactive phase, daytime for the most commonly used model rodents. Naturally, daytime feeding forces the nocturnal animals to display high locomotor activity also during the feeding time, however, the increased activity starts up to several hours before food presentation (Richter, 1922, Bolles & Stokes, 1965, Edmonds & Adler, 1977, Stephan, 1992), and is accompanied by a release of plasma corticosteroids, as well as an increase in the core body temperature (Krieger *et al.,* 1977) and gastrointestinal motility (Comperatore & Stephan, 1987). Daytime feeding was shown to cause a phase shift in the liver, kidney, heart, pancreas, stomach and colon (Damiola *et al.,* 2000, Hara *et al.,* 2001, Stokkan *et al.,* 2001, Davidson *et al.,* 2003), as well as some brain structures, importantly excluding the SCN (Wakamatsu *et al.,* 2001, Gooley *et al.,* 2006, Mieda *et al.,* 2006, Verwey *et al.,* 2007, 2008, Minana-Solis *et al.,* 2009), which results in an uncoupling of the light- and food-sensitive clocks. Moreover, this food-anticipatory activity (FAA) persists in SCN-lesioned, normally arrhythmic animals (Krieger *et al.,* 1977), indicating that the food-entrainable oscillator (FEO) is independent from the master circadian clock. These two, however, interact, as shown by a possibility of SCN entrainment to TRF, but only under constant lighting conditions (Castillo *et al.,* 2004, Lamont *et al.,* 2005).

These results present TRF as a potential solution to the problems of desynchronising body clocks under modern lifestyle. Establishing a regular feeding schedule makes food intake a strong zeitgeber, which could even become dominant, considering omnipresent light pollution.

1.1.4. Dorsomedial Hypothalamus as a part of the food-entrainable oscillator

A long search for the brain site of the FEO, including a multitude of lesioning studies as unsuccessful attempts to abolish the FAA (reviewed in Davidson, 2006 and Carneiro & Araujo, 2009), has proven it to be a network of structures, rather than just one specific locus. Despite some reports presenting an elimination of the FAA after a site-specific lesion, these results were not repetitive. A good example is the Dorsomedial Hypothalamus (DMH), considered

one of the most important parts of the FEO. DMH was shown to respond to TRF, with not only a phase-shift in the clock and immediate early gene expression, but also a large increase in the rhythm amplitude (Gooley *et al.*, 2006, Mieda *et al.*, 2006, Verwey *et al.*, 2007, 2008, Minana-Solis *et al.*, 2009). Some reports claim that DMH only becomes rhythmic under regular feeding restriction (Mieda *et al.*, 2006, Verwey *et al.*, 2007, 2009), however others present DMH rhythmicity not only in the clock gene expression, but also regarding neuronal activity (Guilding *et al.*, 2009), especially in the compact part of the DMH (cDMH). Moreover, even in *ad libitum*-fed animals, DMH lesions cause a reduction of the rhythms in wakefulness, feeding, locomotor activity, and serum corticosteroid levels (Chou *et al.*, 2003). Importantly, DMH lesions also result in a complete FAA elimination, although this effect is only temporary, showing that the FEO network is capable of adjustment and adaptation (Gooley *et al.*, 2006, Landry *et al.*, 2006, Moriya *et al.*, 2009, Acosta-Galvan *et al.*, 2011).

DMH is located bilaterally, on either side of the third ventricle. Structurally and functionally it can be divided into three distinct subdivisions. From its ventromedial corner diagonally extends the already mentioned compact part, composed of small, densely packed cells, and considered the site of the local circadian oscillator (Guilding *et al.*, 2009). The cDMH splits the structure into the ventral (vDMH) and dorsal (dDMH) parts, which are more directly involved in sensing and responding to different metabolic states. DMH receives feeding-related information from the digestive system and adipose tissue, with the non-compact substructures possessing cells responsive to leptin (Elmquist *et al.*, 1998, Bi *et al.*, 2003, Zhang *et al.*, 2011, Faber *et al.*, 2021), ghrelin (Olszewski *et al.*, 2003, Kobelt *et al.*, 2008), and glucagon-like peptide 1 (GLP1; Renner *et al.*, 2012). They are also the site of the highest neuropeptide Y (NPY) fibre density within the DMH (Broberger *et al.*, 1998, Chen *et al.*, 2004, Sanetra *et al.*, 2022), although it is the cDMH that is capable of NPY expression (Guan *et al.*, 1998, Tritos *et al.*, 1998, Bi *et al.*, 2003, Chen *et al.*, 2008). The cDMH is also the only DMH subregion which expresses glucagon-like peptide 2 receptor (GLP2R; Tang-Christensen *et al.*, 2000).

Despite many similarities, a distinction of the non-compact DMH into dDMH and vDMH is justifiable on both molecular and functional levels. The highest GLP1&2 fibre density is observed in the vDMH (Tang-Christensen *et al.*, 2000, Renner *et al.*, 2012), which is also the most responsive to feeding (Poulin & Timofeeva, 2008, Renner *et al.*, 2012, Maejima *et al.*, 2021). The feeding-activated, GLP1R-positive vDMH neurons project to the SCN (Acosta-Galvan *et al.*, 2011, Maejima *et al.*, 2021), whereas the main output projections of the dDMH are those to the ventrolateral medulla and raphe pallidus, relaying the stimulation of the sympathetic nervous system, regulating heart beat and brown adipose tissue (BAT)

thermogenesis (Cano *et al.*, 2003, Cao *et al.*, 2004, Samuels *et al.*, 2004, Zhao *et al.*, 2017, Kono *et al.*, 2020, Brizuela & Ootsuka, 2021). The dDMH is also the location of orexin neurons (De Lecea *et al.*, 1998, Peyron *et al.*, 1998, Nambu *et al.*, 1999), influencing energy homeostasis via both food intake stimulation (Dube *et al.*, 1999) and autonomic nervous system regulation (Zhang *et al.*, 2010, Li *et al.*, 2018, 2021). DMH location, as well as within-structure differences are summarised in Fig. 1.

The DMH is, therefore, involved in sensing the metabolic state of the organism via hunger and satiety signals, and producing a behavioural and autonomic response through efferent projections. On top of these, a presence of a circadian clock enables adjustment of the output depending on the time of the day and feeding schedule.

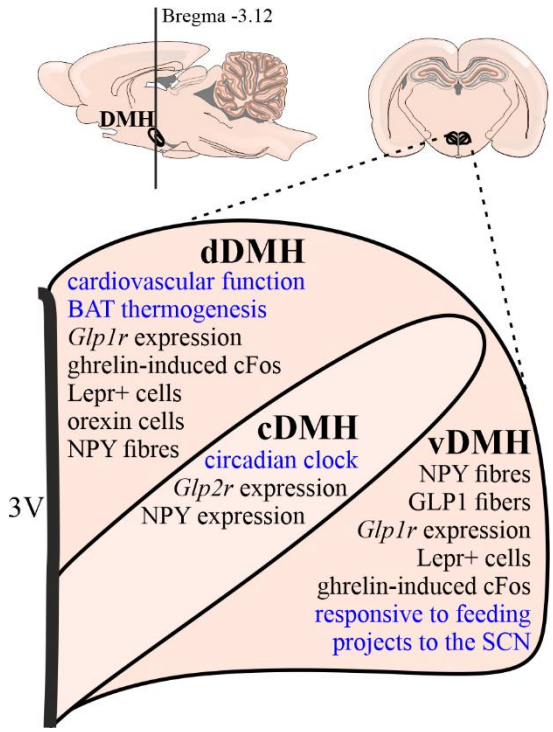

Figure 1. *Location and internal complexity of the Dorsomedial Hypothalamus (DMH). Sagittal (left) and coronal (right) view of the rat brain, followed by a zoomed-in schematic of the internal separation within the structure. Main function of each subdivision (compact - cDMH, dorsal - dDMH and ventral - vDMH) is indicated in blue. 3V - third ventricle, BAT - brown adipose tissue, Glp1/2(r) - glucagon-like peptide 1/2 (receptor), Lepr - leptin receptor, NPY - neuropeptide Y, SCN - Suprachiasmatic Nucleus. Brain schematic obtained from Paxinos & Watson, 2007.*

1.1.5. Obesity-induced changes to the DMH functioning

DMH is affected by diet-induced obesity (DIO) stronger than any other investigated hypothalamic region, with changes in the expression level of 60 genes, encoding proteins participating in cell-to-cell signalling, chemical and glucose homeostasis, hormone secretion, transport and uptake, and intracellular signalling pathways (Zhang *et al.*, 2020). More specifically, these include the overexpression of genes for cholecystokinin, urocortin, melanocortin receptor and GLP1R, as well as downregulation of gastrin-releasing peptide, all of which are, amongst others, involved in feeding behaviour and metabolism control.

Upregulation of cocaine and amphetamine regulated transcript (CART) was shown to mediate HFD-induced hypertension (Chaar *et al.*, 2016), whereas DIO-induced NPY expression in the DMH might further stimulate excessive food intake (Guan *et al.*, 1998, Yang *et al.*, 2009). Studies on DIO animals clearly present DMH as an important part of the metabolism-controlling circuitry, disrupted by obesity. However, whether this structure also plays an active role during obesity development, or its malfunctions are purely a result of an increased body weight, is not currently clear. Although a DMH-specific NPY knockdown was shown to be capable of obesity prevention and even reversal (Chao *et al.*, 2011, Kim & Bi, 2016), NPY is considered to only be expressed there secondary to obesity (Kesterson *et al.*, 1997, Guan *et al.*, 1998, Tritos *et al.*, 1998), as a result of caloric restriction (Bi *et al.*, 2003), or during lactation (Smith, 1993). The possibility of DMH involvement in obesity development needs to be studied more systematically, by addressing diet-induced changes that occur before obesity onset. This was done in the presented thesis, which examines the DMH properties under both control diet (CD) and HFD, at various times of the day, and separately for each of its functionally distinct subdivisions (cDMH, dDMH and vDMH).

1.1.6. The family of the proglucagon-derived peptides

Obesity is a complex and multifactorial disease, and therefore the attempted treatments should approach it from multiple angles. While behavioural and circadian aspects, such as TRF, have shown very promising results, great progress has also been made regarding pharmacology. Recently, two antidiabetic drugs: liraglutide and semaglutide (both produced by Novo Nordisk A/S, Denmark), have been approved for obesity treatment (FDA, 2021, EMA, 2022a, b). Their mechanism of action is based on GLP1R agonism, which mediates the incretin effect, delays gastric emptying and gastric acid secretion, as well as decreases food intake and prolongs the feeling of satiety in human patients (Kreymann *et al.*, 1987, Gutniak *et al.*, 1992, Nathan *et al.*, 1992, Nauck *et al.*, 1993, Wettergren *et al.*, 1993, D'Alessio *et al.*, 1994, Näslund *et al.*, 1998, Kolterman *et al.*, 2003, Dupré *et al.*, 2004, Khera *et al.*, 2016). Using animal models, GLP1 analogues have been shown to stimulate insulin expression in addition to its release, increase pancreatic β-cell mass and improve their sensitivity to glucose, and increase energy expenditure (Drucker *et al.*, 1987, Holz *et al.*, 1993, Schmidt *et al.*, 1985, Wang & Brubaker, 2002, Osaka *et al.*, 2005), which together with decreased feeding (Turton *et al.*, 1996, Dakin *et al.*, 2001) inhibits weight gain even in genetic models of obesity (De Fonseca *et al.*, 2000, Williams *et al.*, 2006).

GLP1 is a member of the preproglucagon (PPG) family, also called the proglucagon-derived peptides (PGDP). Proglucagon is post-translationally cleaved by prohormone convertases (PC), which produces GLP1, GLP2, and either glucagon (in the pancreatic α-cells; cleavage by PC2, Rouille *et al.,* 1994), or glicentin/oxyntomodulin (Oxm, in the intestinal L cells; cleavage by PC1/3; Mojsov *et al.,* 1986, Bataille & Dalle, 2014).

GLP1 and glucagon are the most studied PGDP, with much less known about GLP2 and Oxm. Despite a lack of the incretin effect, GLP2 also promotes glycaemic control and insulin sensitivity, as well as decelerates gastric emptying and enhances intestinal nutrient absorption (Guan, 2014). GLP2 is, however, more often associated with the behavioural aspects of feeding, possessing a great anorexigenic potential, reducing food intake via receptors located in the hypothalamus, particularly in the cDMH (Dalvi & Belsham, 2012, Tang-Christensen *et al.,* 2000).

Unlike GLP1 or GLP2, the Oxm does not possess dedicated receptors. It can, however, bind and activate both GLP1R (Gros *et al.,* 1993, Schepp *et al.,* 1996) and the glucagon receptor (GCGR; Baldissera *et al.,* 1988). As an GLP1R agonist, Oxm also induces insulin release (Schjoldager *et al.,* 1988) and improves glucose metabolism, even in diet-induced insulin-resistant mice (Parlevliet *et al.,* 2008). Moreover, Oxm decreases stomach acid release (Schjoldager *et al.,* 1988), although it does not inhibit gastric emptying (Maida *et al.,* 2008). Most importantly from the neurobiological perspective, Oxm inhibits food intake in humans (Cohen *et al.,* 2003, Wynne *et al.,* 2006) and laboratory animals, when injected peripherally (Dakin *et al.,* 2004) as well as intraventricularly (Dakin *et al.,* 2001).

The PGDP are co-released after a meal, and evert their effects locally, within the digestive system, but also travel via the bloodstream to more distantly located tissues (Kreymann *et al.,* 1987, Le Quellec *et al.,* 1992). The information about food consumption is delivered to the brain by means of both the circulation, carrying the PGDP, amongst other satiety signals, and by stimulating the vagus nerve (Berthoud & Neuhuber, 2000, Bai *et al.,* 2019), which delivers the cue directly into the brainstem Nucleus of the Solitary Tract (NTS; Wan *et al.,* 2007). Interestingly, a subpopulation of the NTS neurons also expresses the gene for PPG (Larsen *et al.,* 1997). With a dominant presence of PC1/3 over PC2 (Perello *et al.,* 2007), the NTS cells produce GLP1 and GLP2 and Oxm, and send axonal projections to other brain structures, with high density in the DMH (Larsen *et al.,* 1997, Vrang *et al.,* 2007).

As already mentioned, DMH possesses not only PPG-positive neuronal endings, but also both GLP1 and GLP2 receptors (Merchenthaler *et al.,* 1999, Tang-Christensen *et al.,* 2000, 2001, *Cork et al.,* 2015, Maejima *et al.,* 2021, Huang *et al.,* 2022), with low amounts of, and less

focus given the GCGR (Hoosein *et al.,* 1984, Svoboda *et al.,* 1994, Hansen *et al.,* 1995). DMH cells have been shown to respond to the PGDP (Tang-Christensen *et al.,* 2000, Maejima *et al.,* 2021, Huang *et al.,* 2022), and mediate their effects on energy expenditure, BAT thermogenesis (Lee *et al.,* 2018) and feeding behaviour (Schick *et al.,* 1996, Renner *et al.,* 2012, Maejima *et al.,* 2021). Moreover, GLP1R knockout specifically in the DMH impairs animals' feeding pattern, induces hyperphagia and obesity (Maejima *et al.,* 2021), as well as alters lipid and glucose metabolism (Lee *et al.,* 2018, Huang *et al.,* 2022), which underlines the importance of the central nervous system, and the DMH in particular, also for peripheral glucose homeostasis. Taking into account the therapeutical potential but not yet fully explored role of the PPG signalling within the hypothalamus, the presented thesis aimed at studying the PGDP in the DMH – their physiological effects, distribution and abundance under different metabolic states, followed by an analysis of the HFD-evoked changes.

1.2. Research objectives

The global aim of the conducted studies was to characterise the DMH in the context of circadian rhythms and meal-entrainment, with special attention to the internal complexity of the structure, as well as to explore the HFD-evoked changes to the DMH physiology before obesity onset, which could be indicative of the mechanisms partaking in its development. The main objectives were, therefore, grouped into 3 general modules:

I. **Physiology** – characterisation of the DMH electrophysiology, circadian and periprandial rhythms.
II. **Pathology** – investigation of the changes occurring during HFD-induced obesity development.
III. **Intervention** – attempt at the prevention of the DMH rhythm disruption under HFD.

Detailed objectives have been divided into sections, which have given rise to three separate publications:

- **Publication 1**:
  - Electrophysiological characterisation of the DMH neurons with a distinction of the three subdivisions (dDMH, cDMH and vDMH) and comparison of their electrophysiological properties between daytime and nighttime, as well as between CD- and HFD-fed animals
- **Publication 2**:

- Assessment of the kinetics of the body weight gain and feeding behaviour under HFD
- Investigation into the day/night rhythm of the cellular activation of the DMH neurons, its dependence on the amount of food eaten at the particular time, and HFD-mediated alterations
- Evaluation of the circadian (intrinsic) nature of the DMH oscillations via long-term activity recordings, with an indication of the time of the highest neuronal activity for both dietary groups
- Verification whether the DMH clock disturbance persists under restricted nighttime feeding (is a direct result of the HFD), or arises secondary to the irregular feeding pattern

- **Publication 3**:
  - Exploration of the spatial distribution and expression levels of the *Glp1/2r* under both CD and HFD
  - Delineation of the DMH neuronal responsiveness to the PGDP during daytime/nighttime and under different diets: proportions and location of responsive cells, types of responses produced and factors determining the amplitude of the response
  - Analysis of the participation of the PGDP in the DMH synaptic transmission at different times of the day and under both CD and HFD
  - Examination of the GLP1 abundance in the DMH under different metabolic states (fasted/fed), both when unexpected and anticipatory, as well as their relationship with the cellular activity.

2. Overview of the methods

2.1. Animals

2.1.1. Animal model

The study utilised male Sprague Dawley rats, divided into two primary groups. At weaning (postnatal day 28), half of the animals received control diet (CD; ~3,514 kcal/kg, fat content 4%, energy from: 10% fat, 24% protein, 66% carbohydrates, cat. no. C1090-10; Altromin International, Germany) and created the control group. On the other hand, the experimental group consisted of rats fed a high-fat diet (HFD; ~5,389 kcal/kg, fat content 42%, energy from: 70% fat, 16% protein, 14% carbohydrates, cat. no. C1090-70; Altromin International). For all but one experiment, the animals were maintained on a respective diet for 2-4 weeks, which precedes excessive weight gain in HFD-fed rats (Chrobok *et al.*, 2022), occurring after 5 weeks of HFD-feeding (**Publication 2**). Nevertheless, for all immunohistochemical studies here, utilising large groups of animals at the time, their weight was also monitored as a confirmation, as well as to find out whether different feeding restrictions influence weight gain kinetics in any way.

Female rats were excluded from the study due to a high probability of interactions between the oestrus cycle and metabolism, especially during puberty.

2.1.2. Animal maintenance

All experiments were carried out in accordance with the Polish Animal Welfare Act of 23 May 2012 (82/2012) and the European Communities Council Directive (86/609/EEC), and had received approval from the Local Ethics Committee in Krakow (No. 18/2018, 349/2022). Animals were maintained in constant environmental conditions (temperature ~23^{o}C, humidity ~65 %) and standard lighting conditions (LD 12:12). Water was provided *ad libitum*, and food either *ad libitum* or accordingly to specific experimental protocols, as follows:

- For the night-feeding (NF) protocol food was available between ZT12-24 (Zeitgeber time, where ZT0 is the onset of the light phase; **Publication 2**).
- For the food deprivation (FD) protocol 2 groups were food-deprived for 48 h, starting at ZT14, after which one of them was refed to satiety during the next 2 h (**Publication 3**).
- For the restricted-feeding (RF) protocol the food was available between ZT14-20 (**Publication 3**).

2.2. Electrophysiology

2.2.1. Patch clamp

Whole-cell patch clamp experiments were utilised in order to investigate electrophysiological parameters of the DMH neurons, their day/night changes and any HFD-mediated alterations. The parameters examined were: resting membrane potential, spontaneous firing rate, threshold for action potential generation, rheobase (defined as the current value at the time at which the cell reaches the threshold minus the holding current; Kania *et al.*, 2020) – in current clamp mode; input resistance and the current-voltage relationship – in voltage clamp (**Publication 1**). Patch clamp recordings in voltage clamp mode were also used to test the effect of Exn4, Oxm and GLP2 on the DMH synaptic network (**Publication 3**).

2.2.2. Multi-electrode array (MEA)

Extracellular MEA recordings were performed to measure DMH neuronal activity on a large group of cells.

First, short recordings at midday and midnight were employed to check potential day/night differences in the firing rate and whether any changes occur under HFD. These experiments were performed on *ad libitum*- and night-fed animals, to check whether the dietary differences observed for *ad libitum*-fed rats persist under a healthy feeding schedule, or depend on a disrupted rhythm in food intake (**Publication 2**).

Second, in order to explore circadian changes in the DMH cellular activity, as well as their dietary influence, long-term recordings (~30 h) were performed, revealing exact times of the peak firing rate for both groups. These experiments were also performed on both *ad libitum*- and night-fed animals (**Publication 2**).

Third, PPG-derived peptides' impact on the DMH activity was tested at night and during daytime for both dietary groups for *ad libitum*-fed rats. Both the amplitude and the frequency of the responses were analysed (**Publication 3**).

2.3. Immunofluorescence

Immunofluorescent staining was performed on brain slices acquired after transcardial perfusion (with an exception of the NF protocol, were fresh slices were cut and then fixed; **Publication 2**). For these experiments, the fixed stomachs were weight as a proxy of the amount of food eaten by the animal, which was then compared between the diets and particular conditions

(time of the day/metabolic state), serving as a confirmation of the protocol assumptions and reflecting the data from the chow weighing.

As a marker of neuronal activity, cFos protein – a product of an immediate early gene, was immunostained for *ad libitum*-fed groups in 4 equally separated time points (ZT0, 6, 12, 18), as well as at midday/midnight (ZT6, 18) for the NF rats (**Publication 2**).

For the FD and RF protocols, the cFos immunofluorescence was accompanied by GLP1 staining, detecting GLP1-positive neuronal fibres at different time points around the meal (**Publication 3**).

2.4. *In situ* hybridisation

RNAscope technique was utilised to explore the presence and precise location of the *Glp1r* and *Glp2r* mRNA, as well as their expression level for both dietary groups (**Publication 3**).

3. Publications

3.1. **Publication 1**: *Electrophysiological complexity in the rat dorsomedial hypothalamus and its susceptibility to daily rhythms and high-fat diet*

2022, European Journal of Neuroscience, 56(4), 4363-4377

Received: 23 December 2021 | Revised: 10 June 2022 | Accepted: 10 June 2022

DOI: 10.1111/ejn.15759

RESEARCH REPORT

EJN European Journal of Neuroscience FENS WILEY

Electrophysiological complexity in the rat dorsomedial hypothalamus and its susceptibility to daily rhythms and high-fat diet

Anna Magdalena Sanetra[1] | **Katarzyna Palus-Chramiec**[1] | **Lukasz Chrobok**[1,2] | **Marian Henryk Lewandowski**[1]

[1]Department of Neurophysiology and Chronobiology, Institute of Zoology and Biomedical Research, Jagiellonian University in Krakow, Krakow, Poland

[2]School of Physiology, Pharmacology, and Neuroscience, University of Bristol, Bristol, UK

Correspondence
Anna Magdalena Sanetra and Marian Henryk Lewandowski, Department of Neurophysiology and Chronobiology, Institute of Zoology and Biomedical Research, Jagiellonian University in Krakow, Gronostajowa Street 9, 30-387 Krakow, Poland.
Email: anna.sanetra@uj.edu.pl; marian.lewandowski@uj.edu.pl

Funding information
This study was supported by Polish National Science Centre grant 2017/25/B/NZ4/01433 awarded to MHL.

Edited by: Rae Silver

Abstract

The dorsomedial hypothalamus (DMH) in amongst the most important brain structures involved in the regulation of feeding behaviour and metabolism. In contrast to other hypothalamic centres, its main role is related to the circadian rhythmicity of food intake and energy homeostasis; both reported to be disrupted in obesity. In modern world, overweight and obesity reached global epidemic proportions. Thus, not only is it important to study their negative implications but also the mechanism responsible for their development. Here, we exposed rats to short-term (2–4 weeks) high-fat diet (HFD)—not long enough to induce obesity. Next, we performed electrophysiological patch-clamp recordings ex vivo from neurons in the DMH either during the day or at night. Our results showed a day-to-night change in the firing frequency of DMH cells, with higher activity during the dark phase. This was abolished by HFD consumption, resulting in a decreased threshold for action potential generation during the day and therefore increased electrical activity at this phase. We propose this electrophysiological disturbance as a mechanism for the induction of abnormal daytime feeding, previously observed for HFD-fed animals, which might in turn contribute to the development of obesity. In addition, we provide an electrophysiological characteristic of DMH neurons with a separation into three anatomically and functionally distinct subpopulations, namely, the compact part, separating the structure into the ventral and dorsal

Abbreviations: ACSF, artificial cerebro-spinal fluid; cACSF, cutting ACSF; cDMH, compact division of the DMH; Cv, coefficient of variation; dDMH, dorsal division of the DMH; DIO, diet-induced obesity; DMH, dorsomedial hypothalamus; FEO, food-entrainable oscillator; FR, firing rate; HFD, high-fat diet; ISI, interspike interval; LD, light/dark; nACSF, normal ACSF; NDS, normal donkey serum; MEA, multielectrode array; PBS, phosphate-buffered saline; R, resistance; Rh, rheobase; SCN, suprachiasmatic nucleus; Th, threshold; vDMH, ventral division of the DMH; Vm, membrane potential; ZT, Zeitgeber time.

divisions. Our study is the first to show electrophysiological complexity of the DMH with its sensitivity to diet and daily rhythms.

KEYWORDS
chronobiology, food intake, metabolism, obesity, patch-clamp

1 | INTRODUCTION

All animals express some form of circadian rhythms—rhythmic physiological processes with a period of about 24 h. Their intrinsic regulation enables the organism to predict changes arising in the environment every day; however, they can adapt, or entrain, when these conditions start to change. Most important cue influencing circadian rhythms is light availability, information about which is received directly from the eye by the master circadian clock, located in the Suprachiasmatic Nucleus (SCN). SCN neurons oscillate around the 24 h clock, changing their activity both as a result of rhythmic clock gene expression, as well as due to the changes in the information received from the retina.

However, circadian rhythms can also be entrained by other factors, for example, food availability. Circadian regulation of food intake is controlled by a complex network of neuronal structures, creating the food-entrainable oscillator (FEO), independent of the SCN. FEO is responsible for the organism's entrainment to different feeding schedules. It is believed that one of the main centres of FEO is located in the dorsomedial hypothalamus (DMH; Mieda et al., 2006), a structure responsive to different metabolic states and affecting food intake and metabolism. Intriguingly, the DMH also exhibits intrinsic circadian clock properties (Guilding et al., 2009), which influence rhythms of feeding, as well as wakefulness and locomotor activity (Chou et al., 2003).

The DMH is located bilaterally in the mediobasal hypothalamus, on either side of the third ventricle. The compact division (cDMH) extends diagonally from its ventromedial corner and is composed of densely packed small neurons, which separate the whole structure into the dorsal (dDMH) and ventral (vDMH) subdivisions. Though the majority of studies treat the DMH as a whole, there are limited data indicating distinct properties differentiating these three parts in terms of molecular characteristics, but also functionally. First, rhythmic clock gene expression and electrical activity ex vivo have been shown to be the strongest in the cDMH (Guilding et al., 2009), suggesting this part to be the local autonomous oscillator. On the other hand, it is the vDMH neurons that create the efferent connection to the SCN (Acosta-Galvan et al., 2011). The vDMH is also the most responsive to different metabolic states and metabolically-relevant signalling molecules (Poulin & Timofeeva, 2008; Renner et al., 2012; our unpublished observation). Lastly, the dDMH sends descending connections to the autonomic nervous system, regulating thermogenesis (Cano et al., 2003, reviewed in DiMicco & Zaretsky, 2007), heart rate (Kono et al., 2020; Samuels et al., 2004) and cardiovascular response (Fontes et al., 2001).

Obesity is a constantly growing health problem in the modern society. Unhealthy diet combined with a sedentary lifestyle creates an imbalance between the amount of calories ingested and spent, resulting in excess storage and fat tissue accumulation. Subsequently, obesity may increase risk of many life-threatening conditions such as cardiovascular disease and stroke (Kenchaiah et al., 2002; Lakka et al., 2001), mental disorders (reviewed in Avila et al., 2015), and even some types of cancer (Calle et al., 2003). As far as negative health implications of obesity have been extensively investigated into, the mechanism for its development is still not well understood. In animal studies, the most common models include feeding a specific diet, high in fat and/or sugar, in order to best reflect the current trends of nutrition. This approach is known as the diet-induced obesity (DIO).

The transcriptome analysis has shown that the DMH is one of the two brain structures most potently affected by DIO. The expression level has been found to be affected for over 80 genes in the DMH, including those involved in the regulation of chemical homeostasis and different aspects of neuropeptide and hormone signalling (Zhang et al., 2020). These complex changes induced by DIO indicate global dysfunction of the entire DMH network. The causal link is bidirectional, as not only does obesity influence the DMH, but also experimental manipulations within this region result in hyperphagic behaviour and obesity (e.g., brain-derived neurotrophic factor deletion; Unger et al., 2007), decreased energy expenditure and impaired sympathetic nerve activity ($G_q a/G_{11} a$ deficiency; Wilson et al., 2021). All of these factors lead to slower metabolism and excessive weight gain. High-fat diet (HFD)-induced hypertension has also been shown to be accompanied by an increase in *Cart* gene expression within the DMH (Chaar et al., 2016).

Therefore, the aim of this study was to characterise neurons in three distinct parts of the DMH during the day and night and investigate electrophysiological changes occurring under HFD. In order to study the possible causes rather than consequences of obesity, we fed rats with HFD for 2–4 weeks, as our previous study has proved that they would not become overweight within this time (Chrobok, Klich, Sanetra, et al., 2022). Then, we performed an extensive electrophysiological characterization of the DMH, with a separation into the three functionally distinct parts, and found substantial differences predominately between the cDMH and the other two, reflected in a variation in resting membrane potential, input resistance and rheobase. The DMH was also shown to exhibit day-to-night changes in the electrical activity, with higher levels observed during the night. These daily changes were abolished by HFD, which increased neuronal firing during the behaviourally quiescent day by lowering the threshold for action potential generation. Bearing in mind the orexigenic character of the DMH activity, we propose that a dysregulation of its circadian rhythmicity, with higher daytime firing, influences animal behaviour by increasing daytime feeding and therefore leads to the development of obesity.

2 | METHODS

2.1 | Animals

The study was performed on 4- to 8-week-old male Sprague–Dawley rats, bred and kept at the Animal Facility in the Institute of Zoology and Biomedical Research, Jagiellonian University in Krakow. Animals were maintained in standard environmental conditions (temperature: 23 ± 2°C, relative humidity: 67 ± 3%, 12:12 h light–dark [LD] cycle), with food and water supplied ad libitum. All experiments were performed according to the Polish Animal Welfare Act of 23 May 2012 (82/2012) and the European Communities Council Directive (86/609/EEC) and had been approved by the II Local Ethics Committee in Krakow (No. 18/2018 and 349/2020).

At 4 weeks of age, rats were weaned and randomly assigned to one of two groups, fed with either control (CD, ∼3,514 kcal/kg, fat content 4%, energy from: 10% fat, 24% protein, 66% carbohydrates; Altromin International, Germany), or high-fat diet (HFD, ∼5389 kcal/kg, fat content 42%, energy from: 70% fat, 16% protein, 14% carbohydrates; Altromin International), and maintained on it for the following 2–4 weeks, after which electrophysiological experiments were performed.

A total of 29 rats were used for the study, out of which 17 fed CD (eight culled at night and nine during the day) and 12 fed HFD (four culled at night and eight during the day).

2.2 | Electrophysiological recordings

2.2.1 | Tissue preparation

Brain tissue for patch-clamp recordings was prepared always 1–3 h after the change in the lighting conditions (ZT1–3 or ZT13–15, where ZT0 is the onset of the light phase). For night-time recordings, the preparation was performed under red light.

Animals were deeply anaesthetized by isoflurane inhalation (2 ml/kg of body weight) and decapitated. Brain was quickly extracted from the skull and placed in ice-cold, carbogenated (95% O_2, 5% CO_2) cutting artificial cerebro-spinal fluid (cACSF), composed of (in mM): 25 $NaHCO_3$, 3 KCl, 1.2 Na_2HPO_4, 2 $CaCl_2$, 10 $MgCl_2$, 10 glucose, 125 sucrose with addition of pH indicator: Phenol Red 0.01 mg/L (osmolality ∼290 mOsmol/kg). Tissue was cut into 250 μm thick coronal slices with a vibroslicer (Leica VT1000S, Heidelberg, Germany) and these containing the DMH (between −3.00 and - 3.48 from bregma; Paxinos & Watson, 2007) were placed in carbogenated normal ACSF (nACSF; warmed up to 32°C), containing (in mM): 125 NaCl, 25 $NaHCO_3$, 3 KCl, 1.2 Na_2HPO_4, 2 $CaCl_2$, 2 $MgCl_2$, 5 glucose, and 0.01 mg/L of Phenol Red, for a minimum of 2 h prior to the recording.

2.2.2 | Patch-clamp recordings

The recordings started around ZT6 or ZT18 (±1 h) and continued until the end of the projected lighting phase: therefore, the data collected constitutes an electrophysiological description and analysis of DMH neurons recorded predominantly during the second part of day/night, respectively. After the incubation, a brain slice was placed in the recording chamber, constantly perfused with carbogenated nACSF (heated to 32°C) with a peristaltic pump at a speed of 2.5 ml/min. Recording chamber was positioned under an Axioskop 2 FS microscope fitted with infrared differential interference contrast (Göttingen, Germany). Whole-cell configuration was acquired under 40x magnification with borosilicate glass pipettes (Sutter Instruments, Novato, USA; resistance = 4–9 MΩ), filled with an intrapipette solution containing (in mM): 125 potassium gluconate, 20 KCl, 10 HEPES,2 $MgCl_2$, 4 Na_2ATP, 0.4 Na_3GTP, 1 EGTA, and 0.05% biocytin (pH = 7.4, adjusted with 5-M KOH; osmolality 300 mOsmol/kg) and mounted onto an Ag/AgCl

electrode. Pressure was applied with Ez-gSEAL100B Pressure Controller (Neo Biosystem, USA) in order to obtain gigaseal as well as to rupture cellular membrane necessary for whole-cell recordings. Recorded signal was amplified by a SC 05LX amplifier (NPI, Tamm, Germany), low-pass filtered at 3 kHz, digitised at 20 kHz, and visualised using the Signal software (Cambridge Electronic Design Inc., UK). A liquid junction potential of −14.8 mV was added to the recorded values of the membrane potential.

Each neuron was subjected to a set of electrophysiological tests. First, a minimum of 30 s of current clamp recording at 0-nA holding current was recorded in order to measure resting membrane potential and spontaneous firing frequency, as well as regularity calculated from the interspike intervals (ISI) as a coefficient of variation: $Cv = \frac{SD(ISI)}{MEAN(ISI)}$ (Young et al., 1988). Then membrane potential was manually set to −90 mV and a 0.15-nA ramp current lasting 1 s was applied. This enabled us to establish the threshold for action potential generation as well as rheobase, defined as the current value at the time at which the cell reaches the threshold minus holding current (Kania et al., 2020). Lastly, current–voltage (IV) relationship was acquired with a set of voltage steps. From a holding potential of −50 mV, 18 0.8-s-long steps ranging from −125 to 45 mV (with 10-mV increments) were applied. Membrane resistance was calculated from the −115-mV step.

2.2.3 | Histological verification

At the end of each experiment, brain slices containing recorded neurons were subjected to an immunohistochemical staining, with the aim of verifying the location of recorded neurons within the DMH. First, each slice was fixed overnight in 4% paraformaldehyde in phosphate-buffered saline (PBS, pH = 7.4). On the following day, slices were rinsed in PBS (2 × 10 min), and underwent membrane permeabilization and non-specific sites blocking with 0.6% Triton-X100 (Sigma-Aldrich, Germany) and 10% normal donkey serum (NDS; Jackson ImmunoResearch, USA) in PBS, for 3 h at room temperature. Next, the slices were transferred to PBS containing 0.3% Triton-X100, 2% NDS and primary rabbit neuropeptide Y (NPY) antisera (1:8000, Sigma-Aldrich), which served to delineate the borders of the DMH. In order to visualise recorded neurons, this solution also contained Cy3-conjugated Extravidin (1:250, Sigma-Aldrich), which binds biocytin present in the intrapipette solution and after the recording—also in a recorded cell. After 72 h at 4°C, the slices were rinsed again (2 × 10 minutes in PBS) and anti-rabbit

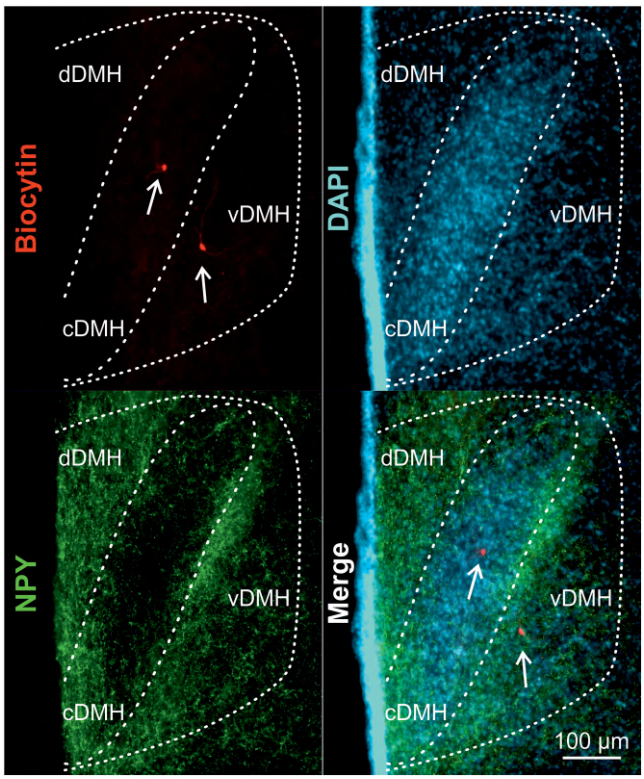

FIGURE 1 Representative photomicrograph of a brain slice immunostained after a patch clamp recording. In order to assign the recorded neurons to either the compact (cDMH), ventral (vDMH), or dorsal (dDMH) part of the dorsomedial hypothalamus, we analysed the signal from DAPI staining (indicating densely packed neurons within the cDMH), as well as neuropeptide Y (NPY) immunoreactivity (visibly lower in the cDMH, with a characteristic region of dense NPY-ir neuronal fibres at its border with the vDMH). Two neurons recorded from this particular slice are pointed to by white arrows.

AlexaFluor 647-conjugated antisera (1:300; Jackson ImmunoResearch) were applied for another 24 h at 4°C. At the end, after another rinsing in PBS (2 × 10 min), slices were placed onto microscope slides and coverslipped with Fluoroshield™ (Sigma-Aldrich). Images were taken with a epifluorescence microscope (Axio Imager M2, Zeiss, Germany) and all the neurons were assigned into one of three distinct parts of the DMH (cDMH, dDMH or vDMH; Figure 1), as well as aligned with a corresponding plate from the rat brain atlas (Paxinos & Watson, 2007) in order to obtain an exact location of the cell within the borders of the DMH, used for further heatmap plotting.

2.3 | Statistical analysis

Statistical analysis was performed in R (Version 4.0.4; Team RC, 2021) and RStudio (Version 1.4.1106, PBC;

RStudio Team, 2019). Outliers were identified by the boxplot method for outlier detection from the *rstatix* package (Kassambara, 2021), as well as with a help of QQ-plots (*ggpubr*; Kassambara, 2020), and were removed from further analysis. For each parameter a linear mixed model was created using the *nlme* package (Pinheiro et al., 2021), with diet, time of day (LD—light/dark), and part of the DMH (referred to as the division—Div. factor) treated as fixed factors. Animal, from which particular brain slices were acquired, was set as a random factor, also accounting for the variation between experimental days (slices from one animal only were recorded per day). However, in no case was the random factor significantly influencing the model; therefore, it was simplified to contain only the fixed factors. Data were analysed with estimation statistics, as well as probability statistics. Type III analysis of variance (ANOVA) was performed with the aid of the *car* package (Fox & Weisberg, 2019) and $P < 0.05$ treated as a threshold for statistical significance. Post hoc analyses were performed using the *emmeans* package (Length, 2021) and *P* value corrected for multiple comparisons with Tukey method. Factors for the multiple comparisons were chosen based on the significance of both the ANOVA and the estimate within the linear model. Results from the statistical analysis, including all *F*, *t*, and *P* values as well as multiple comparisons performed, are presented in Table S1. Assumptions for using a general linear model were checked with Shapiro–Wilk normality test from the *rstatix* package and Levene test for homoscedasticity from the *car* package, normality of the residuals' distribution were analysed with QQ-plots.

To test whether length of a diet within the 2-week period created an effect, we performed a 4-factor multivariate analysis of variance (MANOVA), with the three factors as mentioned above, and the fourth being the time on a diet in weeks (2–3 vs. 3–4). Since no effect of the time on a diet was observed ($F_{6,93} = 1.37$, $P = 0.23$), and the only significant result of such analysis was an interaction between all the other factors (LD:diet: Div.; $F_{12,188} = 2.08$, $P = 0.02$), we decided to keep only them in the final model.

Due to high heteroscedasticity between the groups, the current–voltage relationship was analysed separately for each part of the DMH as well as for each holding potential. A two-way ANOVA was calculated with diet and LD as fixed factors, and a multiple comparison with Tukey correction run in the case of significant interaction. Results from the statistical analysis, including all *F*, *t*, and *P* values as well as multiple comparisons performed, are presented in Table S2.

3 | RESULTS

3.1 | Spontaneous activity of DMH neurons

We recorded a total of 151 neurons (CD daytime: 43, CD night-time: 35, HFD daytime: 37 and HFD night-time: 36; please see Table 1 for details on the number of cells recorded from each group for each parameter). Each cell was assigned to one of three distinct divisions of the DMH. This enabled us not only to compare different electrophysiological parameters between the groups of animals but also to study the variation amongst the DMH divisions.

Vast majority of DMH neurons were spontaneously active, with only nine hyperpolarised below their threshold for action potential generation. Surprisingly, we observed a subpopulation (∼15%) of highly depolarised cells which displayed a distinguishing form of activity manifesting in a delayed after-spike repolarisation during which another action potential of a much smaller amplitude and longer duration was often generated (Figure 2a). Some neurons changed their pattern of activity into depolarised low-amplitude membrane oscillations (DLAMO), similar to the one reported by Belle et al. (2009). Because high values of the recorded membrane potential might be a sign of either a ruptured seal between the recording pipette and the cell, or the neuron itself being in poor condition, each of these neurons was brought down to a more hyperpolarised value by negative current injection in order to check whether the recording was valid. Examples of two cells exhibiting these membrane characteristics are presented in Figure 2a with black traces representing the cell's spontaneous activity, and red—the activity modified by manual setting of the membrane potential at different values. Additionally, the validity of these recordings was confirmed by high input resistance.

Most of these neurons (17/22) were recorded from the cDMH; however, this area was not exclusive for such activity. Their larger proportion in this DMH division was probably due to an overall less negative resting membrane potential in the cDMH comparing to the other subdivisions (cDMH: -48.8 ± 5.0 mV, vDMH: -53.9 ± 5.1 mV, dDMH: -54.2 ± 4.4 mV; $F_{2,139} = 9.14$, $P = 0.00019$; cDMH–dDMH: $t_{139} = 5.29$, $P < 0.0001$, effect size: $t = -3.52$, $P < 0.0001$, cDMH–vDMH: $t_{139} = 5.29$, $P < 0.0001$, effect size: $t = -3.53$, $P < 0.0001$; please see Table 1 for all mean ± SD values for particular variables and Tables S1 and S2 for the results from all models presented in the paper). No differences in membrane potential were observed between the dDMH and vDMH ($t_{139} = 0.12$, $P = 0.99$). For this

TABLE 1 Mean ± SD and *n* values for the recorded parameters for each group

		cDMH				dDMH	
		Day		Night		Day	
Variable		CD	HFD	CD	HFD	CD	HFD
Membrane potential (mV)	Mean ± SD	−48.7 ± 5.9	−50.2 ± 5.4	−47.9 ± 5.0	−48.6 ± 3.4	−55.4 ± 4.8	−54.1 ± 5.6
	n	20	17	12	15	10	8
Firing rate (Hz)	Mean ± SD	3.9 ± 2.3	7.0 ± 3.2	6.4 ± 2.7	7.6 ± 3.0	5.4 ± 5.2	4.9 ± 3.9
	n	18	16	12	15	10	8
log10(Cv)	Mean ± SD	−0.4 ± 0.3	−0.5 ± 0.2	−0.4 ± 0.3	−0.4 ± 0.2	−0.7 ± 0.2	−0.6 ± 0.3
	n	19	17	12	15	7	5[a]
Threshold (mV)	Mean ± SD	−47.4 ± 4.9	−51.9 ± 4.6	−50.5 ± 3.4	−47.0 ± 4.8	−45.7 ± 7.2	−45.4 ± 7.3
	n	20	15	12	12	10	8
log10(Rh[nA])	Mean ± SD	−1.3 ± 0.1	−1.4 ± 0.1	−1.3 ± 0.1	−1.3 ± 0.1	−1.2 ± 0.1	−1.2 ± 0.2
	n	20	16	11	11	9	8
log10(R[Mohm])	Mean ± SD	3.0 ± 0.2	3.1 ± 0.2	2.9 ± 0.2	3.0 ± 0.3	2.8 ± 0.2	2.9 ± 0.2
	n	18	17	10	14	10	8

TABLE 1 (Continued)

	dDMH		vDMH			
	Night		Day		Night	
Variable	CD	HFD	CD	HFD	CD	HFD
Membrane potential (mV)	−54.7 ± 5.0	−51.8 ± 4.7	−54.9 ± 4.4	−53.2 ± 4.4	−54.3 ± 4.5	−54.1 ± 4.6
	15	13	13	10	10	8
Firing rate (Hz)	4.4 ± 4.3	4.9 ± 2.8	2.9 ± 2.1	4.8 ± 3.6	8.3 ± 4.8	7.2 ± 4.5
	15	13	13	10	9	8
log10(Cv)	−0.8 ± 0.5	−0.5 ± 0.3	−0.4 ± 0.2	−0.6 ± 0.5	−0.7 ± 0.3	−0.8 ± 0.3
	13	13	12	10	9	8
Threshold (mV)	−46.6 ± 3.1	−48.2 ± 7.7	−47.4 ± 4.2	−49.3 ± 3.8	−49.3 ± 5.1	−46.3 ± 2.6
	15	12	13	9	10	6
log10(Rh[nA])	−1.2 ± 0.1	−1.3 ± 0.1	−1.3 ± 0.1	−1.3 ± 0.1	−1.3 ± 0.2	−1.2 ± 0.1
	15	12	13	9	10	6
log10(R[Mohm])	2.8 ± 0.3	2.8 ± 0.1	2.9 ± 0.2	2.9 ± 0.2	2.9 ± 0.2	2.8 ± 0.2
	11	13	15	8	8	8

Note: Cv—coefficient of variation, R—resistance, Rh—rheobase.
[a]Low *n* stems from a relatively high number of silent cells in this group.

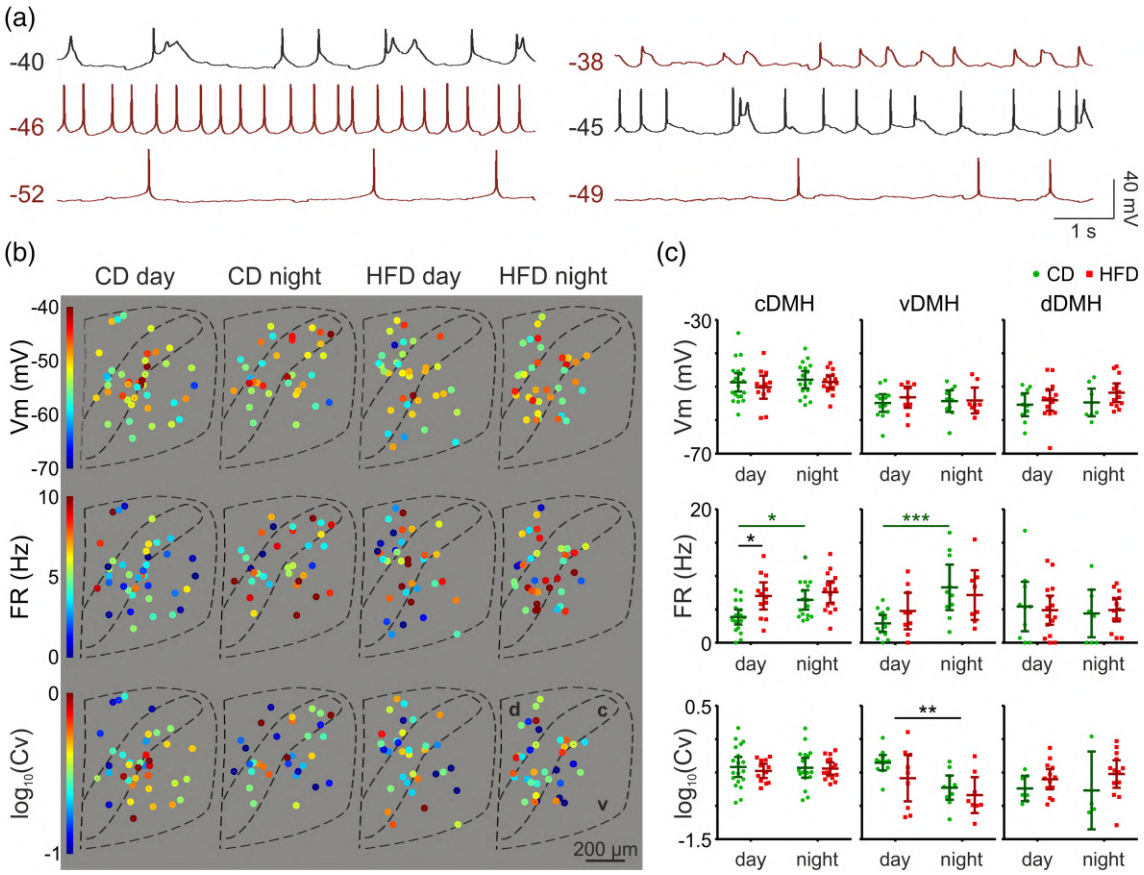

FIGURE 2 Spontaneous activity of dorsomedial hypothalamus (DMH) neurons. (a) Representative recordings of two neurons (traces in each column represent one neuron) displaying delayed repolarisation or DLAMO (depolarised low-amplitude membrane oscillation)-like events. Black traces indicate recordings from native resting membrane potential, whereas the red ones have been manipulated by current injection. (b) Heatmaps presenting spatial distribution of the recorded cells and their values of resting membrane potential (Vm; top row), frequency of action potential generation (FR; middle row) and the coefficient of variation of the interspike interval, representing regularity (Cv—ISI coefficient of variation; bottom row). The three divisions of the DMH are indicated as: c—compact, v—ventral, d—dorsal. (c) Analysis of the abovementioned parameters with the separation into the three divisions of the DMH. Data are presented as mean ± 95% CI. * $P < 0.05$, ** $P < 0.01$, *** $P < 0.001$. CD—control diet, HFD—high-fat diet.

electrophysiological parameter there was also neither a day-night variation ($F_{1,139} = 0.23$, $P = 0.63$) nor was it affected by HFD ($F_{1,139} = 0.66$, $P = 0.42$; Figure 2b,c, top row, analysis presented for DMH as a whole, without separation into subdivisions).

In addition to resting membrane potential, we analysed spontaneous activity of DMH neurons, studying both the frequency and the regularity of action potential generation. Despite higher membrane potential of cDMH cells, compared with other DMH divisions, there were no differences in the firing frequency between the three parts of the DMH (cDMH: 6.1 ± 3.1 Hz, vDMH: 5.5 ± 4.2 Hz, dDMH: 4.9 ± 3.9 Hz; $F_{2,135} = 1.53$, $P = 0.22$). This suggests that different ionic mechanisms guard neuronal excitability amongst the DMH divisions. More importantly though, we observed that both the time of day ($F_{1,135} = 4.67$, $P = 0.032$, effect size: $t = 2.16$, $P = 0.032$) and the diet ($F_{1,135} = 6.04$, $P = 0.015$, effect size: $t = 2.46$, $P = 0.015$) influence the firing rate in the DMH, as well as we noted an interaction between the LD cycle and the location within the DMH ($F_{2,135} = 4.33$, $P = 0.015$). Post hoc analysis revealed that day-night variability in the firing frequency was present in the cDMH (day: 3.9 ± 2.3 Hz, night: 6.4 ± 2.7 Hz; $t_{135} = -2.16$, $P = 0.03$) and vDMH (day: 2.9 ± 2.1 Hz, night: 8.3 ± 4.8 Hz; $t_{135} = -3.72$, $P = 0.0003$) under CD only, with lower neuronal activity recorded during the day, compared with behaviourally active night. Day-to-night variation in neuronal firing was abolished under HFD in both substructures (cDMH day: 7.0 ± 3.2 Hz, cDMH night: 7.6 ± 3.0 Hz; $t_{135} = -0.41$, $P = 0.68$, vDMH day: 4.8 ± 3.6 Hz, vDMH night: 7.2 ± 4.5 Hz; $t_{135} = -1.43$, $P = 0.16$). This effect was attributable to an abnormal increase in neuronal activity during the day (CD vs. HFD during daytime: $t_{135} = -2.46$, $P = 0.016$; Figure 2b,c, middle row), which was most notable for the cDMH.

Regularity of neuronal firing was measured as the coefficient of variation (Cv) of the interspike interval, therefore high values indicate low regularity in the action potential generation. Here, the analysis revealed a significant difference between the DMH divisions ($\log_{10}$(Cv): cDMH: -0.4 ± 0.2, vDMH: -0.6 ± 0.4, dDMH: -0.62 ± 0.3; $F_{2,128} = 4.41$, $P = 0.014$, effect size cDMH-dDMH: $t = -2.56$, $P = 0.012$), and an interaction between the time of day and the localisation in distinct DMH division (ANOVA: $F_{2,128} = 2.95$, $P = 0.056$; effect size: cDMH-vDMH: $t = -2.34$, $P = 0.021$). Therefore, both factors were contrasted in the multiple comparison analysis. This revealed that the day-night variation in regularity of firing only concerned the vDMH (day: -0.5 ± 0.3, night: -0.8 ± 0.3; $t_{128} = 3.4$, $P = 0.0009$), where neurons showed high Cv values during the day (irregular firing) and lower at night (increased regularity). This result may be explained by the fact that higher firing frequency often results in the increased regularity, as observed in the vDMH. Notwithstanding, we also observed differences in regularity amongst the three DMH divisions, despite very similar firing frequency. Namely, during the day neurons located within the vDMH showed higher Cv, similar to that observed in the cDMH regardless of the time of the day (cDMH - vDMH: $F_{128} = 0.28$, $P = 0.96$; cDMH - dDMH: $F_{128} = 2.62$, $P = 0.026$). However vDMH neurons decreased their Cv at night to the range of values observed within the dDMH (vDMH - dDMH: $F_{128} = 1.36$, $P = 0.36$; cDMH - vDMH: $F_{128} = 4.13$, $P = 0.0002$; Figure 2b,c, bottom row).

Altogether, these results suggest that the three DMH divisions display different electrical properties, mostly differentiating the cDMH from the other two. Additionally, they reveal that both the cDMH and vDMH show a day-to-night variation in the neuronal activity, which is abolished by HFD consumption.

3.2 | Excitability of DMH neurons

As the differences in firing frequency of DMH neurons between the day and night, as well as between the diets were shown not to be caused by the variation in the resting membrane potential, we hypothesised that they might be related to changes in the threshold for action potential generation. Therefore, we subjected the recorded cells to a depolarising current ramp and measured the voltage at which they elicit the first action potential. We also calculated the rheobase, defined as the amount of current required to cross that threshold (as done previously by Kania et al., 2020; Figure 3a).

Threshold analysis revealed an effect of the diet ($F_{1,130} = 5.49$, $P = 0.02$, effect size: $t = -2.34$, $P = 0.02$),

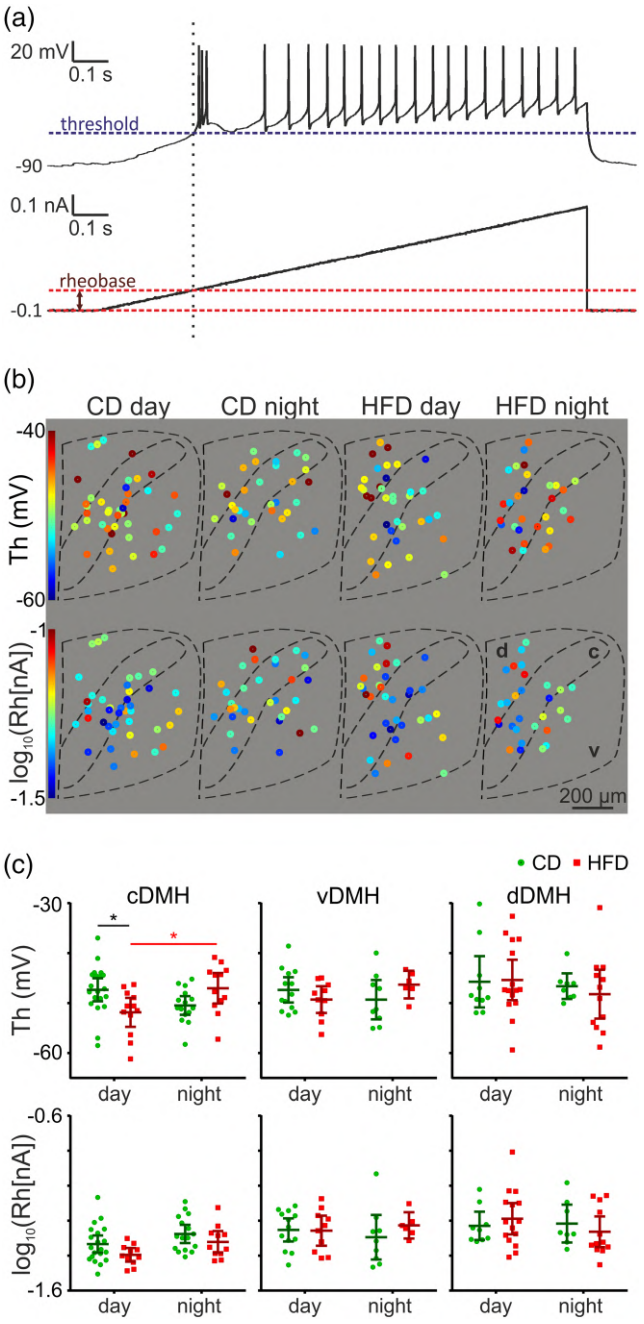

FIGURE 3 Depolarising current ramp. (a) A schematic explanation of the recorded parameters on a representative recording. (b) Heatmaps presenting spatial distribution of the recorded cells and their values of the recorded threshold (upper part) and rheobase (lower part) for the four groups of animals studied. The three divisions of the DMH are indicated as: c—compact, v—ventral, d—dorsal. (c) Analysis of threshold (Th; upper row) and rheobase (Rh; lower row) with the distinction of the three parts of the DMH. Data are presented as mean ± 95% CI. * $P < 0.05$. CD—control diet, HFD—high-fat diet.

an interaction between the diet and time of day ($F_{1,130} = 8.03$, $P = 0.0053$, effect size: $t = 2.83$, $P = 0.01$), and an interaction between all 3 factors ($F_{2,130} = 2.73$,

$P = 0.069$, effect size: $t = -2.32$, $P = 0.02$); therefore, we decided to contrast all groups in the post hoc analysis. Day-to-night differences where only observed in the HFD group in the cDMH ($t_{130} = -2.24$, $P = 0.027$), where the threshold was shown to be significantly decreased during the light phase (day: -51.9 ± 4.6 mV, night: -47.0 ± 4.8 mV). Indeed, neurons in this DMH division significantly differed between the diets during the day (CD day: -47.4 ± 4.9 mV; $t_{130} = 2.34$, $P = 0.02$; Figure 3b,c, upper part). Thus, lowered action potential generation threshold in the cDMH by HFD is most likely to underlay its increased neuronal activity during the behaviourally inactive phase.

Rheobase was shown to vary exclusively between the three divisions of the DMH ($\log_{10}$Rh: cDMH: -1.3 ± 0.1 nA, vDMH: -1.22 ± 0.1 nA, dDMH: -1.26 ± 0.1 nA; $F_{2,128} = 3.21$, $P = 0.044$, effect size: cDMH-dDMH: $t = 2.21$, $P = 0.029$, cDMH-vDMH: $t = 1.94$, $P = 0.055$), with cDMH being significantly more excitable than either the dDMH ($t_{128} = -4.41$, $P = 0.0001$) or vDMH ($t_{128} = -2.9$, $P = 0.012$; Figure 3b, c, lower part). No differences were observed between the dDMH and vDMH ($t_{128} = 1.23$, $P = 0.44$).

These results provide an insight into possible mechanism of the disrupted daily changes in the DMH neuronal activity by HFD—namely, a decreased threshold for action potential generation during the day, resulting in increased daytime firing. Lower rheobase recorded in the cDMH indicates generally higher excitability of these cells, compared with the other subdivisions of the DMH.

3.3 | Current–voltage relationship

In order to study the dependency of the current flowing through the cellular membrane at different membrane potentials, we performed a set of voltage steps, long enough to study steady state current.

In the cDMH, we observed a day-to-night difference in the magnitude of both inward and outward current, flowing at highly hyperpolarised (below -115 mV) and depolarised (-15 mV and above 5 mV; please see Table S2 for details) potentials, respectively. Current magnitude at night was significantly higher than during the day, which was true for both dietary groups. No interaction between the factors were present at any command voltage (Figure 4a, left column).

On the contrary, in the vDMH, only the outward current at highly depolarising steps was affected, but by both diet and time of day. Neurons obtained from rats fed CD displayed a clear day-to-night variation, with a higher current magnitude during the day than at night. Spectacularly, this effect completely disappeared under HFD. This was reflected in the magnitude of current in the HFD group being as high as in CD during daytime regardless of the light phase (Figure 4a, middle column).

No daily changes were observed in the dDMH, neither did the diet affect the magnitude of the current flowing at any recorded potential (Figure 4a, right column).

Following, we calculated membrane resistance as the difference in the applied voltage divided by change in the flowing current from the -115 mV step. We found that membrane resistance was significantly different amongst the three subdivisions of the DMH ($\log_{10}$R: cDMH: 3 ± 0.2 MΩ, vDMH: 2.8 ± 0.2 MΩ, dDMH: 2.8 ± 0.2 MΩ; $F_{2,128} = 3.10$, $P = 0.048$, effect size: cDMH-dDMH: $t = -2.27$, $P = 0.025$, cDMH-vDMH: $t = 1.85$, $P = 0.067$). Similarly to the other parameters measured, the cDMH was shown to stand out with significantly higher resistance compared with the other two part of the DMH (cDMH vs. dDMH: $t_{128} = 3.82$, $P = 0.0006$; cDMH vs. vDMH: $F_{128} = 3.02$, $P = 0.0086$; Figure 4b,c).

Therefore, both the cDMH and vDMH were shown to display daily variability in the magnitude of net current increasing with the distance from the reversal potential. The IV relationship was not affected by HFD in the cDMH nor dDMH; however, in the vDMH, the daily variation of current magnitude was disrupted by HFD consumption. Amongst the DMH subdivisions, the membrane resistance was highest in cDMH neurons, in line with their decreased rheobase.

4 | DISCUSSION

In the presented article, we demonstrate a thorough analysis of various electrophysiological properties of neurons localised in the DMH. We first collated cells recorded within the cDMH, and compared them to the other two divisions located ventrally and dorsally. Neurons recorded in the cDMH varied significantly from these found in the other DMH divisions in parameters, such as the resting membrane potential, input resistance, (all higher in the cDMH), firing regularity and rheobase (lower in the cDMH). We also observed a night-time elevation of the neuronal activity within both the cDMH and vDMH, which diminished under HFD. Abnormally heightened daytime firing in the HFD-fed group is most likely attributed to a decreased threshold for action potential generation during the light phase.

Up until now, only one study has focused on the electrophysiology of DMH neurons (Bailey et al., 2003). However, many of the conclusions presented by authors are contrary to ours. In their paper, Bailey and colleagues compared DMH neurons projecting to the paraventricular nucleus of the hypothalamus to these without

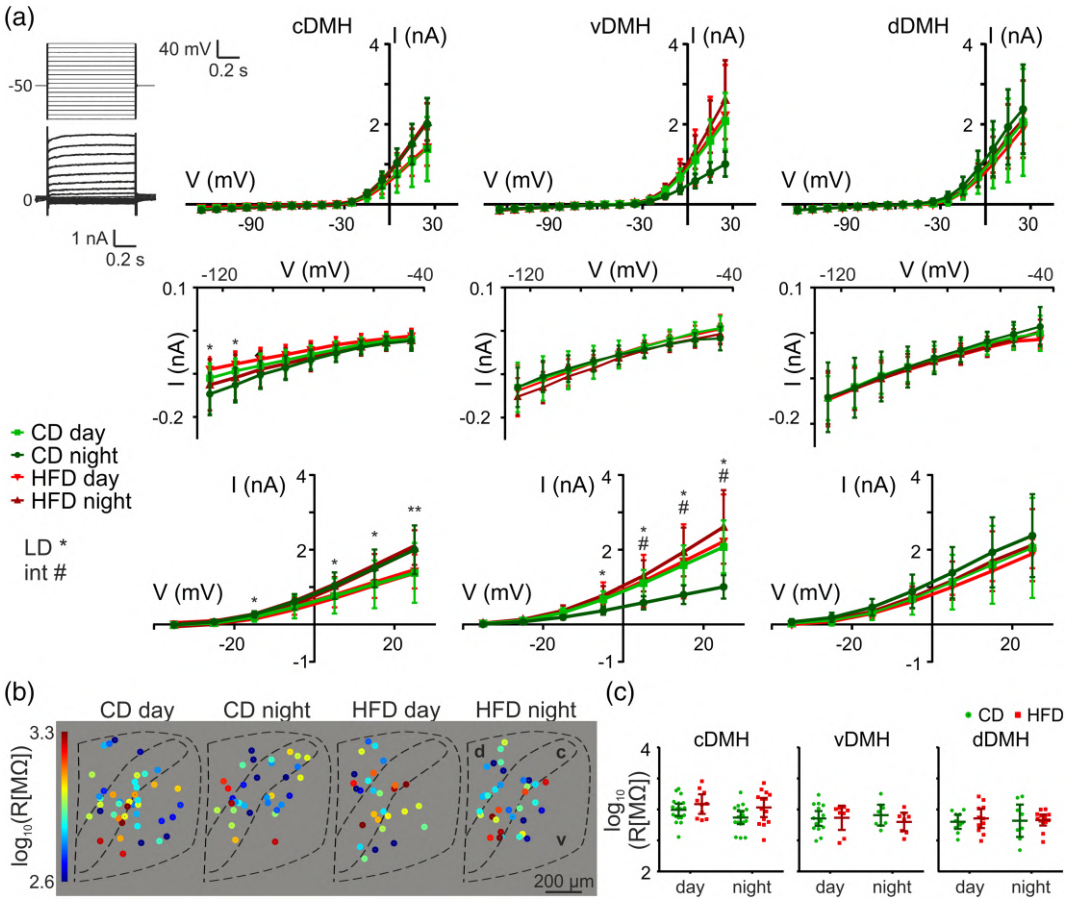

FIGURE 4 Current–voltage (IV) relationship. (a) Representative recording of the voltage steps protocol, followed by the IV curves, presented separately for each division of the dorsomedial hypothalamus (DMH; top row). Middle and bottom rows contain zoomed in views of the left and right part of the curve, respectively. *$P < 0.05$, **$P < 0.01$, significance of the time-of-day factor (LD); # $P < 0.05$, significance of the interaction between diet and LD factors. (b) Heatmaps presenting spatial distribution of the recorded cells and their values of the recorded membrane resistance (R) for the four groups of animals studied. The three divisions of the DMH are indicated as: c—compact, v—ventral, d—dorsal. (c) Analysis of the membrane resistance with the distinction of the three parts of the DMH. Data are presented as mean ± 95% CI. CD—control diet, HFD—high-fat diet.

such projection, which were shown to differ in the excitability. Overall however, that study has proposed that DMH neurons form a very homogenous population in general.

We believe the differences between our results and others may stem from a different experimental setup and analysis methods. Bailey et al. have not separated the recorded DMH neurons into the three divisions; therefore, there is a possibility of oversampling from one of the distinct groups. Additionally, authors have not reported highly depolarized cells (only neurons more hyperpolarized than −50 mV were analysed), whereas our study found the depolarised (but healthy) neurons to be numerous in the DMH. This may provide an additional explanation on why other parameters have been shown not to vary amongst individual cells.

As we included all viable DMH neurons in our analysis, we were able to observe a subpopulation of cells exhibiting DLAMO-like events. This form of activity has been previously reported in the SCN in healthy and functioning neurons (Belle et al., 2009; Belle & Piggins, 2017; Diekman et al., 2013) and characterised in detail with aids of mathematical modelling and pharmacology (i.e., calcium high-voltage activated current blockers). The L-type calcium current specifically was shown to be essential for the propagation of such activity. Resemblance of the neurons recorded by us and those observed in the SCN suggests that a similar mechanism might govern this phenomenon in the DMH. High dependency of our DLAMO-like events on strong membrane depolarisation and their distinctive kinetics indeed point to calcium currents activated at high potentials. However, future pharmacological studies are needed to unravel if specifically the L-type calcium current similarly underlies these DLAMO events in the DMH.

Interestingly, the SCN neurons expressing DLAMOs were observed only during the late day and all of them were classified as clock cells (due to expression of a core clock gene *Per1*; Belle et al., 2009). Together, these strongly imply the dependency of DLAMO on the circadian clock. As the main regulator of circadian rhythms, the SCN generates strong rhythms in both clock gene expression and neuronal membrane potential, influencing the electrical activity. In our study, cells expressing DLAMO were not restricted to any particular time of day, but neither did DMH neurons change their membrane potential between day and night, even though they were firing more action potentials during the night. This observation strengthens the hypothesis, that DLAMO generation is strongly dependent on membrane potential per se, rather than levels of firing rate and excitability.

Apart from the L-type calcium current, other ionic currents driving the day/night changes in the activity of SCN neurons include sodium and potassium leak currents (Belle et al., 2009; Diekman et al., 2013). Even though we have not investigated any specific type of current in our experiment, we believe this might be a major difference between the SCN and DMH. Changes in the magnitude of any leak current should result in a modulation of the resting membrane potential, which could explain the day/night changes in the firing frequency of the SCN neurons, where such a rhythm in membrane potential exists. However, in the DMH, the mechanism responsible for day/night changes in firing activity is more likely due to the changing threshold for action potential generation.

Even though the SCN is considered the master or central circadian clock, many more autonomous or semi-autonomous circadian oscillators are being found in the brain, ranging from the olfactory bulbs (Abe et al., 2002; Granados-Fuentes et al., 2006) through some areas of the cerebral cortex (Prolo et al., 2005), the hippocampus (Wang et al., 2009), parts of the thalamus (Chrobok, Pradel, et al., 2021), hypothalamus (Abe et al., 2002; Guilding et al., 2009), and midbrain (Chrobok, Jeczmien-Lazur, et al., 2021), all the way to the brainstem (Chrobok et al., 2020), and the cerebellum (Rath et al., 2012), including even circumventricular organs (Chrobok et al., 2020; Myung et al., 2018; Northeast et al., 2020). Circadian food intake regulation and entrainment to different feeding schedules have been shown to be independent of the SCN, but controlled by a network of brain structures regarded to as FEO, with the DMH considered to play and important role as one of the proposed main FEO centres. As such, the DMH has been shown to be a weak circadian oscillator in ad libitum fed animals (Guilding et al., 2009) but become much stronger under any form of restricted feeding (Mieda et al., 2006; Minana-Solis et al., 2009; Verwey et al., 2007, 2008). Here, we confirm that even in ad libitum fed animals, the DMH expresses daily changes in the electrical activity. Neurons located in both the cDMH and vDMH fire at a lower frequency during the day, which is the behaviourally quiescent phase for rats, and with a higher rate during the metabolically active night. In the vDMH, this was also accompanied by changes in the regularity of action potential generation, with more active cells recorded at nighttime firing more regularly. Previous data has indicated, that it is mostly the cDMH that displays rhythmic changes in clock gene expression and electrical activity (Guilding et al., 2009). Surprisingly, in our study the daily changes in the firing frequency as well as current–voltage dependencies were even more explicit for the vDMH, which may be related to its involvement in the circadian regulation of food intake. Having observed the strongest cFOS response to satiety in this part of the DMH (our unpublished data, as well as Poulin & Timofeeva, 2008; Renner et al., 2012), we suggest that robust daily changes in the vDMH neuronal activity reflect rats' daily feeding pattern.

Bidirectional relationship between dysregulated circadian feeding pattern and obesity has been shown both in humans as well as in animal models (Chaix et al., 2014; Chrobok, Klich, Jeczmien-Lazur, et al., 2022; Hatori et al., 2012; Kohsaka et al., 2007). Overweight and obese people more often report sleep disturbances such as insomnia (Pearson et al., 2006; Vgontzas et al., 1994) and obstructive sleep apnoea (Ong et al., 2013). On the other hand, shift work-related lack of feeding regularity has been acknowledged as a high risk factor for obesity and related health issues (Di Lorenzo et al., 2003; Kubo et al., 2011; for an extensive review, please see Antunes et al., 2010). As an important part of the FEO and highly responsive to the regularity of food intake, the DMH is a primary candidate for being responsible for the disruption of feeding pattern, leading to obesity in HFD fed animals.

Presented data show that HFD consumption influences neuronal activity in the DMH. Whilst the DMH neurons in rats fed CD displayed a clear daily variation in the firing frequency, it was completely abolished under HFD. During the behaviourally and metabolically inactive daytime, when neuronal activity in the DMH is also normally low, HFD caused an increase in the frequency of neuronal firing. Here, we propose the decrease in the threshold for action potential generation as a potential mechanism of these changes, which was also observed during the same time of day, especially in the

cDMH. It is important to emphasise that even small changes in the firing threshold, due to an all-or-nothing nature of action potential generation, will influence the number of spontaneously firing cells as well as their firing frequency.

The DMH has been classically regarded as an orexigenic centre, as its lesions decrease food intake (Bellinger, 1987; Bernardis, 1970), therefore its increased activity during daytime under HFD might be a stimulator of food intake during this inactive phase. Indeed, we have previously reported, that animals fed with HFD show disrupted circadian feeding pattern, manifested as an enhanced food intake during the day (Chrobok, Klich, Jeczmien-Lazur, et al., 2022).

Importantly, these effects of HFD consumption are present before the onset of obesity, which clarifies that they are not a consequence of it, but a possible mechanism for its development. Here we propose, that HFD dysregulates daily changes in firing frequency of the DMH neurons resulting in the increased activity during the day, which stimulates daytime feeding. Disrupted feeding schedule conduces to the development of obesity (Antunes et al., 2010).

Collectively, the data presented here, as well as our other published results from the studies on the nucleus of the solitary tract as a whole (Chrobok, Klich, Sanetra, et al., 2022), and its output structure separately (the dorsal motor nucleus of the vagus, Chrobok, Klich, Jeczmien-Lazur, et al., 2022) indicate, that HFD changes the physiological functioning and day/night rhythms of brain structures. Even small changes in the brain structures' activity might potently affect animals feeding behaviour, and therefore increase the risk of developing obesity.

Overall, our results indicate changes in the functioning of the DMH neurons under short-term HFD, which broaden our understanding of mechanisms responsible for the development of obesity. Presented data highlight the importance of the circadian rhythms, both behavioural and at the level of the neuronal activity, with their disruptions mediating the deleterious effects of HFD.

5 | CONCLUSION

This is the first paper to investigate electrophysiological characteristics of DMH neurons with a separation into three anatomically and functionally distinct divisions, shown to differ in electrophysiological parameters, such as resting membrane potential, regularity, membrane resistance, and rheobase. Moreover, we propose a novel mechanism for the development of obesity under HFD via the DMH-dependent increase in daytime feeding.

ACKNOWLEDGEMENTS

We would like to thank Kamil Pradel for providing a MATLAB script for heatmap production. We would also like to thank Patrycjusz Nowik for excellent animal care.

CONFLICTS OF INTEREST

The authors declare no conflict of interest.

AUTHOR CONTRIBUTIONS

AMS and KPCH conceived the study. AMS performed electrophysiological recordings. AMS and LCh analysed and interpreted the data. MHL received the funding and supervised the study. AMS wrote the manuscript and all authors agreed to its final form.

PEER REVIEW

The peer review history for this article is available at https://publons.com/publon/10.1111/ejn.15759.

DATA AVAILABILITY STATEMENT

All data are available from the corresponding author upon reasonable request.

ORCID

Anna Magdalena Sanetra https://orcid.org/0000-0002-3070-4688
Katarzyna Palus-Chramiec https://orcid.org/0000-0002-9870-334X
Lukasz Chrobok https://orcid.org/0000-0002-0118-2833
Marian Henryk Lewandowski https://orcid.org/0000-0003-1461-9392

REFERENCES

Abe, M., Herzog, E. D., Yamazaki, S., Straume, M., Tei, H., Sakaki, Y., Menaker, M., & Block, G. D. (2002). Circadian rhythms in isolated brain regions. *Journal of Neuroscience*, *22*(1), 350–356. https://doi.org/10.1523/JNEUROSCI.22-01-00350.2002

Acosta-Galvan, G., Yi, C. X., van der Vliet, J., Jhamandas, J. H., Panula, P., Angeles-Castellanos, M., Basualdo, M. D. C., Escobar, C., & Buijs, R. M. (2011). Interaction between hypothalamic dorsomedial nucleus and the suprachiasmatic nucleus determines intensity of food anticipatory behavior. *Proceedings of the National Academy of Sciences*, *108*(14), 5813–5818. https://doi.org/10.1073/pnas.1015551108

Antunes, L. C., Levandovski, R., Dantas, G., Caumo, W., & Hidalgo, M. P. (2010). Obesity and shift work: Chronobiological aspects. *Nutrition Research Reviews*, *23*(1), 155–168. https://doi.org/10.1017/S0954422410000016

Avila, C., Holloway, A. C., Hahn, M. K., Morrison, K. M., Restivo, M., Anglin, R., & Taylor, V. H. (2015). An overview of links between obesity and mental health. *Current Obesity*

Reports, *4*(3), 303–310. https://doi.org/10.1007/s13679-015-0164-9

Bailey, T. W., Nicol, G. D., Schild, J. H., & DiMicco, J. A. (2003). Synaptic and membrane properties of neurons in the dorsomedial hypothalamus. *Brain Research*, *985*(2), 150–162. https://doi.org/10.1016/S0006-8993(03)03047-6

Belle, M. D., Diekman, C. O., Forger, D. B., & Piggins, H. D. (2009). Daily electrical silencing in the mammalian circadian clock. *Science*, *326*(5950), 281–284. https://doi.org/10.1126/science.1169657

Belle, M. D., & Piggins, H. D. (2017). Circadian regulation of mouse suprachiasmatic nuclei neuronal states shapes responses to orexin. *European Journal of Neuroscience*, *45*(5), 723–732. https://doi.org/10.1111/ejn.13506

Bellinger, L. L. (1987). Ingestive behavior of rats with ibotenic acid lesions of the dorsomedial hypothalamus. *American Journal of Physiology. Regulatory, Integrative and Comparative Physiology*, *252*(5), R938–R946. https://doi.org/10.1152/ajpregu.1987.252.5.R938

Bernardis, L. L. (1970). Participation of the dorsomedial hypothalamic nucleus in the "feeding center" and water intake circuitry of the weanling rat. *Journal of Neuro-Visceral Relations*, *31*(4), 387–398. https://doi.org/10.1007/BF02312740

Calle, E. E., Rodriguez, C., Walker-Thurmond, K., & Thun, M. J. (2003). Overweight, obesity, and mortality from cancer in a prospectively studied cohort of US adults. *New England Journal of Medicine*, *348*(17), 1625–1638. https://doi.org/10.1056/NEJMoa021423

Cano, G., Passerin, A. M., Schiltz, J. C., Card, J. P., Morrison, S. F., & Sved, A. F. (2003). Anatomical substrates for the central control of sympathetic outflow to interscapular adipose tissue during cold exposure. *Journal of Comparative Neurology*, *460*(3), 303–326. https://doi.org/10.1002/cne.10643

Chaar, L. J., Coelho, A., Silva, N. M., Festuccia, W. L., & Antunes, V. R. (2016). High-fat diet-induced hypertension and autonomic imbalance are associated with an upregulation of CART in the dorsomedial hypothalamus of mice. *Physiological Reports*, *4*(11), e12811. https://doi.org/10.14814/phy2.12811

Chaix, A., Zarrinpar, A., Miu, P., & Panda, S. (2014). Time-restricted feeding is a preventative and therapeutic intervention against diverse nutritional challenges. *Cell Metabolism*, *20*(6), 991–1005. https://doi.org/10.1016/j.cmet.2014.11.001

Chou, T. C., Scammell, T. E., Gooley, J. J., Gaus, S. E., Saper, C. B., & Lu, J. (2003). Critical role of dorsomedial hypothalamic nucleus in a wide range of behavioral circadian rhythms. *Journal of Neuroscience*, *23*(33), 10691–10702. https://doi.org/10.1523/JNEUROSCI.23-33-10691.2003

Chrobok, L., Jeczmien-Lazur, J. S., Bubka, M., Pradel, K., Klekocinska, A., Klich, J. D., Rahim, A. R., Myung, J., Kepczynski, M., & Lewandowski, M. H. (2021). Daily coordination of orexinergic gating in the rat superior colliculus—Implications for intrinsic clock activities in the visual system. *The FASEB Journal*, *35*(10), e21930. https://doi.org/10.1096/fj.202100779RR

Chrobok, L., Klich, J. D., Jeczmien-Lazur, J. S., Pradel, K., Palus-Chramiec, K., Sanetra, A. M., Piggins, H. D., & Lewandowski, M. H. (2022). Daily changes in neuronal activities of the dorsal motor nucleus of the vagus under standard and high-fat diet. *The Journal of Physiology*, *600*(4), 733–749. https://doi.org/10.1113/JP281596

Chrobok, L., Klich, J. D., Sanetra, A. M., Jeczmien-Lazur, J. S., Pradel, K., Palus-Chramiec, K., Kepczynski, M., Piggins, H. D., & Lewandowski, M. H. (2022). Rhythmic neuronal activities of the rat nucleus of the solitary tract are impaired by high-fat diet–implications for daily control of satiety. *The Journal of Physiology*, *600*(4), 751–767. https://doi.org/10.1113/JP281838

Chrobok, L., Northeast, R. C., Myung, J., Cunningham, P. S., Petit, C., & Piggins, H. D. (2020). Timekeeping in the hindbrain: A multi-oscillatory circadian centre in the mouse dorsal vagal complex. *Communications Biology*, *3*(1), 1–12. https://doi.org/10.1038/s42003-020-0960-y

Chrobok, L., Pradel, K., Janik, M. E., Sanetra, A. M., Bubka, M., Myung, J., Rahim, A. R., Klich, J. D., Jeczmien-Lazur, J. S., Palus-Chramiec, K., & Lewandowski, M. H. (2021). Intrinsic circadian timekeeping properties of the thalamic lateral geniculate nucleus. *Journal of Neuroscience Research*, *99*(12), 3306–3324. https://doi.org/10.1002/jnr.24973

Di Lorenzo, L., De Pergola, G., Zocchetti, C., L'Abbate, N., Basso, A., Pannacciulli, N., Cignarelli, M., Giorgino, R., Soleo, L., & Soleo, L. (2003). Effect of shift work on body mass index: Results of a study performed in 319 glucose-tolerant men working in a Southern Italian industry. *International Journal of Obesity*, *27*(11), 1353–1358. https://doi.org/10.1038/sj.ijo.0802419

Diekman, C. O., Belle, M. D., Irwin, R. P., Allen, C. N., Piggins, H. D., & Forger, D. B. (2013). Causes and consequences of hyperexcitation in central clock neurons. *PLoS Computational Biology*, *9*(8), e1003196. https://doi.org/10.1371/journal.pcbi.1003196

DiMicco, J. A., & Zaretsky, D. V. (2007). The dorsomedial hypothalamus: A new player in thermoregulation. *American Journal of Physiology. Regulatory, Integrative and Comparative Physiology*, *292*(1), R47–R63. https://doi.org/10.1152/ajpregu.00498.2006

Fontes, M. A. P., Tagawa, T., Polson, J. W., Cavanagh, S. J., & Dampney, R. A. L. (2001). Descending pathways mediating cardiovascular response from dorsomedial hypothalamic nucleus. *American Journal of Physiology. Heart and Circulatory Physiology*, *280*(6), H2891–H2901. https://doi.org/10.1152/ajpheart.2001.280.6.H2891

Fox, J., & Weisberg, S. (2019). *An R companion to applied regression*. Sage Publications. https://socialsciences.mcmaster.ca/jfox/Books/Companion/

Granados-Fuentes, D., Tseng, A., & Herzog, E. D. (2006). A circadian clock in the olfactory bulb controls olfactory responsivity. *Journal of Neuroscience*, *26*(47), 12219–12225. https://doi.org/10.1523/JNEUROSCI.3445-06.2006

Guilding, C., Hughes, A. T., Brown, T. M., Namvar, S., & Piggins, H. D. (2009). A riot of rhythms: Neuronal and glial circadian oscillators in the mediobasal hypothalamus. *Molecular Brain*, *2*(1), 1–19. https://doi.org/10.1186/1756-6606-228

Hatori, M., Vollmers, C., Zarrinpar, A., DiTacchio, L., Bushong, E. A., Gill, S., Leblanc, M., Chaix, A., Joens, M., Fitzpatrick, J. A. J., Ellisman, M. H., & Panda, S. (2012). Time-restricted feeding without reducing caloric intake prevents metabolic diseases in mice fed a high-fat diet. *Cell Metabolism*, *15*(6), 848–860. https://doi.org/10.1016/j.cmet.2012.04.019

Kania, A., Sambak, P., Gugula, A., Szlaga, A., Soltys, Z., Blasiak, T., Hess, G., Rajfur, Z., & Blasiak, A. (2020). Electrophysiology and distribution of oxytocin and vasopressin neurons in the hypothalamic paraventricular nucleus: A study in male and female rats. *Brain Structure and Function*, *225*(1), 285–304. https://doi.org/10.1007/s00429-019-01989-4

Kassambara, A. (2020). ggpubr: 'ggplot2' Based Publication Ready Plots. R Package Version 0.4.0. https://CRAN.R-project.org/package=ggpubr

Kassambara, A. (2021). rstatix: Pipe-Friendly Framework for Basic Statistical Tests. R Package Version 0.7.0 https://CRAN.Rproject.org/package=rstatix

Kenchaiah, S., Evans, J. C., Levy, D., Wilson, P. W., Benjamin, E. J., Larson, M. G., Larson, M. G., Kannel, W. B., & Vasan, R. S. (2002). Obesity and the risk of heart failure. *New England Journal of Medicine*, *347*(5), 305–313. https://doi.org/10.1056/NEJMoa020245

Kohsaka, A., Laposky, A. D., Ramsey, K. M., Estrada, C., Joshu, C., Kobayashi, Y., Turek, F. W., & Bass, J. (2007). High-fat diet disrupts behavioral and molecular circadian rhythms in mice. *Cell Metabolism*, *6*(5), 414–421. https://doi.org/10.1016/j.cmet.2007.09.006

Kono, Y., Yokota, S., Fukushi, I., Arima, Y., Onimaru, H., Okazaki, S., Takeda, K., Yazawa, I., Yoshizawa, M., Hasebe, Y., Koizumi, K., Pokorski, M., Toda, T., Sugita, K., & Okada, Y. (2020). Structural and functional connectivity from the dorsomedial hypothalamus to the ventral medulla as a chronological amplifier of sympathetic outflow. *Scientific Reports*, *10*(1), 1–11. https://doi.org/10.1038/s41598-020-70234-4

Kubo, T., Oyama, I., Nakamura, T., Shirane, K., Otsuka, H., Kunimoto, M., Kadowaki, K., Maruyama, T., Otomo, H., Fujino, Y., Matsumoto, T., & Matsuda, S. (2011). Retrospective cohort study of the risk of obesity among shift workers: Findings from the industry-based shift workers' health study Japan. *Occupational and Environmental Medicine*, *68*(5), 327–331. https://doi.org/10.1136/oem.2009.054445

Lakka, T. A., Lakka, H. M., Salonen, R., Kaplan, G. A., & Salonen, J. T. (2001). Abdominal obesity is associated with accelerated progression of carotid atherosclerosis in men. *Atherosclerosis*, *154*(2), 497–504. https://doi.org/10.1016/S0021-9150(00)00514-1

Length, R. V. (2021). emmeans: Estimated Marginal Means, aka Least-Squares Means. R package version 1.5.5-1. https://CRAN.Rproject.org/package=emmeans

Mieda, M., Williams, S. C., Richardson, J. A., Tanaka, K., & Yanagisawa, M. (2006). The dorsomedial hypothalamic nucleus as a putative food-entrainable circadian pacemaker. *Proceedings of the National Academy of Sciences*, *103*(32), 12150–12155. https://doi.org/10.1073/pnas.0604189103

Minana-Solis, M. C., Angeles-Castellanos, M., Feillet, C., Pevet, P., Challet, E., & Escobar, C. (2009). Differential effects of a restricted feeding schedule on clock-gene expression in the hypothalamus of the rat. *Chronobiology International*, *26*(5), 808–820. https://doi.org/10.1080/07420520903044240

Myung, J., Schmal, C., Hong, S., Tsukizawa, Y., Rose, P., Zhang, Y., Holtzman, M. J., Schutter, E. D., Herzel, H., Bordyugov, G., & Takumi, T. (2018). The choroid plexus is an important circadian clock component. *Nature Communications*, *9*(1), 1–13. https://doi.org/10.1038/s41467-018-03507-2

Northeast, R. C., Chrobok, L., Hughes, A. T., Petit, C., & Piggins, H. D. (2020). Keeping time in the lamina terminalis: Novel oscillator properties of forebrain sensory circumventricular organs. *The FASEB Journal*, *34*(1), 974–987. https://doi.org/10.1096/fj.201901111R

Ong, C. W., O'Driscoll, D. M., Truby, H., Naughton, M. T., & Hamilton, G. S. (2013). The reciprocal interaction between obesity and obstructive sleep apnoea. *Sleep Medicine Reviews*, *17*(2), 123–131. https://doi.org/10.1016/j.smrv.2012.05.002

Paxinos, G., & Watson, C. (2007). *The rat brain in stereotaxic coordinates*. Academic Press.

Pearson, N. J., Johnson, L. L., & Nahin, R. L. (2006). Insomnia, trouble sleeping, and complementary and alternative medicine: Analysis of the 2002 national health interview survey data. *Archives of Internal Medicine*, *166*(16), 1775–1782. https://doi.org/10.1001/archinte.166.16.1775

Pinheiro, J., Bates, D., DebRoy, S., Sarkar, D., R Core Team (2021). nlme: Linear and Nonlinear Mixed Effects Models. R package version 3.1-152, https://CRAN.R-project.org/package=nlme

Poulin, A. M., & Timofeeva, E. (2008). The dynamics of neuronal activation during food anticipation and feeding in the brain of food-entrained rats. *Brain Research*, *1227*, 128–141. https://doi.org/10.1016/j.brainres.2008.06.039

Prolo, L. M., Takahashi, J. S., & Herzog, E. D. (2005). Circadian rhythm generation and entrainment in astrocytes. *Journal of Neuroscience*, *25*(2), 404–408. https://doi.org/10.1523/JNEUROSCI.4133-04.2005

Rath, M. F., Rohde, K., & Møller, M. (2012). Circadian oscillations of molecular clock components in the cerebellar cortex of the rat. *Chronobiology International*, *29*(10), 1289–1299. https://doi.org/10.3109/07420528.2012.728660

Renner, E., Puskas, N., Dobolyi, A., & Palkovits, M. (2012). Glucagon-like peptide-1 of brainstem origin activates dorsomedial hypothalamic neurons in satiated rats. *Peptides*, *35*(1), 14–22. https://doi.org/10.1016/j.peptides.2012.02.018

Samuels, B. C., Zaretsky, D. V., & DiMicco, J. A. (2004). Dorsomedial hypothalamic sites where disinhibition evokes tachycardia correlate with location of raphe-projecting neurons. *American Journal of Physiology. Regulatory, Integrative and Comparative Physiology*, *287*(2), R472–R478. https://doi.org/10.1152/ajpregu.00667.2003

Team, R. (2019). *RStudio: Integrated Development for R*. RStudio, Inc.. http://www.rstudio.com/

Team RC. (2021). *R: A language and environment for statistical computing*. R Foundation for Statistical Computing. https://www.Rproject.org/

Unger, T. J., Calderon, G. A., Bradley, L. C., Sena-Esteves, M., & Rios, M. (2007). Selective deletion of Bdnf in the ventromedial and dorsomedial hypothalamus of adult mice results in hyperphagic behavior and obesity. *Journal of Neuroscience*, *27*(52), 14265–14274. https://doi.org/10.1523/JNEUROSCI.3308-07.2007

Verwey, M., Khoja, Z., Stewart, J., & Amir, S. (2007). Differential regulation of the expression of Period2 protein in the limbic forebrain and dorsomedial hypothalamus by daily limited access to highly palatable food in food-deprived and free-fed

rats. *Neuroscience*, *147*(2), 277–285. https://doi.org/10.1016/j.neuroscience.2007.04.044

Verwey, M., Khoja, Z., Stewart, J., & Amir, S. (2008). Region-specific modulation of PER2 expression in the limbic forebrain and hypothalamus by nighttime restricted feeding in rats. *Neuroscience Letters*, *440*(1), 54–58. https://doi.org/10.1016/j.neulet.2008.05.043

Vgontzas, A. N., Tan, T. L., Bixler, E. O., Martin, L. F., Shubert, D., & Kales, A. (1994). Sleep apnea and sleep disruption in obese patients. *Archives of Internal Medicine*, *154*(15), 1705–1711. https://doi.org/10.1001/archinte.1994.00420150073007

Wang, L. M., Dragich, J. M., Kudo, T., Odom, I. H., Welsh, D. K., O'Dell, T. J., & Colwell, C. S. (2009). Expression of the circadian clock gene Period2 in the hippocampus: Possible implications for synaptic plasticity and learned behaviour. *ASN Neuro*, *1*(3), AN20090020. https://doi.org/10.1042/AN20090020

Wilson, E. A., Sun, H., Cui, Z., Jahnke, M. T., Pandey, M., Metzger, P., Gavrilova, O., Chen, M., Weinstein, L. S., & Weinstein, L. S. (2021). Gqα/G11α deficiency in dorsomedial hypothalamus leads to obesity resulting from decreased energy expenditure and impaired sympathetic nerve activity. *American Journal of Physiology. Endocrinology and Metabolism*, *320*(2), E270–E280. https://doi.org/10.1152/ajpendo.00059.2020

Young, E. D., Robert, J. M., & Shofner, W. P. (1988). Regularity and latency of units in ventral cochlear nucleus: Implications for unit classification and generation of response properties. *Journal of Neurophysiology*, *60*(1), 1–29. https://doi.org/10.1152/jn.1988.60.1.1

Zhang, C., Barkholt, P., Nielsen, J. C., Thorbek, D. D., Rigbolt, K., Vrang, N., Woldbye, D. P. D., & Jelsing, J. (2020). The dorsomedial hypothalamus and nucleus of the solitary tract as key regulators in a rat model of chronic obesity. *Brain Research*, *1727*, 146538. https://doi.org/10.1016/j.brainres.2019.146538

SUPPORTING INFORMATION

Additional supporting information can be found online in the Supporting Information section at the end of this article.

How to cite this article: Sanetra, A. M., Palus-Chramiec, K., Chrobok, L., & Lewandowski, M. H. (2022). Electrophysiological complexity in the rat dorsomedial hypothalamus and its susceptibility to daily rhythms and high-fat diet. *European Journal of Neuroscience*, *56*(4), 4363–4377. https://doi.org/10.1111/ejn.15759

3.2. **Publication 2**: *High-Fat-Diet-Evoked Disruption of the Rat Dorsomedial Hypothalamic Clock Can Be Prevented by Restricted Nighttime Feeding*

2022, Nutrients, 14(23), 5034

nutrients

MDPI

Article

High-Fat-Diet-Evoked Disruption of the Rat Dorsomedial Hypothalamic Clock Can Be Prevented by Restricted Nighttime Feeding

Anna Magdalena Sanetra [1,*], Katarzyna Palus-Chramiec [1], Lukasz Chrobok [1,2], Jagoda Stanislawa Jeczmien-Lazur [1], Emilia Gawron [1], Jasmin Daniela Klich [1,3], Kamil Pradel [1] and Marian Henryk Lewandowski [1,*]

1 Department of Neurophysiology and Chronobiology, Institute of Zoology and Biomedical Research, Jagiellonian University in Krakow, Gronostajowa Street 9, 30-387 Krakow, Poland
2 School of Physiology, Pharmacology, and Neuroscience, University of Bristol, University Walk, Biomedical Sciences Building, Bristol BS8 1TD, UK
3 Max-Delbrück-Center for Molecular Medicine in the Helmholtz Association (MDC), Robert-Rössle-Str. 10, 13125 Berlin, Germany
* Correspondence: anna.sanetra@doctoral.uj.edu.pl (A.M.S.); marian.lewandowski@uj.edu.pl (M.H.L.); Tel.: +48-12-664-53-56 (A.M.S.); +48-12-664-53-73 (M.H.L.)

Abstract: Obesity is a growing health problem for modern society; therefore, it has become extremely important to study not only its negative implications but also its developmental mechanism. Its links to disrupted circadian rhythmicity are indisputable but are still not well studied on the cellular level. Circadian food intake and metabolism are controlled by a set of brain structures referred to as the food-entrainable oscillator, among which the dorsomedial hypothalamus (DMH) seems to be especially heavily affected by diet-induced obesity. In this study, we evaluated the effects of a short-term high-fat diet (HFD) on the physiology of the male rat DMH, with special attention to its day/night changes. Using immunofluorescence and electrophysiology we found that both cFos immunoreactivity and electrical activity rhythms become disrupted after as few as 4 weeks of HFD consumption, so before the onset of excessive weight gain. This indicates that the DMH impairment is a possible factor in obesity development. The DMH cellular activity under an HFD became increased during the non-active daytime, which coincides with a disrupted rhythm in food intake. In order to explore the relationship between them, a separate group of rats underwent time-restricted feeding with access to food only during the nighttime. Such an approach completely abolished the disruptive effects of the HFD on the DMH clock, confirming its dependence on the feeding schedule of the animal. The presented data highlight the importance of a temporally regulated feeding pattern on the physiology of the hypothalamic center for food intake and metabolism regulation, and propose time-restricted feeding as a possible prevention of the circadian dysregulation observed under an HFD.

Keywords: chronobiology; metabolism; time-restricted feeding; obesity; food-entrainable oscillator

Citation: Sanetra, A.M.; Palus-Chramiec, K.; Chrobok, L.; Jeczmien-Lazur, J.S.; Gawron, E.; Klich, J.D.; Pradel, K.; Lewandowski, M.H. High-Fat-Diet-Evoked Disruption of the Rat Dorsomedial Hypothalamic Clock Can Be Prevented by Restricted Nighttime Feeding. *Nutrients* **2022**, *14*, 5034. https://doi.org/10.3390/nu14235034

Academic Editor: Yoon Jung Park

Received: 30 October 2022
Accepted: 24 November 2022
Published: 26 November 2022

1. Introduction

Overweight and obesity have reached pandemic proportions, with almost two billion overweight and more than half a billion obese adults worldwide as of 2016 [1]. A high body mass index (BMI) is a risk factor for many life-threatening disorders, such as cardiovascular disease [2] and various types of cancer [3], which are the two leading causes of death globally. Although the pathophysiology of obesity is complex and multifactorial, it is considered to be mostly the result of an imbalance between the number of calories ingested and spent, followed by the accumulation of the excess in the form of fat tissue. Modern dietary habits promote a disproportionate intake of highly palatable foods, rich in fat and/or sugar, increasing the hedonic motivational drive and disturbing the homeostatic balance.

A relatively new approach to metabolism research involves its circadian regulation. An increased BMI is often associated with shift work [4–8], which disturbs the body clock by its irregular activity and feeding patterns [9,10], raising the question of how much the disruptions in feeding patterns influence weight gain prevalence. Time-restricted feeding with daily periods of food deprivation have been shown to be beneficial for losing weight and improving sleep quality in humans [11], as well as to prevent excessive weight gain in mice fed a high-fat diet (HFD) [12–14] and enhance longevity in rodents [15].

An HFD is the most commonly used animal model of diet-induced obesity (DIO). In addition to body weight gain, it induces leptin resistance [16] and type 2 diabetes, and impairs glucose tolerance [17]. Interestingly, an HFD was also shown to lengthen the circadian period and disrupt the day/night feeding pattern even before obesity development [18,19], further confirming circadian dysregulation as an important factor in its pathophysiology.

The circadian rhythmicity of different functions is controlled by local oscillators, present in the brain as well as different tissues on the periphery. These clocks are synchronized by the light-entrained master circadian clock in the suprachiasmatic nucleus (SCN) of the anterior hypothalamus, which can, however, be uncoupled from its metabolic partners by an unhealthy feeding pattern [20]. The brain structures sensitive to metabolic cues and orchestrating behavioral responsiveness to different feeding schedules collectively form the food-entrainable oscillator (FEO), of which a very important part is the dorsomedial hypothalamus (DMH) [21]. The DMH is sensitive to many hunger and satiety signals, including ghrelin [22–24], orexins [25,26], cholecystokinin [24,27], leptin [28–32] and glucagon-like peptides [33,34], involved in both short- and long-term regulation of feeding behaviour. Moreover, the DMH exhibits an intrinsic circadian rhythm in clock gene expression [35], which can be enhanced and even entirely shifted by restricted feeding [36–40].

DIO has been shown to globally affect the DMH, changing the expression of over 80 genes in this structure [41], which is more than in any other investigated brain structure (importantly including other hypothalamic metabolic centers such as the lateral hypothalamus, the paraventricular nucleus or the arcuate nucleus). However, it is not clear when these changes begin, and whether they are a result of obesity or contribute to its development by affecting feeding behaviour and metabolism. Therefore, in this study, we explored how a short-term (2–4 weeks) HFD (preceding obesity, [19]) influences day/night rhythms in this hypothalamic structure and how this relates to the disrupted pattern of food intake observed under an HFD. Using ex vivo electrophysiology and immunofluorescence we show that even such a short period of an HFD consumption is enough to impair DMH cellular activity rhythms, in the form of an increasing daytime cFos immunoreactivity and neuronal firing rate, as well as by delaying the peak of its electrical activity. Most importantly, these disruptions do not occur under restricted nighttime feeding (NF), indicating their possible prevention by a healthy feeding pattern.

2. Materials and Methods

2.1. Ethical Statement

All experiments were performed in accordance with the Polish Animal Welfare Act of 23 May 2012 (82/2012) and the European Communities Council Directive (86/609/EEC) and were approved by the Local Ethics Committee in Krakow (No. 18/2018, 349/2022). Every possible effort was made to minimize the number of animals used and their suffering.

2.2. Animal Maintenance

The study was performed on male Sprague-Dawley (SD) rats, bred and kept at the Jagiellonian University in Krakow (Poland) in standard lighting conditions (LD 12/12), constant temperature (23 ± 2 °C) and humidity (~65%), with water and food supplied ad libitum (with the exception of the night-feeding protocols). Females were excluded due to probable interactions between the estrous phase and food intake/metabolism, especially during puberty. At 4 weeks of age, the animals were weaned and assigned to either

control or experimental group. The first one was fed control diet (CD; ~3514 kcal/kg, fat content 4%, energy from: 10% fat, 24% protein, 66% carbohydrates, cat. no. C1090-10; Altromin International, Lage, Germany), whereas the experimental group received HFD (~5389 kcal/kg, fat content 42%, energy from: 70% fat, 16% protein, 14% carbohydrates, cat. no. C1090-70; Altromin International). The animals were then fed a respective diet for 2–7 weeks, depending on the experimental protocol, as detailed in the following sections.

2.3. Food Intake and Body Weight Gain Assessment

Food intake and body weight gain assessment was performed on 20 rats (10 of which fed CD and another 10 HFD). In order to measure the amount of food eaten, the rats were housed individually. Starting 3 days after weaning, body weight and the amount of food eaten during 24 h were measured every week for 7 successive weeks, always at the beginning of the light phase (ZT—Zeitgeber time 0). Food ingested was analysed both as the chow mass disappearing from the feeder, as well as after calculating this value into kcal/kg of body weight.

2.4. Immunofluorescence

For the immunofluorescence study, 50 animals were used (24 fed CD and 26 fed HFD). After 4 weeks on either diet, the rats were perfused at one of 4 time points (ZT0, 6, 12 or 18). Each of the new groups formed contained 6 animals, with the exception of HFD—ZT6 and HFD—ZT18, which contained 7 rats.

All animals were anesthetized by isoflurane inhalation (1 mL in the incubation chamber, Baxter, Deerfield, IL, USA; v/v air mixture) followed by sodium pentobarbital injection (100 mg/kg body weight, i.p.; Biowet, Pulawy, Poland). Deep anesthesia was confirmed with a tail pinch, and when no response was observed, the rats were perfused transcardially with phosphate-buffered saline (PBS) followed by 4% paraformaldehyde (PFA) in PBS. Next, the brains were removed and kept in the same PFA solution overnight. A vibroslicer (Leica VT1000S, Heidelberg, Germany) was used to cut 35 µm thick slices containing the DMH, which were then washed out of PFA by two 10 min long incubations with PBS. Non-specific site blocking and membrane permeabilization were performed in one step, with a 30 min long incubation in a PBS solution containing 0.6% Triton-X100 (Sigma-Aldrich, Saint Louis, MO, USA) and 10% normal donkey serum (NDS, Jackson ImmunoResearch, West Grove, PA, USA) at room temperature. Next, the slices were transferred to a PBS solution containing rabbit anti-cFos antibodies (1:2000, Abcam, Cambridge, UK), 2% NDS and 0.3% Triton-X100 and kept in it for 24 h at 4 °C. After this step, the slices were rinsed in PBS (2 × 10 min) and incubated with secondary antibodies (AlexaFluor488-conjugated anti-rabbit antisera; 1:400, Jackson ImmunoResearch, West Grove, PA, USA) in PBS overnight at 4 °C. Finally, the slices were rinsed again (2 × 10 min), mounted onto glass slides and coverslipped with FluoroshieldTM with DAPI (Sigma-Aldrich, Saint Louis, MO, USA).

Slices were scanned using epifluorescence microscope (Axio Imager M2, Zeiss, Jena, Germany) at 20× magnification, cFos-positive cells were counted manually and DMH area measured with the aid of ZEN 2.5 (blue edition) software (Zeiss, Jena, Germany). Only cells immunoreactive for cFos and DAPI-positive were counted. Results present the density of cFos-positive cells within the area occupied by the DMH.

2.5. Electrophysiology

2.5.1. Short-Term Recordings

Tissue Preparation

Multi-electrode array (MEA) ex vivo recordings were performed in the middle of both light and dark phases. A total of 16 animals were used (CD daytime: 5, HFD daytime: 5, CD nighttime: 3, HFD nighttime: 3), fed with a respective diet for 2–4 weeks. Animals were sacrificed between 1–3 h after the onset of each lighting phase (ZT1–3 and ZT13–15), and the recordings were performed around ZT6/18 (±1 h).

Rats were anesthetized with isoflurane (2 mL/kg body weight), then decapitated. The brain was removed while immersed in ice-cold, cutting artificial cerebro-spinal fluid (cACSF), containing (in mM): 25 $NaHCO_3$, 3 KCl, 1.2 Na_2HPO_4, 2 $CaCl_2$, 10 $MgCl_2$, 10 glucose, 125 sucrose with addition of a pH indicator, Phenol Red 0.01 mg/L, osmolality ~290 mOsmol/kg, continuously carbogenated (95% O_2, 5% CO_2). Then, 250 µm thick coronal slices containing the DMH were cut using a vibroslicer (Leica VT1000S, Heidelberg, Germany) and incubated in the recording artificial cerebro-spinal fluid (rACSF), containing: (in mM): 125 NaCl, 25 $NaHCO_3$, 3 KCl, 1.2 Na_2HPO_4, 2 $CaCl_2$, 2 $MgCl_2$, 5 glucose and 0.01 mg/l of Phenol Red (initial temperature: 32 °C, cooled to room temperature) for a minimum of 0.5 h before the recording.

Multi-Electrode Array Recordings

The MEA recordings were performed using MEA2100-System (Multichannel Systems GmbH, Reutlingen, Germany; [42]). Slices containing the DMH were placed onto an 8 × 8 recording array of a perforated MEA (60pMEA100/30iR-Ti, Multichannel Systems), constantly perfused with fresh rACSF, heated up to 32 °C. The slices were positioned to ensure the presence of as many recording spots within the DMH as possible, and then gently sucked into the perforations neighboring the spots by creating imbalance between inward and outward flow through the bottom tubing circuit of the recording chamber. After a proper amount of suction was established, the slices were allowed to settle for half an hour before the start of the recording and were then recorded for another half an hour.

Signal was acquired with Multi Channel Experimenter software (Multichannel Systems), with sampling frequency of 20 kHz. After the experiment, the raw signal was processed as described previously [19,43]. In brief, the signal was exported to HDF5 and CED-64 files with Multi Channel DataManager (Multichannel Systems GmbH). The HDF5 file was mapped and converted into DAT format with a custom-made MatLab script (R2018a version, MathWorks, Natick, MA, USA), followed by an automatic spike sorting with the KiloSort [44] in MatLab environment. Parallelly, the CED-64 files were remapped and filtered with Butterworth band pass filter (fourth order) from 0.3 to 7.5 kHz by a custom-made Spike2 script. Spike-sorting results were then transferred into the prepared CED-64 files (Spike2 8.11; Cambridge Electronic Design Ltd., Cambridge, UK) with a custom-written MatLab script. At the end, each spot was verified manually for errors in the automatized process, and corrected with the aid of autocorrelation, cross-correlation, principal component analysis (PCA) and spike shape inspection.

2.5.2. Long-Term Recordings

For long-term MEA experiments, animals (3 rats per diet) were sacrificed at ZT0, and the recordings started exactly 2 h later. The procedures for both tissue preparation, MEA setup and signal analysis were analogical to those reported in the previous section (2.5.1 Short-Term Recordings) with two differences. First, as the recordings lasted ~30 h, they were not recorded in a continuous way, but one-minute-long sample was recorded every ten minutes. Second, to enhance long-term survival of the tissue, 1 mg/mL of penicillin–streptomycin (Sigma-Aldrich) was added to the rACSF and the recordings were performed at 25 °C.

2.6. Night-Feeding Protocol

After the administration of a respective diet (CD or HFD, at weaning) the animals were fed ad libitum for the first two weeks, after which they were only given access to food during nighttime, for another 2 weeks. Following this, two separate experiments were performed: the long-term MEA recordings, analogically to the procedure described earlier (2.5.2 Long-Term Recordings; 4 rats fed CD and 3 fed HFD), and a combination of short-term MEA recordings with an immunofluorescence study, as follows.

Short-Term MEA Recordings Combined with Immunofluorescence Staining

For these experiments, we used a total of 16 rats (groups included: CD daytime, CD nighttime, HFD daytime, HFD nighttime, 4 animals per group). Tissue was collected as reported in the short-term MEA recordings (2.5.1) section and the MEA experiments performed accordingly to the study on ad libitum-fed animals. From each animal one 250 µm thick slice containing DMH was used for the MEA, and the rest was immediately fixed in a 4% PFA solution overnight. The latter slices were then immersed in a sucrose solution (30% in PBS) for ~24 h, cut into thinner, 35 µm slices using a cold-plate microtome, and further processed as described in the Immunofluorescence (2.4) section. For this experiment the animals were sacrificed at ZT3–4/ZT15–16, to ensure that both slice fixation in the PFA solution, as well as the MEA recordings, happened around ZT6/ZT18 (±1 h).

2.7. Statistical Analysis

Statistical analysis was performed in R (Version 4.0.4; [45]) and RStudio (Version 1.4.1106, PBC; [46]). Outliers were detected with the help of the box-and-whisker method from the rstatix package [47] and those identified as extreme outliers (above Q3 + 3×IQR or below Q1—3×IQR) were removed from further analysis. For independent data, a general linear model was fitted, whereas in the case of multiple observations from the same animals, a random intercept was included in a linear mixed effects model (and a random slope for repeated measures designs). Mixed models were fitted using the lme4 package [48] and analysed with type III ANOVA (with Satterthwaite's method for the degrees of freedom estimation) from the lmerTest [49] package. Post hoc analyses were performed using the emmeans package [50], and *p*-value corrected for multiple comparisons with Tukey method. Assumptions for using a general linear model were checked with Shapiro–Wilk normality test from the rstatix package and Levene test for homoscedasticity from the car package [51], normality of the residuals' distribution were analysed with QQ-plots (ggpubr; [52]). Where necessary, Box–Cox (BC) transformation was applied (package: MASS, [53]), which was defined as: $BC(y) = (y\lambda\text{-}1)/\lambda$, where λ is a value that provides the best approximation for the normal distribution of the response variable [54]. Detailed results from all the models are presented in Table S1.

Circular statistics of the long-term MEA recordings was performed with the CircStat toolbox [55] in the MatLab Environment (R2018a version, MathWorks). Non-uniformity of distributions was confirmed with Rayleigh test and circular means were compared using the circular analogue of ANOVA (Watson-Williams test).

3. Results

3.1. Body Weight Gain and Feeding Assessment

First, we investigated how the body weight of animals changes under an HFD. In order to do so, rats were maintained on either a CD or HFD (10 animals per group) for 7 weeks and weighed every week starting at the time of weaning (week 0). We fitted a mixed effects model with diet and week as fixed factors (including the interaction between them), as well as random intercept and slope for each animal (to account for a repeated measures design of the study).

The analysis revealed significant changes in the rat body weight during the course of the study ($F_{8,18} = 768.27$, $p < 0.0001$), and differences between the diets ($F_{1,18} = 5.08$, $p = 0.037$). Due to a significant interaction ($F_{7,18} = 16.11$, $p < 0.0001$), we performed a post hoc analysis, which indicated that animals fed an HFD become heavier than the control group after 5 weeks ($t_{18} = 2.37$, $p = 0.029$), and this difference increases in the following 2 weeks (week 6: $t_{18} = 2.87$, $p = 0.01$, week 7: $t_{18} = 3.31$, $p = 0.0039$; Figure 1A).

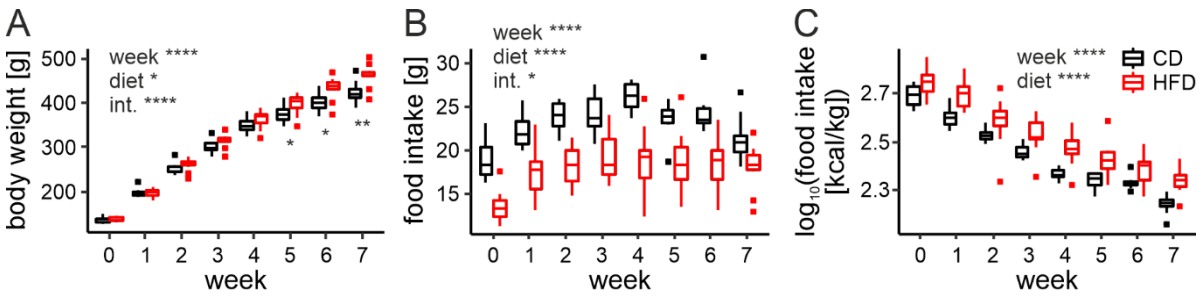

Figure 1. Body weight gain and feeding assessment. (**A**). Body weight gain across 7 weeks on either control (CD) or high-fat diet (HFD; week: F8,18 = 768.27, $p < 0.0001$; diet: F1,18 = 5.08, $p = 0.037$; interaction: F7,18 = 16.11, $p < 0.0001$). Differences between the diets observed from week 5 onwards (t18 = 2.37, $p = 0.029$). (**B**). Daily food intake in grams across 7 weeks on either CD or HFD (week: F7,18 = 35.92, $p < 0.0001$; diet: F1,18 = 45.13, $p < 0.0001$; interaction: F7,18 = 3.00, $p = 0.028$). (**C**). Daily food intake in kcal/kg body mass across 7 weeks on either CD or HFD (week: F7,18 = 183.84, $p < 0.0001$; diet: F1,18 = 30.52, $p < 0.0001$, interaction: F7,18 = 2.33, $p = 0.07$). * $p < 0.05$, ** $p < 0.01$, **** $p < 0.0001$. Box-and-whisker plots present median value, interquartile range (IQR; box) and the minimum-to-maximum range of values, not exceeding 1.5 * IQR (whiskers). Data points outside this range are plotted individually as outliers.

In addition to body mass, we weighed the chow at the beginning and at the end of a day to calculate daily food intake. Rats fed an HFD were shown to eat a significantly lower amount of chow than the control group (F1,18 = 45.13, $p < 0.0001$, Figure 1B). Even though the interaction with the week of the experiment was also observed (F7,18 = 3.00, $p = 0.028$), post hoc analysis confirmed that this difference was present each week (for the results from all multiple comparisons please see Table S1). The amount of food eaten by animals on both diets seemed to increase up until around week 3, which we believe to be due to the continuous growth of the young animals. We hypothesized, that the lower food intake of the HFD-fed group was caused by a higher caloric density of this chow; therefore, we expressed food intake as the number of calories per body mass. With this correction, the HFD-fed group was shown to consume more calories than the control group throughout the entire experiment (F1,18 = 30.52, $p < 0.0001$). Here, we also observed that the number of calories ingested per kg of body weight decreased throughout the course of the study (F7,18 = 183.84, $p < 0.0001$), with no interaction between the factors (F7,18 = 2.33, $p = 0.07$; Figure 1C).

Since our experiments were aimed at investigating changes under an HFD before the onset of obesity, it was important for us to determine how much time is needed for this to happen. The results presented in this section show that rats fed an HFD become significantly heavier than the control group after 5 weeks; therefore, all the following experiments were performed on animals fed the respective diet for a maximum of 4 weeks. Additionally, we show that rats fed an HFD eat fewer grams of food daily, but more calories per body mass, as a result of the distinct caloric density of both chows.

3.2. HFD Advances Daily cFos Rhythm in the DMH

Immunofluorescence staining was performed on coronal brain slices (bregma between −3.00 and −3.48, Figure 2A, [56]) collected from animals that had undergone transcardial perfusion at one of four daily time points (ZT0, 6, 12 and 18; 6 rats per group, with the exception of the HFD group perfused at ZT6 and ZT18, which contained 7 animals), 4 weeks into the experiment. Both the brains and stomachs were collected, and the latter ones immediately weighed.

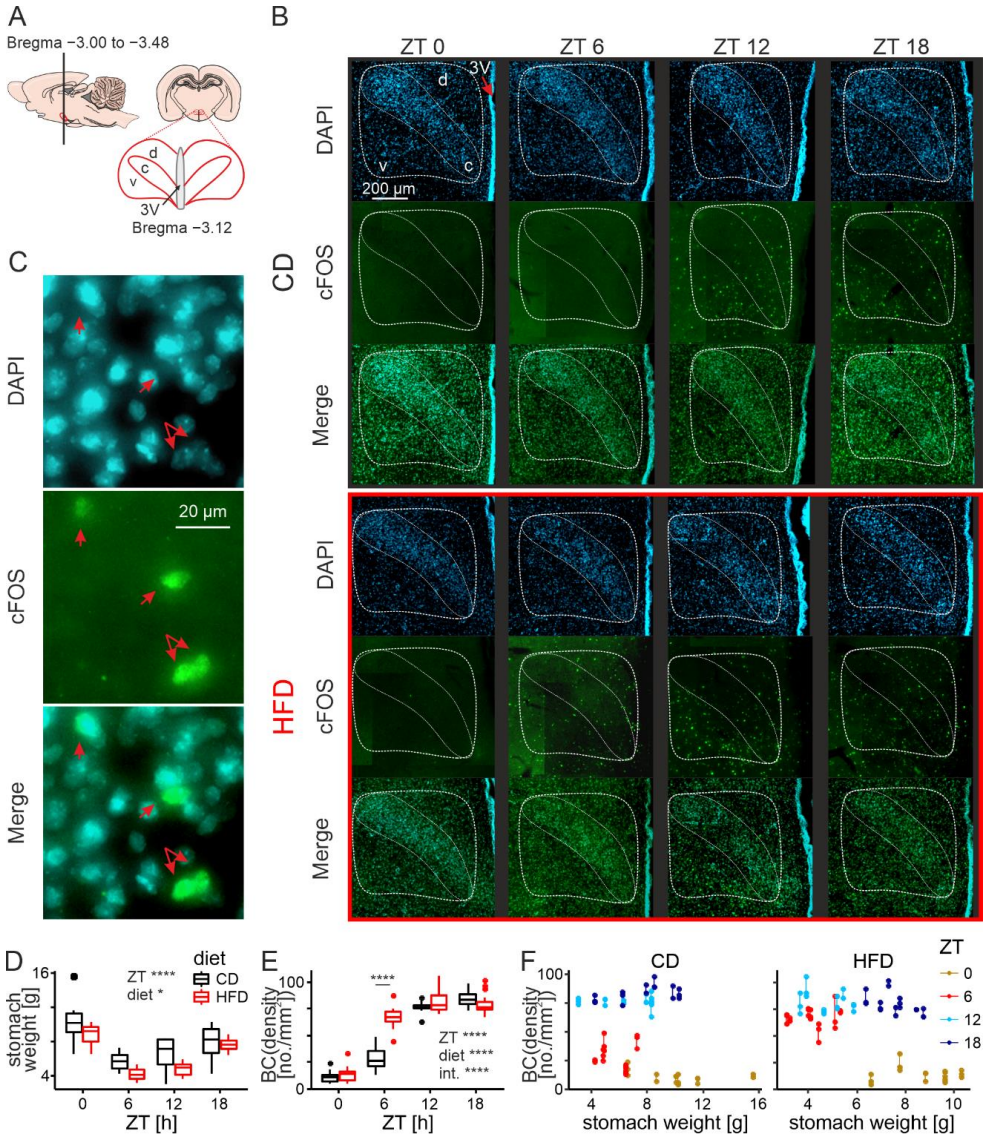

Figure 2. HFD advances daily cFos rhythm in the DMH. (**A**). A schematic drawing indicating the brain sections analysed in reference to bregma. (**B**). Representative microphotographs of DMH-containing brain slices obtained from animals fed either control (CD) or high-fat diet (HFD) at four daily timepoints. The compact part of the DMH, recognized with DAPI staining as the region of densely packed cells, is delineated with the white-bordered shape inside the outline of the entire structure. d—dorsal part of the DMH, c—compact part of the DMH, v—ventral part of the DMH. Please note the layer of ependymal cells indicative of the location of the third ventricle (3V) on the right side of the microphotographs. (**C**). Colocalization of DAPI and cFos within individual cells (red arrows). (**D**). Comparison of stomach weight and its changes across the 24 h between rats fed either CD or HFD (diet: $F1,42 = 7.09$, $p = 0.011$; ZT: $F3,42 = 18.99$, $p < 0.0001$; interaction: $F3,42 = 0.54$, $p = 0.66$). (**E**). Comparison of cFos immunoreactivity and its changes across the 24 h between rats fed either CD or HFD (diet: $F1,41 = 21.16$, $p < 0.0001$; ZT: $F3,41 = 208.55$, $p < 0.0001$; diet: $F1,41 = 0.082$, $p = 0.78$; interaction: $F3,41 = 21.79$, $p < 0.0001$). BC—Box–Cox transformed values; $\lambda = 0.59$. * $p < 0.05$, **** $p < 0.0001$. Box-and-whisker plots present the median value, the interquartile range (IQR; box) and the minimum-to-maximum range of values, not exceeding 1.5 * IQR (whiskers). Data points outside this range are plotted individually as outliers. (**F**). Graphical representation of the relationship between stomach weight and cFos-positive cell density for rats fed CD or HFD. Data points for each brain slice are presented, those acquired from the same animal are connected by a vertical line. ZT—Zeitgeber time (ZT0 at lights on).

Consistently with the results reported in the previous section, stomachs collected from animals fed the HFD were significantly lighter than those of the control group ($F_{1,42} = 7.09$, $p = 0.011$). Nocturnality of the rats was reflected by changes in the stomach weight between time points. For both dietary groups, the stomachs were the lightest at the beginning of the night, and the heaviest at the end of it ($F_{3,42} = 18.98$, $p < 0.0001$, Figure 2D).

Next, we analysed the changes in the number of cFos-positive neurons in the DMH, considering both the time of the day (the ZT factor) and the diet. To account for the day/night changes in stomach weight, we fitted the model including it as a covariate. The density of cFos-positive cells was defined as the number of immunostained neurons per 1 mm^2 of the DMH area. To achieve normality of the distributions and homoscedasticity, we applied Box–Cox (BC) transformation to the data ($\lambda = 0.59$). All cFos-immunoreactive cells were also positive for DAPI (Figure 2C).

We collected and analysed a total of 140 brain slices containing the DMH (hemispheres treated separately), from 50 animals. Differences between the diets were observed (higher cFos for HFD-fed group; $F_{1,41} = 21.16$, $p < 0.0001$), as were changes around the clock, with generally lower values during the day and higher at night (ZT factor: $F_{3,41} = 208.55$, $p < 0.0001$). The cFos-positive cells appeared most densely in the ventral and medial parts of the structure, covering the area of all three previously outlined subdivisions of the DMH (ventral, dorsal and compact; Figure 2B). Most importantly, there was a significant interaction between the two factors analysed ($F_{3,41} = 21.79$, $p < 0.0001$). Whereas around and at nighttime cFos density was similar between the dietary groups, a striking difference was observed in the middle of the day when the HFD-fed group demonstrated an increased number of cFos-positive cells (ZT6, $t_{40} = 9.17$, $p < 0.0001$; Figure 2E).

The DMH is highly responsive to metabolic signals [22–34], which could be the reason for the observed variation in cFos-positive neurons around the clock. What is more, we recently showed that animals fed an HFD change their pattern of feeding and start eating during their normally inactive phase (daytime; [19]), which could explain an increased cFos expression in the DMH during this time of the day. However, stomach weight was shown not to influence the density of cFos-positive cells within our dataset ($F_{1,41} = 0.083$, $p = 0.78$), contradicting the presence of a positive correlation between them. This is most clearly visible at ZT0 when the stomachs are the heaviest but there are very few cFos-positive neurons in the structure (Figure 2F). Even though there appears to be some relationship between stomach weight and cFos immunoreactivity, cFos changes are better explained by the other factors in the model, predominantly the interaction between ZT and diet. Therefore, we believe the day/night rhythm in cFos immunoreactivity in the DMH, as well as its disruption under an HFD, are not simply a consequence of the animals' changed feeding activity.

3.3. HFD Increases Midday Electrical Activity of the DMH

To reveal whether and how increased cFos reflects in the electrical activity of DMH neurons, we performed extracellular MEA recordings in two time points: middle of the day (~ZT6) and middle of the night (~ZT18). We recorded a total of 577 neurons from 16 animals. Since for this experiment rats had been kept on a diet for 2–4 weeks, we added the exact time of diet (in days) to the linear model as a covariate, even though it was not statistically significant ($F_{1,4} = 1.87$, $p = 0.24$).

In line with previous reports [24,35,57], the DMH was shown to possess a day/night rhythm in neuronal activity (LD: $F_{1,5} = 14.14$, $p = 0.011$), with higher firing frequency during the behaviorally active nighttime. However, an interaction with diet was also observed ($F_{1,5} = 6.61$, $p = 0.047$, Figure 3B). Post hoc analysis revealed that this day/night rhythm only concerned the DMH extracted from control animals ($t_9 = 4.14$, $p = 0.0022$), whereas in the HFD-fed group it was completely abolished ($t_6 = 0.85$, $p = 0.43$). Similarly to the results obtained with immunofluorescence, it was in the middle of the day that the activity of the cells in the experimental group was abnormally increased (day: $t_6 = 3.37$, $p = 0.017$,

night: t10 = 0.35, $p = 0.73$). No clear pattern in the spatial distribution of neurons firing with similar frequency was observed (Figure 3A).

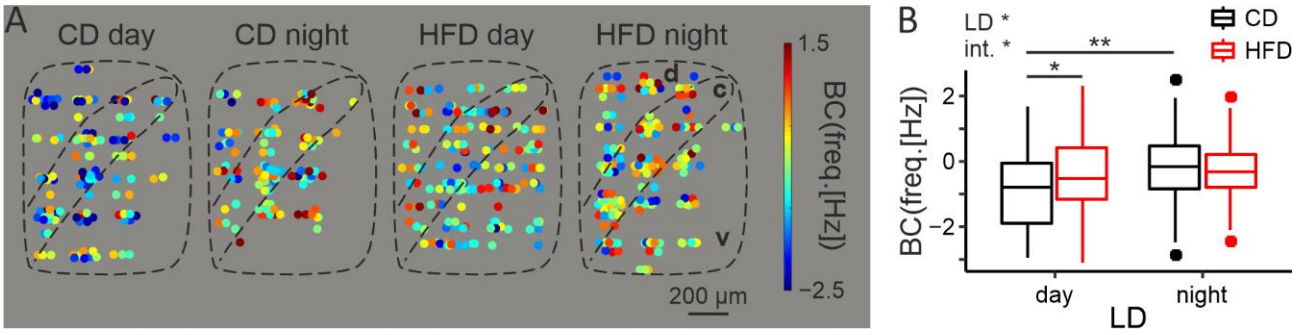

Figure 3. HFD increases midday electrical activity of the DMH. (**A**). Heatmaps illustrating spatial distribution of the recorded neurons and their firing frequency with color-coding. Data points from the same location (recording electrode) were scattered around it. d—dorsal part of the DMH, c—compact part of the DMH, v—ventral part of the DMH. (**B**). Comparison of the spontaneous neuronal activity between cells obtained from animals fed either control (CD) or high-fat diet (HFD), either during the day or at night (LD—light/dark; diet: $F1,6 = 4$, $p = 0.096$; LD: $F1,5 = 14.14$, $p = 0.011$, diet day: $F1,4 = 1.87$, $p = 0.24$; interaction: $F1,5 = 6.61$, $p = 0.047$). BC—Box–Cox transformed values; $\lambda = 0.26$. * $p < 0.05$, ** $p < 0.01$. Box-and-whisker plots present the median value, the interquartile range (IQR; box) and the minimum-to-maximum range of values, not exceeding 1.5 * IQR (whiskers). Data points outside this range are plotted individually as outliers.

3.4. HFD Delays Circadian Patterning of Neuronal Activity of the DMH

3.4.1. Ad Libitum Feeding Experiment

The DMH is highly responsive to metabolic information arriving from the digestive system; however, it possesses an intrinsic circadian clock as well, driving spontaneous activity changes even in the absence of external synchronizers [35]. Therefore, we next aimed at investigating the influence of the HFD on the intrinsic clock properties of this structure. To do so, we performed another set of MEA recordings, starting at projected (p)ZT2 and continuing for ~30 h, which enabled us to monitor spontaneous changes in neuronal activity.

We spike-sorted a total of 390 units, out of which 264 were labelled "rhythmic" (presenting a single peak of activity within a 24 h window). For both dietary groups, the majority of the neurons were rhythmic: 70.65% (130/184) under CD and 65.05% (134/206) under HFD (three rats per group; $\chi 21 = 1.15$, $p = 0.28$). An example recording from one electrode is presented in Figure 4A, with extracted action potentials and their frequency change over time for two cells (one rhythmic and one non-rhythmic). Consistently with previous data, the mean peak time appeared during the nighttime; however, a 2 h delay was observed for the HFD group in respect to the control (all peak times presented as mean ± SD; for CD: pZT14.43 ± 1.03, for HFD: pZT16.58 ± 1.14, $F1,262 = 9.82$, $p = 0.0019$, Watson-Williams test; Figure 4B). No clear spatial pattern in either the presence of rhythmic cells or peak time values was observed, although for the control group the neurons with an earlier peak time seemed to appear closer to the compact part of the DMH (Figure 4C).

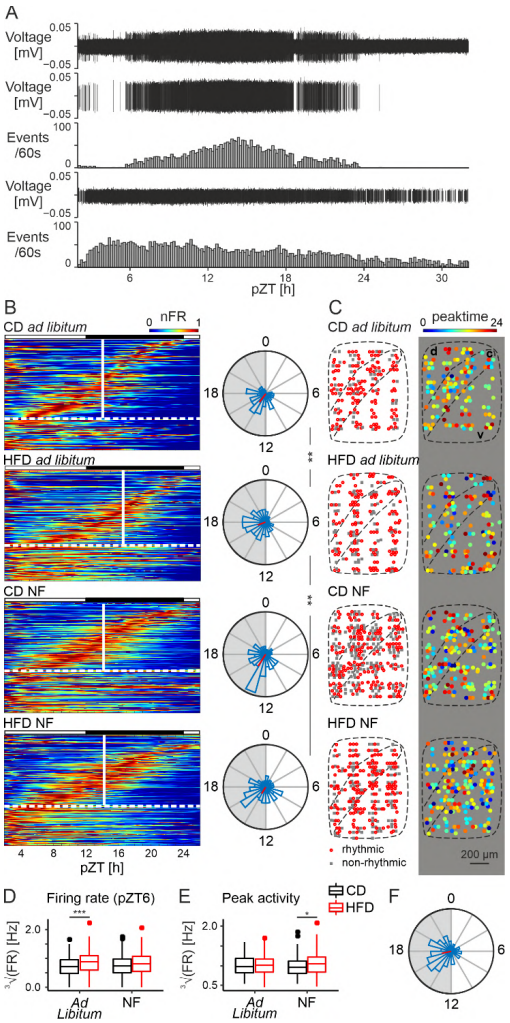

Figure 4. HFD delays circadian patterning of neuronal activity of the DMH. (**A**). Representative recording of a raw signal (top trace), followed by 2 spike-sorted cells (one rhythmic and one non-rhythmic), for which extracted action potentials and their frequency (extrapolated activity over 10 min) are presented. (**B**). (left) Heatmaps presenting the activity of all recorded neurons across the 24 h of recording. Cells with a single activity peak are called rhythmic and sorted by peak time. They are followed by the non-rhythmic cells, from which they are separated with a horizontal dotted line. Average peak value for each group is represented by white, vertical lines. Black and white rectangles above each heatmap reflect projected light–dark phases. (right) Rose petal diagrams (circular histograms of peak times) for each group (bin width: 1 h). The length of the vector (in red) codes the strength of the clustering. Asterisks present the results of the Watson-Williams test: ** $p < 0.01$. Shaded semi-circles represent the dark phase. CD—control diet, HFD—high-fat diet, NF—night feeding, nFR—normalized firing rate. (**C**). Heatmaps presenting spatial distribution of the rhythmic cells (left) and peak time values (right) throughout the structure. d—dorsal part of the DMH, c—compact part of the DMH, v—ventral part of the DMH. (**D**). Comparison of the firing rate at projected Zeitgeber time 6 (pZT6; Ad libitum: $F_{1,388} = 11.338$, $p = 0.00084$; NF: $F_{1,5} = 2.98$, $p = 0.15$). *** $p < 0.001$. FR—firing rate. (**E**). Comparison of the firing rate at the time of peak activity (Ad libitum: $F_{1,4} = 0.019$, $p = 0.9$; NF: $F_{1,352} = 5.86$, $p = 0.016$). * $p < 0.05$. Box-and-whisker plots present the median value, the interquartile range (IQR; box) and the minimum-to-maximum range of values, not exceeding 1.5 * IQR (whiskers). Data points outside this range are plotted individually as outliers. (**F**). Rose petal diagram (circular histogram of peaks) for an experiment starting at pZT12 (bin width: 1 h). The length of the vector (in red) codes the strength of the clustering. Shaded semi-circle represents the dark phase.

The results presented in the previous section (3.3. HFD increases midday electrical activity of the DMH), showing mainly an increased daytime activity of DMH neurons for the HFD-fed rats, could be explained by their daytime feeding behaviour, which might be stimulating DMH activity via a release of satiety signals. In the case of our long-term recordings, brain slice preparation started at ZT0 when both groups of animals should be fully satiated. Yet, the neuronal activity of the HFD group was still higher at pZT6 ($F_{1,388} = 11.338$, $p = 0.00084$, Figure 4D), confirming the results from the short MEA recordings and indicating that this difference is not due to a simple satiety effect from daytime food intake preceding the cull. In order to investigate possible differences in the strength of the rhythm, we also analysed the neuronal firing rate at the time of peak activity but found it unchanged by the diet ($F_{1,3.74} = 0.019$, $p = 0.9$, Figure 4E).

The presented results indicate that the neuronal activity in the DMH is the highest at night, which is in line with its involvement in feeding behaviour. However, to exclude possible phase shifts due to the procedure, we also performed a set of long-term experiments for the CD group, which started at ZT12. Even though the mean peak time value in this case appeared slightly later than previously (around ZT17.21 $\pm$ 1.15; Figure 4F), it confirmed the first half of the night as a time of the peak firing rate in this structure.

3.4.2. Night-Feeding Experiment

The DMH is known to entrain to feeding schedules, participating in the anticipation of an upcoming meal [36–40]. Our long-term experiments on ad libitum-fed animals showed that the increased daytime activity of DMH neurons is not caused by their daytime feeding on the particular day of the experiment. However, it might be related to a repeated disturbance in the feeding behaviour, which shifted the DMH clock over a period of time. To find out whether this is true, we performed a similar set of experiments on animals that had undergone nighttime feeding (food available between ZT12–24) for 2 weeks prior to the recordings.

Night-feeding (NF) turned out to prevent the delay in peak neuronal activity of the HFD group (HFD ad libitum vs. HFD NF: $F_{1,308} = 10.51$, $p = 0.0013$, Watson-Williams test), shifting it back to pZT14.16 $\pm$ 1.21, which was not significantly different from the CD (CD ad libitum vs. HFD NF: $F_{1,304} = 0.16$, $p = 0.69$, Watson-Williams test). As expected, this feeding restriction did not cause any effect in the CD-fed animals (peak at pZT14.15 $\pm$ 1.14 for CD NF; $F_{1,306} = 0.2$, $p = 0.65$, Watson-Williams test; Figure 4B). What is more, the difference in neuronal activity at pZT6, observed between the ad libitum-fed dietary groups, was also abolished by night feeding ($F_{1,4.92} = 2.98$, $p = 0.15$, Figure 4D). Surprisingly though, NF caused an increase in the peak firing rate of the HFD-fed group ($F_{1,352} = 5.86$, $p = 0.016$, Figure 4E). This result could be related to the fact that circadian rhythms in the DMH become much stronger under many different forms of restricted feeding [37–40], and in this case it was predominantly the HFD group that was restricted since these were the animals that would otherwise consume more food during the day.

3.5. Rhythm Disruption in cFos Immunoreactivity and Neuronal Activity Are Prevented by Night Feeding

Following the promising results obtained on night-fed animals, indicating the possible prevention of an HFD-mediated disturbance of the DMH clock, we decided to study NF effects in more detail. For this, we repeated previous experiments on NF animals. As for the long-term recordings, they were fed ad libitum for the first 2 weeks (when no changes in the feeding pattern are yet observed between the diets [19], which was then followed by 2 weeks of NF. For these, we used a total of 16 rats, 8 per diet.

In line with the data on ad libitum-fed animals reported here, as well as previously [19], under NF, the dietary groups did not differ in body weight for the first 4 weeks either (diet: $F_{1,14} = 0.0001$, $p = 0.99$, week: $F_{4,14} = 629.74$, $p < 0.0001$, interaction: $F_{4,14} = 1.66$, $p = 0.22$; Figure 5A). The HFD-fed animals ate less grams of chow daily ($F_{1,14} = 56.28$, $p < 0.0001$; Figure 5B), but this contributed to more calories per body mass ($F_{1,14} = 19.14$, $p = 0.00063$;

Figure 5C), also matching the data obtained with ad libitum-fed groups. Interestingly, total food intake (in kcal/kg) did not differ between the protocols (ad libitum vs. NF: F1,32 = 3.46, $p = 0.07$; Figure 5D), suggesting that when the animals did not have access to food during the day, they would consume their daily requirement completely during the night. This is important information, especially regarding the HFD group, which were shown to neither overeat in response to the restriction, nor stick to the amount normally ingested during the nighttime without the additional daytime feeding.

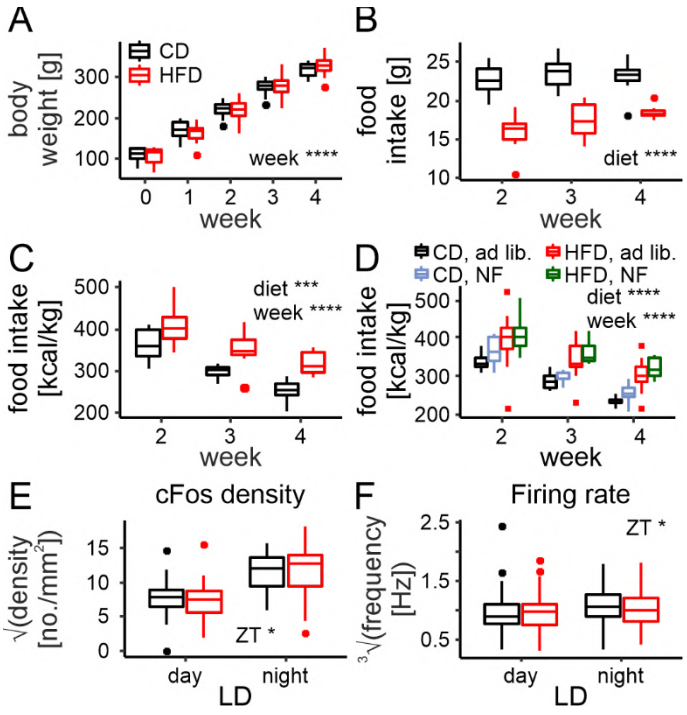

Figure 5. Rhythm disruption in cFos immunoreactivity and neuronal activity are prevented by night feeding (NF). (**A**). Body weight gain across 4 weeks (including 2 weeks on restricted nighttime feeding) on either control (CD) or high-fat diet (HFD; diet: F1,14 = 0.0001, $p = 0.99$, week: F4,14 = 629.74, $p < 0.0001$, interaction: F4,14 = 1.66, $p = 0.22$). (**B**). Nighttime-restricted food intake in grams for CD and HFD (diet: F1,14 = 56.28, $p < 0.0001$, week: F2,14 = 3.56, $p = 0.056$, interaction: F2,14 = 1.91, $p = 0.18$). (**C**). Nighttime-restricted food intake in kcal/kg body mass across the 2 week period (diet: F1,14 = 19.14, $p = 0.00063$, week: F2,14 = 33.71, $p < 0.0001$, interaction: F2,14 = 0.44, $p = 0.66$). (**D**). Comparison of total daily food intake between ad libitum and NF protocols for both diets (diet: F1,32 = 30.89, $p < 0.0001$, week: F2,64 = 69.14, $p < 0.0001$, protocol: F1,32 = 3.46, $p = 0.072$). (**E**). Comparison of cFos immunoreactivity and its changes between midday and midnight (LD—light/dark) between rats fed either CD or HFD during nighttime only (diet: F1,6 = 0.017, $p = 0.9$, LD: F1,6 = 10.11, $p = 0.019$, interaction: F1,6 = 0.023, $p = 0.88$. (**F**). Comparison of the neuronal firing rate and its changes between midday and midnight between rats fed either CD or HFD during nighttime only (diet: F1,12 = 0.1, $p = 0.75$, LD: F1,12 = 5.56, $p = 0.037$, interaction: F1,12 = 0.47, $p = 0.51$. * $p < 0.05$, *** $p < 0.001$, **** $p < 0.0001$. Box-and-whisker plots present the median value, the interquartile range (IQR; box) and the minimum-to-maximum range of values, not exceeding 1.5 * IQR (whiskers). Data points outside this range are plotted individually as outliers.

These animals were then used for the immunostaining and short-term MEA recordings in order to systematically compare the results to the ones obtained from previous experiments on ad libitum-fed rats.

For the cFos immunoreactivity analysis, we collected a total of 68 brain slices from 16 animals (which were included in the model as a random intercept). In contrast to the analysis of the ad libitum-fed animals, here we omitted stomach weight (as a covariate), as they were not collected (no PFA perfusion performed). The number of cFos-positive cells

turned out to vary between day and night (F1,6 = 10.11, $p = 0.019$); however, no difference between the diets was found (F1,6 = 0.017, $p = 0.9$), nor was there an interaction between the two (F1,6 = 0.023, $p = 0.88$, Figure 5E).

As for the MEA recordings, we spike-sorted 574 neurons from the same animals (1 brain slice per animal). In this case, all rats had been on a diet for 4 weeks; therefore, in contrast to the analysis performed for the ad libitum cohort, the exact time on a diet (in days, as a covariate) was excluded from the model. Similar to the immunofluorescence, the neuronal firing rate was also observed to change between day and night (F1,12 = 5.56, $p = 0.037$) but not differ between the diets (F1,12 = 0.1, $p = 0.75$, interaction: F1,12 = 0.47, $p = 0.51$; Figure 5F).

These results confirm that the disruption of DMH daily rhythms in neuronal activity is caused by a prolonged disruption in the rhythm of food intake and can be prevented by restricted nighttime feeding.

4. Discussion

The presented data support the DMH involvement in the processing of metabolic information with an emphasis on its chronoregulation. First, we confirm the DMH day/night changes in the neuronal activity, observed previously [24,57], and their circadian nature [35]. Moreover, we show that an HFD can impair the observed rhythms by increasing the daytime firing rate and cFos immunoreactivity, as well as by delaying the phase of the circadian rhythm in the electrical activity of DMH neurons. Lastly and most importantly, we provide an insight into the possible prevention of such dysregulation by time-dependent feeding, restricted to the active phase of the animal.

Since this study was designed to investigate the effects of an HFD but not obesity, we started off by determining the kinetics of body weight gain for both diets and pinpointing the time necessary for them to divert. This occurred 5 weeks after the onset of the experiment (assignment into CD or HFD groups); therefore, all successive procedures were performed on animals fed either chow for a maximum of 4 weeks. For the night-feeding protocols, the animals were fed ad libitum for the first 2 weeks, followed by 2 weeks of NF, as our previous data showed that the feeding pattern changes between the dietary groups after 3 weeks [19]. Interestingly, the same study found that even though after 4 weeks of the experiment the HFD-fed group had not become significantly heavier than the control, an interaction between diet and time was observed, suggesting faster weight gain of the HFD-fed rats [19]. This was, however, not observed for our NF animals, which, together with other reports [12–14], indicates restricted feeding as a potent therapeutical strategy slowing down or even preventing excessive weight gain. This highlights the importance of the temporal regulation of feeding behaviour, as these animals ingest the same amount of food when fed only during the night, as they would with ad libitum access. What makes it even more striking is that animals fed an HFD consume more calories daily than the control group, yet the timing of the meals seems to matter more than this difference in its amount.

Considering the role of DMH neurons in the regulation of metabolism and food intake [58,59], it is not surprising that their peak activity is confined to the active phase of the rats (nighttime). This was true for both the intrinsic electrical firing and expression of early-response genes (cFos), possibly indicating changes in the incoming stimuli. Interestingly, this day/night rhythm is impaired by a short-term HFD lasting no more than 4 weeks. Together with our previous data [19] showing a disrupted feeding pattern under HFD, these results indicated a general metabolic dysregulation, which required further exploration. Our NF experiments clearly showed that disrupted rhythms in the DMH functioning are not a cause but an effect of an irregular food intake and can therefore be prevented by restricted nighttime feeding. Other studies have also reported the beneficial effects of time-restricted feeding, which prevents not only excessive weight gain [12–14], but also fat accumulation and associated inflammation, glucose intolerance and insulin resistance, as well as improves nutrient homeostasis [14].

The DMH is well known for its ability to enhance its circadian rhythm under restricted feeding [21] and entrain to different meal schedules, which has been shown for both clock gene expression and cFos immunoreactivity [36–40], but so far not for its electrophysiology. With our long-term MEA recordings, we were able to examine the intrinsic circadian properties of DMH neurons and found early night to be the time of their highest firing frequency. An HFD delayed that peak in activity by ~2 h, although not when the animals had been night-fed, once again confirming this to be a result of a disrupted feeding pattern. Moreover, the strength of the rhythm, indicated by the firing rate at the peak time of each individual cell, was enhanced only in the HFD NF group, as this was the group most affected by the feeding restriction that may have required the DMH clock's adaptation.

Importantly, DMH neurons' activity peaked in the early night, even when the slice preparation had been shifted by 10 h, negating the possible effects of the procedure itself on the circadian rhythm within the structure. Even though in this second set (starting at pZT12) the mean peak was a little bit later than the one observed for the experiments starting at pZT2, we believe this may have been caused by the immediacy of the preparation time and peak time, which might have negatively influenced the cells firing at their highest frequency at the time of the procedure, either excitotoxically killing them or at least phase shifting their rhythm.

We recently performed an extensive electrophysiological study into different subregions of the DMH, indicating important differences between its three subdivisions: compact, ventral and dorsal ([57]; Figures 2A, 3A and 4C). In this case, however, such a distinction did not seem reasonable. First, cFos-positive cells were the most densely observed in the ventral part, but also medially, extending through all the abovementioned subdivisions. Because of that, a separate analysis of each one of them produced the same result. Second, spatial distribution of the MEA electrodes does not allow for a clear identification of the borders between the subdivisions of the DMH; therefore, instead, we presented the results from it in a graphical form with spatial heatmaps. In line with our patch clamp study [57], the firing rate did not seem to differ between the three parts of the structure.

Interestingly though, the distribution of the rhythmic cells also did not show any pattern, despite the compact part of the DMH being recognised as the main site of its circadian clock and most pronounced in the clock gene expression [35]. We suspect this inconsistency stems from an intense network signaling within the structure, preserved in our slice preparation. The most rhythmical, compact part of the DMH might be regulating firing frequency of the cells located outside of it; however, more research into the DMH network is needed to confirm it and determine the details. Even though cells within the compact part seemed to peak earlier in the CD-ad libitum group, this trend was not clear enough to conclude from and disappeared in other groups tested, importantly including CD NF, where it should have been even more visible.

Our results indicate that HFD dysregulates feeding behaviour, which in turn impairs the DMH clock. However, the mechanisms for either of these processes remain unknown. Diet has been shown to potently influence the composition of the gut microbiome [60,61], which affects circadian rhythms in both the liver and the hypothalamus [62]. Moreover, gut microbiota composition changes depending not only on the type of ingested food but also its timing [63], suggesting some relationship to the result observed here. Germ-free mice have increased levels of two obesity-suppressing agents: BDNF in the hypothalamus and proglucagon (precursor of glucagon-like peptides—GLP1 and 2) within the digestive system [64]. Interestingly, the DMH is among the brain structures with the highest expression for the GLP1 receptor [65], and the only hypothalamic structure expressing the GLP2 receptor [66]. Moreover, the expression of the GLP1 receptor in the DMH increases in DIO [41], whereas BDNF deletion in the DMH has been shown to result in hyperphagia [67]. Therefore, we believe studying gut microbiota could prove beneficial for uncovering the mechanism responsible for the DMH clock disruption. Additionally, investigating specific subpopulations of DMH neurons, expressing different neurotransmitters, could shed some light on the pathways involved.

Regarding possible effects of DMH rhythm impairment on the development of obesity, DMH is generally considered an orexigenic structure (for a review please see [68], so its increased activity during daytime could feed back into further food intake stimulation. On the other hand, the dorsal part of the DMH connects to the autonomic nervous system, regulating metabolism and thermogenesis [58], which can influence weight gain independently of food intake. However, more research is needed to uncover whether and how the DMH clock disruption participates in the development of obesity.

In conclusion, our work presents a clear dysregulation of the DMH circadian clock under a short-term HFD. We propose that this effect is mediated by a change in the animals' feeding behaviour and can be avoided if a healthy feeding pattern (eating only during the active phase) is kept, even without altering the amount of food ingested. Possible obesity prevention by time-restricted feeding has already been indicated elsewhere; however, to the best of our knowledge, this is the first study to prove its beneficial effects also for the hypothalamic processing including its circadian rhythmicity. This is extremely important considering the brain's top-down control of the metabolism and feeding behaviour, clearly disrupted by an HFD even before the onset of obesity.

Supplementary Materials: The following supporting information can be downloaded at: https://www.mdpi.com/article/10.3390/nu14235034/s1, Table S1: Results of the statistical analyses of all linear models fitted in the study.; Table S2: Data file for the analysis of body weight gain and food intake (*ad libitum*); Table S3: Data file for the analysis of the cFos immunoreactivity (*ad libitum*); Table S4: Data file for the analysis of the neuronal firing rate (*ad libitum*); Table S5: Data file for the analysis of the longterm MEA experiments; Table S6: Data file for the analysis of body weight gain and food intake (NF); Table S7: Data file for the analysis of food intake (*ad libitum* vs. NF); Table S8: Data file for the analysis of the cFos immunoreactivity (NF); Table S9: Data file for the analysis of the neuronal firing rate (NF).

Author Contributions: Conceptualization, A.M.S., K.P.-C., L.C., J.S.J.-L. and M.H.L.; data curation, A.M.S., K.P.-C., L.C. and E.G.; formal analysis, A.M.S., L.C. and K.P.; funding acquisition, A.M.S. and M.H.L.; investigation, A.M.S., K.P.-C., L.C., J.S.J.-L., E.G. and J.D.K.; methodology, A.M.S., K.P.-C., L.C. and J.S.J.-L.; project administration, M.H.L.; resources, A.M.S., L.C., K.P. and M.H.L.; software, K.P.; supervision, M.H.L.; visualization, A.M.S., L.C. and K.P.; writing—original draft, A.M.S.; writing—review and editing, K.P.-C., L.C., J.S.J.-L., E.G., J.D.K., K.P. and M.H.L. All authors have read and agreed to the published version of the manuscript.

Funding: This study was supported by the Polish National Science Centre grant 2017/25/B/NZ4/01433 ("Opus 13" to MHL) and by the Faculty of Biology of the Jagiellonian University in Krakow N18/MNS/000033 and U1U/W18/NO/28.16 (both awarded to AMS).

Institutional Review Board Statement: The animal study protocol was approved by the Local Ethics Committee in Krakow (No. 18/2018, 349/2022).

Data Availability Statement: The data presented in this study are available in Tables S2–S9.

Acknowledgments: The work was supported by the programme "Excellence Initiative–Research University" at the Jagiellonian University in Krakow, Poland. We would like to thank Patrycjusz Nowik for their excellent animal care.

Conflicts of Interest: These authors declare no conflict of interests.

Abbreviations

ACSF—artificial cerebro-spinal fluid, BC—Box–Cox, cACSF—cutting ACSF, BMI—body mass index, CD—control diet, cDMH—compact DMH, dDMH—dorsal DMH, DMH—dorsomedial hypothalamus, FEO—food-entrainable oscillator, FR—firing rate, HFD—high-fat diet, LD—light/dark, NDS—normal donkey serum, NF—night feeding, MEA—multi-electrode array, PBS—phosphate-buffered saline, rACSF—recording ACSF, SCN—suprachiasmatic nucleus, vDMH—ventral DMH, ZT—Zeitgeber time.

References

1. World Health Organization. *Health at a Glance: Asia/Pacific 2020 Measuring Progress towards Universal Health Coverage: Measuring Progress towards Universal Health Coverage*; OECD Publishing: Paris, France, 2020.
2. Ortega, F.B.; Lavie, C.J.; Blair, S.N. Obesity and cardiovascular disease. *Circ. Res.* **2016**, *118*, 1752–1770. [CrossRef] [PubMed]
3. Lauby-Secretan, B.; Scoccianti, C.; Loomis, D.; Grosse, Y.; Bianchini, F.; Straif, K. Body fatness and cancer—Viewpoint of the IARC Working Group. *N. Engl. J. Med.* **2016**, *375*, 794–798. [CrossRef] [PubMed]
4. Parkes, K.R. Shift work and age as interactive predictors of body mass index among offshore workers. *Scand. J. Work. Environ. Health* **2002**, *28*, 64–71. [CrossRef] [PubMed]
5. Di Lorenzo, L.; De Pergola, G.; Zocchetti, C.; L'Abbate, N.; Basso, A.; Pannacciulli, N.; Soleo, L. Effect of shift work on body mass index: Results of a study performed in 319 glucose-tolerant men working in a Southern Italian industry. *Int. J. Obes.* **2003**, *27*, 1353–1358. [CrossRef] [PubMed]
6. Kubo, T.; Oyama, I.; Nakamura, T.; Shirane, K.; Otsuka, H.; Kunimoto, M.; Matsuda, S. Retrospective cohort study of the risk of obesity among shift workers: Findings from the Industry-based Shift Workers' Health study, Japan. *Occup. Environ. Med.* **2011**, *68*, 327–331. [CrossRef] [PubMed]
7. Tada, Y.; Kawano, Y.; Maeda, I.; Yoshizaki, T.; Sunami, A.; Yokoyama, Y.; Togo, F. Association of body mass index with lifestyle and rotating shift work in J apanese female nurses. *Obesity* **2014**, *22*, 2489–2493. [CrossRef]
8. Brum, M.C.B.; Dantas Filho, F.F.; Schnorr, C.C.; Bertoletti, O.A.; Bottega, G.B.; da Costa Rodrigues, T. Night shift work, short sleep and obesity. *Diabetol. Metab. Syndr.* **2020**, *12*, 1–9. [CrossRef]
9. Shaw, E.; Dorrian, J.; Coates, A.M.; Leung, G.K.; Davis, R.; Rosbotham, E.; Bonham, M.P. Temporal pattern of eating in night shift workers. *Chronobiol. Int.* **2019**, *36*, 1613–1625. [CrossRef]
10. Kosmadopoulos, A.; Kervezee, L.; Boudreau, P.; Gonzales-Aste, F.; Vujovic, N.; Scheer, F.A.; Boivin, D.B. Effects of shift work on the eating behavior of police officers on patrol. *Nutrients* **2020**, *12*, 999. [CrossRef]
11. Gill, S.; Panda, S. A smartphone app reveals erratic diurnal eating patterns in humans that can be modulated for health benefits. *Cell Metab.* **2015**, *22*, 789–798. [CrossRef]
12. Sherman, H.; Genzer, Y.; Cohen, R.; Chapnik, N.; Madar, Z.; Froy, O. Timed high-fat diet resets circadian metabolism and prevents obesity. *FASEB J.* **2012**, *26*, 3493–3502. [CrossRef] [PubMed]
13. Hatori, M.; Vollmers, C.; Zarrinpar, A.; DiTacchio, L.; Bushong, E.A.; Gill, S.; Panda, S. Time-restricted feeding without reducing caloric intake prevents metabolic diseases in mice fed a high-fat diet. *Cell Metab.* **2012**, *15*, 848–860. [CrossRef]
14. Chaix, A.; Zarrinpar, A.; Miu, P.; Panda, S. Time-restricted feeding is a preventative and therapeutic intervention against diverse nutritional challenges. *Cell Metab.* **2014**, *20*, 991–1005. [CrossRef] [PubMed]
15. Acosta-Rodríguez, V.; Rijo-Ferreira, F.; Izumo, M.; Xu, P.; Wight-Carter, M.; Green, C.B.; Takahashi, J.S. Circadian alignment of early onset caloric restriction promotes longevity in male C57BL/6J mice. *Science* **2022**, *376*, 1192–1202. [CrossRef] [PubMed]
16. Lin, S.; Thomas, T.C.; Storlien, L.H.; Huang, X.F. Development of high fat diet-induced obesity and leptin resistance in C57Bl/6J mice. *Int. J. Obes.* **2000**, *24*, 639–646. [CrossRef] [PubMed]
17. Winzell, M.S.; Ahrén, B. The high-fat diet–fed mouse: A model for studying mechanisms and treatment of impaired glucose tolerance and type 2 diabetes. *Diabetes* **2004**, *53* (Suppl. 3), S215–S219. [CrossRef] [PubMed]
18. Kohsaka, A.; Laposky, A.D.; Ramsey, K.M.; Estrada, C.; Joshu, C.; Kobayashi, Y.; Bass, J. High-fat diet disrupts behavioral and molecular circadian rhythms in mice. *Cell Metab.* **2007**, *6*, 414–421. [CrossRef]
19. Chrobok, L.; Klich, J.D.; Sanetra, A.M.; Jeczmien-Lazur, J.S.; Pradel, K.; Palus-Chramiec, K.; Lewandowski, M.H. Rhythmic neuronal activities of the rat nucleus of the solitary tract are impaired by high-fat diet–implications for daily control of satiety. *J. Physiol.* **2022**, *600*, 751–767. [CrossRef]
20. Damiola, F.; Le Minh, N.; Preitner, N.; Kornmann, B.; Fleury-Olela, F.; Schibler, U. Restricted feeding uncouples circadian oscillators in peripheral tissues from the central pacemaker in the suprachiasmatic nucleus. *Genes Dev.* **2000**, *14*, 2950–2961. [CrossRef]
21. Mieda, M.; Williams, S.C.; Richardson, J.A.; Tanaka, K.; Yanagisawa, M. The dorsomedial hypothalamic nucleus as a putative food-entrainable circadian pacemaker. *Proc. Natl. Acad. Sci. USA* **2006**, *103*, 12150–12155. [CrossRef]
22. Kobelt, P.; Wisser, A.S.; Stengel, A.; Goebel, M.; Inhoff, T.; Noetzel, S.; Mönnikes, H. Peripheral injection of ghrelin induces Fos expression in the dorsomedial hypothalamic nucleus in rats. *Brain Res.* **2008**, *1204*, 77–86. [CrossRef]
23. Hyland, L.; Park, S.B.; Abdelaziz, Y.; Abizaid, A. Ghrelin infused into the dorsomedial hypothalamus of male mice increases food intake and adiposity. *Physiol. Behav.* **2020**, *220*, 112882. [CrossRef]
24. Palus-Chramiec, K.; Sanetra, A.M.; Lewandowski, M.H. Day/night changes in the dorsomedial hypothalamus firing responses to ghrelin are modulated by high-fat diet. *Neuroscience* **2022**, *494*, 167–177. [CrossRef]
25. Li, T.L.; Chen, J.Y.; Huang, S.C.; Dai, Y.W.E.; Hwang, L.L. Cardiovascular pressor effects of orexins in the dorsomedial hypothalamus. *Eur. J. Pharmacol.* **2018**, *818*, 343–350. [CrossRef]
26. Li, T.L.; Lee, Y.H.; Wu, F.H.; Hwang, L.L. Orexin-A directly depolarizes dorsomedial hypothalamic neurons, including those innervating the rostral ventrolateral medulla. *Eur. J. Pharmacol.* **2021**, *899*, 174033. [CrossRef]
27. Chen, J.; Scott, K.A.; Zhao, Z.; Moran, T.H.; Bi, S. Characterization of the feeding inhibition and neural activation produced by dorsomedial hypothalamic cholecystokinin administration. *Neuroscience* **2008**, *152*, 178–188. [CrossRef] [PubMed]

28. Marsh, A.J.; Fontes, M.A.; Killinger, S.; Pawlak, D.B.; Polson, J.W.; Dampney, R.A. Cardiovascular responses evoked by leptin acting on neurons in the ventromedial and dorsomedial hypothalamus. *Hypertension* **2003**, *42*, 488–493. [CrossRef] [PubMed]
29. Enriori, P.J.; Sinnayah, P.; Simonds, S.E.; Rudaz, C.G.; Cowley, M.A. Leptin action in the dorsomedial hypothalamus increases sympathetic tone to brown adipose tissue in spite of systemic leptin resistance. *J. Neurosci.* **2011**, *31*, 12189–12197. [CrossRef] [PubMed]
30. Zhang, Y.; Kerman, I.A.; Laque, A.; Nguyen, P.; Faouzi, M.; Louis, G.W.; Münzberg, H. Leptin-receptor-expressing neurons in the dorsomedial hypothalamus and median preoptic area regulate sympathetic brown adipose tissue circuits. *J. Neurosci.* **2011**, *31*, 1873–1884. [CrossRef]
31. Faber, C.L.; Deem, J.D.; Phan, B.A.; Doan, T.P.; Ogimoto, K.; Mirzadeh, Z.; Morton, G.J. Leptin receptor neurons in the dorsomedial hypothalamus regulate diurnal patterns of feeding, locomotion, and metabolism. *Elife* **2021**, *10*, e63671. [CrossRef]
32. Huang, Z.; Liu, L.; Zhang, J.; Conde, K.; Phansalkar, J.; Li, Z.; Liu, J. Glucose-sensing glucagon-like peptide-1 receptor neurons in the dorsomedial hypothalamus regulate glucose metabolism. *Sci. Adv.* **2022**, *8*, eabn5345. [CrossRef] [PubMed]
33. Renner, E.; Puskas, N.; Dobolyi, A.; Palkovits, M. Glucagon-like peptide-1 of brainstem origin activates dorsomedial hypothalamic neurons in satiated rats. *Peptides* **2012**, *35*, 14–22. [CrossRef] [PubMed]
34. Tang-Christensen, M.; Larsen, P.J.; Thulesen, J.; Rømer, J.; Vrang, N. The proglucagon-derived peptide, glucagon-like peptide-2, is a neurotransmitter involved in the regulation of food intake. *Nat. Med.* **2000**, *6*, 802–807. [CrossRef] [PubMed]
35. Guilding, C.; Hughes, A.T.; Brown, T.M.; Namvar, S.; Piggins, H.D. A riot of rhythms: Neuronal and glial circadian oscillators in the mediobasal hypothalamus. *Mol. Brain* **2009**, *2*, 1–19. [CrossRef] [PubMed]
36. Gooley, J.J.; Schomer, A.; Saper, C.B. The dorsomedial hypothalamic nucleus is critical for the expression of food-entrainable circadian rhythms. *Nat. Neurosci.* **2006**, *9*, 398–407. [CrossRef]
37. Verwey, M.; Khoja, Z.; Stewart, J.; Amir, S. Differential regulation of the expression of Period2 protein in the limbic forebrain and dorsomedial hypothalamus by daily limited access to highly palatable food in food-deprived and free-fed rats. *Neuroscience* **2007**, *147*, 277–285. [CrossRef]
38. Verwey, M.; Khoja, Z.; Stewart, J.; Amir, S. Region-specific modulation of PER2 expression in the limbic forebrain and hypothalamus by nighttime restricted feeding in rats. *Neurosci. Lett.* **2008**, *440*, 54–58. [CrossRef]
39. Verwey, M.; Lam, G.Y.; Amir, S. Circadian rhythms of PERIOD1 expression in the dorsomedial hypothalamic nucleus in the absence of entrained food-anticipatory activity rhythms in rats. *Eur. J. Neurosci.* **2009**, *29*, 2217–2222. [CrossRef]
40. Minana-Solis, M.C.; Angeles-Castellanos, M.; Feillet, C.; Pevet, P.; Challet, E.; Escobar, C. Differential effects of a restricted feeding schedule on clock-gene expression in the hypothalamus of the rat. *Chronobiol. Int.* **2009**, *26*, 808–820. [CrossRef]
41. Zhang, C.; Barkholt, P.; Nielsen, J.C.; Thorbek, D.D.; Rigbolt, K.; Vrang, N.; Jelsing, J. The dorsomedial hypothalamus and nucleus of the solitary tract as key regulators in a rat model of chronic obesity. *Brain Res.* **2020**, *1727*, 146538. [CrossRef]
42. Belle, M.D.; Baño-Otalora, B.; Piggins, H.D. Perforated multi-electrode array recording in hypothalamic brain slices. In *Circadian Clocks*; Humana: New York, NY, USA, 2021; pp. 263–285.
43. Sanetra, A.M.; Palus-Chramiec, K.; Lewandowski, M.H. Modulation of the Rat Intergeniculate Leaflet of the Thalamus Network by Norepinephrine. *Neuroscience* **2021**, *469*, 1–16. [CrossRef] [PubMed]
44. Pachitariu, M.; Steinmetz, N.; Kadir, S.; Carandini, M.; Harris, K.D. Kilosort: Realtime spike-sorting for extracellular electrophysiology with hundreds of channels. *bioRxiv* **2016**, 061481.
45. Team, R.C. *R: A Language and Environment for Statistical Computing*; R Foundation for Statistical Computing: Vienna, Austria, 2021. Available online: https://www.R-project.org/ (accessed on 1 April 2022).
46. Team, R. *RStudio: Integrated Development for R*; RStudio, Inc.: Boston, MA, USA, 2015; Available online: http://www.rstudio.com/ (accessed on 1 April 2022).
47. Kassambara, A. Rstatix: Pipe-Friendly Framework for Basic Statistical Tests. R Package Version 0.7.0. 2021. Available online: https://CRAN.R-project.org/package=rstatix (accessed on 1 April 2022).
48. Bates, D.; Maechler, M.; Bolker, B.M.; Walker, S. Fitting linear mixed-effects models using lme4. *J. Stat. Softw.* **2015**, *67*, 1–48. [CrossRef]
49. Kunzetsova, A.; Brockhoff, P.; Christensen, R. lmerTest package: Tests in linear mixed effect models. *J. Stat. Softw.* **2017**, *82*, 1–26.
50. Lenth, R.V. Emmeans: Estimated Marginal Means, aka Least-Squares Means. R Package Version 1.5.5-1. 2021. Available online: https://CRAN.R-project.org/package=emmeans (accessed on 1 April 2022).
51. Fox, J.; Weisberg, S. *An R Companion to Applied Regression*; Sage Publications: Newbury Park, CA, USA, 2019. Available online: https://socialsciences.mcmaster.ca/jfox/Books/Companion/ (accessed on 1 April 2022).
52. Kassambara, A. ggpubr: 'ggplot2' Based Publication Ready Plots. R Package Version 0.4.0. 2020. Available online: https://CRAN.R-project.org/package=ggpubr (accessed on 1 April 2022).
53. Venables, W.N.; Ripley, B.D. *Modern Applied Statistics with S*; Springer Science & Business Media: New York, NY, USA, 2002; Volume 200, pp. 183–206.
54. Box, G.E.P.; Cox, D.R. An analysis of transformations. *J. R. Stat. Soc. Ser. B* **1964**, *26*, 211–252. [CrossRef]
55. Berens, P. CircStat: A MATLAB Toolbox for Circular Statistics. *J. Stat. Softw.* **2009**, *31*, 1–21. [CrossRef]
56. Paxinos, G.; Watson, C. *The Rat Brain in Stereotaxic Coordinates*; Academic Press: Cambridge, MA, USA, 2007.
57. Sanetra, A.M.; Palus-Chramiec, K.; Chrobok, L.; Lewandowski, M.H. Electrophysiological complexity in the rat dorsomedial hypothalamus and its susceptibility to daily rhythms and high-fat diet. *Eur. J. Neurosci.* **2022**, *56*, 4363–4377. [CrossRef]

58. DiMicco, J.A.; Zaretsky, D.V. The dorsomedial hypothalamus: A new player in thermoregulation. *Am. J. Physiol. Regul. Integr. Comp. Physiol.* **2007**, *292*, R47–R63. [CrossRef]
59. Yang, L.; Scott, K.A.; Hyun, J.; Tamashiro, K.L.; Tray, N.; Moran, T.H.; Bi, S. Role of dorsomedial hypothalamic neuropeptide Y in modulating food intake and energy balance. *J. Neurosci.* **2009**, *29*, 179–190. [CrossRef]
60. Hildebrandt, M.A.; Hoffmann, C.; Sherrill–Mix, S.A.; Keilbaugh, S.A.; Hamady, M.; Chen, Y.Y.; Wu, G.D. High-fat diet determines the composition of the murine gut microbiome independently of obesity. *Gastroenterology* **2009**, *137*, 1716–1724. [CrossRef]
61. Murphy, E.F.; Cotter, P.D.; Healy, S.; Marques, T.M.; O'sullivan, O.; Fouhy, F.; Shanahan, F. Composition and energy harvesting capacity of the gut microbiota: Relationship to diet, obesity and time in mouse models. *Gut* **2010**, *59*, 1635–1642. [CrossRef] [PubMed]
62. Leone, V.; Gibbons, S.M.; Martinez, K.; Hutchison, A.L.; Huang, E.Y.; Cham, C.M.; Chang, E.B. Effects of diurnal variation of gut microbes and high-fat feeding on host circadian clock function and metabolism. *Cell Host Microbe* **2015**, *17*, 681–689. [CrossRef] [PubMed]
63. Zarrinpar, A.; Chaix, A.; Yooseph, S.; Panda, S. Diet and feeding pattern affect the diurnal dynamics of the gut microbiome. *Cell Metab.* **2014**, *20*, 1006–1017. [CrossRef] [PubMed]
64. Schéle, E.; Grahnemo, L.; Anesten, F.; Hallén, A.; Bäckhed, F.; Jansson, J.O. The gut microbiota reduces leptin sensitivity and the expression of the obesity-suppressing neuropeptides proglucagon (Gcg) and brain-derived neurotrophic factor (Bdnf) in the central nervous system. *Endocrinology* **2013**, *154*, 3643–3651. [CrossRef] [PubMed]
65. Merchenthaler, I.; Lane, M.; Shughrue, P. Distribution of pre-pro-glucagon and glucagon-like peptide-1 receptor messenger RNAs in the rat central nervous system. *J. Comp. Neurol.* **1999**, *403*, 261–280. [CrossRef]
66. Tang-Christensen, M.; Vrang, N.; Larsen, P.J. Glucagon-like peptide containing pathways in the regulation of feeding behaviour. *Int. J. Obes.* **2001**, *25*, S42–S47. [CrossRef]
67. Unger, T.J.; Calderon, G.A.; Bradley, L.C.; Sena-Esteves, M.; Rios, M. Selective deletion of Bdnf in the ventromedial and dorsomedial hypothalamus of adult mice results in hyperphagic behavior and obesity. *J. Neurosci.* **2007**, *27*, 14265–14274. [CrossRef]
68. Bellinger, L.L.; Bernardis, L.L. The dorsomedial hypothalamic nucleus and its role in ingestive behavior and body weight regulation: Lessons learned from lesioning studies. *Physiol. Behav.* **2002**, *76*, 431–442. [CrossRef]

3.3. **Publication 3**: *Proglucagon signalling in the rat Dorsomedial Hypothalamus – Physiology and high-fat diet-mediated alterations*

2023, Molecular and Cellular Neuroscience, published online

Molecular and Cellular Neuroscience 126 (2023) 103873

Contents lists available at ScienceDirect

Molecular and Cellular Neuroscience

journal homepage: www.elsevier.com/locate/ymcne

Proglucagon signalling in the rat Dorsomedial Hypothalamus – Physiology and high-fat diet-mediated alterations

A.M. Sanetra [a,*], K. Palus-Chramiec [a], L. Chrobok [a,b], J.S. Jeczmien-Lazur [a], J.D. Klich [a,c], M. H. Lewandowski [a,*]

[a] Department of Neurophysiology and Chronobiology, Institute of Zoology and Biomedical Research, Jagiellonian University in Krakow, Gronostajowa Street 9, 30-387 Krakow, Poland
[b] School of Physiology, Pharmacology, and Neuroscience, University of Bristol, University Walk, Biomedical Sciences Building, Bristol BS8 1TD, UK
[c] Max-Delbrück-Center for Molecular Medicine in the Helmholtz Association (MDC), Robert-Rössle Street 10, 13125 Berlin, Germany

ARTICLE INFO

Keywords:
Metabolism
Restricted feeding
Obesity
Food-entrainable oscillator
Glucagon-like peptide
Oxyntomodulin

ABSTRACT

A relatively new pharmacological target in obesity treatment has been the preproglucagon (PPG) signalling, predominantly with glucagon-like peptide (GLP) 1 receptor agonists. As far as the PPG role within the digestive system is well recognised, its actions in the brain remain understudied. Here, we investigated PPG signalling in the Dorsomedial Hypothalamus (DMH), a structure involved in feeding regulation and metabolism, using in situ hybridisation, electrophysiology, and immunohistochemistry. Our experiments were performed on animals fed both control, and high-fat diet (HFD), uncovering HFD-mediated alterations. First, sensitivity to exendin-4 (Exn4, a GLP1R agonist) was shown to increase under HFD, with a higher number of responsive neurons. The amplitude of the response to both Exn4 and oxyntomodulin (Oxm) was also altered, diminishing its relationship with the cells' spontaneous firing rate. Not only neuronal sensitivity, but also GLP1 presence, and therefore possibly release, was influenced by HFD. Immunofluorescent labelling of the GLP1 showed changes in its density depending on the metabolic state (fasted/fed), but this effect was eliminated by HFD feeding. Interestingly, these dietary differences were absent after a period of restricted feeding, allowing for an anticipation of the alternating metabolic states, which suggests possible prevention of such outcome.

1. Introduction

Increasing prevalence of obesity along with its multiple pathophysiological consequences have resulted in an urgent need for both treatment and prevention options. Amongst various treatment attempts, promising results have been obtained with analogues of glucagon-like peptides (GLP; for a review see Trujillo et al., 2021). These include GLP1 and GLP2, which are posttranslationally cleaved from preproglucagon (PPG) by prohormone convertases (PC 1/3 or PC 2), also producing oxyntomodulin (Oxm), glucagon, miniglucagon or glicentin (Bataille and Dalle, 2014). The PPG peptide family are responsible for glucose homeostasis, with a recognised and widely exploited potential in the treatment of both types of diabetes (Kolterman et al., 2003; Dupré et al., 2004). However, they are also potent satiety signals influencing behaviour (decreasing food intake), and metabolism (stimulating energy expenditure; Hwa et al., 1998, Dakin et al., 2001, 2002, Baggio et al., 2004, Osaka et al., 2005, Wynne et al., 2006, Pocai et al., 2009, Kosinski et al., 2012). These properties make them an interesting therapeutical target for obesity, however, they are mediated by the central nervous system, which in comparison to the digestive system has been hugely

Abbreviations: 3V, Third ventricle; ACSF, Artificial cerebro-spinal fluid; BC, Box-Cox; cACSF, Cutting ACSF; CD, Control diet; cDMH, Compact DMH; dDMH, Dorsal DMH; DLAMO, Depolarised low-amplitude membrane oscillation; DMH, Dorsomedial Hypothalamus; Exn4, Exendin-4; FD, Food deprivation; FEO, Food-entrainable oscillator; FR, Firing rate; GABA, Gamma-aminobutyric acid; GCGR, Glucagon receptor; GLP1/2, Glucagon-like peptide 1/2; GLP1/2R, GLP1/2 receptor; HFD, High-fat diet; HVA, High-voltage activated; LD, Light/dark; NDS, Normal donkey serum; NTS, Nucleus of the Solitary Tract; MEA, Multi-electrode array; Oxm, Oxyntomodulin; PC, Prohormone convertase; PBS, Phosphate-buffered saline; rACSF, Recording ACSF; PGDP, Proglucagon-derived peptides; PPG, Preproglucagon; RF, Restricted feeding; SCN, Suprachiasmatic Nucleus; vDMH, Ventral DMH; VMH, Ventromedial Hypothalamus; ZT, Zeitgeber time.

* Corresponding authors at: Department of Neurophysiology and Chronobiology, Institute of Zoology and Biomedical Research, Jagiellonian University, Gronostajowa Str 9, 30-387 Krakow, Poland.

E-mail addresses: anna.sanetra@doctoral.uj.edu.pl (A.M. Sanetra), marian.lewandowski@uj.edu.pl (M.H. Lewandowski).

https://doi.org/10.1016/j.mcn.2023.103873
Received 28 March 2023; Received in revised form 24 May 2023; Accepted 6 June 2023
Available online 8 June 2023

underexplored in the context of PPG signalling.

The main central source of PPG is located in the brainstem Nucleus of the Solitary Tract (NTS, Larsen et al., 1997). NTS PPG neurons send projections to various brain sites including the Dorsomedial Hypothalamus (DMH; Renner et al., 2012), which expresses receptors for both GLP1 (Merchenthaler et al., 1999; Tang-Christensen et al., 2001; Cork et al., 2015; Lee et al., 2018; Maejima et al., 2021) and GLP2 (Tang-Christensen et al., 2000, 2001). Furthermore, amongst the hypothalamic regions, the DMH shows the highest susceptibility to diet-induced obesity (DIO, Zhang et al., 2020), which includes overexpression of the GLP1 receptor (GLP1R), binding both GLP1 and Oxm. We have also recently shown that high-fat diet (HFD; a rodent model of obesity, Winzell and Ahrén, 2004) disrupts the day/night rhythm in the neuronal activity of DMH cells down to the level of their electrophysiological properties (Sanetra et al., 2022a, 2022b) even before the development of obesity. Therefore, as a next step, we performed a complex analysis of GLP1, GLP2 and Oxm actions in the DMH, with a separation into three main sections: GLP1 and GLP2 receptor expression, neuronal sensitivity to the peptides of interest, and their abundance in different conditions.

First, in situ hybridisation was used to detect *Glp1r* and *Glp2r* mRNA and investigate their spatial distribution, as well as HFD-induced changes in their expression. Next, using ex vivo electrophysiology we recorded changes in the neuronal sensitivity to the PPG-derived peptides between light and dark phases of the 24 h cycle. Finally, as a representative of all three co-released substances we investigated the GLP1 immunoreactivity in the DMH under different metabolic states – fasted and fed, occurring either unpredictably, or after a period of time-restricted feeding. Here, we observed lower density of GLP1 immunoreactivity in hungry animals, but only for non-anticipated fasted state.

All protocols were performed on animals fed control (CD), or high-fat diet (HFD) for no longer than 4 weeks, in order to study potential HFD-evoked changes to the PPG signalling, developing even before the onset of obesity, at the time when the DMH circadian rhythmicity is already being altered (Sanetra et al., 2022a, 2022b). Our data show that short-term HFD impacts DMH neuronal responsiveness to Oxm and exendin-4 (Exn4, a selective GLP1R agonist), completely abolishing its dependence on the spontaneous activity. Furthermore, HFD-induced changes in the amount of GLP1 in various subdivisions of the DMH (compact – cDMH, dorsal – dDMH and ventral – vDMH), suppress its relationship with the metabolic state of the animal, indicating an uncoupling between peripheral and central regulators of metabolism. Finally, no difference between the diets occurs under restricted feeding (RF), when GLP1 immunoreactivity remains constant throughout the feeding cycle.

2. Materials and methods

2.1. Animal maintenance

All experiments were carried out in accordance with the Polish Animal Welfare Act of 23 May 2012 (82/2012) and the European Communities Council Directive (86/609/EEC), and had received approval from the Local Ethics Committee in Krakow (No. 18/2018, 349/2022).

Animals used in the study were male Sprague-Dawley (SD) rats, bred at the animal facility of the Institute of Zoology and Biomedical Research, Jagiellonian University in Krakow (Poland). Females were excluded due to probable interactions between the oestrous cycle and metabolism, especially during puberty. Rats were kept in constant environmental conditions (temperature ~ 23 °C, humidity ~65 %) and standard lighting conditions (LD 12:12), with water supplied ad libitum, and food supplied either also ad libitum or accordingly to the experimental protocols, as described in the following sections.

At the age of weaning (4 weeks), the animals were assigned to either control or experimental group. The first one was fed control diet (CD; ~3514 kcal/kg, fat content 4 %, energy from: 10 % fat, 24 % protein, 66 % carbohydrates, cat. no. C1090–10; Altromin International, Germany), whereas the experimental group received HFD (~5389 kcal/kg, fat content 42 %, energy from: 70 % fat, 16 % protein, 14 % carbohydrates, cat. no. C1090–70; Altromin International). Animals were maintained on the assigned diet until the end of the experiment (between 2 and 4 weeks).

2.2. In situ hybridisation

2.2.1. Tissue preparation

For the in situ hybridisation 6 rats (3 per diet) were used, after 4 weeks on a respective diet. The animals were sacrificed in the middle of the light phase (zeitgeber time - ZT6, where ZT0 is the onset of the light phase) by isoflurane inhalation (1 ml in the incubation chamber, Baxter, USA) followed by decapitation. Brains were quickly extracted, frozen on dry ice and stored at −80 °C. Sections including the DMH were cut on a cryostat (Leica CM1950, Germany) at −20 °C and thaw-mounted on Superfrost-Plus slides (Fisher Scientific, USA). Slices were then fixed for 15 min in a 4 % paraformaldehyde solution (PFA) in phosphate-buffered saline (PBS), rinsed in PBS (2 × 1 min), dehydrated in ethanol solutions of increasing concentrations (50 %, 70 % and 2 × 100 %, 5 min in each) and circled with a hydrophobic marker.

2.2.2. RNAscope assay

The assay was performed with the RNAscope multiplex in situ hybridization protocol (Advanced Cell Diagnostics—ACD, USA), which started with a 12-min long pre-treatment with protease IV. Next, the slides were rinsed in PBS (2 × 1 min) and incubated with probes targeting *Glp1r* and *Glp2r* (2 h at 40 °C). After that, the slides were rinsed in wash buffer (2 × 2 min) and a four-step-long signal amplification protocol was applied (3 × 30 min with AMP1–3 and 15 min with fluorophores: Atto 647 for *Glp1r* and Atto 550 for *Glp2r*, all at 40 °C). Following, the slides were rinsed again in wash buffer (2 × 2 min), and coverslipped with DAPI.

2.2.3. Image processing and analysis

Microphotographs were taken with an epifluorescence microscope (Axio Imager M2, Zeiss, Germany) and visualised in ZEN software (ZEN 2.5. blue edition, Zeiss), where *Glp1r*-positive neurons were manually counted, for each part of the DMH separately, and divided by the substructure area to obtain the density. Both probes, were also analysed as the density of the fluorescent signal, reflecting *Glp1r/Glp2r* mRNA abundance. For this, stacks were processed into a maximum intensity projection in ZEN 2.3. (black edition, Zeiss), followed by contrast enhancement and maxima count in ImageJ software (NIH, USA; Fiji: Schindelin et al., 2012).

2.3. Electrophysiology

2.3.1. Tissue preparation

All electrophysiological recordings were performed either during the day (cull between ZT1–3, recording starting at ZT6 ± 1 h) or at night (cull at ZT13–15, recording starting at ZT18 ± 1 h). Recording time never exceeded the end of the projected lighting phase (ZT12 for daytime or ZT24 for nighttime recordings).

After 2–4 weeks on a diet, the animals were anaesthetized with isoflurane (1 ml in the incubation chamber, Baxter) and sacrificed by decapitation. The brains were quickly removed and cut into 250 μm thick coronal slices containing the DMH with a vibroslicer (Leica VT1000S). Throughout the entire procedure, the brains were immersed in ice-cold, cutting artificial cerebro-spinal fluid (cACSF), containing (in mM): 25 $NaHCO_3$, 3 KCl, 1.2 Na_2HPO_4, 2 $CaCl_2$, 10 $MgCl_2$, 10 glucose, 125 sucrose with addition of a pH indicator, Phenol Red 0.01 mg/l, osmolality ~290 mOsmol/kg, continuously carbogenated (95 % O_2, 5 % CO_2). Before the start of the recoding, the slices were incubated for at least half an hour (MEA) or 2 h (patch clamp) in the recording artificial cerebro-spinal fluid (rACSF), containing: (in mM): 125 NaCl, 25 $NaHCO_3$, 3 KCl, 1.2 Na_2HPO_4, 2 $CaCl_2$, 2 $MgCl_2$, 5 glucose and 0.01 mg/l

of Phenol Red (initial temperature: 32 °C, cooled to room temperature).

2.3.2. Multi-electrode array recordings

2.3.2.1. Recording. Multi-electrode array recordings (MEA) were performed on a total of 17 animals (CD daytime: 3, HFD daytime: 3, CD nighttime: 5, HFD nighttime: 6), using MEA2100-System (Multichannel Systems GmbH, Germany; Belle et al., 2021). DMH-containing brain slices were placed on an 8 × 8 perforated electrode matrix (60pMEA100/30iR-Ti, Multichannel Systems), which ensured electrode coverage of the entire structure. Double perfusion system of the recording chamber was used, with the top circuit used for constant perfusion with fresh rACSF as well as drug application, and the bottom circuit crucial for establishing slight pressure sucking the slices into proximity with the recording electrodes. At least half an hour was waited for the set up to stabilise, after which the recordings started with another half an hour of baseline recording. Then, proglucagon-derived peptides were applied, one at a time, with at least an hour between consecutive applications, after the responding cells had fully recovered from the previous effect.

Signal was acquired with Multi Channel Experimenter software (Multichannel Systems), with a sampling frequency of 20 kHz.

2.3.2.2. Data analysis. Single-unit activity analysis was employed in order to quantify the percentage of responsive cells, and evaluate possible changes in the amplitude of the effect between the groups.

Multi Channel DataManager (Multichannel Systems GmbH) was used to export raw signal into HDF5 and CED-64 files. The HDF5 file was mapped and converted into DAT format, which then underwent automated spike-sorting with KiloSort programme (Pachitariu et al., 2016) in the MatLab environment. Parallelly, the CED-64 file was remapped and filtered with Butterworth band pass filter (fourth order) from 0.3 to 7.5 kHz by a custom-made Spike2 script. Spike-sorting results were merged with the CED-64 files (Spike2 8.11; Cambridge Electronic Design Ltd.) with a custom-written MatLab script. Such prepared files were then inspected manually, and all errors corrected using autocorrelation, crosscorrelation, principal component analysis (PCA) and spike shape inspection.

Data were analysed as firing frequency averaged over 30 s. Cells whose firing rate during the drug application varied from their mean baseline (~10 min) value by at least three standard deviations were pronounced sensitive and included in the analysis of the amplitude of the effect, with an exception of those not active spontaneously. The amplitude of the response was calculated as the maximal value during the response minus the averaged baseline.

2.3.3. Patch clamp

2.3.3.1. Recording. A brain slice containing the DMH was placed in the recording chamber positioned under an Axioskop 2 FS microscope fitted with infrared differential interference contrast (Göttingen, Germany). The chamber was constantly perfused with carbogenated rACSF, heated to 32 °C. The structure of interest was localised under 5× magnification, after which 40× objective was used to acquire whole-cell configuration. For this, borosilicate glass pipettes (Sutter Instruments, USA; resistance = 4–9 MΩ) filled with an intrapipette solution containing (in mM): 125 potassium gluconate, 20 KCl, 10 HEPES,2 MgCl2, 4 Na2ATP, 0.4 Na3GTP, 1 EGTA, and 0.05 % biocytin (pH = 7.4, adjusted with 5 M KOH; osmolality 300 mOsmol/kg) and mounted onto an Ag/AgCl electrode were used. Pressure necessary to obtain gigaseal, as well as rupture cellular membrane, was applied with Ez-gSEAL100B Pressure Controller (Neo Biosystem, USA). Recorded signal was amplified by a SC 05LX amplifier (NPI, Germany), low-pass filtered at 3 kHz, digitised at 20 kHz, and visualised using Signal and Spike 2 software (Cambridge Electronic Design Inc., UK).

Patch clamp experiments were performed in voltage clamp mode at −60 mV holding potential. A minimum of 300 s of stable baseline was recorded before Exn4/GLP2/Oxm administration and the recording continued for at least 1000 s after peptide application in order to ensure a complete washout of the drug. Throughout the entire recording, patch clamp stability was monitored by applying a rectangular voltage pulse (duration 1 s, amplitude 35 mV) every 60 s.

2.3.3.2. Immunohistochemical verification. At the end of the experiment the location of each recorded neuron was verified with immunofluorescence. All brain slices containing a recorded cell were fixed in 4 % PFA in PBS overnight. They were then rinsed in PBS (2 × 10 min) and incubated with 0.6 % Triton-X100 (Sigma-Aldrich, USA) and 10 % normal donkey serum (NDS; Jackson ImmunoResearch, USA) in PBS, for 3 h at room temperature. Primary antibodies solution (72 h at 4 °C) included Cy3-conjugated Extravidin (1:250, Sigma-Aldrich), binding biocytin in the recorded neuron, rabbit neuropeptide Y (NPY) antisera (1:8000, Sigma-Aldrich), used as a marker of the DMH, as well as 0.3 % Triton-X100 and 2 % NDS. After this step, the slices were rinsed in PBS (2 × 10 min) and incubated with secondary, anti-rabbit AlexaFluor 647-conjugated antisera (1:300; Jackson ImmunoResearch) in PBS for 24 h at 4 °C. Finally, the slices were rinsed once more (2 × 10 min), placed onto slides and coverslipped with Fluoroshield™ with DAPI (Sigma-Aldrich).

Immunostained slices were scanned with an epifluorescence microscope (Axio Imager M2, Zeiss). Different subdivisions of the DMH were recognised based on DAPI (smaller, densely packed cells in the cDMH), as well as NPY (dense fibres in both dDMH and vDMH, visibly less dense in cDMH or the neighbouring VMH; Fig. 3A).

2.3.3.3. Data analysis. From each recording we extracted three 100 s long segments, representative of the cells' postsynaptic activity during the baseline, peptide application, and after the washout of the drug. This enabled us to distinguish between genuine effect of the drug and a continuous drift in PSC generation during the experiment, independent of the tested stimulus. Postsynaptic currents (PSC) were counted in Mini Analysis Software (Synaptosoft, USA). Amplitude of the effect to the drug was calculated as the frequency of PSC during its application minus PSC frequency during the baseline, and compared between daytime/nighttime and dietary groups.

2.3.4. Drugs

Exendin-4 (Exn4; Tocris, UK) glucagon-like peptide 2 (GLP2; Sigma-Aldrich) and oxyntomodulin (Oxm; Tocris) were dissolved in 0.9 % NaCl at 100× concentration, aliquoted, and kept at −20 °C. During the experiment, the stock was diluted in fresh rACSF and applied by bath perfusion. The target concentration of all three drugs was 1 μM.

2.4. Immunofluorescence

2.4.1. Food deprivation (FD) protocol

The food deprivation (FD) protocol was performed on 36 rats (18 fed CD and another 18 fed HFD). After 4 weeks on a diet, the animals were divided into three treatment groups. The first group was an ad libitum-fed control, perfused at ZT14. The further two were food deprived for 48 h (starting and ending at ZT14), after which one of them was perfused straight away (the fasted condition, representing hunger), while the other one was allowed free access to food for the next 2 h (the refeed condition, representing satiety).

All animals were sacrificed between ZT14–17. First, the rats were anaesthetised by isoflurane inhalation (1 ml in the incubation chamber, Baxter) and sodium pentobarbital injection (100 mg/kg body weight, i.p.; Biowet, Poland). After no response to a tail pinch could be observed, transcardial perfusion was performed with PBS followed by 4 % PFA in PBS. Fixed brains were extracted and kept overnight in the same PFA

solution. The next day, 35 μm thick brain slices were cut using a vibroslicer (Leica VT1000S, Germany).

Immunofluorescent labelling started with a 30-min long non-specific site blocking and membrane permeabilization in PBS containing 0.5 % Triton-X100 (Sigma-Aldrich) and 5 % normal donkey serum (NDS, Jackson ImmunoResearch), at room temperature. Then, the slices were incubated with 0.5 % NDS, 0.3 % Triton-X100 and either rabbit anti-cFos antibodies (1:2000, Abcam, UK) or mouse anti-GLP1 antibodies (1:500, Santa Cruz Biotechnology, USA) in PBS for 24 h at 4 °C. After this step, the slices were rinsed in PBS (2 × 10 min) and transferred to a secondary antibodies solution (either AlexaFluor488-conjugated anti-rabbit or Cy3-conjugated anti-mouse antisera; 1:300, Jackson ImmunoResearch) in PBS overnight at 4 °C. After that, the slices were rinsed again (2 × 10 min), mounted onto glass slides and coverslipped with Fluoroshield™ with DAPI (Sigma-Aldrich).

Microphotographs were taken using an epifluorescence microscope (Axio Imager M2, Zeiss, Germany). The compact part of the DMH was recognised with DAPI, as a region of small, densely packed cells, of a characteristic shape. Then, three circular regions of interest (300 px in diameter) were outlined inside each of the DMH subdivisions. Density of the GLP1 fibres was analysed as area fraction (immunoreactive pixels/area) after background subtraction and image binarization via thresholding, averaged over the three measurements.

Cells immunoreactive for cFos were counted manually by a blinded experimenter, separately for each DMH subdivision within a particular slice, and the total area of each part was measured with ZEN 2.5 (blue edition; Zeiss). All cFos-immunoreactive neurons were also DAPI-positive. The analysis was performed on the density of the cFos-positive cells (cell count/area).

2.4.2. Restricted feeding (RF) protocol

The restricted feeding (RF) protocol was performed on 37 rats (18 fed CD and 19 fed HFD). The animals underwent 2 weeks of ad libitum feeding, after which they were fed in a restricted manner (food available between ZT14–20) for the following 2 weeks. Then, they were assigned to one of three groups. The first one was sacrificed 0.5 h before the scheduled meal, the second 1.5 h and the third 3.5 h after the onset of the scheduled meal. The perfusion, the immunofluorescent staining and the microphotograph processing were performed analogically to the procedure described in *2.4.1. Food deprivation protocol*, with the only differences being the concentration of the primary anti-GLP1 antibody (1:400) and both secondary antibodies (1:400).

2.5. Statistical analysis

Statistical analysis was performed in R (Version 4.0.4; Team, 2021) and RStudio (Version 1.4.1106, PBC; Team, 2015). Frequency of the response to the applied peptides was analysed with binomial regression (a generalised linear mixed effects model with a binomial response value), whereas for continuous outcome variables general linear models were fitted. To account for multiple observations from the same animal and/or brain slice a random effect was included in a mixed model (random intercepts for nested designs and random slopes for repeated measures). Mixed models were fitted with *lme4* and *lmerTest* packages (Bates et al., 2015; Kunzetsova et al., 2017) and analysed with type III ANOVA (with Satterthwaite's method for the degrees of freedom estimation). Outliers were detected with Bonferroni test from *car* package (Fox and Weisberg, 2019), detecting mean-shifting (influential) data points within the model. Post hoc analyses were performed using *emmeans* package (Lenth, 2021), and *p*-value corrected for multiple comparisons with Tukey method. Assumptions of a general linear model were checked with Shapiro-Wilk normality test from *rstatix* package (Kassambara, 2021) and Levene test for homoscedasticity from *car* package, normality of the residuals' distribution was analysed with QQ-plots (*ggpubr*; Kassambara, 2020). In the case of not meeting the normality or homogeneity assumptions the values were transformed either using odd roots (MEA and patch clamp – response amplitude: both positive and negative values) or Box-Cox (BC) transformation (for immunofluorescence – only positive values; package: *MASS*; Venables and Ripley, 2002), defined as: $BC(y) = (y^{\lambda}-1)/\lambda$, where λ is a value that provides the best approximation for the normal distribution of the response variable (Box and Cox, 1964). Detailed results from all the models are presented in Tables S1 (ANOVA results of the generalised linear models), S2 (ANOVA results of the general linear models), S3 (results of the multiple comparisons) and S4 (mean, SD and n values).

3. Results

3.1. Localisation of Glp1r and Glp2r mRNA in the DMH

Our study on the high-fat diet-evoked changes in the PPG signalling within the DMH started with a confirmation of *Glp1r* and *Glp2r* expression in the structure as well as its precise localisation using in situ hybridisation. In line with previous reports (Merchenthaler et al., 1999; Tang-Christensen et al., 2000, 2001; Cork et al., 2015; Lee et al., 2018; Maejima et al., 2021; Huang et al., 2022), we observed fluorescent signal from both *Glp1r*- and *Glp2r*-targeting probes within the DMH. Moreover, the two types of receptors appeared to occupy distinct subdivisions of the DMH, with little if any overlap or colocalization (Fig. 1A). *Glp1r* expression was restricted to individual cells within vDMH and dDMH, densely filled with the fluorescent probe. The analysis of the density of the *Glp1r*-positive cells confirmed the observed distribution ($F_{2,26} = 80.06$, $p < 0.0001$, $n = 36$), showing the highest abundance per area in the dDMH (dDMH vs vDMH: $t_{20} = 5.28$, $p = 0.0001$; dDMH vs cDMH: $t_{20} = 12.6$, $p < 0.0001$), followed by vDMH (vDMH vs cDMH: $t_{20} = 7.32$, $p < 0.0001$). No differences between the dietary groups were observed in any DMH subdivision (diet: $F_{1,4} = 0.009$, $p = 0.93$; diet × DMH div.: $F_{2,26} = 0.79$, $p = 0.46$, $n = 36$, Fig. 1B).

The intensity of *Glp1r* expression was analysed as the density of the fluorescent signal. Here, also differences within the DMH were spotted, with no dietary influence (diet: $F_{1,4} = 0.1$, $p = 0.76$; DMH div.: $F_{2,22} = 21.98$, $p < 0.0001$; diet × DMH div.: $F_{2,22} = 0.0061$, $p = 0.99$, $n = 39$). Interestingly, in this case vDMH and dDMH showed the same level of *Glp1r* expression ($t_{22} = 1.63$, $p = 0.25$), again higher than in the cDMH (vDMH vs cDMH: $t_{22} = 4.75$, $p = 0.0003$; dDMH vs cDMH: $t_{22} = 6.83$, $p < 0.0001$; Fig. 1C).

On the other hand, *Glp2r* mRNA was present predominantly in the cDMH ($F_{2,22} = 30.41$, $p < 0.0001$, $n = 39$; cDMH vs vDMH: $t_{22} = 7.31$, $p < 0.0001$; cDMH vs. dDMH: $t_{22} = 6.00$, $p < 0.0001$), with equally little *Glp2r* expressed in the other two subdivisions ($t_{22} = 1.31$, $p = 0.4$; Fig. 1C). Its expression appeared diffused across the entire cDMH area, which together with compactly packed neurons did not allow for a distinction of individual, *Glp2r*-positive cells.

3.2. Exn4/Oxm/GLP2 impact on the DMH neuronal firing

Despite extensive data on the presence of the GLP1 and GLP2 receptors in the DMH (Merchenthaler et al., 1999, Tang-Christensen et al., 2000, 2001, Cork et al., 2015, Lee et al., 2018, Maejima et al., 2021, Huang et al., 2022), their ability to induct cFos expression in the DMH (Tang-Christensen et al., 2000; Maejima et al., 2021; Huang et al., 2022), as well as the DMH-mediated influence of the PPG-derived peptides on the animals feeding behaviour (Maejima et al., 2021), our knowledge of their impact on the DMH electrophysiology is limited. Therefore, we performed a set of multi-electrode array (MEA) experiments on brain slices acquired from animals fed either CD or HFD, both during the day and at night (factor - LD).

All three tested peptides (Exn4, GLP2 and Oxm) were shown to impact the electrical activity of the DMH neurons, predominantly causing an increase in their firing rate. Although these receptors had been shown to localise in very specific parts of the structure, neurons responsive to the applied substances were spotted all over the structure,

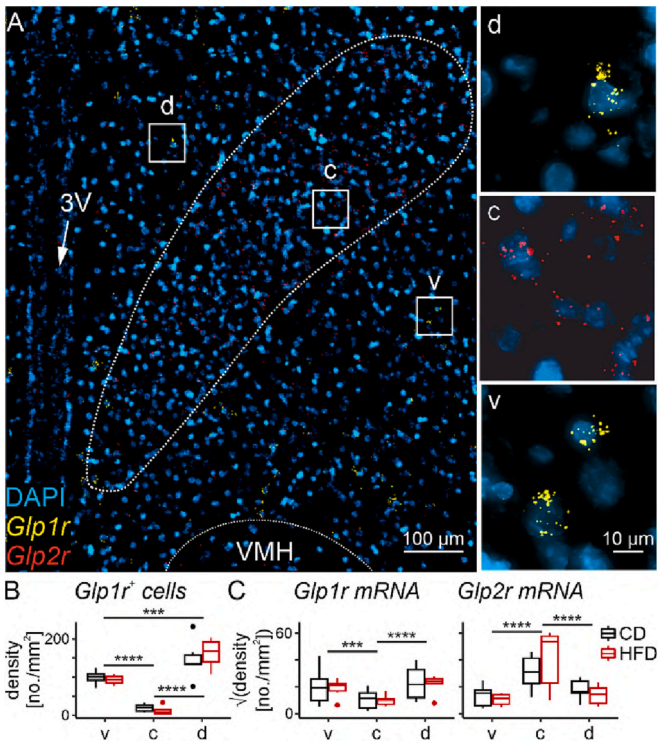

Fig. 1. *Localisation of Glp1r and Glp2r mRNA in the DMH*

A. Representative microphotograph of a brain slice acquired from a HFD-fed rat, tagged with probes for glucagon-like peptide 1 receptor (*Glp1r*) and glucagon-like peptide 2 receptor (*Glp2r*), together with DAPI staining, indicating the location of the compact part of the DMH (c) as the region of densely packed cells. Each of the DMH subdivisions was additionally zoomed-in, in order to better visualise the specific distribution of both signals, with *Glp1r* being restricted to the ventral (v) and dorsal (d) parts of the structure, and *Glp2r* mostly present in the cDMH. 3 V – third ventricle, VMH – Ventromedial Hypothalamus.

B. Graphs presenting the results from the analysis of the density of *Glp1r*-positive cells (diet: $F_{1,4} = 0.009$, $p = 0.93$; DMH div.: $F_{2,26} = 80.06$, $p < 0.0001$; diet × DMH div.: $F_{2,26} = 0.79$, $p = 0.46$, $n = 36$).

C. Graphs presenting the results from the analysis of the density of *Glp1r* (diet: $F_{1,4} = 0.1$, $p = 0.76$; DMH div.: $F_{2,22} = 21.98$, $p < 0.0001$; diet × DMH div.: $F_{2,22} = 0.0061$, $p = 0.99$, $n = 39$) and *Glp2r* mRNA (diet: $F_{1,4} = 0.015$, $p = 0.91$; DMH div.: $F_{2,22} = 30.41$, $p < 0.0001$; diet × DMH div.: $F_{2,22} = 2.93$, $p = 0.074$, $n = 39$). ***$p < 0.001$, ****$p < 0.0001$. Box-and-whisker plots present the median value, the interquartile range (IQR; box) and the minimum-to-maximum range of values, not exceeding 1.5 * IQR (whiskers). Data points outside this range are plotted individually.

with no clear spatial pattern in the magnitude of the effect either (Fig. 2A, E, I). The percentage of cells responsive to GLP2 and Oxm did not differ between the experimental groups (GLP2: CD daytime - 34.48 %, CD nighttime - 52.63 %, HFD daytime - 35.46 %, HFD nighttime - 44.68 %; diet: $\chi^2_1 = 0.0051$, $p = 0.94$; LD: $\chi^2_1 = 2.98$, $p = 0.085$, diet × LD: $\chi^2_1 = 0.15$, $p = 0.7$, $n = 352$; Oxm: CD daytime: 50 %, CD nighttime: 38.46 %, HFD daytime: 44.79 %, HFD nighttime: 44.74 %%; diet: $\chi^2_1 = 0.19$, $p = 0.67$; LD: $\chi^2_1 = 1.4$, $p = 0.24$, diet × LD: $\chi^2_1 = 1.09$, $p = 0.3$, $n = 363$), however the sensitivity to Exn4 was increased under HFD (CD daytime: 42.86 %, CD nighttime: 46 %, HFD daytime: 65.05 %, HFD nighttime: 50 %; diet: $\chi^2_1 = 7.68$, $p = 0.0056$; LD: $\chi^2_1 = 0.11$, $p = 0.74$, diet × LD: $\chi^2_1 = 2.46$, $p = 0.12$, $n = 316$). Moreover, when comparing the types of responses (increase vs. decrease in firing rate) we noticed a higher percentage of cells lowering their frequency of action potential generation at night than during the day, for all three peptides (Exn4: diet: $\chi^2_1 = 1.14$, $p = 0.29$; LD: $\chi^2_1 = 5.08$, $p = 0.024$, $n = 167$; Oxm: diet: $\chi^2_1 = 1.11$, p = 0.29; LD: $\chi^2_1 = 4.33$, $p = 0.037$, $n = 163$; GLP2: diet: $\chi^2_1 = 0.3$, $p = 0.59$; LD: $\chi^2_1 = 4.69$, p = 0.03, $n = 143$; Fig. 2D, H, L). Nevertheless, those cells constituted a vast minority, and their total number did not allow for statistical comparison of the amplitude of the effect between the groups. We also excluded cells which were completely silent during baseline recording ($n = 8$; total for all peptides), as their response could be highly dependent on the magnitude of hyperpolarisation below the threshold for action potential generation.

We have previously shown that HFD-feeding increases spontaneous activity in the DMH during the day (Sanetra et al., 2022b). Baseline firing rate might alone be an important factor influencing the magnitude of a response to a drug, therefore we have added it to the model as a covariate, and run an ANCOVA to find out whether there are any differences in the relationship between neuronal spontaneous activity and the amplitude of the response to Exn4/GLP2/Oxm between our dietary/LD groups.

Taking into account all predictors in the model, HFD was shown to reduce the amplitude of the response to both Exn4 ($F_{1,73} = 4.78$, $p = 0.032$, $n = 122$) and Oxm ($F_{1,77} = 7.91$, $p = 0.0062$, $n = 130$). However, a strong correlation with baseline activity was also observed (Exn4: $F_{1,106} = 9.04$, $p = 0.0033$, n = 122; Oxm: $F_{1,122} = 11.78$, $p = 0.00082$, n = 130), as well as an interaction between the diet and the baseline activity (Exn4: $F_{1,106} = 6.05$, $p = 0.016$, n = 122; Oxm: $F_{1,122} = 6.31$, $p = 0.013$, n = 130; Fig. 2B-C, 2F-G), indicating that the link between cells' spontaneous and evoked activity becomes disrupted under HFD. In the case of GLP2, only an effect of baseline firing rate was significant ($F_{1,107} = 10.69$, $p = 0.0015$, $n = 115$), with no changes between the dietary groups ($F_{1,107} = 0.0052$, $p = 0.94$, n = 115; Fig. 2J-K).

These results provide an insight into HFD-mediated changes in DMH neurons' sensitivity to Exn4 and Oxm, and negate HFD influence on the responsiveness to GLP2.

3.3. Exn4/Oxm/GLP2 impact on the synaptic network in the DMH

Lack of a specific spatial distribution in the responsiveness to the PPG-derived peptides contrasting a clear separation in the receptor expression led us to hypothesise that observed effects may attribute to a mix of postsynaptic and network-driven actions of PPGs. In order to confirm such phenomenon, we performed a patch-clamp study in voltage clamp mode, and analysed changes in the frequency of the postsynaptic currents (PSC) due to the drug application between our diet/LD groups. Thanks to the post-recording immunostaining, we were able to pinpoint the exact location on the recorded cell (DMH division: dDMH, cDMH or vDMH; Fig. 3A) and add it to the model as a covariate, however in no case was it statistically significant (Exn4: $F_{2,43} = 2.78$, $p = 0.073$, $n = 57$; Oxm: $F_{2,43} = 1.45$, $p = 0.25$, $n = 49$; GLP2: $F_{2,36} = 0.33$, $p = 0.72$, $n = 43$).

Various responses were spotted after Exn4/Oxm/GLP2 bath application, including both an increase (Fig, 3B) and a decrease in PSC frequency, as well as no effect. The response to GLP2 was shown to depend only on the time of day ($F_{1,26} = 10.14$, $p = 0.0038$, n = 43) with higher values during daytime regardless of the diet fed ($F_{1,26} = 0.33$, $p = 0.57$, n = 43), whereas the responsiveness to Exn4 was also influenced by the diet (diet × LD: $F_{1,22} = 5.01$, $p = 0.036$, n = 57). HFD group presented a higher response amplitude than the CD during the day ($t_{24} = 2.08$, $p = 0.048$), which caused a strong day/night difference in this group ($t_{27} = 3.73$, $p = 0.0009$). Contrary to the results obtained with the MEA, the PSC frequency response to Oxm did not follow the pattern observed for Exn4, as no changes were spotted between any of the groups (LD: $F_{1,25} = 0.96$, $p = 0.34$, diet: $F_{1,25} = 3.76$, $p = 0.064$, LD × diet: $F_{1,25} = 0.59$, $p = 0.45$, $n = 49$; Fig. 3C).

These data confirm the synaptic mediation of Exn4 and GLP2 effects, which could be happening either directly by activating presynaptic receptors or via postsynaptic response. Either way, the cue of the PPG-derived peptides, despite locally distributed receptors, appears to get spread out throughout the entire structure due to the synaptic network. On top of that, our results suggest that this process varies between day and night for both Exn4 and GLP2, and changes under HFD for Exn4, but

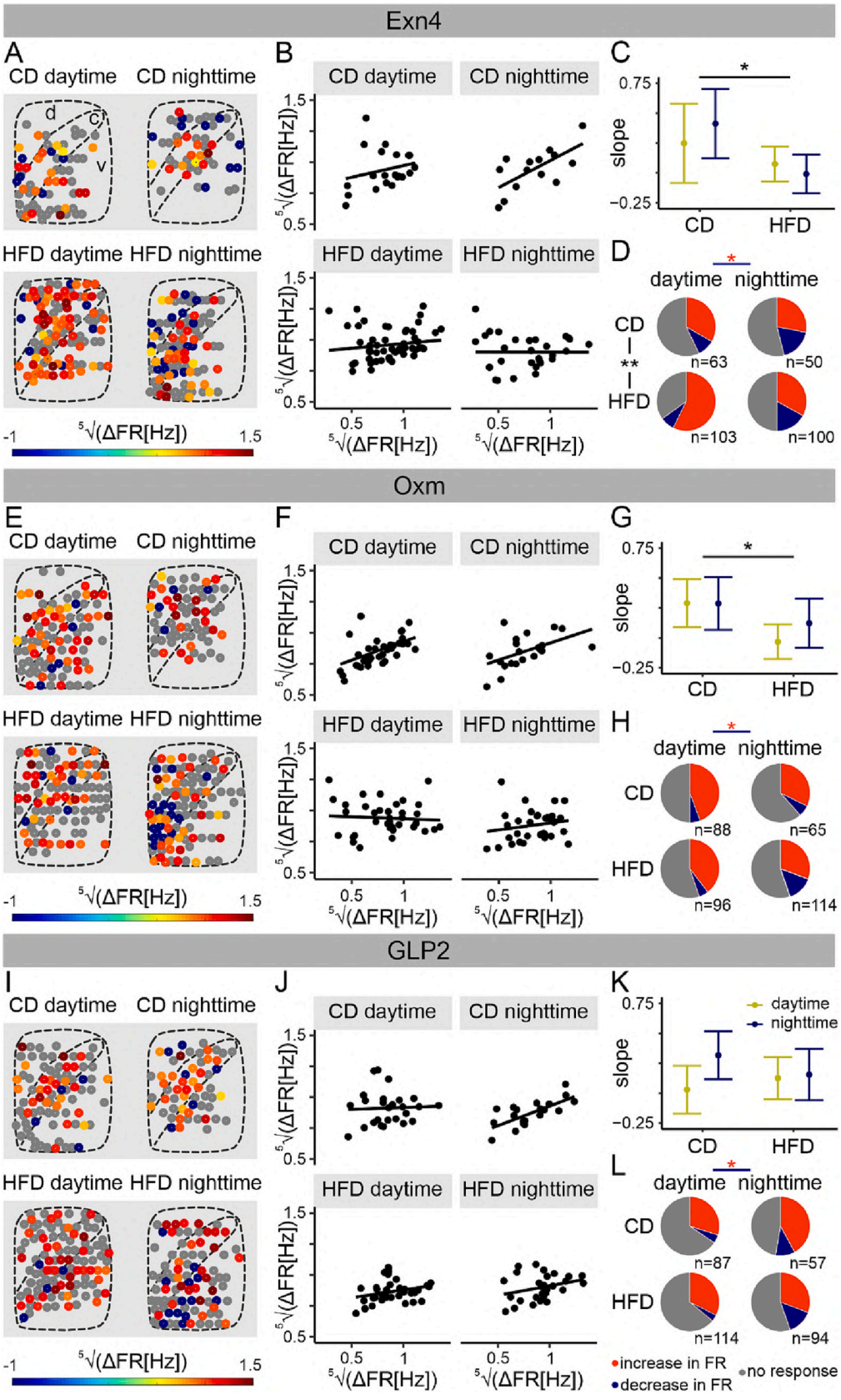

Fig. 2. *Exn4/Oxm/GLP2 impact on the DMH neuronal firing*

A, E, I. Spatial distribution of the cells sensitive to Exn4 (A)/Oxm (E)/GLP2 (I) together with colour-coded amplitude of the response to the tested peptides. Grey colour indicates non-responsive neurons. DMH subdivisions are indicated as: c – compact, d – dorsal, v – ventral.

B - C, F - G, J - K. Correlation of the amplitude of the excitatory response to Exn4 (B)/Oxm (F)/GLP2 (J) and the baseline activity for each of the diet/LD groups. Analysis of the regression slopes revealed differences between the diets for Exn4 ($F_{1,106} = 6.05$, $p = 0.016$, $n = 122$; C) and Oxm ($F_{1,122} = 6.31$, $p = 0.013$, $n = 130$; G), but not for GLP2 ($F_{1,107} = 0.11$, $p = 0.74$, $n = 115$; K). Slope values presented as estimate ±95 % CI.

D, H, L. Pie charts representing proportions of cells sensitive to Exn4 (D)/Oxm (H)/GLP2 (L), as well as responding with increase and decrease in firing rate (FR). Higher number of neurons was sensitive to Exn4 in the HFD group compared to CD ($\chi^2_1 = 7.68$, $p = 0.0056$, $n = 316$). For each peptide, the percentage of cells responding with a decrease in FR was higher at night than during the day (Exn4: $\chi^2_1 = 5.08$, $p = 0.024$, $n = 167$, Oxm: $\chi^2_1 = 4.33$, $p = 0.037$, $n = 163$, GLP2: $\chi^2_1 = 4.69$, $p = 0.03$). Black asterisks indicate differences in the total number of responsive cells, whereas red ones present the results of the analysis comparing cells responding in different ways within the sensitive population. CD – control diet, Exn4 – exendin-4, GLP2 – glucagon-like peptide 2, HFD – high-fat diet, Oxm – oxyntomodulin. *$p < 0.05$, **$p < 0.01$.

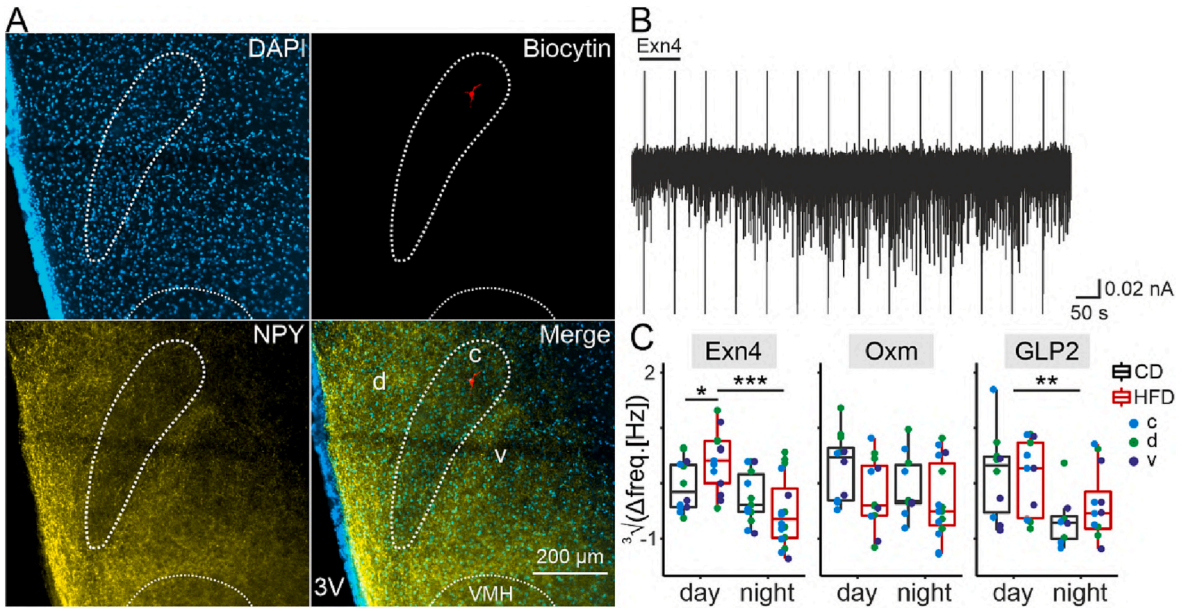

Fig. 3. *Exn4/Oxm/GLP2 impact on the synaptic network in the DMH*

A. Representative microphotographs presenting a post-recording immunostained brain slice. The recorded neuron is visible due to biocytin presence inside the intrapipette solution. DAPI, and well as neuropeptide Y (NPY) were used to outline the different subdivisions of the DMH: the compact (c) part, recognised as densely packed cells with little NPY immunoreactivity, separating the structure into dorsal (d) and ventral (v) parts. 3 V – third ventricle, VMH – Ventromedial Hypothalamus.

B. Representative recording showing a transient increase in post-synaptic currents (PSC) after exendin-4 (Exn4) application.

C. Comparison of the PSC frequency (freq.) between dietary (control – CD vs high-fat diet – HFD) and LD (day/night) groups for each of the investigated peptides: Exn4 (diet: $F_{1,21} = 0.76$, $p = 0.39$; LD: $F_{1,22} = 9.79$, $p = 0.0048$, DMH div.: $F_{2,43} = 2.78$, $p = 0.073$; diet × LD: $F_{1,22} = 5.01$, $p = 0.036$, $n = 57$; day: $t_{24} = 2.08$, $p = 0.048$, HFD: $t_{27} = 3.73$, $p = 0.0009$), Oxm (LD: $F_{1,25} = 0.96$, $p = 0.34$, diet: $F_{1,25} = 3.76$, $p = 0.064$, DMH div.: $F_{2,43} = 1.45$, $p = 0.25$, LD × diet: $F_{1,25} = 0.59$, $p = 0.45$, $n = 49$) and GLP2 (LD: $F_{1,26} = 10.14$, $p = 0.0038$, diet: $F_{1,26} = 0.33$, $p = 0.57$, DMH div.: $F_{2,36} = 0.33$, $p = 0.72$, LD × diet: $F_{1,26} = 0.73$, p = 0.4, $n = 43$). $^{*}p < 0.05$, $^{**}p < 0.01$, $^{***}p < 0.001$. Box-and-whisker plots present the median value, the interquartile range (IQR; box) and the minimum-to-maximum range of values, not exceeding 1.5 * IQR (whiskers). Data points are colour coded to visualise the lack of differences between DMH subdivisions.

not Oxm, also signalising differences between the mechanisms underlying the action of these two peptides.

3.4. Density and distribution of GLP1-immunoreactive fibres and cFos-positive cells in the DMH under different metabolic states

Potential changes in PPG signalling could be occurring on two distinct levels: sensitivity of the DMH neurons to these peptides, and/or the amount of the peptides released. Therefore, after observing differences in the responsiveness of the DMH cells between the diets, we decided to investigate the density of GLP1-positive neuronal fibres, as a representative of the amount of the co-released peptides present in the structure. Keeping in mind, that PPG-derived peptides are involved in satiety signalling, and their production as well as release might depend on the animals' metabolic states, we performed the immunofluorescence staining under three different conditions for each dietary group. The first group was an ad libitum-fed control, the second was food-deprived for 48 h (hunger state), and the third one was also food-deprived for 48 h, but then refed for 2 h (satiety state).

In order to confirm a lack of difference in body weight after 4 weeks on a diet the animals were weighed once a week, starting at week 0 (the onset of the experiment). As previously (Chrobok et al., 2022; Sanetra et al., 2022b), we observed time-related increase in the weight of the rats ($F_{4,34} = 1636.53$, $p < 0.0001$, $n = 36$) and an interaction between the diet and the week ($F_{4,34} = 8.34$, $p < 0.0001$, $n = 36$), but no significant effect of HFD feeding at any time point ($F_{1,34} = 0.022$, $p = 0.88$, n = 36; week 4: $t_{34} = -0.73$, $p = 0.47$; Fig. 4B). The adequacy of the experimental protocol was verified by analysing stomach mass after cull. Food-deprived group (FD) had significantly lighter stomachs than either the ad libitum (AL, $F_{2,30} = 255.83$, $p < 0.0001$, n = 36, $t_{30} = -7.68$, $p < 0.0001$), or refed groups ($t_{30} = -22.27$, $p < 0.0001$), and the latter one was also heavier than the control group ($t_{30} = 14.59$, $p < 0.0001$). On top of that, stomachs obtained from HFD-fed animals were lighter than the CD group ($F_{1,30} = 6.45$, $p = 0.017$, n = 36; Fig. 4C), also in line with our previous reports of decreased food intake (total food mass) in these rats (Chrobok et al., 2022, Sanetra et al., 2022b).

As documented by Renner et al. (2012), vast majority of the GLP1-positive fibres occupied the ventral subdivision of the DMH, with some present in the dorsal part, and very little in *pars compacta* ($F_{2,112} = 129.23$, $p < 0.0001$, $n = 186$). However, an interaction with the diet was also noted ($F_{2,112} = 3.46$, $p = 0.035$, n = 186), suggesting different susceptibility of the three substructures to HFD. Furthermore, a significant interaction between diet and treatment (metabolic state) indicated changes in the dependence of the GLP1-immunoreactivity on the satiety state between the dietary groups ($F_{2,28} = 3.74$, $p = 0.036$, n = 186). Indeed, the GLP1 fibre density was greater after the refeed than during food deprivation in both dDMH ($t_{72} = 2.84$, $p = 0.016$) and vDMH ($t_{72} = 2.95$, $p = 0.012$) and also during ad libitum feeding in vDMH ($t_{66} = 2.83$, $p = 0.017$), but only for CD-fed rats. HFD completely abolished the observed phenomenon. In dDMH this happened due to an increased GLP1-immunoreactivity during food deprivation ($t_{72} = 2.62$, $p = 0.011$), whereas in the vDMH, fibre density during the refeed appeared near-to-significantly lower than for the control diet ($t_{62} = -1.94$, $p = 0.057$; Fig. 4A, D). All back-transformed mean + 95 % CI values for each group can be found in Table S4.

DMH has been shown to respond to satiety with an intense cFos expression, predominantly in cells located in close proximity to the GLP1-immunoreactive fibres (Renner et al., 2012; Huang et al., 2022). The study by Renner et al. (2012) also showed that this cFos expression is partially mediated by the GLP1-positive NTS neurons sending projections to the DMH. Therefore, we also analysed the density of cFos-positive cells in the same conditions as done for GLP1

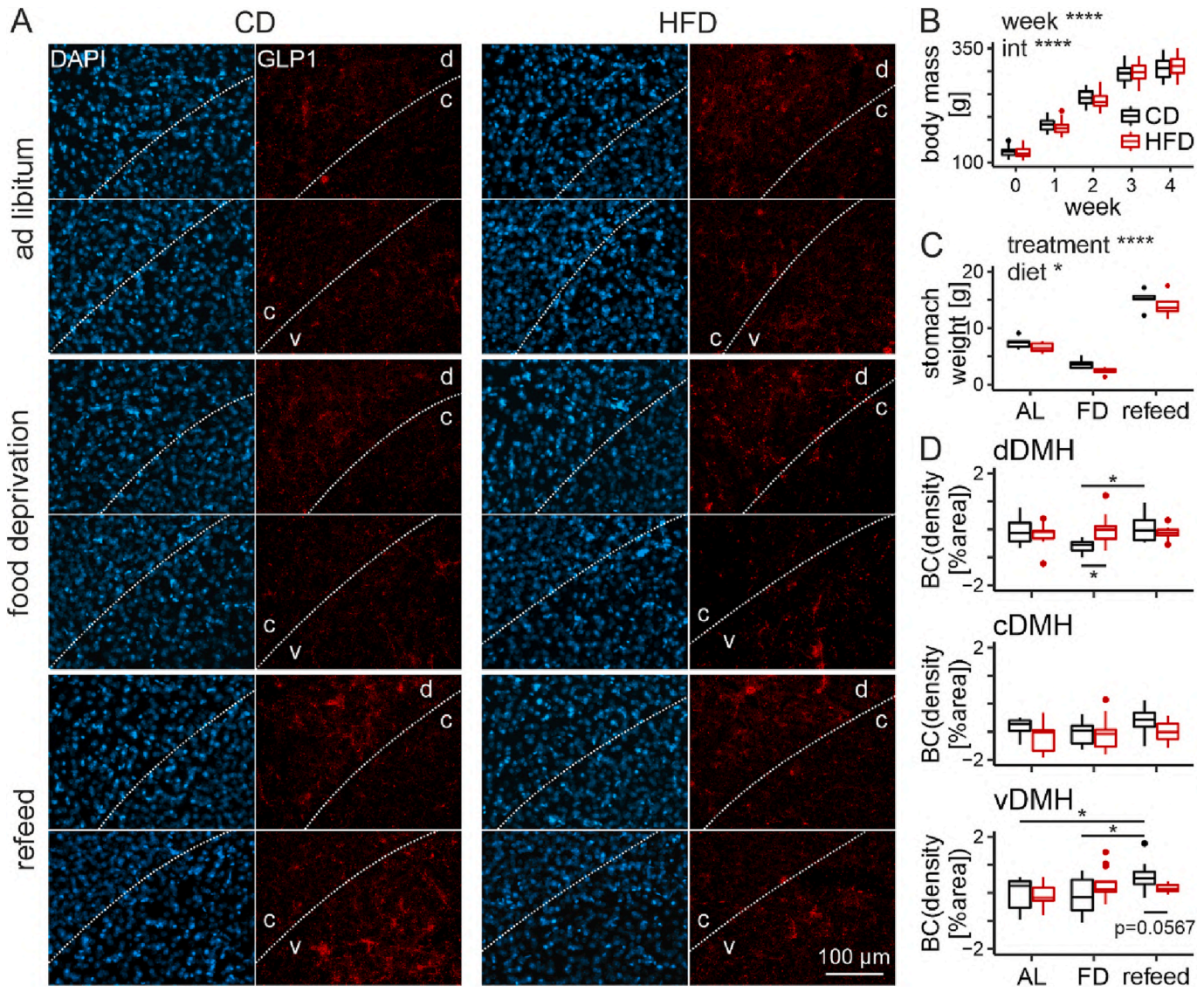

Fig. 4. *GLP1-immunoreactive fibre density in the DMH under different metabolic states*

A. Representative microphotographs visualising GLP1-positive fibres in different parts of the DMH. The highest density was observed in the ventral part of the structure (v), followed by the dorsal part (d) and the lowest in the compact part (c; $F_{2,112} = 129.23$, $p < 0.0001$, $n = 186$).

B. Comparison of body mass for control (CD) and high-fat diet (HFD)-fed rats across the 4 weeks of the experiment (week: $F_{4,34} = 1636.53$, $p < 0.0001$; diet: $F_{1,34} = 0.022$, $p = 0.88$; week × diet: $F_{4,34} = 8.34$, $p < 0.0001$, $n = 36$).

C. Comparison of the stomach weight at the end of the experimental procedure (treatment: $F_{2,30} = 255.83$, $p < 0.0001$; diet: $F_{1,30} = 6.45$, $p = 0.017$; treatment × diet: $F_{2,30} = 0.084$, $p = 0.92$, n = 36).

D. Comparison of the GLP1 immunoreactivity between dietary/treatment groups for each of the DMH subdivisions (diet: $F_{1,28} = 0.4$, $p = 0.53$; treatment: $F_{2,28} = 3.17$, $p = 0.058$; DMH div.: $F_{2,112} = 129.23$, $p < 0.0001$; diet × treatment: $F_{2,28} = 3.74$, $p = 0.036$; diet × DMH div.: $F_{2,112} = 3.46$, $p = 0.035$; treatment × DMH div.: $F_{4,112} = 1.41$ $p = 0.24$; diet × treatment × DMH: $F_{4,112} = 0.83$, $p = 0.51$; $n = 186$). BC—Box–Cox transformed values ($\lambda = 0.1414$), AL – ad libitum, FD – food deprivation, *$p < 0.05$, ****$p < 0.0001$. Box-and-whisker plots present the median value, the interquartile range (IQR; box) and the minimum-to-maximum range of values, not exceeding 1.5 * IQR (whiskers). Data points outside this range are plotted individually.

immunoreactivity, to see whether HFD-related changes in GLP density translate onto cellular activity of the DMH neurons.

Similarly to the results from the analysis of the GLP1-immunoreactivity, the density of cFos positive cells in the vDMH was also higher after the refeed comparing to either FD or AL groups ($F_{2,29} = 13.86$, $p < 0.0001$, $n = 204$; CD FD vs refeed: $t_{46} = -4.07$, $p = 0.0005$; AL vs refeed: $t_{50} = -3.23$, $p = 0.0062$), however in the case of cFos this effect was also present for the HFD-fed rats (FD vs refeed: $t_{46} = -4.95$, $p < 0.0001$; AL vs refeed: $t_{48} = -3.4$, $p = 0.0039$). Interestingly, a difference between the diets was observed in the density of cFos-positive cells after refeeding in the cDMH ($t_{41} = -2.87$, $p = 0.0064$), with higher numbers under HFD, which caused cFos density to vary between FD and refeed conditions also in this part of the structure ($t_{46} = -4.8$, $p = 0.0001$; Fig. 5). Same as for GLP1 immunoreactivity, generally the highest density of cFos-positive cells was observed in the vDMH, and the lowest in the cDMH ($F_{2,124} = 154.85$, $p < 0.0001$, n = 204), which was most apparent for the refed groups (Fig. 5A).

These results show that although HFD disrupts GLP1 satiety signalling in relation to the amount of peptide present in the structure, the cellular response to a refeed condition in the form of cFos expression remains mostly unchanged, possibly due to the abundance of other signalling molecules, or various compensatory mechanisms.

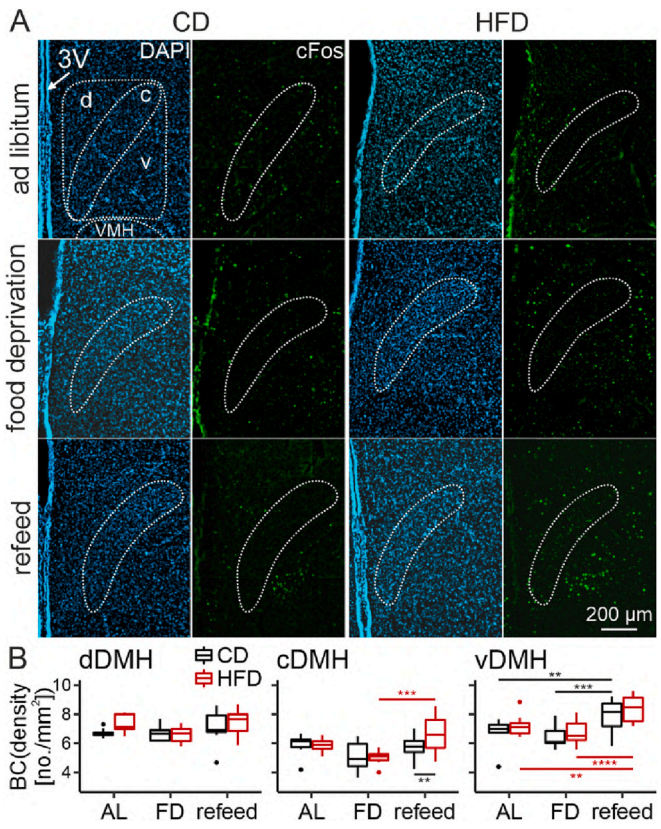

Fig. 5. *Density and distribution of cFos-positive cells in the DMH under different metabolic states*

A. Representative microphotographs presenting brain slices acquired from each dietary (CD – control diet, HFD – high-fat diet) and treatment group (AL – ad libitum, FD – food deprivation, and refeed). 3 V – third ventricle, VMH – Ventromedial Hypothalamus.

B. Graphs presenting the results from the analysis performed for each DMH subdivision separately (c – compact, d – dorsal, v – ventral; diet: $F_{1,29} = 2.87$, $p = 0.1$; treatment: $F_{2,29} = 13.86$, $p < 0.0001$; DMH div.: $F_{2,124} = 154.85$, $p < 0.0001$; diet × treatment: $F_{2,29} = 0.66$, $p = 0.53$; diet × DMH div.: $F_{2,124} = 0.21$, $p = 0.81$; treatment × DMH div.: $F_{4,124} = 7.98$, $p < 0.0001$; diet × treatment × DMH: $F_{4,124} = 2.88$, $p = 0.026$; $n = 204$). BC—Box–Cox transformed values ($\lambda = 0.1010$). $^{**}p < 0.01$, $^{***}p < 0.001$, $^{****}p < 0.0001$. Box-and-whisker plots present the median value, the interquartile range (IQR; box) and the minimum-to-maximum range of values, not exceeding 1.5 * IQR (whiskers). Data points outside this range are plotted individually.

3.5. Density and distribution of GLP1-immunoreactive fibres and cFos-positive cells in the DMH under restricted feeding (RF)

The DMH is well known for its susceptibility to time-restricted feeding, influencing clock gene expression (Mieda et al., 2006; Verwey et al., 2007, 2008, 2009; Minana-Solis et al., 2009), cFos immunoreactivity (Gooley et al., 2006; Verwey et al., 2007) and electrical activity (Sanetra et al., 2022b) within the structure. Thus, we repeated our immunofluorescent staining on animals which had been fed in a restricted manner. For this we used 37 rats (18 fed CD and 19 fed HFD), which were initially fed ad libitum (first 2 weeks), and then for the next 2 weeks were allowed unlimited access to food but only between ZT14–20. At the end of the protocol animals were perfused either half an hour before (time point −0.5 h), 1.5 h or 3.5 h after the onset of the scheduled meal.

Consistently with the FD protocol the rats were weighed every week (for the duration of the RF protocol – weeks 2–4), and again despite a significant interaction between diet and week ($F_{2,28} = 4.13$, $p = 0.027$, $n = 37$; Fig. 6A) the HFD-fed group did not become heavier than the control during the experiment (week 4: $t_{35} = 0.9$, $p = 0.37$). Here, we also weighed the food provided, and left after the meal in order to calculate the amount eaten during the 6 h window. Similarly to the data presented before (Chrobok et al., 2022; Sanetra et al., 2022b), HFD-fed animals were shown to eat fewer grams ($F_{1,35} = 104.8$, $p < 0.0001$, $n = 37$), but more calories per kilogram of body mass ($F_{1,35} = 56.64$, $p < 0.0001$, n = 37), however in the second case, this effect was only temporary, and disappeared completely by the end of the 4th week ($t_{35} = 1.3$, $p = 0.2$; Fig. 6A). Surprisingly, and unlike previously, the stomachs of HFD-fed animals were not lighter than the control group ($F_{1,31} = 0.035$, $p = 0.85$, n = 37), only differences between conditions (time before/after the meal onset) were spotted ($F_{2,31} = 139.24$, $p < 0.0001$, n = 37; Fig. 6A).

Also contrary to the FD protocol, the density of GLP1-positive neuronal fibres remained unaltered by the anticipated metabolic state ($F_{2,25} = 0.054$, $p = 0.95$, $n = 234$), neither did it depend on the diet ($F_{1,25} = 0.42$, $p = 0.52$, n = 234). The only significant factor here was the DMH division ($F_{2,144} = 146.05$, $p < 0.0001$, n = 234), which unsurprisingly showed the same pattern as in the previous experiment – majority of the GLP1 fibres located in the vDMH, and the lowest density in the cDMH (Fig. 6B-C).

The same spatial distribution was observed for the density of cFos-positive cells ($F_{2,170} = 104.37$, $p < 0.0001$, $n = 273$). On the other hand, cFos-immunoreactivity, unlike the GLP1 density, varied depending on the perfusion time in relation to meal onset ($F_{2,28} = 21.7$, $p < 0.0001$, n = 273). Although the effect of the diet was not significant ($F_{1,28} = 0.067$, $p = 0.8$, n = 273), we observed an interaction between diet and DMH division ($F_{2,170} = 5.78$, $p = 0.0037$, n = 273), as well as between the DMH division and the time of cull ($F_{4,170} = 3.96$, $p = 0.0042$, n = 273; Fig. 6D-E). For each structure and both diets the lowest density of cFos-positive cells was recorded before the scheduled meal, comparing to both time points after the onset of the meal. The only difference between the diets regarded the density of cFos-immunoreactive cells 1.5 h after meal onset in the vDMH, being lower under HFD ($t_{33} = -2.15$, $p = 0.039$; Fig. 6D-E). All cFos-immunoreactive cells colocalised with DAPI (Fig. 6F).

The results presented in this section indicate differences in both GLP1 and cFos immunoreactivity in response to hunger and satiety depending on their predictability. Moreover, the susceptibility to HFD also appears to change when these metabolic states had been anticipated.

4. Discussion

The presented study investigated PPG signalling in the DMH, together with its HFD-induced alterations, on multiple levels from the distribution of the receptors, through the peptide amount in different conditions, up to the neuronal sensitivity.

4.1. GLP1 and GLP2 receptor and GLP1 fibre spatial distribution

First, in situ hybridisation was used to confirm a very specific spatial pattern of the *Glp1r* and *Glp2r* mRNA for both diets. As observed by others (Merchenthaler et al., 1999; Tang-Christensen et al., 2000, 2001; Cork et al., 2015; Lee et al., 2018; Maejima et al., 2021), both receptors were found by us to be expressed within the DMH, with GLP2R present almost exclusively within the cDMH (Tang-Christensen et al., 2000, 2001), and GLP1R mostly outside of it (Renner et al., 2012), although in the second case there are inconsistencies between studies, with some showing a more even coverage of the *Glp1r*-expressing cells across the structure (Cork et al., 2015; Maejima et al., 2021). Differences could stem from species-specificity (mouse vs. rat), or probe sensitivity, failing to detect the signal in some cells. Even though the signal acquired appeared very intense and dense in the neurons where it was spotted, there is a possibility of much lower expression in other cells, resulting in a barely detectable signal, which would not have been counted as a *Glp1r*-expressing cell. For this reason, as well as to investigate the level

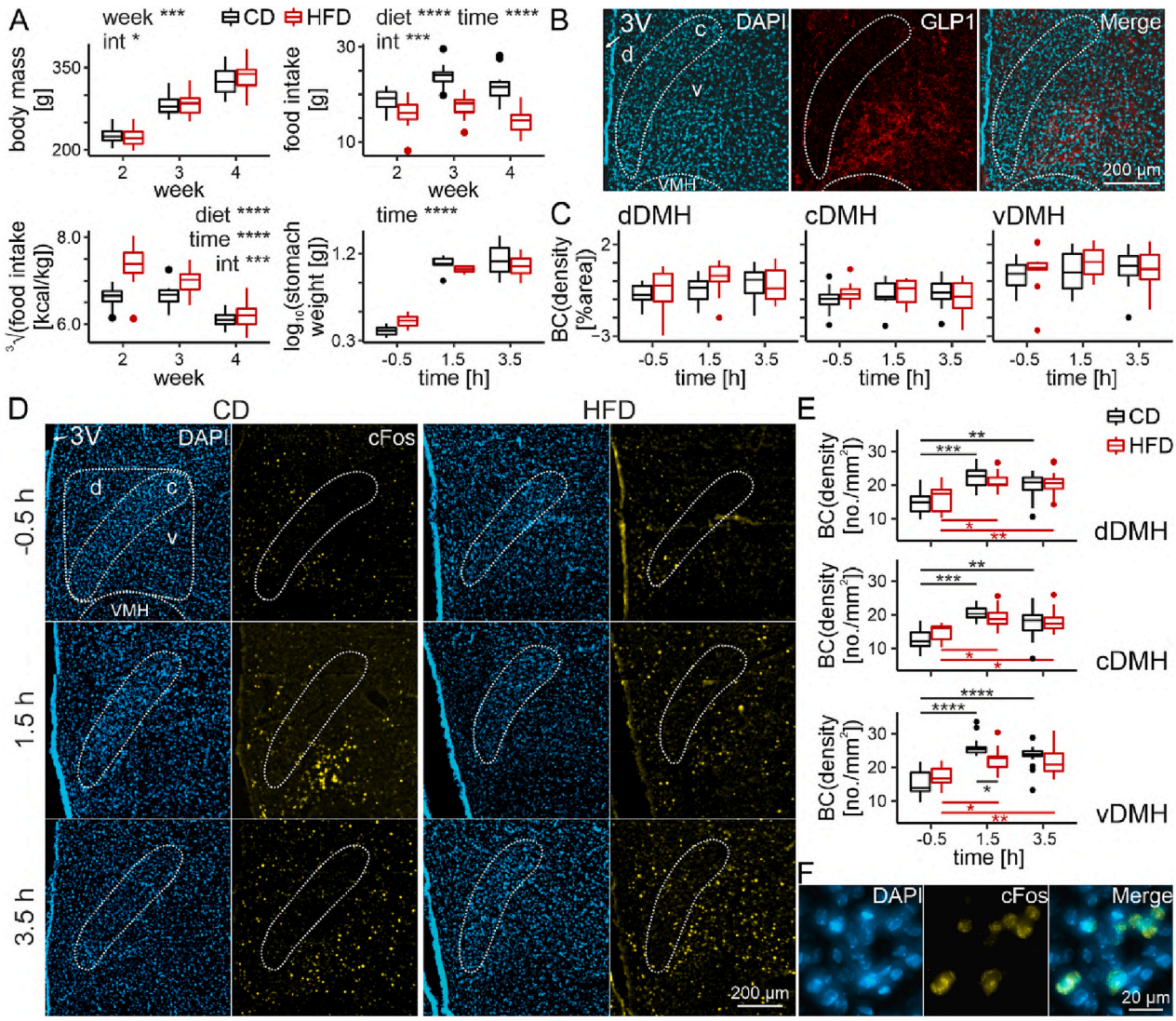

Fig. 6. *Density and distribution of GLP1-immunoreactive fibres and cFos-positive cells in the DMH under restricted feeding (RF)*

A. Graphs presenting body weight (week: $F_{2,28} = 1485.61$, $p < 0.0001$; diet: $F_{1,35} = 0.098$, $p = 0.76$; week × diet: $F_{2,28} = 4.13$, $p = 0.027$, $n = 37$), total meal size in grams (week: $F_{2,35} = 30.96$, $p < 0.0001$; diet: $F_{1,35} = 104.8$, $p < 0.0001$; week × diet: $F_{2,35} = 11.64$, $p = 0.00013$, $n = 37$) and in kcal/kg body weight (week: $F_{2,35} = 68.35$, $p < 0.0001$; diet: $F_{1,35} = 56.64$, $p < 0.0001$; week × diet: $F_{2,35} = 9.71$, $p = 0.00044$, $n = 37$) throughout the 4 weeks of control (CD)- or high-fat diet (HFD)-feeding, as well as stomach weight at the end of the experiment (time: $F_{2,31} = 139.24$, $p < 0.0001$; diet: $F_{1,31} = 0.035$, $p = 0.85$; time × diet: $F_{2,31} = 2.31$, $p = 0.12$, $n = 37$).

B. Representative microphotographs presenting spatial distribution of GLP1-immunoreactive fibres in relation to the different subdivisions of the DMH (c – compact, d – dorsal, v – ventral). 3 V – third ventricle, VMH – Ventromedial Hypothalamus.

C. Graphs presenting the results from the analysis of GLP1-positive fibres, performed for each DMH subdivision separately (diet: $F_{1,25} = 0.42$, $p = 0.52$; time: $F_{2,25} = 0.054$, $p = 0.95$; DMH div.: $F_{2,144} = 146.05$, $p < 0.0001$; diet × time: $F_{2,25} = 0.71$, $p = 0.5$; diet × DMH div.: $F_{2,144} = 0.76$, $p = 0.47$; time × DMH div.: $F_{4,144} = 0.96$, $p = 0.43$; diet × time × DMH: $F_{4,144} = 0.55$, $p = 0.7$; $n = 234$). BC—Box–Cox transformed values ($\lambda = 0.0202$).

D. Representative microphotographs presenting the density of cFos-positive cells depending on the time of meal onset and diet.

E. Graphs presenting the results from the analysis of the density of cFos-positive cells, performed for each DMH subdivision separately (diet: $F_{1,28} = 0.067$, $p = 0.8$; time: $F_{2,28} = 21.7$, $p < 0.0001$; DMH div.: $F_{2,170} = 104.37$, $p < 0.0001$; diet × time: $F_{2,28} = 1.2$, $p = 0.32$; diet × DMH div.: $F_{2,170} = 5.78$, $p = 0.0037$; time × DMH div.: $F_{4,170} = 3.96$, $p = 0.0042$; diet × time × DMH: $F_{4,170} = 2.16$, $p = 0.075$; $n = 273$). BC—Box–Cox transformed values ($\lambda = 0.3030$). *$p < 0.05$, **$p < 0.01$, ***$p < 0.001$, ****$p < 0.0001$. Box-and-whisker plots present the median value, the interquartile range (IQR; box) and the minimum-to-maximum range of values, not exceeding 1.5 * IQR (whiskers). Data points outside this range are plotted individually.

F. Representative microphotographs presenting colocalization of cFos and DAPI.

of expression, we analysed the mRNA density independently, where every fluorescent signal was included. In both cases, *Glp1r* showed very little expression in the cDMH. Surprisingly, even though the density of *Glp1r*-positive cells was higher in the dDMH than vDMH, signal density was equal between them, indicating higher *Glp1r* expression in fewer vDMH cells. Most importantly, we observed neither the general pattern, nor the level of expression of either receptor to change under HFD, despite literature presenting enhanced *Glp1r* expression in DIO (Zhang et al., 2020). The fact that this gene is overexpressed in obesity, but not during its development could indicate that it is a result of the increased body mass, possibly as some form of a compensatory mechanism.

As for the distribution of the GLP1-positive neuronal fibres, our results are in line with others (Renner et al., 2012), showing the highest density within the vDMH, followed by the dDMH, with an observable gap in between. GLP1, GLP2 and Oxm are all products of one pro-hormone and are released from the same, PPG-expressing neurons

(Vrang et al., 2007), therefore the spatial pattern of GLP1 fibres observed by us will presumably also reflect that of the other PPG products. Indeed, the GLP2-positive fibres have also been observed mostly in the vDMH (Tang-Christensen et al., 2000).

The rationale for a separation of the DMH into the three outlined subdivisions is based on both molecular and functional characteristics. The cDMH has been postulated as a site for the local circadian oscillator, as the clock gene expression rhythm is the strongest within this part of the structure (Guilding et al., 2009). The vDMH seems to be the most involved with feeding-related cues (Poulin and Timofeeva, 2008; Kobelt et al., 2008; Renner et al., 2012) and transmitting the information to the master circadian clock in the Suprachiasmatic Nucleus (SCN, Acosta-Galvan et al., 2011). Last, the dDMH sends projections to the sympathetic premotor neurons in the rostral medullary raphe (Zhang et al., 2011; Kataoka et al., 2014), serving as a regulator of the thermogenesis and other autonomic nervous system functions (for a review see DiMicco and Zaretsky, 2007).

Indeed it was the vDMH which responded to feeding with the highest cFos expression, with the other two only doing so under restricted feeding. Feeding scheduled to regular, few-hour-long meals at the same time every day has been shown to alter DMH physiology increasing its circadian oscillatory properties, and switching phase depending on the meal time, so as to enable its anticipation (Mieda et al., 2006; Gooley et al., 2006; Verwey et al., 2007, 2008, 2009; Minana-Solis et al., 2009; Sanetra et al., 2022b). Our data indicate that this entrainment engages all three DMH subdivisions, as opposed to the vDMH simply responding to the post-meal satiety.

4.2. Exn4/Oxm/GLP2 influence on the DMH electrophysiology

Contrary to the receptor expression or fibre immunoreactivity, cells sensitive to the PPG-derived peptides were not restrained to any specific part of the structure. Moreover, despite a spatial separation in *Glp1r* and *Glp2r* expression, we spotted cells responsive to both Exn4 and GLP2, Oxm and GLP2, and even all three peptides. As far as the responsiveness to both Exn4 and Oxm did not surprise us, since both of these peptides bind GLP1R, either of them activating the same cell as GLP2 was unforeseen. Alternatively, the information delivered by these satiety signals is probably received by distinct neuronal subpopulations, but then spread across the entire structure via the synaptic network.

Regarding the peptides binding GLP1R, many of the recorded cells were indeed activated by both, but not all of them. Exn4 and Oxm have previously been shown to activate different hypothalamic structures (Chaudhri et al., 2006; Parkinson et al., 2009), suggesting a functional separation between them. Many of the neurons recorded in this study responded to Exn4 but not Oxm, possibly due to a higher affinity of Exn4 to the GLP1R (Baggio et al., 2004; Jorgensen et al., 2007). On the other hand, some neurons responded only to Oxm, which could also be explained as Oxm binds glucagon receptors (GCGR; Baldissera et al., 1988) in addition to GLP1R; however, GCGR expression in the DMH is questionable. Historically, many have failed to detect its presence in the entire brain completely, or found it to be generally low (Svoboda et al., 1994; Hansen et al., 1995), especially in the hypothalamus (Hoosein and Gurd, 1984). Others have spotted GCGR, with the highest density in the brainstem, only followed by the hypothalamus (Campos et al., 1994), but even within the hypothalamus the highest levels seem to occupy the Arcuate Nucleus and the Ventromedial Hypothalamus rather than the DMH (Quinones et al., 2015). This issue, however, remains to be clarified.

Acting through different receptors would also explain why some neurons responded differently to both peptides (i.e. an increase in the firing rate to one of them and a decrease to the other), however it is not the only explanation. Apart from the already mentioned possibility of a presynaptic influence, distinct intracellular pathways might be stimulated in the presence of different preferential allosteric ligands (Koole et al., 2010). The GLP1R is a complex protein with an ability to bind various G proteins (Montrose-Rafizadeh et al., 1999), although the predominant mechanism involves the stimulation of adenyl cyclase by the G_{α} protein, which then induces phospholipase C activity via Epac2, leading to an increase in the intracellular Ca^{2+} concentration (Wheeler et al., 1993; Dzhura et al., 2010). Such pathway is extremely interesting to consider for the DMH, as our previous data indicate a presence of high-voltage activated (HVA) calcium channels, responsible for cells experiencing depolarised low-amplitude membrane oscillations (DLAMOs) under strong depolarisation (Sanetra et al., 2022a) in this structure. The involvement of calcium channels activating at strong depolarisation seems a plausible mechanism also for the dependence of the response amplitude on baseline firing rate, indicative of the strength of depolarisation. Since this relationship completely disappears under HFD for both Exn4 and Oxm, it might be in fact these channels, rather than the receptors themselves, that become altered by the diet. On the other hand, L-type HVA calcium channels, participating in DLAMO generation in the SCN (Pennartz et al., 2002; Belle et al., 2009), have also been linked to the actions of GLP2R (Wang and Guan, 2010), which appeared unaffected by the diet. Additionally, a new study by Huang et al. (2022) suggests a different mechanism of the GLP1 action in the DMH, via a decrease in the delayed rectifier potassium current, causing cell depolarisation. However, in this patch clamp study no change in the firing rate was observed after Exn4 application, which is in contradiction to our results. We believe inconsistencies might stem from a different recording method (extracellular vs intracellular recording), and propose both mechanisms as plausible to mediate GLP1 effect on the DMH neurons. Interestingly, during our patch clamp recordings we failed to observe a postsynaptic effect on the neurons, which might be another argument for the necessity of a specific membrane potential for the signal transduction through voltage-gated channels.

A switch from regular, sodium-dependent spiking into slower DLAMOs could also provide another explanation as to why some cells lowered their firing rate in response to the PPG-derived peptides. The fact that we observed a higher number of such neurons at night than during the day for all three peptides suggests a common underlying process. Whereas one option is of course the variation in the intensity of the GABAergic transmission, another could be related to the depolarisation above the threshold for DLAMOs or complete spiking blockage.

As suggested by the higher-than-expected number and a lack of spatial distribution of the cells responsive to Exn4/Oxm/GLP2, as well as verified with our patch clamp study, the DMH synaptic network is involved in signal transmission. For the GLP2 this was shown to differ between day and night, with a stronger decrease in the PSC frequency during the dark phase, which could also underlie the decrease in postsynaptic cells' firing rate more commonly observed at night. Same as for the MEA experiment, no effect of the diet was observed.

Also in line with the MEA results, the synaptic response to Exn4 was changed under HFD, in a form of an increased frequency of PSC during the day. Interestingly, we have previously observed an increased spontaneous firing rate during the light phase in the DMH (Sanetra et al., 2022b), which could be related to a malfunctioning of GLP1 signalling. On the other hand, the PSC response to Oxm application did not differ between either day/night or the diets, which once again indicates a distinct mechanism of action for the two GLP1R agonists.

It is important to note, that the investigation of the PSC frequency changes was performed in the absence of any specific synaptic blockers, or tetrodotoxin. The main rationale for these experiments was to confirm, that despite a moderate number of cells expressing the receptors for the PGDP, the ones which do, distribute this information throughout the structure resulting in an activation of about 40–50 % of the recorded cells. However, the investigation of the PGDP effect on the synaptic network functions, such as neurotransmitter release from the presynaptic terminal, would need to be addressed under pharmacological isolation. Further studies including a distinction of the type of current analysed (excitatory/inhibitory, type of ionic conductance), are needed to provide more in depth explanation on the nature of

phenomena observed.

4.3. GLP1 and cFos immunoreactivity under different metabolic states

The PPG family of peptides is responsible for satiety signalling; therefore, it could be assumed that their production as well as release is regulated by the animals' metabolic state. To explore that area, we studied the amount of GLP1 in the DMH by analysing GLP1-immunoreactive fibre density, under both hunger (48 h-long food deprivation) and satiety (2 h-long refeed). Since the DMH is well known for its entrainment to feeding schedules (Mieda et al., 2006; Gooley et al., 2006; Verwey et al., 2007, 2008, 2009; Minana-Solis et al., 2009; Sanetra et al., 2022b), we also applied a RF protocol (6 h long meal every night), which mimicked anticipated hunger/satiety. In order to monitor DMH cellular response to the same conditions, we also immunostained the cFos protein, as a marker of neuronal activity.

A 6 h-long mealtime was chosen as middle-length, when compared to others. While some researchers shorten it to 2 or 4 h (Gooley et al., 2006; Mieda et al., 2006; Verwey et al., 2007, 2008; Minana-Solis et al., 2009; Acosta-Rodríguez et al., 2022), far longer time windows are also common, even up to 8, 12 or 15 h (Hatori et al., 2012; Chaix et al., 2014; Vieira et al., 2022). In this case, we wanted to ensure the time restriction is strong enough to cause DMH anticipatory rhythms, while keeping the mealtime long enough to prevent caloric restriction, which could be an additional factor influencing the outcome of the study. Moreover, since the DMH had been observed to express day/night changes in cFos immunoreactivity (Gooley et al., 2006; Sanetra et al., 2022a), the meal onset was chosen as ZT14, so that the time point before the scheduled meal is also sampled during nighttime.

Throughout the CD/HFD feeding part of the experiment, the rats were weighed once a week. It was crucial to confirm that the HFD-fed group does not become significantly heavier than the controls at any point, since we were interested in studying potential mechanisms responsible for the development of obesity, rather than its consequences. Similarly to our previous reports (Chrobok et al., 2022; Sanetra et al., 2022b), an interaction between diet and week on a diet was observed, suggesting that the growth speed of the dietary groups differs, however up until the end of week 4, HFD-fed animals had not become heavier.

The fact that continuous body weight increase was present for both dietary groups throughout the experiment was related to the age of the animals at the start of it. Assigning the rats into CD- of HFD-fed groups, and the onset of specialist diet-feeding began at weaning, typically done at 4 weeks of age. Therefore, the rats at the time are still rapidly growing, which is well visible in the graphs presenting body mass changes from both FD and RF protocols. Our approach, aimed at modelling adolescent high-fat diet intake, does raise a question of how much the observed alterations, both behavioural and cellular, reflect also adult-onset obesity.

Also in line with previous reports, HFD-fed rats were shown to eat fewer grams of food, but more calories, due to the higher caloric value of the high-fat chow. Surprisingly though, the difference in the number of calories ingested during the 6 h window started declining immediately after RF onset and by the 4th week had completely vanished. On the other hand, our data on the 12 h-long RF did not follow the same trend, with an increased caloric intake throughout the entire experiment (Sanetra et al., 2022b). This discrepancy indicates meal length as an important factor determining the amount of food eaten, and suggests slower kinetics of the HFD consumption, additionally backed up by a lower density of cFos evoked 1.5 h after meal onset in the vDMH for the HFD group (Fig. 6E), as well as a slight (but not significant) trend implying lighter HFD stomachs at the same time point, despite lack of such difference before the meal, or 3.5 h after its onset (Fig. 6A). However, it is important to point out, that the HFD-fed animals decreased not only the caloric intake during the 2 weeks on the RF, but also total chow weight, indicating that the caloric restriction was voluntary, and the 6 h-long mealtime was enough for them to eat more, had there been such a subjective need.

Previous studies revealed that food deprivation decreases the PPG neurons' activity (Maniscalco and Rinaman, 2013; Maniscalco et al., 2015) and GLP1 efficiency at inhibiting food intake (Sandoval et al., 2012). This was attributed to an interaction with feeding-related changes in the levels of circulating leptin (Williams et al., 2006). Consistently with these observations of a reduced GLP1 signalling in a fasted state, we found GLP1 fibre density to be lower under starvation and increase after refeeding. Interestingly, this dynamic was lost in animals fed HFD. In the vDMH the satiety-induced GLP1 immunofluorescence failed to reach such a high level, whereas in the dDMH higher GLP1 density was observed during FD. This second result is particularly surprising, but might point to differences in the hunger-related metabolic processes, regulated by this part of the structure.

On the other hand, under RF the GLP1 fibre density remained unchanged by the scheduled meal. The reason for it might be the lack of FD-caused drop due to a shorter time window without any food during the RF protocol in comparison with the 48 h starvation. However, the stomachs weighed very similarly at the end of both protocols regarding the hungry groups. Instead, the lack of changes might also indicate meal anticipation in a form of neuronal terminals storing GLP1 so as to enable a swift response to the scheduled feeding.

Importantly, GLP1 fibre immunoreactivity was constant across the feeding cycle also for the HFD-fed rats, neither did it differ between the diets at any time point. Scheduled feeding has been proven beneficial for longevity (Acosta-Rodríguez et al., 2022), as well as metabolic health, even capable of preventing obesity altogether (Hatori et al., 2012; Sherman et al., 2012; Chaix et al., 2014; Vieira et al., 2022). Lately, we have also shown that 12 h-long RF can prevent the disturbance in the DMH circadian clock (Sanetra et al., 2022b). Results presented in this article provide another example of the advantageous influence of time-restricted feeding.

Concluding, in this study we investigated PPG signalling in the DMH, confirming the presence and specific spatial distribution of GLP1-positive neuronal fibres, GLP1 and GLP2 receptors, as well as investigated Exn4/Oxm/GLP2 influence on the DMH neurons and the synaptic network. Most importantly, our results provide an insight into HFD-mediated changes in the PPG signalling on two distinct levels: disrupted feeding-related dynamics of GLP1 density in the structure, and altered neuronal responsiveness to the GLP1R agonists, despite a lack of change in the receptor expression. Presented study is an important step towards understanding PPG signalling in the brain, especially vital with the view of an already wide usage of GLP1R agonists in therapy.

Funding

This study was supported by Polish National Science Centre (grant 2017/25/B/NZ4/01433 'Opus 13' awarded to MHL).

CRediT authorship contribution statement

A.M. Sanetra: Conceptualization, Data curation, Formal analysis, Investigation, Methodology, Visualization, Writing – original draft. **K. Palus-Chramiec:** Conceptualization, Data curation, Formal analysis, Investigation, Methodology, Writing – review & editing. **L. Chrobok:** Conceptualization, Data curation, Formal analysis, Investigation, Methodology, Writing – review & editing. **J.S. Jeczmien-Lazur:** Conceptualization, Investigation, Methodology, Writing – review & editing. **J.D. Klich:** Investigation, Writing – review & editing. **M.H. Lewandowski:** Conceptualization, Funding acquisition, Project administration, Resources, Supervision, Writing – review & editing.

Declaration of competing interest

Authors declare no conflict of interests.

Data availability

The data presented in this study are available upon request.

Acknowledgements

We would like to thank Patrycjusz Nowik for excellent animal care.

Appendix A. Supplementary data

Supplementary data to this article can be found online at https://doi.org/10.1016/j.mcn.2023.103873.

References

Acosta-Galvan, G., Yi, C.X., van der Vliet, J., Jhamandas, J.H., Panula, P., Angeles-Castellanos, M., Buijs, R.M., 2011. Interaction between hypothalamic dorsomedial nucleus and the suprachiasmatic nucleus determines intensity of food anticipatory behavior. Proc. Natl. Acad. Sci. 108 (14), 5813–5818.

Acosta-Rodríguez, V., Rijo-Ferreira, F., Izumo, M., Xu, P., Wight-Carter, M., Green, C.B., Takahashi, J.S., 2022. Circadian alignment of early onset caloric restriction promotes longevity in male C57BL/6J mice. Science 376 (6598), 1192–1202.

Baggio, L.L., Huang, Q., Brown, T.J., Drucker, D.J., 2004. Oxyntomodulin and glucagon-like peptide-1 differentially regulate murine food intake and energy expenditure. Gastroenterology 127 (2), 546–558.

Baldissera, F.G., Holst, J.J., Knuhtsen, S., Hilsted, L., Nielsen, O.V., 1988. Oxyntomodulin (glicentin-(33–69)): pharmacokinetics, binding to liver cell membranes, effects on isolated perfused pig pancreas, and secretion from isolated perfused lower small intestine of pigs. Regul. Pept. 21 (1–2), 151–166.

Bataille, D., Dalle, S., 2014. The forgotten members of the glucagon family. Diabetes Res. Clin. Pract. 106 (1), 1–10.

Bates, D., Maechler, M., Bolker, B.M., Walker, S., 2015. Fitting linear mixed-effects models using lme4. J. Stat. Softw. 67, 1–48.

Belle, M.D., Diekman, C.O., Forger, D.B., Piggins, H.D., 2009. Daily electrical silencing in the mammalian circadian clock. Science 326 (5950), 281–284.

Belle, M.D., Baño-Otalora, B., Piggins, H.D., 2021. Perforated multi-electrode array recording in hypothalamic brain slices. In: Circadian Clocks. Humana, New York, NY, pp. 263–285.

Box, G.E.P., Cox, D.R., 1964. An analysis of transformations. J. R. Stat. Soc. Ser. B 26, 211–252.

Campos, R.V., Lee, Y.C., Drucker, D.J., 1994. Divergent tissue-specific and developmental expression of receptors for glucagon and glucagon-like peptide-1 in the mouse. Endocrinology 134 (5), 2156–2164.

Chaix, A., Zarrinpar, A., Miu, P., Panda, S., 2014. Time-restricted feeding is a preventative and therapeutic intervention against diverse nutritional challenges. Cell Metab. 20 (6), 991–1005.

Chaudhri, O.B., Parkinson, J.R., Kuo, Y.T., Druce, M.R., Herlihy, A.H., Bell, J.D., Bloom, S.R., 2006. Differential hypothalamic neuronal activation following peripheral injection of GLP-1 and oxyntomodulin in mice detected by manganese-enhanced magnetic resonance imaging. Biochem. Biophys. Res. Commun. 350 (2), 298–306.

Chrobok, L., Klich, J.D., Sanetra, A.M., Jeczmien-Lazur, J.S., Pradel, K., Palus-Chramiec, K., Lewandowski, M.H., 2022. Rhythmic neuronal activities of the rat nucleus of the solitary tract are impaired by high-fat diet–implications for daily control of satiety. J. Physiol. 600 (4), 751–767.

Cork, S.C., Richards, J.E., Holt, M.K., Gribble, F.M., Reimann, F., Trapp, S., 2015. Distribution and characterisation of glucagon-like peptide-1 receptor expressing cells in the mouse brain. Molecular metabolism 4 (10), 718–731.

Dakin, C.L., Gunn, I., Small, C.J., Edwards, C.M.B., Hay, D.L., Smith, D.M., Bloom, S.R., 2001. Oxyntomodulin inhibits food intake in the rat. Endocrinology 142 (10), 4244–4250.

Dakin, C.L., Small, C.J., Park, A.J., Seth, A., Ghatei, M.A., Bloom, S.R., 2002. Repeated ICV administration of oxyntomodulin causes a greater reduction in body weight gain than in pair-fed rats. American Journal of Physiology-Endocrinology and Metabolism 283 (6), E1173–E1177.

DiMicco, J.A., Zaretsky, D.V., 2007. The dorsomedial hypothalamus: a new player in thermoregulation. Am. J. Phys. Regul. Integr. Comp. Phys. 292 (1), R47–R63.

Dupré, J., Behme, M.T., McDonald, T.J., 2004. Exendin-4 normalized postcibal glycemic excursions in type 1 diabetes. The journal of clinical endocrinology & metabolism 89 (7), 3469–3473.

Dzhura, I., Chepurny, O.G., Kelley, G.G., Leech, C.A., Roe, M.W., Dzhura, E., Holz, G.G., 2010. Epac2-dependent mobilization of intracellular Ca2+ by glucagon-like peptide-1 receptor agonist exendin-4 is disrupted in β-cells of phospholipase C-ε knockout mice. J. Physiol. 588 (24), 4871–4889.

Fox, J., Weisberg, S., 2019. An R Companion to Applied Regression. Sage Publications. https://socialsciences.mcmaster.ca/jfox/Books/Companion/.

Gooley, J.J., Schomer, A., Saper, C.B., 2006. The dorsomedial hypothalamic nucleus is critical for the expression of food-entrainable circadian rhythms. Nat. Neurosci. 9 (3), 398–407.

Guilding, C., Hughes, A.T., Brown, T.M., Namvar, S., Piggins, H.D., 2009. A riot of rhythms: neuronal and glial circadian oscillators in the mediobasal hypothalamus. Molecular brain 2 (1), 1–19.

Hansen, L.H., Abrahamsen, N., Nishimura, E., 1995. Glucagon receptor mRNA distribution in rat tissues. Peptides 16 (6), 1163–1166.

Hatori, M., Vollmers, C., Zarrinpar, A., DiTacchio, L., Bushong, E.A., Gill, S., Panda, S., 2012. Time-restricted feeding without reducing caloric intake prevents metabolic diseases in mice fed a high-fat diet. Cell Metab. 15 (6), 848–860.

Hoosein, N.M., Gurd, R.S., 1984. Identification of glucagon receptors in rat brain. Proc. Natl. Acad. Sci. 81 (14), 4368–4372.

Huang, Z., Liu, L., Zhang, J., Conde, K., Phansalkar, J., Li, Z., Liu, J., 2022. Glucose-sensing glucagon-like peptide-1 receptor neurons in the dorsomedial hypothalamus regulate glucose metabolism. Science Advances 8 (23), eabn5345.

Hwa, J.J., Ghibaudi, L., Williams, P., Witten, M.B., Tedesco, R., Strader, C.D., 1998. Differential effects of intracerebroventricular glucagon-like peptide-1 on feeding and energy expenditure regulation. Peptides 19 (5), 869–875.

Jorgensen, R., Kubale, V., Vrecl, M., Schwartz, T.W., Elling, C.E., 2007. Oxyntomodulin differentially affects glucagon-like peptide-1 receptor β-arrestin recruitment and signaling through Gα. J. Pharmacol. Exp. Ther. 322 (1), 148–154.

Kassambara, A., 2020. ggpubr: 'ggplot2' Based Publication Ready Plots. R package version 0.4.0. https://CRAN.R-project.org/package=ggpubr.

Kassambara, A., 2021. rstatix: Pipe-Friendly Framework for Basic Statistical Tests. R package version 0.7.0. https://CRAN.R-project.org/package=rstatix.

Kataoka, N., Hioki, H., Kaneko, T., Nakamura, K., 2014. Psychological stress activates a dorsomedial hypothalamus-medullary raphe circuit driving brown adipose tissue thermogenesis and hyperthermia. Cell Metab. 20 (2), 346–358.

Kobelt, P., Wisser, A.S., Stengel, A., Goebel, M., Inhoff, T., Noetzel, S., Mönnikes, H., 2008. Peripheral injection of ghrelin induces Fos expression in the dorsomedial hypothalamic nucleus in rats. Brain Res. 1204, 77–86.

Kolterman, O.G., Buse, J.B., Fineman, M.S., Gaines, E., Heintz, S., Bicsak, T.A., Baron, A. D., 2003. Synthetic exendin-4 (exenatide) significantly reduces postprandial and fasting plasma glucose in subjects with type 2 diabetes. The Journal of Clinical Endocrinology & Metabolism 88 (7), 3082–3089.

Koole, C., Wootten, D., Simms, J., Valant, C., Sridhar, R., Woodman, O.L., Sexton, P.M., 2010. Allosteric ligands of the glucagon-like peptide 1 receptor (GLP-1R) differentially modulate endogenous and exogenous peptide responses in a pathway-selective manner: implications for drug screening. Mol. Pharmacol. 78 (3), 456–465.

Kosinski, J.R., Hubert, J., Carrington, P.E., Chicchi, G.G., Mu, J., Miller, C., Pocai, A., 2012. The glucagon receptor is involved in mediating the body weight-lowering effects of oxyntomodulin. Obesity 20 (8), 1566–1571.

Kunzetsova, A., Brockhoff, P., Christensen, R., 2017. lmerTest package: tests in linear mixed effect models. J. Stat. Softw. 82, 1–26.

Larsen, P.J., Tang-Christensen, M., Holst, J.J., Ørskov, C., 1997. Distribution of glucagon-like peptide-1 and other preproglucagon-derived peptides in the rat hypothalamus and brainstem. Neuroscience 77 (1), 257–270.

Lee, S.J., Sanchez-Watts, G., Krieger, J.P., Pignalosa, A., Norell, P.N., Cortella, A., Watts, A.G., 2018. Loss of dorsomedial hypothalamic GLP-1 signaling reduces BAT thermogenesis and increases adiposity. Molecular metabolism 11, 33–46.

Lenth, R.V., 2021. emmeans: Estimated Marginal Means, aka Least-Squares Means. R package version 1.5.5-1. https://CRAN.R-project.org/package=emmeans.

Maejima, Y., Yokota, S., Shimizu, M., Horita, S., Kobayashi, D., Hazama, A., Shimomura, K., 2021. The deletion of glucagon-like peptide-1 receptors expressing neurons in the dorsomedial hypothalamic nucleus disrupts the diurnal feeding pattern and induces hyperphagia and obesity. Nutrition & metabolism 18 (1), 1–15.

Maniscalco, J.W., Rinaman, L., 2013. Overnight food deprivation markedly attenuates hindbrain noradrenergic, glucagon-like peptide-1, and hypothalamic neural responses to exogenous cholecystokinin in male rats. Physiol. Behav. 121, 35–42.

Maniscalco, J.W., Zheng, H., Gordon, P.J., Rinaman, L., 2015. Negative energy balance blocks neural and behavioral responses to acute stress by "silencing" central glucagon-like peptide 1 signaling in rats. J. Neurosci. 35 (30), 10701–10714.

Merchenthaler, I., Lane, M., Shughrue, P., 1999. Distribution of pre-pro-glucagon and glucagon-like peptide-1 receptor messenger RNAs in the rat central nervous system. J. Comp. Neurol. 403 (2), 261–280.

Mieda, M., Williams, S.C., Richardson, J.A., Tanaka, K., Yanagisawa, M., 2006. The dorsomedial hypothalamic nucleus as a putative food-entrainable circadian pacemaker. Proc. Natl. Acad. Sci. 103 (32), 12150–12155.

Minana-Solis, M.C., Angeles-Castellanos, M., Feillet, C., Pevet, P., Challet, E., Escobar, C., 2009. Differential effects of a restricted feeding schedule on clock-gene expression in the hypothalamus of the rat. Chronobiol. Int. 26 (5), 808–820.

Montrose-Rafizadeh, C., Avdonin, P., Garant, M.J., Rodgers, B.D., Kole, S., Yang, H., Bernier, M., 1999. Pancreatic glucagon-like peptide-1 receptor couples to multiple G proteins and activates mitogen-activated protein kinase pathways in Chinese hamster ovary cells. Endocrinology 140 (3), 1132–1140.

Osaka, T., Endo, M., Yamakawa, M., Inoue, S., 2005. Energy expenditure by intravenous administration of glucagon-like peptide-1 mediated by the lower brainstem and sympathoadrenal system. Peptides 26 (9), 1623–1631.

Pachitariu, M., Steinmetz, N., Kadir, S., Carandini, M., Harris, K.D., 2016. Kilosort: realtime spike-sorting for extracellular electrophysiology with hundreds of channels. bioRxiv, 061481. https://doi.org/10.1101/061481.

Parkinson, J.R., Chaudhri, O.B., Kuo, Y.T., Field, B.C., Herlihy, A.H., Dhillo, W.S., Bell, J. D., 2009. Differential patterns of neuronal activation in the brainstem and hypothalamus following peripheral injection of GLP-1, oxyntomodulin and lithium chloride in mice detected by manganese-enhanced magnetic resonance imaging (MEMRI). Neuroimage 44 (3), 1022–1031.

Pennartz, C.M., de Jeu, M.T., Bos, N.P., Schaap, J., Geurtsen, A.M., 2002. Diurnal modulation of pacemaker potentials and calcium current in the mammalian circadian clock. Nature 416 (6878), 286–290.

Pocai, A., Carrington, P.E., Adams, J.R., Wright, M., Eiermann, G., Zhu, L., SinhaRoy, R., 2009. Glucagon-like peptide 1/glucagon receptor dual agonism reverses obesity in mice. Diabetes 58 (10), 2258–2266.
Poulin, A.M., Timofeeva, E., 2008. The dynamics of neuronal activation during food anticipation and feeding in the brain of food-entrained rats. Brain Res. 1227, 128–141.
Quinones, M., Al-Massadi, O., Gallego, R., Fernø, J., Diéguez, C., López, M., Nogueiras, R., 2015. Hypothalamic CaMKKβ mediates glucagon anorectic effect and its diet-induced resistance. Molecular metabolism 4 (12), 961–970.
Renner, E., Puskas, N., Dobolyi, A., Palkovits, M., 2012. Glucagon-like peptide-1 of brainstem origin activates dorsomedial hypothalamic neurons in satiated rats. Peptides 35 (1), 14–22.
Sandoval, D., Barrera, J.G., Stefater, M.A., Sisley, S., Woods, S.C., D'Alessio, D.D., Seeley, R.J., 2012. The anorectic effect of GLP-1 in rats is nutrient dependent. PLoS One 7 (12), e51870.
Sanetra, A.M., Palus-Chramiec, K., Chrobok, L., Lewandowski, M.H., 2022a. Electrophysiological complexity in the rat dorsomedial hypothalamus and its susceptibility to daily rhythms and high-fat diet. Eur. J. Neurosci. 56 (4), 4363–4377.
Sanetra, A.M., Palus-Chramiec, K., Chrobok, L., Jeczmien-Lazur, J.S., Gawron, E., Klich, J.D., Lewandowski, M.H., 2022b. High-fat-diet-evoked disruption of the rat dorsomedial hypothalamic clock can be prevented by restricted nighttime feeding. Nutrients 14 (23), 5034.
Schindelin, J., Arganda-Carreras, I., Frise, E., Kaynig, V., Longair, M., Pietzsch, T., Cardona, A., 2012. Fiji: an open-source platform for biological-image analysis. Nat. Methods 9 (7), 676–682.
Sherman, H., Genzer, Y., Cohen, R., Chapnik, N., Madar, Z., Froy, O., 2012. Timed high-fat diet resets circadian metabolism and prevents obesity. FASEB J. 26 (8), 3493–3502.
Svoboda, M., Tastenoy, M., Vertongen, P., Robberecht, P., 1994. Relative quantitative analysis of glucagon receptor mRNA in rat tissues. Mol. Cell. Endocrinol. 105 (2), 131–137.
Tang-Christensen, M., Larsen, P.J., Thulesen, J., Rømer, J., Vrang, N., 2000. The proglucagon-derived peptide, glucagon-like peptide-2, is a neurotransmitter involved in the regulation of food intake. Nat. Med. 6 (7), 802–807.
Tang-Christensen, M., Vrang, N., Larsen, P.J., 2001. Glucagon-like peptide containing pathways in the regulation of feeding behaviour. Int. J. Obes. 25 (5), S42–S47.
Team, R., 2015. 2019. Integrated Development for R. RStudio, Inc., Boston, MA, RStudio. http://www.rstudio.com/.
Team, R.C., 2021. R: A Language and Environment for Statistical Computing. R Foundation for Statistical Computing, Vienna, Austria. https://www.R-project.org/.
Trujillo, J.M., Nuffer, W., Smith, B.A., 2021. GLP-1 receptor agonists: an updated review of head-to-head clinical studies. In: Therapeutic Advances in Endocrinology and Metabolism, 12, 2042018821997320.
Venables, W.N., Ripley, B.D., 2002. Modern Applied Statistics with S, , Fourth edition53. World, p. 578.
Verwey, M., Khoja, Z., Stewart, J., Amir, S., 2007. Differential regulation of the expression of Period2 protein in the limbic forebrain and dorsomedial hypothalamus by daily limited access to highly palatable food in food-deprived and free-fed rats. Neuroscience 147 (2), 277–285.
Verwey, M., Khoja, Z., Stewart, J., Amir, S., 2008. Region-specific modulation of PER2 expression in the limbic forebrain and hypothalamus by nighttime restricted feeding in rats. Neurosci. Lett. 440 (1), 54–58.
Verwey, M., Lam, G.Y., Amir, S., 2009. Circadian rhythms of PERIOD1 expression in the dorsomedial hypothalamic nucleus in the absence of entrained food-anticipatory activity rhythms in rats. Eur. J. Neurosci. 29 (11), 2217–2222.
Vieira, R.F.L., Muñoz, V.R., Junqueira, R.L., de Oliveira, F., Gaspar, R.C., Nakandakari, S. C.B.R., Pauli, J.R., 2022. Time-restricted feeding combined with aerobic exercise training can prevent weight gain and improve metabolic disorders in mice fed a high-fat diet. J. Physiol. 600 (4), 797–813.
Vrang, N., Hansen, M., Larsen, P.J., Tang-Christensen, M., 2007. Characterization of brainstem preproglucagon projections to the paraventricular and dorsomedial hypothalamic nuclei. Brain Res. 1149, 118–126.
Wang, Y., Guan, X., 2010. GLP-2 potentiates L-type Ca2+ channel activity associated with stimulated glucose uptake in hippocampal neurons. American Journal of Physiology-Endocrinology and Metabolism 298 (2), E156–E166.
Wheeler, M.B., Lu, M.I.N.G., Dillon, J.S., Leng, X.H., Chen, C.H.U.A.N., Boyd 3rd, A.E., 1993. Functional expression of the rat glucagon-like peptide-I receptor, evidence for coupling to both adenylyl cyclase and phospholipase-C. Endocrinology 133 (1), 57–62.
Williams, D.L., Baskin, D.G., Schwartz, M.W., 2006. Leptin regulation of the anorexic response to glucagon-like peptide-1 receptor stimulation. Diabetes 55 (12), 3387–3393.
Winzell, M.S., Ahrén, B., 2004. The high-fat diet–fed mouse: a model for studying mechanisms and treatment of impaired glucose tolerance and type 2 diabetes. Diabetes 53 (suppl_3), S215–S219.
Wynne, K., Park, A.J., Small, C.J., Meeran, K., Ghatei, M.A., Frost, G.S., Bloom, S.R., 2006. Oxyntomodulin increases energy expenditure in addition to decreasing energy intake in overweight and obese humans: a randomised controlled trial. Int. J. Obes. 30 (12), 1729–1736.
Zhang, C., Barkholt, P., Nielsen, J.C., Thorbek, D.D., Rigbolt, K., Vrang, N., Jelsing, J., 2020. The dorsomedial hypothalamus and nucleus of the solitary tract as key regulators in a rat model of chronic obesity. Brain Res. 1727, 146538.
Zhang, Y., Kerman, I.A., Laque, A., Nguyen, P., Faouzi, M., Louis, G.W., Münzberg, H., 2011. Leptin-receptor-expressing neurons in the dorsomedial hypothalamus and median preoptic area regulate sympathetic brown adipose tissue circuits. J. Neurosci. 31 (5), 1873–1884.

4. Summary of the results

In accordance with the presented study objectives, the following results were obtained:

- **Publication 1**:
  - ✓ DMH substructures were shown to differ in the electrophysiological properties, with the cDMH displaying less negative resting membrane potential (Vm), higher input resistance (R), lower rheobase (Rh) and less regular action potential generation (higher interspike interval coefficient of variation – Cv) when compared to the non-compact subdivisions (dDMH and vDMH). Regularity of the vDMH firing was shown to change between day and night, with higher Cv (lower regularity) during the day than at night (Fig. 2, left side). In both vDMH and cDMH of the CD-fed animals the spontaneous firing rate (FR) presented a day/night rhythm, with higher activity during the active phase of the rats - nighttime. This rhythmicity was, however, disrupted under HFD, which at least in the cDMH appears to be caused by a decrease in the threshold for action potential generation during the day (Th; Fig. 2, right side).

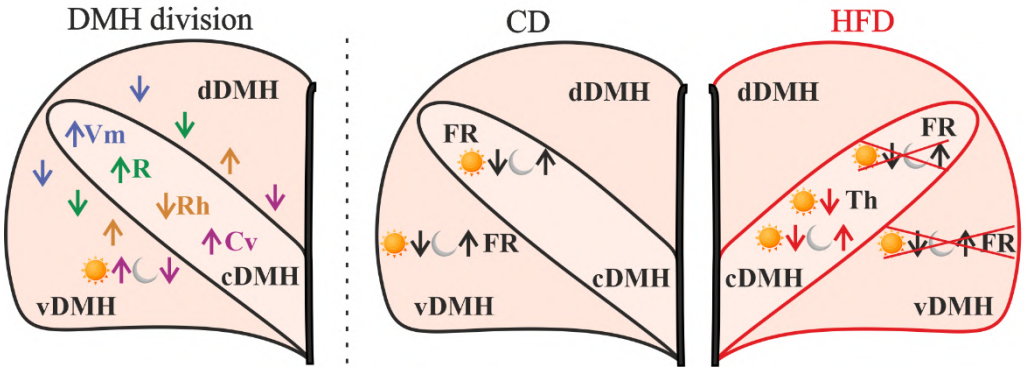

Figure 2. *Graphical summary of the results presented in Publication 1. Left side of the graphic presents differences within the DMH, with up/down arrows indicating whether a particular parameter is higher or lower in relation to the other DMH subdivisions. The right side focuses on the day/night rhythms (indicated with a sun and moon symbols) and HFD-caused alterations of them (HFD-mediated changes presented in red). CD – control diet, cDMH – compact DMH, Cv – coefficient of variation of the interspike interval, dDMH – dorsal DMH, DMH – Dorsomedial Hypothalamus, FR – firing rate, R – input resistance, Rh – rheobase, vDMH – ventral DMH, Vm – membrane potential.*

- **Publication 2**:
  - ✓ The body mass of the rats fed either CD or HFD diverged after 5 weeks, during which the HFD-fed animals consumed less amount, but more calories daily.
  - ✓ DMH neurons were shown to possess a day/night rhythm in the spontaneous firing rate and cFos protein immunoreactivity, with higher values of both during nighttime. However, HFD-feeding completely abolished this rhythmicity, by increasing both the firing frequency and cFos expression in the middle of the day. The around-the-clock changes in the density of the cFos-positive cells were at least partially independent of the amount of food ingested at the particular time point.
  - ✓ The circadian nature of the neuronal activity rhythm in the DMH was confirmed, time of the peak activity was detected around ZT14, but it was delayed by HFD-feeding by ~2 h.
  - ✓ The dependence of the DMH clock impairment on the animals arrhythmic feeding behaviour was demonstrated, as under restricted nighttime feeding, all HFD-evoked rhythm alterations have been prevented (Fig. 3).

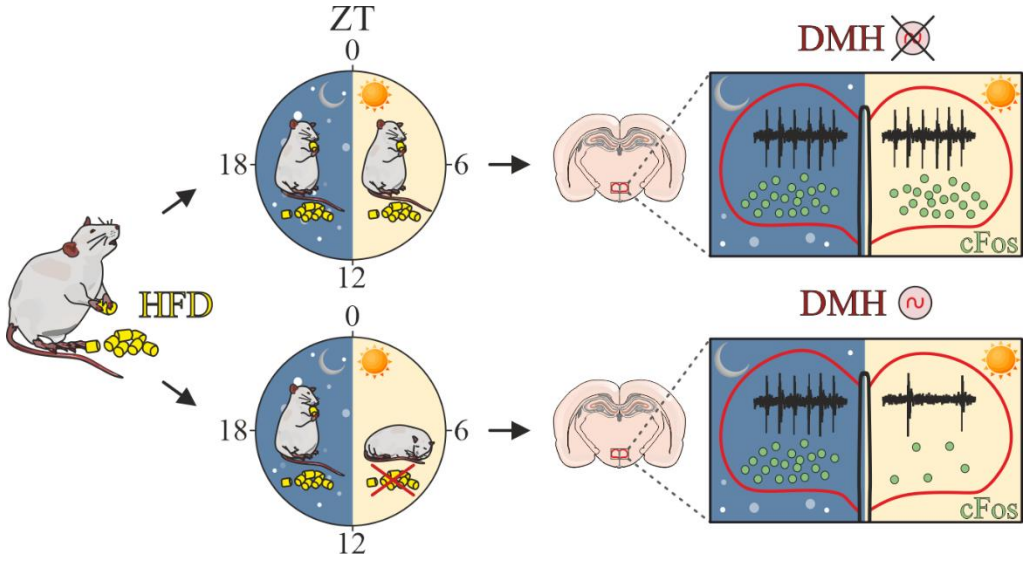

Figure 3. *Graphical summary of the results presented in Publication 2. HFD causes an alteration in the animals feeding pattern, increasing food intake during daytime. This behavioural arrhythmicity disrupts the DMH clock. Restricting food intake to nighttime restores the circadian properties of the DMH cells. DMH – Dorsomedial Hypothalamus, HFD – high-fat diet, ZT – Zeitgeber time.*

- **Publication 3**:
  - ✓ The *Glp1r* was confirmed to be expressed mostly by the non-compact DMH subdivisions, whereas *Glp2r* within the cDMH. No differences in the level of expression were detected between the dietary groups.
  - ✓ DMH neurons responsive to the PGDP were spotted across the entire structure. Vast majority of the sensitive cells responded with an increase in the firing rate to all three peptides (Exn4, Oxm and GLP2). The amplitude of the excitatory response was shown to depend on the spontaneous firing rate, but this correlation for Exn4 and Oxm disappeared under HFD. The less commonly observed response – a decrease in the firing rate, was more frequently observed at night than during the day for all 3 PGDP and both diets.
  - ✓ As the spatial distribution of the cells expressing the genes for the PGDP receptors differed from the location of the responsive cells, the influence of the PGDP on the synaptic transmission was studied. The effect of GLP2 on the frequency of the postsynaptic current (PSC) generation differed between day and night. On the other hand, diet-dependent changes were observed after Exn4 application, especially during daytime, when Exn4 created a stronger effect for the HFD-fed group.
  - ✓ PGDP abundance in the DMH, measured as the density of the GLP1-immunoreactive fibres, was shown to change depending on the animals' metabolic state (being lower when hungry and higher when satiated), but only for the CD-fed group. On the other hand, the cellular activity in the vDMH, where most of these neuronal endings are located, remained unaltered by HFD. When 6h-long restricted feeding protocol had been applied, no dynamic changes in the GLP1-density was observed around the anticipated meal, whereas the cFos was now induced by satiety also in the other DMH subdivisions.

    The results from **Publication 3** are graphically presented in Fig. 4.

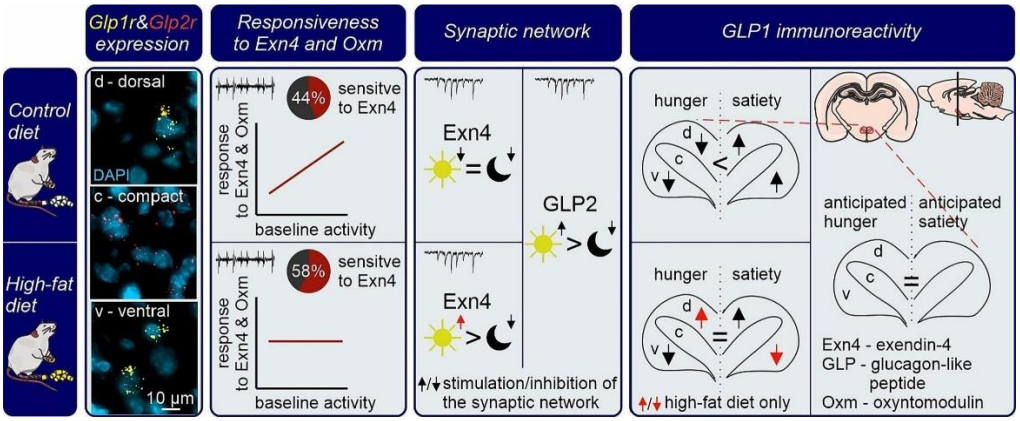

Figure 4. *Sprague-Dawley rats were fed either control (CD) or high-fat diet (HFD) for 2–4 weeks, after which preproglucagon (PPG) signalling was investigated in the Dorsomedial Hypothalamus. In situ hybridisation was used to detect glucagon-like peptide (GLP) 1 and 2 receptor (Glp1r/Glp2r) mRNA, shown to localise within different parts of the structure, with the same level and spatial distribution for both dietary groups. Electrophysiological recordings revealed changes in the sensitivity of the DMH neurons to exendin-4 (Exn4, a GLP1R agonist), with a higher number of responsive cells in the HFD-fed group. Moreover, the amplitude of the excitatory response to both Exn4 and oxyntomodulin (Oxm) correlated positively with the neurons' spontaneous firing rate, but only for the CD. The PPG-derived peptides were also shown to influence the synaptic network in the DMH. GLP2 caused opposite effects depending on the time of day for both diets, whereas daytime response to Exn4 was altered by HFD. Last, immunofluorescent labelling of GLP1 indicated variation in its density depending on the animals' metabolic state (fasted/fed), but this effect was also completely abolished by HFD. The dietary differences, as well as metabolic-state-dependent changes, were absent for animals fed in a time-restricted manner (anticipated hunger/satiety).*

Graphical abstract and text acquired from the on-line version of ***Publication 3****.*

5. Discussion

5.1. Body weight gain and feeding behaviour under HFD

Due to a constantly growing obesity pandemic, extensive research is being performed to increase our knowledge within the subject area. Nonetheless, vast majority of the studies investigate fully developed obesity and its detrimental consequences, focusing on the treatment rather than prevention. Therefore, for the studies presented in the thesis I took a different approach and employed HFD-fed, but not-yet-obese animals, to explore alterations of the hypothalamic functioning during obesity development. Observation of such would indicate mechanisms partaking in the process, the knowledge of which could possibly be applied to avoid obesity onset.

Thus, the starting point of the study was to examine the kinetics of the body weight gain, with a comparison between CD and HFD groups, and determine the time point at which they divert. This was shown to require at least 5 weeks of HFD-feeding, which was also confirmed by a lack of diet-dependent differences in the body mass during all the 4-week-lasting protocols (**Publication 2**: NF protocol, **Publication 3**: FD and RF protocols, as well as previous data published in Chrobok *et al.,* 2022). Even though all the protocols (except the NF) revealed a statistically significant interaction between the diet and the time on it, indicating a faster growth of the HFD-fed animals, the average values did not differ between the dietary groups even at the last body mass measurement of the experiment (at week 4). The fact, that this interaction between diet and week was not observed for the NF protocol could suggest that the night-fed rats do not put on weight as quickly as when fed *ad libitum*, emphasising the importance of the proper day/night feeding pattern. However, for the 6h RF protocol the interaction was surprisingly observed once again, not confirming the phenomenon. Instead, lack of the statistical significance for the NF protocol could have simply been caused by a decreased statistical power of the test, due to a lower number of animals used (n=16). Of course, in order to confidently conclude, whether restricted feeding slows down obesity development, the experiment would have had to continue for a longer period of time, at least until the *ad-libitum*-HFD-fed animals start becoming heavier than the controls. Nevertheless, the literature supports the hypothesis of possible obesity prevention by TRF, which has been show to substantially slow down the excessive weight gain of HFD-fed mice (Hatori *et al.,* 2012, Sherman *et al.,* 2012, Chaix *et al.,* 2014, Zarrinpar *et al.,* 2014).

Both dietary groups exhibited a body weight increase throughout the experiment, which was related to their age at the start of it. Assigning the rats into CD- of HFD-fed groups, and the

onset of specialist diet-feeding began at weaning, typically done at 4 weeks of age. Therefore, the rats at the time are still rapidly growing, which is well visible in each one of the graphs presenting body weight analyses throughout the thesis. The rationale for using such young animals were both technical (such as better survival of the brain tissue for the electrophysiological recordings in younger animals), but also reasonable from the epidemiological point of view, with data showing increasing obesity prevalence amongst children and young adults (Hawkes & Fanzo, 2017). However, this approach does raise a question of how much the observed alterations, both behavioural and cellular, reflect adult-onset obesity, and whether the cause for some rhythms' disturbance by HFD could have been the prevention of their proper development, rather that post-formation alteration.

One such example could be the disrupted day/night feeding pattern, observed by our team previously (Chrobok *et al.*, 2022). The CD and HFD groups were shown to eat similar amounts during the day up until week 3 of the experiment, after which the daytime feeding of the HFD-fed rats became increased in comparison to the CD. Looking at the data more closely, is becomes apparent, that it is in fact the CD group which changes its feeding behaviour, steadily decreasing daytime food intake, whereas the HFD groups continues to eat the same amount of food during the day throughout the 4 weeks of the experiment (Fig. 5). The relatively high percentage of daytime food intake at the start of the experiment might be related to a yet undeveloped day/night feeding pattern, as up until then the animals had been few by the mother at various times of the day. This hypothesis is, to a certain degree, supported by the literature, showing a wide range of time frames necessary for different rhythms' development, e.g. sleep/wake rhythms and different sleep-states maturation between 2-4 postnatal weeks (Frank *et al.*, 2017), whereas the rhythm in body temperature even until the postnatal day 50 (Kittrell & Satinoff, 1986). Alternatively, such feeding behaviour could have been caused by the novelty effect of the chow change, which has been shown to stimulate general food intake especially in males in the presence of a new environment (such as the new cage; Greiner & Petrovich, 2020).

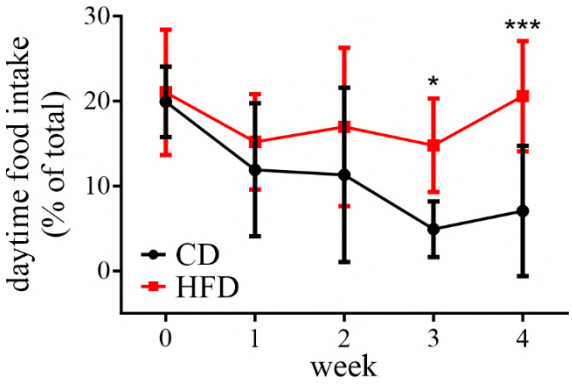

Figure 5. *Percentage of daily food intake consumed during the inactive daytime. Differences between the diets first appear at week 3, and continue onto the following week 4 with an increasing trend. Data reproduced from Chrobok et al., 2022 and presented as mean ± SD.*

Regardless of the underlying cause, the information that the feeding pattern changes between the diets sometime between the 2nd and the 3rd week of the experiment was important when planning the TRF experiments. In both NF and RF protocols, feeding restriction was, therefore, applied from the 2nd week onwards, after the first 2 weeks of *ad libitum* feeding.

Differences in food intake between the dietary groups were evident. The CD-fed animals consumed bigger amounts of chow than the HFD group in every protocol where it was measured (**Publication 2**: *ad libitum* and NF, **Publication 3**: RF), which was most probably caused by the higher caloric density of the HFD. On the other hand, when the amount of calories per body mass was calculated out of the ingested chow weight, higher calorie intake could generally be observed within the HFD group. Both results are in line with the literature. First, caloric value of the consumed food is an important factor determining the amount eaten, leading to lower volume of calorie-dense food ingestion (Johnson *et al.,* 1986, Oscai *et al.*, 1987). At the same time though, the stomach requires a certain amount of stretch or fullness, which interestingly can inhibit food intake even in the absence of any nutrient content (Smith *et al.,* 1962, Fuller *et al.,* 2013). This could be why larger amount or HFD is ingested than would be required to meet the caloric needs. Indeed, enhanced daily intake of HFD has been shown to be at least partially independent of the differences in the caloric density between diets (Warwick & Weingarten, 1995, Lucas *et al.,* 1998, Warwick *et al.,* 2002), although the hedonic value of the highly palatable HFD, in addition to simply not having enough food volume in the stomach, is often postulated a cause of it (Lutter & Nestler, 2009).

Interestingly, the two TRF protocols were observed to differently influence the caloric intake of HFD-fed animals. Under NF (12h-long meals) the general pattern described above persisted throughout the entire experiment, with HFD-fed animals eating fewer grams, but more calories daily, than the control group. However, when mealtime was shortened to just 6 h per night, the difference in the caloric intake between the dietary groups diminished, and disappeared entirely by the end of the 2nd week of RF. Although is it hard to pinpoint a specific reason for such a result without further studies, foods high in fat have been shown to delay stomach emptying (Valenzuela & Defilippi, 1981, Gentilcore et al., 2006, Özdemir-Kumral *et al.,* 2021), which could provide an explanation for a slower, more time-spread intake of the HFD, requiring longer food availability to achieve the subjective daily requirements. On the other hand though, this decrease in the caloric input of the HFD-fed animals was only observable after two weeks of RF, when not only the amount of calories per body mass, but also a total ingested food weight was lowered in comparison with the prior 2 weeks. This shows, that the 6 h of mealtime is in fact enough for them to ingest more chow, was there such a demand. Nevertheless, the

hypothesis regarding the behavioural aspects of HFD feeding, including smaller, more frequent meals (Kohsaka *et al.,* 2007, Pendergast *et al.,* 2013, Branecky *et al.,* 2015), could help to explain the mechanism disrupting the day/night feeding pattern.

5.2. Internal complexity of the DMH

DMH performs a multitude of autonomic, endocrine and behavioural functions, including the already mentioned regulation of food intake, metabolism, thermogenesis and cardiovascular output, as well as others, such as the involvement in the stress response and anxiety (Shekhar, 1993, Lowry *et al.,* 2003, Cullinan *et al.,* 2008, de Noronha *et al.,* 2017, Stamper *et al.,* 2017). Together with a high neurochemical variety within the structure (Kristensen *et al.,* 1998, Molnar *et al.,* 2011, Wagner *et al.,* 2013, Dodd *et al.,* 2014, Zhang & Bi, 2018) and a specific cytoarchitecture, these strongly indicate an existence of various subpopulations of cells within it, possibly located in distinct subregions.

Indeed, the three DMH divisions (cDMH, dDMH and vDMH) have been shown to possess distinct afferent and efferent projections and evert different functions (Larsen *et al.,* 1997, Cano *et al.,* 2003, Chou *et al.,* 2003, Cao *et al.,* 2004, Samuels *et al.,* 2004, Guilding *et al.,* 2009, Acosta-Galvan *et al.,* 2011, Renner *et al.,* 2012, Zhao *et al.,* 2017, Kono *et al.,* 2020). On the other hand, previous patch clamp study on the DMH neurons summarised them as an electrophysiologically uniform population (Bailey *et al.,* 2003). Therefore, predominantly in order to compare day/night and HFD-mediated changes, I performed a patch clamp study, and surprisingly observed vast differences between the DMH subdivisions, namely the cDMH and both vDMH and dDMH, with much less variety between the non-compact parts of the structure. On top of that, for the first time in the DMH, DLAMO (depolarised low-amplitude membrane oscillation)-like activity was spotted. This type of discharge had been described in the SCN, where the DLAMO events were restricted to late day, highly depolarised, *Per1*-expressing (clock) cells, and mediated by L-type, high-voltage-activated (HVA) calcium current, as well as changes in potassium conductance, affecting the resting membrane potential (Pennartz *et al.,* 2002, Belle *et al.,* 2009, Diekman *et al.,* 2013). Since the membrane potential of the SCN neurons is under a very tight circadian control (Belle *et al.,* 2009), it is reasonable to expect the extreme-depolarisation-dependent DLAMOs to occur only at the particular time of the day. Contrary to this, no rhythm in the resting membrane potential was observed amongst the DMH cells, and therefore also the DLAMO-like activity was detected at various times of the day. Even though the similarity of the observed signal to the DLAMOs described in the SCN, and their dependence on high depolarisation make it very tempting to conclude about, regarding a

similar mechanism of generation, i.e. modulation by the HVA calcium channels, a proper pharmacological study would need to be performed to clarify this issue. Moreover, genetically modified animals, with fluorescent reporter proteins under the control of one of the clock genes could be used to answer whether it is just the oscillatory neurons that express the DLAMO-like activity in the DMH. Since, contrary the SCN, the DMH oscillations are enhanced and strongly entrained not by light, but feeding cues, it would also be interesting to investigate the changes in the membrane potential, and prevalence of the DLAMO-like activity in TRF animals.

Even though the resting membrane potential did not change around the clock, the firing rate of both cDMH and vDMH did. The presence of such rhythm in the vDMH and a lack of it in the dDMH is one of the few differences spotted between the non-compact parts of the DMH. While it is in fact the cDMH, which is postulated to perform the circadian clock function (Guilding *et al.,* 2009), the difference in the firing rate between day and night observed in the vDMH appeared even larger. However, it is important to note, that this may not be an endogenous property, but simply a response to feeding, known to affect the vDMH stronger than the other DMH subdivisions (Poulin & Timofeeva, 2008, Renner *et al.,* 2012, Maejima *et al.,* 2021). Increased food intake during the behaviourally active night could be causing higher firing rate of the vDMH neurons. Meanwhile, the disturbance of the animals day/night feeding pattern under HFD abolishes the rhythm, as was observed here. Taking these into account, it is almost surprising, that the metabolism- and thermogenesis-regulating dDMH did not express similar rhythmicity, as these are clearly time-of-day-dependent, and strongly connected to the timing of food intake (Blessing *et al.,* 2013, de Goede *et al.,* 2018). This result could indicate, that the responsiveness and top-down control from this part of the DMH is more phasic, and rapidly-adapting.

Another parameter examined, highly related to the frequency of the action potential generation, was firing regularity. Generally, higher firing rate will decrease the interspike interval (ISI), causing the consecutive action potentials to appear more regularly. This was indeed observed within the vDMH. During the day, when the firing rate is lower, the ISI coefficient of variation (Cv) was high, implying irregularity in the activity. On the contrary, at night the firing rate was higher, and the regularity increased (lower Cv). Even the HFD-mediated trend in the daytime firing rate is reflected by the regularity parameter.

However, in the cDMH such phenomenon was not observed. Even though the changes in the firing rate were present, they were not associated with a similar shift in the firing regularity. This might be related to the higher prevalence of the strong-depolarisation-evoked DLAMO-like activity in the cDMH, which had the least negative resting membrane potential among the

DMH subdivisions. A switch from sodium-dependent spikes to much slower, calcium-mediated discharges of various lengths could be the reason the firing rate and regularity do not show the same concurrence.

As neither the day/night rhythm in the firing rate, nor the HFD-mediated disruption of it, was related to changes in the membrane potential, the next possible candidate was the threshold for the action potential firing. Although the statistical significance was only reached in the case of the cDMH, the vDMH showed a very similar trend, with HFD-evoked decrease in the threshold during the day (a shift towards more negative values), possibly responsible for the increased firing rate during the inactive phase. This parameter is directly dependent on the opening of the voltage-gated sodium channels, suggesting changes in their functioning under HFD, which could have many underlying reasons. Sodium currents can be modulated by signalling molecules, e.g. secondary messengers through phosphorylation, influencing the magnitude of the current, the probability of channel opening, and voltage-dependence of both activation and inactivation (Li *et al.,* 1992, Ma *et al.,* 1994, Maurice *et al.,* 2001, Goldfarb *et al.,* 2007). The subunit composition of a particular channel also influences such properties (Patton *et al.,* 1994, Isom *et al.,* 1995, Lopez-Santiago *et al.,* 2006). Lastly, an addition of low-voltage-activated calcium channels, generating the low-threshold spikes during the ramp stimulation also cannot be excluded, as the DMH has been shown to express the genes encoding subunits of the T-type calcium channels (Qiu *et al.,* 2006).

Contrary to the firing threshold, the rheobase (defined as the minimal amount of current needed to reach the threshold from a uniform starting voltage, Kania *et al.,* 2020) did not exhibit any changes, but still varied between the DMH subdivisions. Lower values of this parameter in the cDMH were probably related to an increased input resistance recorded from these neurons. As these cells are visibly smaller than those of the non-compact DMH, it was also anticipated that the steady-state currents recorded at various potentials during the IV curve generation were smaller. Moreover, the day/night changes in the amount of current flowing at the very negative and positive potentials were detected, even in the absence of a co-occuring membrane resistance shift, confirming the oscillatory properties of this DMH subdivision. Higher current amplitudes were observed at night, which strikingly contrasted with the rhythm observed in the vDMH, also showing day/night differences at the depolarised states, but in the other direction. Surprisingly, the vDMH was the only one to present any HFD-induced changes, and even more peculiarly, these appeared at nighttime. Occurrence of the observed alterations specifically at highly depolarised membrane potentials, coinciding with the range of HVA channel activation (Fox *et al.,* 1987, Catterall *et al.,* 2005) once again calls for a deeper investigation of the

DLAMO-like activity. Unfortunately, as the presented patch clamp study did not aim specifically at the cells expressing this type of activity, the amount of collected neurons did not allow for any sensible analysis between the groups.
As before, no day/night or HFD-mediated changes were observed in the dDMH, confirming its lack of dependence on the LD and diet factors.

5.3. Circadian and periprandial rhythms in the DMH

Taking into consideration various results obtained by others, regarding the expression of circadian rhythms by the DMH (Mieda *et al.,* 2006, Verwey *et al.,* 2007, 2009, Guilding *et al.,* 2009), and seeking possible disturbances of the DMH physiology by the HFD, the occurrence of different types of rhythms had to be confirmed first. This was done with a use of multiple methods, starting with the discussed above patch clamp study, which showed a clear day/night changes in the cellular activity in two out of three DMH subdivisions. Same differences were also observed with the extracellular MEA recordings, which in spite of lower spatial resolution, not allowing for a confident separation of the distinct subdivisions, confirmed the presence of the rhythm on a much larger group of cells, therefore showing its presence at the level of an entire structure. The endogenous component of the rhythm was verified with the longterm recordings, during which a spontaneous rise in the cellular activity could be observed at the beginning of the night, despite a complete isolation of the structure from the SCN and any environmental cues.
There was no day/night rhythm in the responsiveness to the PGDP, measured as the percentage of the sensitive cells or the amplitude of the excitatory response, although more neurons responded with a decrease in the firing rate at night than during the day. In the case of extracellular recordings, performed without pharmacological isolation, a decrease in the firing frequency is difficult to conclude about. Even though GLP1R and GLP2R are generally considered to be excitatory, both of them have been confirmed to be able to produce a direct inhibitory response. GLP1R can bind multiple G-proteins, including G_i (Montrose-Rafizadeh *et al.*, 1999), whereas GLP2R has been shown to stimulate various intracellular pathways depending on the cell type, leading to different whole-cell effects (Shi *et al.,* 2013). Therefore a direct inhibitory effect on the DMH neurons cannot be excluded. Moreover, network effects (e.g. stimulation of GABA-ergic interneurons) are a very probable cause, whose confirmation could indicate differences in the level of activity of the inhibitory DMH network between day and night. Lastly, a decrease in the firing rate might also be caused by an extreme excitation, inducing depolarisation blockage, or alternative firing modes. For DMH neurons, capable of

switching into slower DLAMO-like activity, and very prone to a depolarisation block, this argument must be acknowledged, especially considering that both GLP1R and GLP2R activation leads to calcium current flow (Wheeler *et al.*, 1993, Dzhura *et al.*, 2010, Guan, 2014). Differences in the PGDP effect on the PSC frequency between day and night were only observed in the case of GLP2, which presented an enhanced inhibitory effect at night. Although based on these experiments it cannot be concluded what type of currents are affected, a decrease in the inhibitory drive could partake in the generation of a higher neuronal activity during the night.

Importantly, and surprisingly, no clear whole-cells effect of the PGDP was observed during the patch clamp recordings. Lack of a response during the voltage clamp protocol, could have been related to a fixed holding potential, suggesting an involvement of some voltage-gated channels in the response generation. An unpublished series of current clamp recordings produced the same result, however it is important to mention that the highly depolarised cells were not targeted here. On the other hand, our RNAscope revealed a relatively low number of cells expressing the receptor gene, especially in the case of GLP1, therefore to confirm a true lack of effect on these cells during the intracellular recordings it would be best to combine patch clamp experiments with fluorescent labelling of the *Glp1/2r*-expressing cells, to ensure they are properly sampled.

The electrophysiological recordings were complemented by an immunofluorescence study, where the immunoreactivity of the cFos protein, a product of an immediate early gene, was analysed in 4 time points, separated by 6 h. Consistently with the results from the electrophysiological recordings, and with the literature linking cFos expression to neuronal activation (Morgan & Curran, 1986, Sheng *et al.*, 1993), higher density of cFos-positive cells was observed at night than during the day. The location of the cFos-positive cells was predominantly the ventral and medial sections of the structure, and therefore included all three DMH subdivisions.

Although cFos immunoreactivity is probably the most commonly used marker of neuronal activity, it is important to remember that these two do not always have to co-occur, as the expression of cFos is specifically induced by high levels of intracellular calcium, flowing through either HVA L-type channels or the NMDA receptors and activating MAPK pathway (Chung, 2015). Importantly, this might happen not only after a direct stimulation, but also after disinhibition of a cell (Zaretskaia *et al.*, 2008). Moreover, the time needed for the cFos expression induction, and translation into a protein might vary between different types of cells and stimuli. While in cell cultures this might happen as quickly as within few minutes (Müller

et al., 1984) but also half an hour (Cavigelli *et al.,* 1995), food intake-induced rise in cFos immunoreactivity in the DMH was shown to require up to an hour (Imoto *et al.,* 2021). On top of that, the fact that this happens in response to a scheduled meal even in the absence of feeding on a particular day suggests that the induction might be caused by food anticipation as well, in which case the time required for an increase in cFos immunoreactivity might be even longer (Johnstone *et al.,* 2006, Poulin & Timofeeva, 2008). Therefore, high cFos density, measured at ZT12 is definitely not a result of food intake at the start of the dark phase, but might be its anticipation, and/or a result of the circadian clock ticking. Similarly, low cFos density at ZT0, right after the last meal of the night, when the stomachs extracted from the animals were the heaviest, also contradicts changes in cFos immunoreactivity as being caused by feeding cues alone.

Nevertheless, even without any anticipation, feeding does induce cFos in the DMH, as shown by others (Imoto *et al.,* 2021) and observed here for the FD protocol. This effect was confined to the vDMH, and co-occurred with refeed-induced increase in the GLP1 density, which has been shown to mediate the effect (Renner *et al.,* 2012). On the contrary, under RF the feeding-related rise in cFos density was detected in all three DMH subdivisions, suggesting meal entrainment by cDMH and dDMH. Surprisingly, this periprandial rhythm was not reflected by GLP1 immunoreactivity, which remained on the same level around the meal. This might indicate another way of feeding anticipation in a form of peptide amount adjustment before the scheduled meal, however with immunofluorescence alone it is difficult to link these measurements to the release of the PGDP from the neuronal axons present in the structure.

5.4. HFD-induced alterations of the DMH physiology

Previous studies have established that the DMH is susceptible to diet-induced obesity (Guan *et al.,* 1998, Chaar *et al.,* 2016, Zhang *et al.,* 2020). However, the underlying processes, including the time during obesity development when they appear, have been understudied. Therefore, it has been unknow, whether the DMH disruptions are just a result, or a part of the pathophysiological mechanism. By examining the DMH physiology under short-term HFD, I aimed at verifying the hypothesis, that some alterations will already be present at this stage, and might be important for obesity generation.

A disruption of the DMH day/night activity rhythm by HFD-feeding was observed using 3 different experimental methods, proving the repetitiveness of the obtained result. An increase in the daytime firing rate was detected with patch clamp and the MEA, while the cFos density rise at ZT6 was spotted with immunofluorescence staining. As discussed in the previous

section, the increased daytime firing under HFD need not necessarily be a result of an intrinsic mechanism, but could simply be due to enhanced food intake during the light phase, which had been shown in our former study (Chrobok *et al.*, 2022). Therefore, in order to extract the endogenous component of the DMH rhythms, a new set of MEA experiments was performed, in which the animals were sacrificed with the start of the light phase (ZT0), and the recordings persisted throughout the entire 24 h cycle and even longer, in the absence of any environmental cues, including those related to feeding.

Removing the possibility of daytime feeding by the HFD-fed rats did not eliminate the elevated firing rate of the DMH neurons at ZT6, denying its direct dependence on the feeding cues. Moreover, time of the highest (peak) neuronal activity was delayed by 2 h for the HFD group, confirming an alteration of not only behaviour-dependent, but also the intrinsic, circadian rhythms. Neither the proportion of the rhythmic cells, nor the peak level of activity differed between the groups, highlighting that the activity rhythm within individual neurons persists under HFD, but might have a longer period, be out of phase with the LD cycle and/or internally desynchronised. The circular histograms illustrating the distribution of peaktimes generally contradicted the desynchronisation hypothesis, as both dietary groups had very similarly shaped histograms, whereas occurrence of a continuous out-of-phase rhythm under normal environmental LD cycle is quite unlikely, although not impossible, as the disruption of the feeding rhythm was also observed under LD12/12. On the other hand, lengthening of the circadian rhythm in the locomotor activity by HFD has been shown for mice (Kohsaka *et al.*, 2007), therefore a similar elongation of the activity rhythm in the DMH appears the most probable, although all three possibilities are worth exploring.

HFD-induced alterations have also been observed regarding DMH neurons' responsiveness to the PGDP. The close relationship between the spontaneous neuronal activity and the amplitude of the response to the GLP1R agonists (Exn4 and Oxm), observed for the control group, was completely abolished under HFD. Given that GLP1R stimulation leads to calcium flow across the membrane (Wheeler *et al.*, 1993, Dzhura *et al.*, 2010) the correlation observed for the CD-fed animals, between the spontaneous and Exn4-evoked activity, is likely to be due to an involvement of voltage-dependent currents, such as the HVA calcium channels, the presence of which is postulated in the DMH (Matsumoto *et al.*, 2004, Cole *et al.*, 2005). The lack of such correlation for the HFD-fed group could indicate a disruption of the voltage-gated calcium currents, once again argumenting for their further study. Additionally, a recent study revealed GLP1 action through voltage-dependent potassium channels in the DMH, namely an inhibition of potassium outflow through the delayed rectifier channels (K_{dr}; Huang *et al.*, 2022). These

channels open during prolonged depolarisation, require a membrane potential of around -25 mV and function to repolarise the neuronal membrane during continuous firing (Kang *et al.*, 2000). This mechanism on its own does not explain the correlation between spontaneous and evoked activity observed here, however the K_{dr} blockage by GLP1R agonists could participate in the generation and prolongation of the highly-depolarised state, necessary for HVA current flow.

Despite an unchanged level of the receptor expression, HFD increased the fraction of cells responding to Exn4, which was most visible during the day and coincided with Exn4-evoked increase in the PSC frequency. Therefore, the enhanced number of responsive cells is caused indirectly, via an augmented synaptic network function, rather than higher number of *Glp1r*-expressing cells. Interestingly, *Glp1r* expression has been shown to be increased in DIO (Zhang *et al.*, 2020), perhaps as a compensatory mechanism due to diminished peptide signalling.

When comparing to the CD-fed rats, the feeding-induced increase in the GLP1 immunoreactivity was indeed attenuated under HFD, especially in the vDMH, which is the most densely innervated by the PPG-positive neuronal fibres (Renner *et al.*, 2012). This could suggest less efficient satiety signalling after a meal, however, it was not reflected by a lower number of activated neurons, as cFos density did not differ between the dietary groups. Since the DMH is affected by a number of different satiety signals, including leptin (Elmquist *et al.*, 1998, Bi *et al.*, 2003, Zhang *et al.*, 2011, Faber *et al.*, 2021) and cholecystokinin (CCK; Chen *et al.*, 2008, Palus-Chramiec *et al.*, 2022), these might transmit the feeding information as well, resulting in an activation of a similar number of the DMH neurons. However, despite a similar main behavioural output (food intake suppression), various satiety signals might bind to receptors located on different cells and result in the activation of entirely distinct pathways. While the CCK appears to activate solely the cDMH (Chen *et al.*, 2008), which is also the site of the *Glp2r*-expressing neurons (Tang-Christensen *et al.*, 2000), both leptin receptors and GLP1R localise in the non-compact parts of the structure, predominantly the vDMH (Elmquist *et al.*, 1998, Bi *et al.*, 2003, Enriori *et al.*, 2011, Zhang *et al.*, 2011, Renner *et al.*, 2012, Faber *et al.*, 2021). Moreover, it is unknown whether the receptors for the peptides activating the same DMH subregion colocalise within individual cells, and even if they were – whether they produce the same neuronal output. It is also important to remember that the number of cFos-positive cells does not inform about the strength of the stimulation, so even if the PGDP activate the same amount of cells after the refeed, this excitation could be weaker, and/or last shorter.

GLP1 fibre pre/post meal kinetics were also abolished by the HFD in the dDMH, however in this case it was due to an increase in the GLP1 fibre density under food deprivation. Since this

part of the DMH is predominantly involved in the sympathetic nervous system stimulation (Cano *et al.*, 2003, Cao *et al.*, 2004, Samuels *et al.*, 2004, Zhao *et al.*, 2017, Kono *et al.*, 2020, Brizuela & Ootsuka, 2021), changes in the GLP1-induced activation could result in altered autonomic functions, such as BAT thermoregulation and cardiovascular response, under prolonged hunger. Animal models of obesity have indeed been observed to exhibit decreased BAT thermogenesis (Himms-Hagen & Desautels, 1978, Trayhurn & James, 1978, Trayhurn & Fuller, 1980) and even BAT atrophy (Himms-Hagen, 1990), while in humans BAT activity has been shown to inversely correlate with BMI (Cypess *et al.*, 2009, Pfannenberg *et al.*, 2010). While the direction of causality within this correlation is unknown, an altered GLP1 immunoreactivity in hungry HFD-fed animals supports a hypothesis of a presence of changes in the autonomic response to hunger before obesity development. Further studies of the alterations of the GLP1 signalling under HFD specifically in this part of the DMH could aid in clarifying this issue.

Lastly, contrary to the control group, HFD-fed animals demonstrated feeding-evoked rise in cFos density not only in the traditionally feeding-responsive vDMH, but also in the cDMH. This surprising result could be attributed to the disruption in the circadian clock properties under HFD, including the delay in the peak activity. Since the refeeding took 2 h, the sampling time for this group was pushed to ZT16, which was also the time of the highest neuronal activity driven by the intrinsic clock for the HFD-fed group. The internal clock ticking with an altered phase seems a more probable explanation of the observed result, than the cDMH becoming activated by satiety itself, however based on this experiment this probability cannot be excluded.

5.5. Insights into behavioural and pharmacological chronotherapy

In the presented study, HFD-feeding was shown to influence various aspects of the DMH physiology, from the neurons' electrophysiological properties, to their intrinsic and evoked activity, including inter-neuronal communication. In a previous study by my team (Chrobok *et al.*, 2022) we found that the HFD attenuates animals' day/night behavioural rhythm in food intake, by increasing daytime feeding. Since the DMH is both responsive to feeding cues (Imoto *et al.*, 2021), and capable of influencing feeding behaviour, the possibility of the two phenomena being related could not have been ignored.

On one hand, DMH is well known for its meal entrainment (Gooley *et al.*, 2006, Mieda *et al.*, 2006, Verwey *et al.*, 2007, 2008, Minana-Solis *et al.*, 2009). Although it is normally recorded using various TRF protocols, animals have a naturally occurring feeding pattern, with nocturnal

rats being active and consequently eating predominantly at night. It is, therefore, probable that a disrupted feeding rhythm would result in the DMH clock disruption. A positive verification of this hypothesis would underline the importance of the temporal feeding pattern and suggest possible prevention of the DMH clock impairment.

On the other hand, since the DMH is generally considered an orexigenic structure, as its lesions lead to a decrease in food intake (Bernardis, 1970, Bellinger, 1987), it would also be reasonable to assume that its increased activity during daytime, as observed for the HFD group, could be a cause rather than a result of a stimulation of feeding at this time of the day. While the two mechanisms are not exclusive, the NF protocol was designed and performed to evaluate the first one – that it is the feeding irregularity that causes the DMH impairment.

The disruption of the day/night rhythm in firing rate, observed under HFD, was successfully counteracted by NF, as revealed by the acute MEA recordings. The longterm MEA experiments, together with cFos immunofluorescence confirmed a lack of the increase in the cellular activity at ZT6, as well. The peaktime delay was also prevented, although the peak activity was increased for the HFD-fed group, perhaps as a result of DMH adaptation to the feeding restriction. It is important to highlight, that these effects were independent of the amount of food ingested, as the night-fed animals continued to eat more calories than the control group, only the timing of food intake changed.

Therefore, the results led to a conclusion that HFD induced daytime feeding, which negatively impacts the DMH clock. Nevertheless, positive validation of this hypothesis does not contradict the second one entirely, as they could both be partaking in obesity development as a positive feedback loop, with daytime food intake activating DMH neurons, which in turn continues to stimulate feeding. However, this study revealed, that the irregular food intake precedes DMH clock disruption, as under a healthy feeding pattern the circadian rhythm of the DMH remains unaltered.

Regarding the periprandial rhythm, TRF changed DMH responsiveness to hunger and satiety by stimulating cFos expression after the anticipated meal in all 3 DMH subdivisions, in contrast to only vDMH being affected by unforeseeable feeding. This result might reflect an enhancement of the oscillatory properties at the level of the entire structure, documented by others (Gooley *et al.,* 2006, Mieda *et al.,* 2006, Verwey *et al.,* 2007, 2008, Minana-Solis *et al.,* 2009). No differences were observed here between the dietary groups, with an exception of a lower density of cFos-positive cells in the vDMH 1.5 h after meal onset. Considering this substructure's direct responsiveness to feeding cues, this might just be a result of a slower HFD intake, especially with a statistically insignificant, but well visible trend in the stomach weight

at this time point (lighter stomachs of the HFD-fed group), as well as in view of the fact that 2 h later the cFos density did not differ between the dietary groups anymore.

Changes in the GLP1 immunoreactivity in the non-compact DMH between hungry and satiate metabolic state, altered by the HFD, were entirely gone under RF. On one hand, the result was incredibly surprising, since an enhancement of the periprandial rhythm in the PGDP content was expected, but instead the result imitated the rhythm disruption by the HFD. However, it should be argued, that RF- and HFD-mediated influence on the metabolic state-related GLP1 immunoreactivity probably have completely different underlying mechanisms, with HFD disturbing the physiological responses to both hunger and satiety in different parts of the DMH (dDMH and vDMH, respectively), and RF possibly resulting in some form of anticipatory accumulation of PGDP in the neuronal endings before the scheduled meal.

Decreased immunoreactivity of the PGDP post-meal in the vDMH is especially interesting, since GLP1 blood levels have been shown to also be lower after a meal in obese individuals, despite faster and elevated food intake (Meyer-Gerspach *et al.*, 2014), suggesting both peripheral and central reduction in the GLP1 signalling. These results highlight the importance of a proper periprandial timing of GLP1 agonist administration for successful obesity treatment, however any more specific pharmacological conclusions are beyond the scope of this thesis.

Reduced amount of GLP1 is likely to cause compensatory mechanisms, aimed at enhancing the sensitivity to the peptide, which was observed here as an increased number of Exn4-responsive neurons. Since the density of the *Glp1r*-expressing cells did not change, this increased sensitivity was probably caused by augmented synaptic network function, as the HFD was seen to intensify the effect of Exn4 on the PSC frequency.

Evidently, the DMH is targeted by the GLP1R-agonist-based anti-diabetic and anti-obesity drugs. With the MEA study I aimed at finding out whether the responsiveness of the DMH neurons to the PGDP changes under HFD. Considering the DMH neurons' increased firing rate under HFD, especially during daytime, the amplitude of the response to both Exn4 and Oxm was smaller than predicted by the model. This was because the model included the spontaneous firing rate as a covariate, which appeared highly significant, however only for the control group. While a loss of this dependence under HFD could be indicative of disrupted signalling pathways, it could also be a compensatory mechanism, preventing these already highly active neurons from overstimulation, and allowing them to further increase their firing rate only up to a certain level, similar as the one observed for the CD. Moreover, it is possible that this excitation level is simply the maximum achievable firing frequency of these cells, before

seizing to fire from a depolarisation block, which they have been observed to be susceptible to (an unpublished observation).

Overall, I believe the presented results support the already established role of the GLP1R as a potent, well selected target in the fight against obesity and diabetes (Crane & McGowan, 2016, Pedrosa *et al.*, 2022). Moreover, they propose chrononutrition and chronopharmacology as the direction of research worth further exploration and application in therapy, where the meal-driven timing of drug administration follows the establishment of a healthy feeding schedule.

Conclusions

I. **Physiology** – DMH was characterised electrophysiologically as a complex structure, with vast differences between the three outlined subdivisions. Presence of a day/night rhythm in the cellular activity was confirmed, as well as its endogenous nature. Moreover, the responsiveness of the DMH neurons to the PGDP was shown to depend on the cells' spontaneous activity, and the abundance of the GLP1 to change depending on the animals' metabolic state. The cellular reaction to satiety was enhanced when the meal had been anticipated, engaging not only the ventral, but all three parts of the structure.

II. **Pathology** – HFD was shown to abolish the day/night rhythms observed in the DMH, and delay the mean activity peak by ~2 h. Responsiveness to the GLP1R agonists no longer correlated with the cells' spontaneous activity, and the fraction of the neurons sensitive to the Exn4 increased via the enhanced synaptic network function. Metabolic state-dependent kinetics of the PGDP abundance in the structure were eliminated.

III. **Intervention** – With restricted nighttime feeding, the DMH circadian rhythmicity was successfully prevented from being attenuated by HFD.

References

1. Aaron, S. D., Fergusson, D., Dent, R., Chen, Y., Vandemheen, K. L., & Dales, R. E. (2004). Effect of weight reduction on respiratory function and airway reactivity in obese women. Chest, 125(6), 2046-2052.
2. Abe, M., Herzog, E. D., Yamazaki, S., Straume, M., Tei, H., Sakaki, Y., ... & Block, G. D. (2002). Circadian rhythms in isolated brain regions. Journal of Neuroscience, 22(1), 350-356.
3. Acosta-Galvan, G., Yi, C. X., van der Vliet, J., Jhamandas, J. H., Panula, P., Angeles-Castellanos, M., ... & Buijs, R. M. (2011). Interaction between hypothalamic dorsomedial nucleus and the suprachiasmatic nucleus determines intensity of food anticipatory behavior. Proceedings of the National Academy of Sciences, 108(14), 5813-5818.
4. Acosta-Rodríguez, V., Rijo-Ferreira, F., Izumo, M., Xu, P., Wight-Carter, M., Green, C. B., & Takahashi, J. S. (2022). Circadian alignment of early onset caloric restriction promotes longevity in male C57BL/6J mice. Science, 376(6598), 1192-1202.
5. Ando, H., Yanagihara, H., Hayashi, Y., Obi, Y., Tsuruoka, S., Takamura, T., ... & Fujimura, A. (2005). Rhythmic messenger ribonucleic acid expression of clock genes and adipocytokines in mouse visceral adipose tissue. Endocrinology, 146(12), 5631-5636.
6. Arendt, J., & Broadway, J. (1987). Light and melatonin as zeitgebers in man. Chronobiology international, 4(2), 273-282.
7. Aschoff, J. (1960, January). Exogenous and endogenous components in circadian rhythms. In Cold Spring Harbor symposia on quantitative biology (Vol. 25, pp. 11-28). Cold Spring Harbor Laboratory Press.
8. Bai, L., Mesgarzadeh, S., Ramesh, K. S., Huey, E. L., Liu, Y., Gray, L. A., ... & Knight, Z. A. (2019). Genetic identification of vagal sensory neurons that control feeding. Cell, 179(5), 1129-1143.
9. Bailey, T. W., Nicol, G. D., Schild, J. H., & DiMicco, J. A. (2003). Synaptic and membrane properties of neurons in the dorsomedial hypothalamus. Brain research, 985(2), 150-162.
10. Baker, C. L., Loros, J. J., & Dunlap, J. C. (2012). The circadian clock of Neurospora crassa. FEMS microbiology reviews, 36(1), 95-110.
11. Baldissera, F. G., Holst, J. J., Knuhtsen, S., Hilsted, L., & Nielsen, O. V. (1988). Oxyntomodulin (glicentin-(33–69)): pharmacokinetics, binding to liver cell membranes, effects on isolated perfused pig pancreas, and secretion from isolated perfused lower small intestine of pigs. Regulatory peptides, 21(1-2), 151-166.
12. Barrington, W. E., & Beresford, S. A. (2019). Eating occasions, obesity and related behaviors in working adults: Does it matter when you snack?. Nutrients, 11(10), 2320.
13. Bataille, D., & Dalle, S. (2014). The forgotten members of the glucagon family. Diabetes Research and Clinical Practice, 106(1), 1-10.
14. Belle, M. D., Diekman, C. O., Forger, D. B., & Piggins, H. D. (2009). Daily electrical silencing in the mammalian circadian clock. Science, 326(5950), 281-284.

15. Bellinger, L. L. (1987). Ingestive behavior of rats with ibotenic acid lesions of the dorsomedial hypothalamus. American Journal of Physiology-Regulatory, Integrative and Comparative Physiology, 252(5), R938-R946.
16. Bernardis, L. L. (1970). Participation of the dorsomedial hypothalamic nucleus in the "feeding center" and water intake circuitry of the weanling rat. Journal of neuro-visceral relations, 31, 387-398.
17. Berthoud, H. R., & Neuhuber, W. L. (2000). Functional and chemical anatomy of the afferent vagal system. Autonomic Neuroscience, 85(1-3), 1-17.
18. Bertisch, S. M., Sillau, S., De Boer, I. H., Szklo, M., & Redline, S. (2015). 25-Hydroxyvitamin D concentration and sleep duration and continuity: multi-ethnic study of atherosclerosis. Sleep, 38(8), 1305-1311.
19. Bi, S., Robinson, B. M., & Moran, T. H. (2003). Acute food deprivation and chronic food restriction differentially affect hypothalamic NPY mRNA expression. American Journal of Physiology-Regulatory, Integrative and Comparative Physiology, 285(5), R1030-R1036.
20. Blessing, W., Mohammed, M., & Ootsuka, Y. (2013). Brown adipose tissue thermogenesis, the basic rest–activity cycle, meal initiation, and bodily homeostasis in rats. Physiology & behavior, 121, 61-69.
21. Bolles, R. C., & Stokes, L. W. (1965). Rat's anticipation of diurnal and a-diurnal feeding. Journal of comparative and physiological psychology, 60(2), 290.
22. Branecky, K. L., Niswender, K. D., & Pendergast, J. S. (2015). Disruption of daily rhythms by high-fat diet is reversible. PloS one, 10(9), e0137970.
23. Brizuela, M., & Ootsuka, Y. (2021). Inhibition of the dorsomedial hypothalamus substantially decreases brown adipose tissue sympathetic discharge induced by activation of the lateral habenula. Autonomic Neuroscience, 230, 102745.
24. Broberger, C., Johansen, J., Johansson, C., Schalling, M., & Hökfelt, T. (1998). The neuropeptide Y/agouti gene-related protein (AGRP) brain circuitry in normal, anorectic, and monosodium glutamate-treated mice. Proceedings of the National Academy of Sciences, 95(25), 15043-15048.
25. Camargo, C. A., Weiss, S. T., Zhang, S., Willett, W. C., & Speizer, F. E. (1999). Prospective study of body mass index, weight change, and risk of adult-onset asthma in women. Archives of internal medicine, 159(21), 2582-2588.
26. Cano, G., Passerin, A. M., Schiltz, J. C., Card, J. P., Morrison, S. F., & Sved, A. F. (2003). Anatomical substrates for the central control of sympathetic outflow to interscapular adipose tissue during cold exposure. Journal of Comparative Neurology, 460(3), 303-326.
27. Canoy, D., Luben, R., Welch, A., Bingham, S., Wareham, N., Day, N., & Khaw, K. T. (2004). Abdominal obesity and respiratory function in men and women in the EPIC-Norfolk Study, United Kingdom. American journal of epidemiology, 159(12), 1140-1149.
28. Cao, W. H., Fan, W., & Morrison, S. F. (2004). Medullary pathways mediating specific sympathetic responses to activation of dorsomedial hypothalamus. Neuroscience, 126(1), 229-240.

29. Carneiro, B. T. S., & Araujo, J. F. (2009). The food-entrainable oscillator: a network of interconnected brain structures entrained by humoral signals?. Chronobiology international, 26(7), 1273-1289.
30. Castillo, M. R., Hochstetler, K. J., Tavernier Jr, R. J., Greene, D. M., & Bult-Ito, A. (2004). Entrainment of the master circadian clock by scheduled feeding. American Journal of Physiology-Regulatory, Integrative and Comparative Physiology, 287(3), R551-R555.
31. Catterall, W. A., Perez-Reyes, E., Snutch, T. P., & Striessnig, J. (2005). International Union of Pharmacology. XLVIII. Nomenclature and structure-function relationships of voltage-gated calcium channels. Pharmacological reviews, 57(4), 411-425.
32. Cavigelli, M., Dolfi, F., Claret, F. X., & Karin, M. (1995). Induction of c-fos expression through JNK-mediated TCF/Elk-1 phosphorylation. The EMBO journal, 14(23), 5957-5964.
33. Centofanti, S., Dorrian, J., Hilditch, C., Grant, C., Coates, A., & Banks, S. (2018). Eating on nightshift: A big vs small snack impairs glucose response to breakfast. Neurobiology of sleep and Circadian Rhythms, 4, 44-48.
34. Chaar, L. J., Coelho, A., Silva, N. M., Festuccia, W. L., & Antunes, V. R. (2016). High-fat diet-induced hypertension and autonomic imbalance are associated with an upregulation of CART in the dorsomedial hypothalamus of mice. Physiological Reports, 4(11), e12811.
35. Chabot, C. C., & Taylor, D. H. (1992). Circadian modulation of the rat acoustic startle response. Behavioral neuroscience, 106(5), 846.
36. Chaix, A., Zarrinpar, A., Miu, P., & Panda, S. (2014). Time-restricted feeding is a preventative and therapeutic intervention against diverse nutritional challenges. Cell metabolism, 20(6), 991-1005.
37. Chan, J. M., Rimm, E. B., Colditz, G. A., Stampfer, M. J., & Willett, W. C. (1994). Obesity, fat distribution, and weight gain as risk factors for clinical diabetes in men. Diabetes care, 17(9), 961-969.
38. Chang, A. M., Aeschbach, D., Duffy, J. F., & Czeisler, C. A. (2015). Evening use of light-emitting eReaders negatively affects sleep, circadian timing, and next-morning alertness. Proceedings of the National Academy of Sciences, 112(4), 1232-1237.
39. Chao, P. T., Yang, L., Aja, S., Moran, T. H., & Bi, S. (2011). Knockdown of NPY expression in the dorsomedial hypothalamus promotes development of brown adipocytes and prevents diet-induced obesity. Cell metabolism, 13(5), 573-583.
40. Chen, J., Scott, K. A., Zhao, Z., Moran, T. H., & Bi, S. (2008). Characterization of the feeding inhibition and neural activation produced by dorsomedial hypothalamic cholecystokinin administration. Neuroscience, 152(1), 178-188.
41. Chen, P., Williams, S. M., Grove, K. L., & Smith, M. S. (2004). Melanocortin 4 receptor-mediated hyperphagia and activation of neuropeptide Y expression in the dorsomedial hypothalamus during lactation. Journal of Neuroscience, 24(22), 5091-5100.
42. Chou, T. C., Scammell, T. E., Gooley, J. J., Gaus, S. E., Saper, C. B., & Lu, J. (2003). Critical role of dorsomedial hypothalamic nucleus in a wide range of behavioral circadian rhythms. Journal of Neuroscience, 23(33), 10691-10702.

43. Chrobok, L., Jeczmien-Lazur, J. S., Bubka, M., Pradel, K., Klekocinska, A., Klich, J. D., ... & Lewandowski, M. H. (2021a). Daily coordination of orexinergic gating in the rat superior colliculus—Implications for intrinsic clock activities in the visual system. The FASEB Journal, 35(10), e21930.
44. Chrobok, L., Klich, J. D., **Sanetra, A. M**., Jeczmien-Lazur, J. S., Pradel, K., Palus-Chramiec, K., ... & Lewandowski, M. H. (2022). Rhythmic neuronal activities of the rat nucleus of the solitary tract are impaired by high-fat diet–implications for daily control of satiety. The Journal of Physiology, 600(4), 751-767.
45. Chrobok, L., Northeast, R. C., Myung, J., Cunningham, P. S., Petit, C., & Piggins, H. D. (2020). Timekeeping in the hindbrain: a multi-oscillatory circadian centre in the mouse dorsal vagal complex. Communications biology, 3(1), 225.
46. Chrobok, L., Pradel, K., Janik, M. E., **Sanetra, A. M**., Bubka, M., Myung, J., ... & Lewandowski, M. H. (2021b). Intrinsic circadian timekeeping properties of the thalamic lateral geniculate nucleus. Journal of Neuroscience Research, 99(12), 3306-3324.
47. Chua, E. C. P., Shui, G., Lee, I. T. G., Lau, P., Tan, L. C., Yeo, S. C., ... & Gooley, J. J. (2013). Extensive diversity in circadian regulation of plasma lipids and evidence for different circadian metabolic phenotypes in humans. Proceedings of the National Academy of Sciences, 110(35), 14468-14473.
48. Chung, L. (2015). A brief introduction to the transduction of neural activity into Fos signal. Development & reproduction, 19(2), 61.
49. Cicuttini, F. M., Baker, J. R., & Spector, T. D. (1996). The association of obesity with osteoarthritis of the hand and knee in women: a twin study. The Journal of rheumatology, 23(7), 1221-1226.
50. Cohen, M. A., Ellis, S. M., Le Roux, C. W., Batterham, R. L., Park, A., Patterson, M., ... & Bloom, S. R. (2003). Oxyntomodulin suppresses appetite and reduces food intake in humans. The Journal of Clinical Endocrinology & Metabolism, 88(10), 4696-4701.
51. Colditz, G. A., Willett, W. C., Rotnitzky, A., & Manson, J. E. (1995). Weight gain as a risk factor for clinical diabetes mellitus in women. Annals of internal medicine, 122(7), 481-486.
52. Cole, R. L., Lechner, S. M., Williams, M. E., Prodanovich, P., Bleicher, L., Varney, M. A., & Gu, G. (2005). Differential distribution of voltage-gated calcium channel alpha-2 delta (α2δ) subunit mRNA-containing cells in the rat central nervous system and the dorsal root ganglia. Journal of Comparative Neurology, 491(3), 246-269.
53. Comperatore, C. A., & Stephan, F. K. (1987). Entrainment of duodenal activity to periodic feeding. Journal of biological rhythms, 2(3), 227-242.
54. Cork, S. C., Richards, J. E., Holt, M. K., Gribble, F. M., Reimann, F., & Trapp, S. (2015). Distribution and characterisation of Glucagon-like peptide-1 receptor expressing cells in the mouse brain. Molecular metabolism, 4(10), 718-731.
55. Crane, J., & McGowan, B. (2016). The GLP-1 agonist, liraglutide, as a pharmacotherapy for obesity. Therapeutic advances in chronic disease, 7(2), 92-107.
56. Cullinan, W. E., Ziegler, D. R., & Herman, J. P. (2008). Functional role of local GABAergic influences on the HPA axis. Brain Structure and Function, 213, 63-72.

57. Cypess, A. M., Lehman, S., Williams, G., Tal, I., Rodman, D., Goldfine, A. B., ... & Kahn, C. R. (2009). Identification and importance of brown adipose tissue in adult humans. New England journal of medicine, 360(15), 1509-1517.
58. D'Alessio, D. A., Kahn, S. E., Leusner, C. R., & Ensinck, J. W. (1994). Glucagon-like peptide 1 enhances glucose tolerance both by stimulation of insulin release and by increasing insulin-independent glucose disposal. The Journal of clinical investigation, 93(5), 2263-2266.
59. Daan, S., & Pittendrigh, C. S. (1976). A functional analysis of circadian pacemakers in nocturnal rodents. Journal of Comparative Physiology A, 106(3), 253-266.
60. Dakin, C. L., Gunn, I., Small, C. J., Edwards, C. M. B., Hay, D. L., Smith, D. M., ... & Bloom, S. R. (2001). Oxyntomodulin inhibits food intake in the rat. Endocrinology, 142(10), 4244-4250.
61. Dakin, C. L., Small, C. J., Batterham, R. L., Neary, N. M., Cohen, M. A., Patterson, M., ... & Bloom, S. R. (2004). Peripheral oxyntomodulin reduces food intake and body weight gain in rats. Endocrinology, 145(6), 2687-2695.
62. Dallmann, R., Viola, A. U., Tarokh, L., Cajochen, C., & Brown, S. A. (2012). The human circadian metabolome. Proceedings of the National Academy of Sciences, 109(7), 2625-2629.
63. Dalvi, P. S., & Belsham, D. D. (2012). Glucagon-like peptide-2 directly regulates hypothalamic neurons expressing neuropeptides linked to appetite control in vivo and in vitro. Endocrinology, 153(5), 2385-2397.
64. Damiola, F., Le Minh, N., Preitner, N., Kornmann, B., Fleury-Olela, F., & Schibler, U. (2000). Restricted feeding uncouples circadian oscillators in peripheral tissues from the central pacemaker in the suprachiasmatic nucleus. Genes & development, 14(23), 2950-2961.
65. Davidson, A. J. (2006). Search for the feeding-entrainable circadian oscillator: a complex proposition. American Journal of Physiology-Regulatory, Integrative and Comparative Physiology, 290(6), R1524-R1526.
66. Davidson, A. J., Poole, A. S., Yamazaki, S., & Menaker, M. (2003). Is the food-entrainable circadian oscillator in the digestive system?. Genes, Brain and Behavior, 2(1), 32-39.
67. Davidson, T. M., & Patel, M. R. (2008). Waist circumference and sleep disordered breathing. The Laryngoscope, 118(2), 339-347.
68. Davies, S. K., Ang, J. E., Revell, V. L., Holmes, B., Mann, A., Robertson, F. P., ... & Skene, D. J. (2014). Effect of sleep deprivation on the human metabolome. Proceedings of the National Academy of Sciences, 111(29), 10761-10766.
69. De Fonseca, F. R., Navarro, M., Alvarez, E., Roncero, I., Chowen, J. A., Maestre, O., ... & Blázquez, E. (2000). Peripheral versus central effects of glucagon-like peptide-1 receptor agonists on satiety and body weight loss in Zucker obese rats. Metabolism, 49(6), 709-717.
70. de Goede, P., Sen, S., Oosterman, J. E., Foppen, E., Jansen, R., La Fleur, S. E., ... & Kalsbeek, A. (2018). Differential effects of diet composition and timing of feeding behavior on rat brown adipose tissue and skeletal muscle peripheral clocks. Neurobiology of sleep and circadian rhythms, 4, 24-33.

71. De Lecea, L., Kilduff, T. S., Peyron, C., Gao, X. B., Foye, P. E., Danielson, P. E., ... & Sutcliffe, J. (1998). The hypocretins: hypothalamus-specific peptides with neuroexcitatory activity. Proceedings of the National Academy of Sciences, 95(1), 322-327.
72. De Mairan, J. (1729). Observation Botanique. Hist. L'Academie R. Sci. Paris, 1729, 35.
73. de Noronha, S. R., Campos, G. V., Abreu, A. R., de Souza, A. A., Chianca Jr, D. A., & de Menezes, R. C. (2017). High fat diet induced-obesity facilitates anxiety-like behaviors due to GABAergic impairment within the dorsomedial hypothalamus in rats. Behavioural brain research, 316, 38-46.
74. Di Lorenzo, L., De Pergola, G., Zocchetti, C., L'Abbate, N., Basso, A., Pannacciulli, N., ... & Soleo, L. (2003). Effect of shift work on body mass index: results of a study performed in 319 glucose-tolerant men working in a Southern Italian industry. International journal of obesity, 27(11), 1353-1358.
75. Diekman, C. O., Belle, M. D., Irwin, R. P., Allen, C. N., Piggins, H. D., & Forger, D. B. (2013). Causes and consequences of hyperexcitation in central clock neurons. PLoS computational biology, 9(8), e1003196.
76. Dixon, J. B., Schachter, L. M., & O'brien, P. E. (2001). Sleep disturbance and obesity: changes following surgically induced weight loss. Archives of internal medicine, 161(1), 102-106.
77. Dodd, G. T., Worth, A. A., Nunn, N., Korpal, A. K., Bechtold, D. A., Allison, M. B., ... & Luckman, S. M. (2014). The thermogenic effect of leptin is dependent on a distinct population of prolactin-releasing peptide neurons in the dorsomedial hypothalamus. Cell metabolism, 20(4), 639-649.
78. Drucker, D. J., Philippe, J., Mojsov, S., Chick, W. L., & Habener, J. F. (1987). Glucagon-like peptide I stimulates insulin gene expression and increases cyclic AMP levels in a rat islet cell line. Proceedings of the National Academy of Sciences, 84(10), 3434-3438.
79. Drucker-Colín, R., Aguilar-Roblero, R., García-Hernández, F., Fernández-Cancino, F., & Rattoni, F. B. (1984). Fetal suprachiasmatic nucleus transplants: diurnal rhythm recovery of lesioned rats. Brain research, 311(2), 353-357.
80. Dube, M. G., Kalra, S. P., & Kalra, P. S. (1999). Food intake elicited by central administration of orexins/hypocretins: identification of hypothalamic sites of action. Brain research, 842(2), 473-477.
81. Dupré, J., Behme, M. T., & McDonald, T. J. (2004). Exendin-4 normalized postcibal glycemic excursions in type 1 diabetes. The journal of clinical endocrinology & metabolism, 89(7), 3469-3473.
82. Dzhura, I., Chepurny, O. G., Kelley, G. G., Leech, C. A., Roe, M. W., Dzhura, E., ... & Holz, G. G. (2010). Epac2-dependent mobilization of intracellular Ca2+ by glucagon-like peptide-1 receptor agonist exendin-4 is disrupted in β-cells of phospholipase C-ε knockout mice. The Journal of physiology, 588(24), 4871-4889.
83. Edgar, R. S., Green, E. W., Zhao, Y., Van Ooijen, G., Olmedo, M., Qin, X., ... & Reddy, A. B. (2012). Peroxiredoxins are conserved markers of circadian rhythms. Nature, 485(7399), 459-464.

84. Edmonds, S. C., & Adler, N. T. (1977). The multiplicity of biological oscillators in the control of circadian running activity in the rat. Physiology & behavior, 18(5), 921-930.
85. Elmquist, J. K., Bjørbæk, C., Ahima, R. S., Flier, J. S., & Saper, C. B. (1998). Distributions of leptin receptor mRNA isoforms in the rat brain. Journal of Comparative Neurology, 395(4), 535-547.
86. EMA (2022a, July 6). Saxenda - European Medicines Agency. European Medicines Agency. https://www.ema.europa.eu/en/medicines/human/EPAR/saxenda
87. EMA (2022b, August 26). Wegovy - European Medicines Agency. European Medicines Agency. https://www.ema.europa.eu/en/medicines/human/EPAR/wegovy
88. Enriori, P. J., Sinnayah, P., Simonds, S. E., Rudaz, C. G., & Cowley, M. A. (2011). Leptin action in the dorsomedial hypothalamus increases sympathetic tone to brown adipose tissue in spite of systemic leptin resistance. Journal of Neuroscience, 31(34), 12189-12197.
89. Eslick, G. D., & Talley, N. J. (2016). Gastrointestinal symptoms negatively impact on sleep quality among obese individuals: a population-based study. Sleep and Breathing, 20, 363-367.
90. Faber, C. L., Deem, J. D., Phan, B. A., Doan, T. P., Ogimoto, K., Mirzadeh, Z., ... & Morton, G. J. (2021). Leptin receptor neurons in the dorsomedial hypothalamus regulate diurnal patterns of feeding, locomotion, and metabolism. Elife, 10, e63671.
91. FDA. (2021, June 4). FDA Approves New Drug Treatment for Chronic Weight Management, First Since 2014 [Press release]. https://www.fda.gov/news-events/press-announcements/fda-approves-new-drug-treatment-chronic-weight-management-first-2014
92. Felson, D. T., Zhang, Y., Anthony, J. M., Naimark, A., & Anderson, J. J. (1992). Weight loss reduces the risk for symptomatic knee osteoarthritis in women: the Framingham Study. Annals of internal medicine, 116(7), 535-539.
93. Ford, N. D., Patel, S. A., & Narayan, K. V. (2017). *Obesity in low-and middle-income countries: burden, drivers, and emerging challenges.* Annual review of public health, 38, 145-164.
94. Fox, A. P., Nowycky, M. C., & Tsien, R. W. (1987). Kinetic and pharmacological properties distinguishing three types of calcium currents in chick sensory neurones. The Journal of physiology, 394(1), 149-172.
95. Frank, M. G., Ruby, N. F., Heller, H. C., & Franken, P. (2017). Development of circadian sleep regulation in the rat: a longitudinal study under constant conditions. Sleep, 40(3).
96. Frisch, B., Hardin, P. E., Hamblen-Coyle, M. J., Rosbash, M., & Hall, J. C. (1994). A promoterless period gene mediates behavioral rhythmicity and cyclical per expression in a restricted subset of the Drosophila nervous system. Neuron, 12(3), 555-570.
97. Fuller, N. R., Lau, N. S., Denyer, G., & Caterson, I. D. (2013). An intragastric balloon produces large weight losses in the absence of a change in ghrelin or peptide YY. Clinical Obesity, 3(6), 172-179.
98. Gamaldo, C. E., Shaikh, A. K., & McArthur, J. C. (2012). The sleep-immunity relationship. Neurologic clinics, 30(4), 1313-1343.

99. Gamble, K. L., Berry, R., Frank, S. J., & Young, M. E. (2014). Circadian clock control of endocrine factors. Nature Reviews Endocrinology, 10(8), 466-475.
100. Ganle, J. K., Boakye, P. P., & Baatiema, L. (2019). Childhood obesity in urban Ghana: evidence from a cross-sectional survey of in-school children aged 5–16 years. BMC public health, 19(1), 1-12.
101. Gao, X., Schwarzschild, M. A., Wang, H., & Ascherio, A. (2009). Obesity and restless legs syndrome in men and women. Neurology, 72(14), 1255-1261.
102. Gaston, K. J., Davies, T. W., Nedelec, S. L., & Holt, L. A. (2017). Impacts of artificial light at night on biological timings. Annual Review of Ecology, Evolution, and Systematics, 48, 49-68.
103. Gentilcore, D., Chaikomin, R., Jones, K. L., Russo, A., Feinle-Bisset, C., Wishart, J. M., ... & Horowitz, M. (2006). Effects of fat on gastric emptying of and the glycemic, insulin, and incretin responses to a carbohydrate meal in type 2 diabetes. The Journal of Clinical Endocrinology & Metabolism, 91(6), 2062-2067.
104. Gill, S., & Panda, S. (2015). A smartphone app reveals erratic diurnal eating patterns in humans that can be modulated for health benefits. Cell metabolism, 22(5), 789-798.
105. Goldfarb, M., Schoorlemmer, J., Williams, A., Diwakar, S., Wang, Q., Huang, X., ... & D'Angelo, E. (2007). Fibroblast growth factor homologous factors control neuronal excitability through modulation of voltage-gated sodium channels. Neuron, 55(3), 449-463.
106. Gooley, J. J., Lu, J., Chou, T. C., Scammell, T. E., & Saper, C. B. (2001). Melanopsin in cells of origin of the retinohypothalamic tract. Nature neuroscience, 4(12), 1165-1165.
107. Gooley, J. J., Schomer, A., & Saper, C. B. (2006). The dorsomedial hypothalamic nucleus is critical for the expression of food-entrainable circadian rhythms. Nature neuroscience, 9(3), 398-407.
108. Granados-Fuentes, D., Tseng, A., & Herzog, E. D. (2006). A circadian clock in the olfactory bulb controls olfactory responsivity. Journal of Neuroscience, 26(47), 12219-12225.
109. Greenwell, B. J., Trott, A. J., Beytebiere, J. R., Pao, S., Bosley, A., Beach, E., ... & Menet, J. S. (2019). Rhythmic food intake drives rhythmic gene expression more potently than the hepatic circadian clock in mice. Cell reports, 27(3), 649-657.
110. Greiner, E. M., & Petrovich, G. D. (2020). The effects of novelty on food consumption in male and female rats. Physiology & behavior, 223, 112970.
111. Grobbelaar, N., Huang, T. C., Lin, H. Y., & Chow, T. J. (1986). Dinitrogen-fixing endogenous rhythm in Synechococcus RF-1. FEMS Microbiology Letters, 37(2), 173-177.
112. Gros, L., Thorens, B., Bataille, D., & Kervran, A. (1993). Glucagon-like peptide-1-(7-36) amide, oxyntomodulin, and glucagon interact with a common receptor in a somatostatin-secreting cell line. Endocrinology, 133(2), 631-638.
113. Guan, X. (2014). The CNS glucagon-like peptide-2 receptor in the control of energy balance and glucose homeostasis. American Journal of Physiology-Regulatory, Integrative and Comparative Physiology, 307(6), R585-R596.

114. Guan, X. M., Yu, H., Trumbauer, M., Frazier, E., Van der Ploeg, L. H., & Chen, H. (1998). Induction of neuropeptide Y expression in dorsomedial hypothalamus of diet-induced obese mice. Neuroreport, 9(15), 3415-3419.
115. Guilding, C., Hughes, A. T., Brown, T. M., Namvar, S., & Piggins, H. D. (2009). A riot of rhythms: neuronal and glial circadian oscillators in the mediobasal hypothalamus. Molecular brain, 2(1), 1-19.
116. Gutniak, M., Ørkov, C., Holst, J. J., Ahrén, B., & Efendić, S. (1992). Antidiabetogenic effect of glucagon-like peptide-1 (7–36) amide in normal subjects and patients with diabetes mellitus. New England Journal of Medicine, 326(20), 1316-1322.
117. Hamaguchi, M., Kojima, T., Takeda, N., Nakagawa, T., Taniguchi, H., Fujii, K., ... & Ida, K. (2005). The metabolic syndrome as a predictor of nonalcoholic fatty liver disease. Annals of internal medicine, 143(10), 722-728.
118. Hansen, L. H., Abrahamsen, N., & Nishimura, E. (1995). Glucagon receptor mRNA distribution in rat tissues. Peptides, 16(6), 1163-1166.
119. Hara, R., Wan, K., Wakamatsu, H., Aida, R., Moriya, T., Akiyama, M., & Shibata, S. (2001). Restricted feeding entrains liver clock without participation of the suprachiasmatic nucleus. Genes to Cells, 6(3), 269-278.
120. Harmer, S. L. (2009). The circadian system in higher plants. Annual review of plant biology, 60, 357-377.
121. Hart, D. J., & Spector, T. D. (1993). The relationship of obesity, fat distribution and osteoarthritis in women in the general population: the Chingford Study. The Journal of rheumatology, 20(2), 331-335.
122. Hatori, M., Vollmers, C., Zarrinpar, A., DiTacchio, L., Bushong, E. A., Gill, S., ... & Panda, S. (2012). Time-restricted feeding without reducing caloric intake prevents metabolic diseases in mice fed a high-fat diet. Cell metabolism, 15(6), 848-860.
123. Hattar, S., Liao, H. W., Takao, M., Berson, D. M., & Yau, K. W. (2002). Melanopsin-containing retinal ganglion cells: architecture, projections, and intrinsic photosensitivity. Science, 295(5557), 1065-1070.
124. Hawkes, C., & Fanzo, J. (2017). Nourishing the sdgs: global nutrition report. Bristol, UK: Development Initiatives Poverty Research Ltd.
125. He, K., Hu, F. B., Colditz, G. A., Manson, J. E., Willett, W. C., & Liu, S. (2004). Changes in intake of fruits and vegetables in relation to risk of obesity and weight gain among middle-aged women. International journal of obesity, 28(12), 1569-1574.
126. Hendrickson, A. E., Wagoner, N., & Cowan, W. M. (1972). An autoradiographic and electron microscopic study of retino-hypothalamic connections. Zeitschrift für Zellforschung und mikroskopische Anatomie, 135(1), 1-26.
127. Herzog, E. D., Takahashi, J. S., & Block, G. D. (1998). Clock controls circadian period in isolated suprachiasmatic nucleus neurons. Nature neuroscience, 1(8), 708-713.
128. Himms-Hagen, J. (1990). Brown adipose tissue thermogenesis: interdisciplinary studies. The FASEB Journal, 4(11), 2890-2898.
129. Himms-Hagen, J., & Desautels, M. (1978). A mitochondrial defect in brown adipose tissue of the obese (obob) mouse: reduced binding of purine nucleotides and a failure to respond to cold by an increase in binding. Biochemical and biophysical research communications, 83(2), 628-634.

130. Holz IV, G. G., Kiihtreiber, W. M., & Habener, J. F. (1993). Pancreatic beta-cells are rendered glucose-competent by the insulinotropic hormone glucagon-like peptide-1 (7-37). Nature, 361, 362-365.
131. Hoosein, N. M., & Gurd, R. S. (1984). Identification of glucagon receptors in rat brain. Proceedings of the National Academy of Sciences, 81(14), 4368-4372.
132. Hruby, A., & Hu, F. B. (2015). The epidemiology of obesity: a big picture. Pharmacoeconomics, 33, 673-689.
133. Hsieh, M. C., Yang, S. C., Tseng, H. L., Hwang, L. L., Chen, C. T., & Shieh, K. R. (2010). Abnormal expressions of circadian-clock and circadian clock-controlled genes in the livers and kidneys of long-term, high-fat-diet-treated mice. International Journal of Obesity, 34(2), 227-239.
134. Huang, Z., Liu, L., Zhang, J., Conde, K., Phansalkar, J., Li, Z., ... & Liu, J. (2022). Glucose-sensing glucagon-like peptide-1 receptor neurons in the dorsomedial hypothalamus regulate glucose metabolism. Science Advances, 8(23), eabn5345.
135. Imoto, D., Yamamoto, I., Matsunaga, H., Yonekura, T., Lee, M. L., Kato, K. X., ... & Toda, C. (2021). Refeeding activates neurons in the dorsomedial hypothalamus to inhibit food intake and promote positive valence. Molecular Metabolism, 54, 101366.
136. Isom, L. L., Scheuer, T., Brownstein, A. B., Ragsdale, D. S., Murphy, B. J., & Catterall, W. A. (1995). Functional Co-expression of the β1 and Type IIA α Subunits of Sodium Channels in a Mammalian Cell Line (∗). Journal of Biological Chemistry, 270(7), 3306-3312.
137. Jakobsen, H. H., & Strom, S. L. (2004). Circadian cycles in growth and feeding rates of heterotrophic protist plankton. Limnology and oceanography, 49(6), 1915-1922.
138. Johnson, C. H., Egli, M., & Stewart, P. L. (2008). Structural insights into a circadian oscillator. Science, 322(5902), 697-701.
139. Johnson, D. F., Ackroff, K., Peters, J., & Collier, G. H. (1986). Changes in rat's meal patterns as a function of the caloric density of the diet. Physiology & behavior, 36(5), 929-936.
140. Johnstone, L. E., Fong, T. M., & Leng, G. (2006). Neuronal activation in the hypothalamus and brainstem during feeding in rats. Cell metabolism, 4(4), 313-321.
141. Kang, J., Huguenard, J. R., & Prince, D. A. (2000). Voltage-gated potassium channels activated during action potentials in layer V neocortical pyramidal neurons. Journal of neurophysiology.
142. Kania, A., Sambak, P., Gugula, A., Szlaga, A., Soltys, Z., Blasiak, T., ... & Blasiak, A. (2020). Electrophysiology and distribution of oxytocin and vasopressin neurons in the hypothalamic paraventricular nucleus: a study in male and female rats. Brain Structure and Function, 225(1), 285-304.
143. Karlsson, B., Knutsson, A., & Lindahl, B. (2001). Is there an association between shift work and having a metabolic syndrome? Results from a population based study of 27 485 people. Occupational and environmental medicine, 58(11), 747-752.
144. Karlsson, B. H., Knutsson, A. K., Lindahl, B. O., & Alfredsson, L. S. (2003). Metabolic disturbances in male workers with rotating three-shift work. Results of the WOLF study. International archives of occupational and environmental health, 76, 424-430.

145. Kesterson, R. A., Huszar, D., Lynch, C. A., Simerly, R. B., & Cone, R. D. (1997). Induction of neuropeptide Y gene expression in the dorsal medial hypothalamic nucleus in two models of the agouti obesity syndrome. Molecular endocrinology, 11(5), 630-637.
146. Khera, R., Murad, M. H., Chandar, A. K., Dulai, P. S., Wang, Z., Prokop, L. J., ... & Singh, S. (2016). Association of pharmacological treatments for obesity with weight loss and adverse events: a systematic review and meta-analysis. Jama, 315(22), 2424-2434.
147. Kim, Y. J., & Bi, S. (2016). Knockdown of neuropeptide Y in the dorsomedial hypothalamus reverses high-fat diet-induced obesity and impaired glucose tolerance in rats. American Journal of Physiology-Regulatory, Integrative and Comparative Physiology, 310(2), R134-R142.
148. Kittrell, E. M. W., & Satinoff, E. (1986). Development of the circadian rhythm of body temperature in rats. Physiology & behavior, 38(1), 99-104.
149. Kobelt, P., Wisser, A. S., Stengel, A., Goebel, M., Inhoff, T., Noetzel, S., ... & Mönnikes, H. (2008). Peripheral injection of ghrelin induces Fos expression in the dorsomedial hypothalamic nucleus in rats. Brain research, 1204, 77-86.
150. Kohsaka, A., Laposky, A. D., Ramsey, K. M., Estrada, C., Joshu, C., Kobayashi, Y., ... & Bass, J. (2007). High-fat diet disrupts behavioral and molecular circadian rhythms in mice. Cell metabolism, 6(5), 414-421.
151. Kolterman, O. G., Buse, J. B., Fineman, M. S., Gaines, E., Heintz, S., Bicsak, T. A., ... & Baron, A. D. (2003). Synthetic exendin-4 (exenatide) significantly reduces postprandial and fasting plasma glucose in subjects with type 2 diabetes. The Journal of Clinical Endocrinology & Metabolism, 88(7), 3082-3089.
152. Kono, Y., Yokota, S., Fukushi, I., Arima, Y., Onimaru, H., Okazaki, S., ... & Okada, Y. (2020). Structural and functional connectivity from the dorsomedial hypothalamus to the ventral medulla as a chronological amplifier of sympathetic outflow. Scientific reports, 10(1), 1-11.
153. Kosmadopoulos, A., Kervezee, L., Boudreau, P., Gonzales-Aste, F., Vujovic, N., Scheer, F. A., & Boivin, D. B. (2020). Effects of shift work on the eating behavior of police officers on patrol. Nutrients, 12(4), 999.
154. Kreymann, B., Ghatei, M. A., Williams, G., & Bloom, S. R. (1987). Glucagon-like peptide-1 7-36: a physiological incretin in man. The Lancet, 330(8571), 1300-1304.
155. Krieger, D. T., Hauser, H., & Krey, L. C. (1977). Suprachiasmatic nuclear lesions do not abolish food-shifted circadian adrenal and temperature rhythmicity. Science, 197(4301), 398-399.
156. Kristensen, P., Judge, M. E., Thim, L., Ribel, U., Christjansen, K. N., Wulff, B. S., ... & Hastrup, S. (1998). Hypothalamic CART is a new anorectic peptide regulated by leptin. Nature, 393(6680), 72-76.
157. Lamont, E. W., Diaz, L. R., Barry-Shaw, J., Stewart, J., & Amir, S. (2005). Daily restricted feeding rescues a rhythm of period2 expression in the arrhythmic suprachiasmatic nucleus. Neuroscience, 132(2), 245-248.
158. Landry, G. J., Simon, M. M., Webb, I. C., & Mistlberger, R. E. (2006). Persistence of a behavioral food-anticipatory circadian rhythm following dorsomedial hypothalamic

ablation in rats. American Journal of Physiology-Regulatory, Integrative and Comparative Physiology, 290(6), R1527-R1534.
159. Larsen, P. J., Tang-Christensen, M., Holst, J. J., & Ørskov, C. (1997). Distribution of glucagon-like peptide-1 and other preproglucagon-derived peptides in the rat hypothalamus and brainstem. Neuroscience, 77(1), 257-270.
160. Lauby-Secretan, B., Scoccianti, C., Loomis, D., Grosse, Y., Bianchini, F., & Straif, K. (2016). Body fatness and cancer—viewpoint of the IARC Working Group. New England journal of medicine, 375(8), 794-798.
161. Le Quellec, A., Kervran, A., Blache, P., Ciurana, A. J., & Bataille, D. (1992). Oxyntomodulin-like immunoreactivity: diurnal profile of a new potential enterogastrone. The Journal of Clinical Endocrinology & Metabolism, 74(6), 1405-1409.
162. LeCheminant, J. D., Christenson, E., Bailey, B. W., & Tucker, L. A. (2013). Restricting night-time eating reduces daily energy intake in healthy young men: a short-term cross-over study. British journal of nutrition, 110(11), 2108-2113.
163. Lee, S. J., Sanchez-Watts, G., Krieger, J. P., Pignalosa, A., Norell, P. N., Cortella, A., ... & Watts, A. G. (2018). Loss of dorsomedial hypothalamic GLP-1 signaling reduces BAT thermogenesis and increases adiposity. Molecular metabolism, 11, 33-46.
164. Li, M., West, J. W., Lai, Y., Scheuer, T., & Catterall, W. A. (1992). Functional modulation of brain sodium channels by cAMP-dependent phosphorylation. Neuron, 8(6), 1151-1159.
165. Li, T. L., Chen, J. Y., Huang, S. C., Dai, Y. W. E., & Hwang, L. L. (2018). Cardiovascular pressor effects of orexins in the dorsomedial hypothalamus. European Journal of Pharmacology, 818, 343-350.
166. Li, T. L., Lee, Y. H., Wu, F. H., & Hwang, L. L. (2021). Orexin-A directly depolarizes dorsomedial hypothalamic neurons, including those innervating the rostral ventrolateral medulla. European Journal of Pharmacology, 899, 174033.
167. Lopez-Santiago, L. F., Pertin, M., Morisod, X., Chen, C., Hong, S., Wiley, J., ... & Isom, L. L. (2006). Sodium channel β2 subunits regulate tetrodotoxin-sensitive sodium channels in small dorsal root ganglion neurons and modulate the response to pain. Journal of Neuroscience, 26(30), 7984-7994.
168. Lowry, C. A., Plant, A., Shanks, N., Ingram, C. D., & Lightman, S. L. (2003). Anatomical and functional evidence for a stress-responsive, monoamine-accumulating area in the dorsomedial hypothalamus of adult rat brain. Hormones and behavior, 43(1), 254-262.
169. Lucas, F., Ackroff, K., & Sclafani, A. (1998). High-fat diet preference and overeating mediated by postingestive factors in rats. American Journal of Physiology-Regulatory, Integrative and Comparative Physiology, 275(5), R1511-R1522.
170. Luppino, F. S., de Wit, L. M., Bouvy, P. F., Stijnen, T., Cuijpers, P., Penninx, B. W., & Zitman, F. G. (2010). Overweight, obesity, and depression: a systematic review and meta-analysis of longitudinal studies. Archives of general psychiatry, 67(3), 220-229.
171. Lutter, M., & Nestler, E. J. (2009). Homeostatic and hedonic signals interact in the regulation of food intake. The Journal of nutrition, 139(3), 629-632.

172. Ma, J. Y., Li, M. I. N. G., Catterall, W. A., & Scheuer, T. (1994). Modulation of brain Na+ channels by a G-protein-coupled pathway. Proceedings of the National Academy of Sciences, 91(25), 12351-12355.
173. Maejima, Y., Yokota, S., Shimizu, M., Horita, S., Kobayashi, D., Hazama, A., & Shimomura, K. (2021). The deletion of glucagon-like peptide-1 receptors expressing neurons in the dorsomedial hypothalamic nucleus disrupts the diurnal feeding pattern and induces hyperphagia and obesity. Nutrition & Metabolism, 18(1), 58.
174. Maida, A., Lovshin, J. A., Baggio, L. L., & Drucker, D. J. (2008). The glucagon-like peptide-1 receptor agonist oxyntomodulin enhances β-cell function but does not inhibit gastric emptying in mice. Endocrinology, 149(11), 5670-5678.
175. Mallon, L., Broman, J. E., & Hetta, J. (2008). Restless legs symptoms with sleepiness in relation to mortality: 20-year follow-up study of a middle-aged Swedish population. Psychiatry and clinical neurosciences, 62(4), 457-463.
176. Manella, G., Sabath, E., Aviram, R., Dandavate, V., Ezagouri, S., Golik, M., ... & Asher, G. (2021). The liver-clock coordinates rhythmicity of peripheral tissues in response to feeding. Nature metabolism, 3(6), 829-842.
177. Matsumoto, N., Sorimachi, M., & Akaike, N. (2004). Excitatory effects of ATP on rat dorsomedial hypothalamic neurons. Brain research, 1009(1-2), 234-237.
178. Maurice, N., Tkatch, T., Meisler, M., Sprunger, L. K., & Surmeier, D. J. (2001). D1/D5 dopamine receptor activation differentially modulates rapidly inactivating and persistent sodium currents in prefrontal cortex pyramidal neurons. Journal of Neuroscience, 21(7), 2268-2277.
179. McCarty, D. E., Reddy, A., Keigley, Q., Kim, P. Y., Cohen, S., & Marino, A. A. (2013). Nonspecific pain is a marker for hypovitaminosis D in patients undergoing evaluation for sleep disorders: a pilot study. Nature and science of sleep, 37-42.
180. McHill, A. W., Phillips, A. J., Czeisler, C. A., Keating, L., Yee, K., Barger, L. K., ... & Klerman, E. B. (2017). Later circadian timing of food intake is associated with increased body fat. The American journal of clinical nutrition, 106(5), 1213-1219.
181. Merchenthaler, I., Lane, M., & Shughrue, P. (1999). Distribution of pre-pro-glucagon and glucagon-like peptide-1 receptor messenger RNAs in the rat central nervous system. Journal of Comparative Neurology, 403(2), 261-280.
182. Meyer-Gerspach, A. C., Wölnerhanssen, B., Beglinger, B., Nessenius, F., Napitupulu, M., Schulte, F. H., ... & Beglinger, C. (2014). Gastric and intestinal satiation in obese and normal weight healthy people. Physiology & behavior, 129, 265-271.
183. Mieda, M., Williams, S. C., Richardson, J. A., Tanaka, K., & Yanagisawa, M. (2006). The dorsomedial hypothalamic nucleus as a putative food-entrainable circadian pacemaker. Proceedings of the National Academy of Sciences, 103(32), 12150-12155.
184. Miller, W. C., Niederpruem, M. G., Wallace, J. P., & Lindeman, A. K. (1994). Dietary fat, sugar, and fiber predict body fat content. Journal of the American Dietetic Association, 94(6), 612-615.
185. Minana-Solis, M. C., Angeles-Castellanos, M., Feillet, C., Pevet, P., Challet, E., & Escobar, C. (2009). Differential effects of a restricted feeding schedule on clock-gene

expression in the hypothalamus of the rat. Chronobiology international, 26(5), 808-820.
186. Mojsov, S., Heinrich, G., Wilson, I. B., Ravazzola, M., Orci, L., & Habener, J. F. (1986). Preproglucagon gene expression in pancreas and intestine diversifies at the level of post-translational processing. Journal of Biological Chemistry, 261(25), 11880-11889.
187. Molnar, C. S., Kallo, I., Liposits, Z., & Hrabovszky, E. (2011). Estradiol down-regulates RF-amide-related peptide (RFRP) expression in the mouse hypothalamus. Endocrinology, 152(4), 1684-1690.
188. Montrose-Rafizadeh, C., Avdonin, P., Garant, M. J., Rodgers, B. D., Kole, S., Yang, H., ... & Bernier, M. (1999). Pancreatic glucagon-like peptide-1 receptor couples to multiple G proteins and activates mitogen-activated protein kinase pathways in Chinese hamster ovary cells. Endocrinology, 140(3), 1132-1140.
189. Moore, R. Y., & Lenn, N. J. (1972). A retinohypothalamic projection in the rat. Journal of Comparative Neurology, 146(1), 1-14.
190. Moreno-Vecino, B., Arija-Blázquez, A., Pedrero-Chamizo, R., Gómez-Cabello, A., Alegre, L. M., Pérez-López, F. R., ... & EXERNET Group. (2017). Sleep disturbance, obesity, physical fitness and quality of life in older women: EXERNET study group. Climacteric, 20(1), 72-79.
191. Morgan, J. I., & Curran, T. (1986). Role of ion flux in the control of c-fos expression. Nature, 322(6079), 552-555.
192. Moriya, T., Aida, R., Kudo, T., Akiyama, M., Doi, M., Hayasaka, N., ... & Shibata, S. (2009). The dorsomedial hypothalamic nucleus is not necessary for food-anticipatory circadian rhythms of behavior, temperature or clock gene expression in mice. European Journal of Neuroscience, 29(7), 1447-1460.
193. Morris, C. J., Yang, J. N., Garcia, J. I., Myers, S., Bozzi, I., Wang, W., ... & Scheer, F. A. (2015). Endogenous circadian system and circadian misalignment impact glucose tolerance via separate mechanisms in humans. Proceedings of the National Academy of Sciences, 112(17), E2225-E2234.
194. Müller, R., Bravo, R., Burckhardt, J., & Curran, T. (1984). Induction of c-fos gene and protein by growth factors precedes activation of c-myc. Nature, 312(5996), 716-720.
195. Muscogiuri, G., Sorice, G. P., Prioletta, A., Policola, C., Della Casa, S., Pontecorvi, A., & Giaccari, A. (2010). 25-Hydroxyvitamin D concentration correlates with insulin-sensitivity and BMI in obesity. Obesity, 18(10), 1906-1910.
196. Myung, J., Schmal, C., Hong, S., Tsukizawa, Y., Rose, P., Zhang, Y., ... & Takumi, T. (2018). The choroid plexus is an important circadian clock component. Nature communications, 9(1), 1062.
197. Nambu, T., Sakurai, T., Mizukami, K., Hosoya, Y., Yanagisawa, M., & Goto, K. (1999). Distribution of orexin neurons in the adult rat brain. Brain research, 827(1-2), 243-260.
198. Näslund, E., Gutniak, M., Skogar, S., Rössner, S., & Hellström, P. M. (1998). Glucagon-like peptide 1 increases the period of postprandial satiety and slows gastric emptying in obese men. The American journal of clinical nutrition, 68(3), 525-530.

199. Nathan, D. M., Schreiber, E., Fogel, H., Mojsov, S., & Habener, J. F. (1992). Insulinotropic action of glucagonlike peptide-I-(7–37) in diabetic and nondiabetic subjects. Diabetes care, 15(2), 270-276.
200. Nauck, M. A., Heimesaat, M. M., Orskov, C., Holst, J. J., Ebert, R., & Creutzfeldt, W. (1993). Preserved incretin activity of glucagon-like peptide 1 [7-36 amide] but not of synthetic human gastric inhibitory polypeptide in patients with type-2 diabetes mellitus. The Journal of clinical investigation, 91(1), 301-307.
201. Ng, M., Fleming, T., Robinson, M., Thomson, B., Graetz, N., Margono, C., ... & Gakidou, E. (2014). Global, regional, and national prevalence of overweight and obesity in children and adults during 1980–2013: a systematic analysis for the Global Burden of Disease Study 2013. The lancet, 384(9945), 766-781.
202. Ni, Y., Wu, L., Jiang, J., Yang, T., Wang, Z., Ma, L., ... & Fu, Z. (2019). Late-Night Eating-Induced Physiological Dysregulation and Circadian Misalignment Are Accompanied by Microbial Dysbiosis. Molecular nutrition & food research, 63(24), 1900867.
203. Northeast, R. C., Chrobok, L., Hughes, A. T., Petit, C., & Piggins, H. D. (2020). Keeping time in the lamina terminalis: Novel oscillator properties of forebrain sensory circumventricular organs. The FASEB Journal, 34(1), 974.
204. Olszewski, P. K., Grace, M. K., Billington, C. J., & Levine, A. S. (2003). Hypothalamic paraventricular injections of ghrelin: effect on feeding and c-Fos immunoreactivity. Peptides, 24(6), 919-923.
205. Opp, M. R., Kapas, L., & Toth, L. A. (1992). Cytokine involvement in the regulation of sleep. Proceedings of the society for Experimental Biology and Medicine, 201(1), 16-27.
206. Osaka, T., Endo, M., Yamakawa, M., & Inoue, S. (2005). Energy expenditure by intravenous administration of glucagon-like peptide-1 mediated by the lower brainstem and sympathoadrenal system. Peptides, 26(9), 1623-1631.
207. Oscai, L. B., Miller, W. C., & Arnall, D. A. (1987). Effects of dietary sugar and of dietary fat on food intake and body fat content in rats. Growth, 51(1), 64-73.
208. Özdemir-Kumral, Z. N., Koyuncuoğlu, T., Arabacı-Tamer, S., Çilingir-Kaya, Ö. T., Köroğlu, A. K., Yüksel, M., & Yeğen, B. Ç. (2021). High-fat diet enhances gastric contractility, but abolishes nesfatin-1-induced inhibition of gastric emptying. Journal of Neurogastroenterology and Motility, 27(2), 265.
209. Palus-Chramiec, K., **Sanetra, A. M.,** & Lewandowski, M. H. (2022). Day/night changes in the dorsomedial hypothalamus firing responses to ghrelin are modulated by high-fat diet. Neuroscience, 494, 167-177.
210. Panda, S., Sato, T. K., Castrucci, A. M., Rollag, M. D., DeGrip, W. J., Hogenesch, J. B., ... & Kay, S. A. (2002). Melanopsin (Opn4) requirement for normal light-induced circadian phase shifting. Science, 298(5601), 2213-2216.
211. Parlevliet, E. T., Heijboer, A. C., Schroder-van der Elst, J. P., Havekes, L. M., Romijn, J. A., Pijl, H., & Corssmit, E. P. (2008). Oxyntomodulin ameliorates glucose intolerance in mice fed a high-fat diet. American Journal of Physiology-Endocrinology and Metabolism, 294(1), E142-E147.

212. Patton, D. E., Isom, L. L., Catterall, W. A., & Goldin, A. L. (1994). The adult rat brain beta 1 subunit modifies activation and inactivation gating of multiple sodium channel alpha subunits. Journal of Biological Chemistry, 269(26), 17649-17655.
213. Paxinos, G., & Watson, C. (2007). The rat brain in stereotaxic coordinates. Academic Press.
214. Pedrosa, M. R., Franco, D. R., Gieremek, H. W., Vidal, C. M., Bronzeri, F., de Cassia Rocha, A., ... & Eliaschewitz, F. G. (2022). GLP-1 Agonist to Treat Obesity and Prevent Cardiovascular Disease: What Have We Achieved so Far?. Current Atherosclerosis Reports, 24(11), 867-884.
215. Pendergast, J. S., Branecky, K. L., Yang, W., Ellacott, K. L., Niswender, K. D., & Yamazaki, S. (2013). High-fat diet acutely affects circadian organisation and eating behavior. European Journal of Neuroscience, 37(8), 1350-1356.
216. Pennartz, C. M., de Jeu, M. T., Bos, N. P., Schaap, J., & Geurtsen, A. M. (2002). Diurnal modulation of pacemaker potentials and calcium current in the mammalian circadian clock. Nature, 416(6878), 286-290.
217. Perello, M., Stuart, R. C., & Nillni, E. A. (2007). Differential effects of fasting and leptin on proopiomelanocortin peptides in the arcuate nucleus and in the nucleus of the solitary tract. American Journal of Physiology-Endocrinology and Metabolism, 292(5), E1348-E1357.
218. Peyron, C., Tighe, D. K., Van Den Pol, A. N., de Lecea, L., Heller, H. C., Sutcliffe, J. G., & Kilduff, T. S. (1998). Neurons containing hypocretin (orexin) project to multiple neuronal systems. Journal of Neuroscience, 18(23), 9996-10015.
219. Pfannenberg, C., Werner, M. K., Ripkens, S., Stef, I., Deckert, A., Schmadl, M., ... & Stefan, N. (2010). Impact of age on the relationships of brown adipose tissue with sex and adiposity in humans. Diabetes, 59(7), 1789-1793.
220. Poulin, A. M., & Timofeeva, E. (2008). The dynamics of neuronal activation during food anticipation and feeding in the brain of food-entrained rats. Brain research, 1227, 128-141.
221. Provencio, I., Rodriguez, I. R., Jiang, G., Hayes, W. P., Moreira, E. F., & Rollag, M. D. (2000). A novel human opsin in the inner retina. Journal of Neuroscience, 20(2), 600-605.
222. Qiu, J., Bosch, M. A., Jamali, K., Xue, C., Kelly, M. J., & Rønnekleiv, O. K. (2006). Estrogen upregulates T-type calcium channels in the hypothalamus and pituitary. Journal of Neuroscience, 26(43), 11072-11082.
223. Quintas-Neves, M., Preto, J., & Drummond, M. (2016). Assessment of bariatric surgery efficacy on Obstructive Sleep Apnea (OSA). Revista Portuguesa de Pneumologia (English Edition), 22(6), 331-336.
224. Ralph, M. R., Foster, R. G., Davis, F. C., & Menaker, M. (1990). Transplanted suprachiasmatic nucleus determines circadian period. Science, 247(4945), 975-978.
225. Reddy, P., Zehring, W. A., Wheeler, D. A., Pirrotta, V., Hadfield, C., Hall, J. C., & Rosbash, M. (1984). Molecular analysis of the period locus in Drosophila melanogaster and identification of a transcript involved in biological rhythms. Cell, 38(3), 701-710.

226. Renner, E., Puskas, N., Dobolyi, A., & Palkovits, M. (2012). Glucagon-like peptide-1 of brainstem origin activates dorsomedial hypothalamic neurons in satiated rats. Peptides, 35(1), 14-22.
227. Resta, O., Foschino Barbaro, M. P., Bonfitto, P., Giliberti, T., Depalo, A., Pannacciulli, N., & De Pergola, G. (2003). Low sleep quality and daytime sleepiness in obese patients without obstructive sleep apnoea syndrome. Journal of internal medicine, 253(5), 536-543.
228. Richter, C. P. (1922). A behavioristic study of the activity of the rat (No. 2). Williams & Wilkins.
229. Ritchie, H., Spooner, F., & Roser, M. (2018). Causes of death. Our world in data.
230. Rouille, Y., Westermark, G., Martin, S. K., & Steiner, D. F. (1994). Proglucagon is processed to glucagon by prohormone convertase PC2 in alpha TC1-6 cells. Proceedings of the National Academy of Sciences, 91(8), 3242-3246.
231. Ruby, N. F., Brennan, T. J., Xie, X., Cao, V., Franken, P., Heller, H. C., & O'Hara, B. F. (2002). Role of melanopsin in circadian responses to light. Science, 298(5601), 2211-2213.
232. Ruiz-Lozano, T., Vidal, J., De Hollanda, A., Scheer, F. A. J. L., Garaulet, M., & Izquierdo-Pulido, M. (2016). Timing of food intake is associated with weight loss evolution in severe obese patients after bariatric surgery. Clinical nutrition, 35(6), 1308-1314.
233. Sadacca, L. A., Lamia, K. A., Delemos, A. S., Blum, B., & Weitz, C. J. (2011). An intrinsic circadian clock of the pancreas is required for normal insulin release and glucose homeostasis in mice. Diabetologia, 54, 120-124.
234. Sagbo, H., Ekouevi, D. K., Ranjandriarison, D. T., Niangoran, S., Bakai, T. A., Afanvi, A., ... & Khanafer, N. (2018). Prevalence and factors associated with overweight and obesity among children from primary schools in urban areas of Lomé, Togo. Public Health Nutrition, 21(6), 1048-1056.
235. Samuels, B. C., Zaretsky, D. V., & DiMicco, J. A. (2004). Dorsomedial hypothalamic sites where disinhibition evokes tachycardia correlate with location of raphe-projecting neurons. American Journal of Physiology-Regulatory, Integrative and Comparative Physiology, 287(2), R472-R478.
236. Sanches, I., Teixeira, F., dos Santos, J. M., & Ferreira, A. J. (2015). Effects of acute sleep deprivation resulting from night shift work on young doctors. Acta medica portuguesa, 28(4), 457-462.
237. Sanders, D., Frago, E., Kehoe, R., Patterson, C., & Gaston, K. J. (2021). A meta-analysis of biological impacts of artificial light at night. Nature Ecology & Evolution, 5(1), 74-81.
238. **Sanetra, A. M.,** Palus-Chramiec, K., Chrobok, L., & Lewandowski, M. H. (2022). Electrophysiological complexity in the rat dorsomedial hypothalamus and its susceptibility to daily rhythms and high-fat diet. European Journal of Neuroscience, 56(4), 4363-4377.
239. Scheer, F. A., Hilton, M. F., Mantzoros, C. S., & Shea, S. A. (2009). Adverse metabolic and cardiovascular consequences of circadian misalignment. Proceedings of the National Academy of Sciences, 106(11), 4453-4458.

240. Schepp, W., Dehne, K., Riedel, T., Schmidtler, J., Schaffer, K., & Classen, M. (1996). Oxyntomodulin: a cAMP-dependent stimulus of rat parietal cell function via the receptor for glucagon-like peptide-1 (7-36) NH2. Digestion, 57(6), 398-405.
241. Schick, R. R., Zimmermann, J. P., Walde, T. V., & Schusdziarra, V. (2003). Glucagon-like peptide 1-(7–36) amide acts at lateral and medial hypothalamic sites to suppress feeding in rats. American Journal of Physiology-Regulatory, Integrative and Comparative Physiology, 284(6), R1427-R1435.
242. Schjoldager, B. T. G., Baldissera, F. G. A., Mortensen, P. E., Holst, J. J., & Christiansen, J. (1988). Oxyntomodulin: a potential hormone from the distal gut. Pharmacokinetics and effects on gastric acid and insulin secretion in man. European journal of clinical investigation, 18(5), 499-503.
243. Schlesinger, I., Erikh, I., Avizohar, O., Sprecher, E., & Yarnitsky, D. (2009). Cardiovascular risk factors in restless legs syndrome. Movement disorders: official journal of the Movement Disorder Society, 24(11), 1587-1592.
244. Schmidt, W. E., Siegel, E. G., & Creutzfeldt, W. (1985). Glucagon-like peptide-1 but not glucagon-like peptide-2 stimulates insulin release from isolated rat pancreatic islets. Diabetologia, 28, 704-707.
245. Shaw, E., Dorrian, J., Coates, A. M., Leung, G. K., Davis, R., Rosbotham, E., ... & Bonham, M. P. (2019). Temporal pattern of eating in night shift workers. Chronobiology international, 36(12), 1613-1625.
246. Shekhar, A. (1993). GABA receptors in the region of the dorsomedial hypothalamus of rats regulate anxiety in the elevated plus-maze test. I. Behavioral measures. Brain research, 627(1), 9-16.
247. Sheng, H. Z., Fields, R. D., & Nelson, P. G. (1993). Specific regulation of immediate early genes by patterned neuronal activity. Journal of neuroscience research, 35(5), 459-467.
248. Sherman, H., Genzer, Y., Cohen, R., Chapnik, N., Madar, Z., & Froy, O. (2012). Timed high-fat diet resets circadian metabolism and prevents obesity. The FASEB Journal, 26(8), 3493-3502.
249. Shi, X., Zhou, F., Li, X., Chang, B., Li, D., Wang, Y., ... & Guan, X. (2013). Central GLP-2 enhances hepatic insulin sensitivity via activating PI3K signaling in POMC neurons. Cell metabolism, 18(1), 86-98.
250. Shigeyoshi, Y., Taguchi, K., Yamamoto, S., Takekida, S., Yan, L., Tei, H., ... & Okamura, H. (1997). Light-induced resetting of a mammalian circadian clock is associated with rapid induction of the mPer1 transcript. Cell, 91(7), 1043-1053.
251. Smith, M., Pool, R., & Weinberg, H. (1962). Role of bulk in the control of eating. Journal of Comparative and Physiological Psychology, 55(1), 115.
252. Smith, M. S. (1993). Lactation alters neuropeptide-Y and proopiomelanocortin gene expression in the arcuate nucleus of the rat. Endocrinology, 133(3), 1258-1265.
253. Spiegel, K., Leproult, R., & Van Cauter, E. (1999). Impact of sleep debt on metabolic and endocrine function. The lancet, 354(9188), 1435-1439.
254. Stamper, C. E., Hassell Jr, J. E., Kapitz, A. J., Renner, K. J., Orchinik, M., & Lowry, C. A. (2017). Activation of 5-HT1A receptors in the rat dorsomedial hypothalamus

inhibits stress-induced activation of the hypothalamic–pituitary–adrenal axis. Stress, 20(2), 223-230.
255. Stephan, F. K. (1992). Resetting of a feeding-entrainable circadian clock in the rat. Physiology & behavior, 52(5), 985-995.
256. Stephan, F. K., & Zucker, I. (1972). Circadian rhythms in drinking behavior and locomotor activity of rats are eliminated by hypothalamic lesions. Proceedings of the National Academy of Sciences, 69(6), 1583-1586.
257. Stokkan, K. A., Yamazaki, S., Tei, H., Sakaki, Y., & Menaker, M. (2001). Entrainment of the circadian clock in the liver by feeding. Science, 291(5503), 490-493.
258. Suwazono, Y., Dochi, M., Sakata, K., Okubo, Y., Oishi, M., Tanaka, K., ... & Nogawa, K. (2008). A longitudinal study on the effect of shift work on weight gain in male Japanese workers. Obesity, 16(8), 1887-1893.
259. Svoboda, M., Tastenoy, M., Vertongen, P., & Robberecht, P. (1994). Relative quantitative analysis of glucagon receptor mRNA in rat tissues. Molecular and cellular endocrinology, 105(2), 131-137.
260. Taheri, S., Lin, L., Austin, D., Young, T., & Mignot, E. (2004). Short sleep duration is associated with reduced leptin, elevated ghrelin, and increased body mass index. PLoS medicine, 1(3), e62.
261. Taheri, S. (2006). The link between short sleep duration and obesity: we should recommend more sleep to prevent obesity. Archives of disease in childhood, 91(11), 881-884. Thomson, C. C., Clark, S., Camargo Jr, C. A., & Marc Investigators. (2003). Body mass index and asthma severity among adults presenting to the emergency department. Chest, 124(3), 795-802.
262. Tang-Christensen, M., Larsen, P. J., Thulesen, J., Rømer, J., & Vrang, N. (2000). The proglucagon-derived peptide, glucagon-like peptide-2, is a neurotransmitter involved in the regulation of food intake. Nature medicine, 6(7), 802-807.
263. Tang-Christensen, M., Vrang, N., & Larsen, P. J. (2001). Glucagon-like peptide containing pathways in the regulation of feeding behaviour. International journal of obesity, 25(5), S42-S47.
264. Tei, H., Okamura, H., Shigeyoshi, Y., Fukuhara, C., Ozawa, R., Hirose, M., & Sakaki, Y. (1997). Circadian oscillation of a mammalian homologue of the Drosophila period gene. Nature, 389(6650), 512-516.
265. Trayhurn, P., & Fuller, L. (1980). The development of obesity in genetically diabetic-obese (db/db) mice pair-fed with lean siblings: The importance of thermoregulatory thermogenesis. Diabetologia, 19, 148-153.
266. Trayhurn, P., & James, W. P. (1978). Thermoregulation and non-shivering thermogenesis in the genetically obese (ob/ob) mouse. Pflugers Archiv: European journal of physiology, 373(2), 189-193.
267. Tritos, N. A., Elmquist, J. K., W. Mastaitis, J., Flier, J. S., & Maratos-Flier, E. (1998). Characterization of expression of hypothalamic appetite-regulating peptides in obese hyperleptinemic brown adipose tissue-deficient (uncoupling protein-promoter-driven diphtheria toxin A) mice. Endocrinology, 139(11), 4634-4641.

268. Turton, M. D., O'shea, D., Gunn, I., Beak, S. A., Edwards, C. M. B., Meeran, K., ... & Bloom, S. R. (1996). A role for glucagon-like peptide-1 in the central regulation of feeding. Nature, 379(6560), 69-72.
269. Valenzuela, J. E., & Defilippi, C. (1981). Inhibition of gastric emptying in humans by secretin, the octapeptide of cholecystokinin, and intraduodenal fat. Gastroenterology, 81(5), 898-902.
270. Van Amelsvoort, L. G. P. M., Schouten, E. G., & Kok, F. J. (1999). Duration of shiftwork related to body mass index and waist to hip ratio. International journal of obesity, 23(9), 973-978.
271. Verwey, M., Khoja, Z., Stewart, J., & Amir, S. (2007). Differential regulation of the expression of Period2 protein in the limbic forebrain and dorsomedial hypothalamus by daily limited access to highly palatable food in food-deprived and free-fed rats. Neuroscience, 147(2), 277-285.
272. Verwey, M., Khoja, Z., Stewart, J., & Amir, S. (2008). Region-specific modulation of PER2 expression in the limbic forebrain and hypothalamus by nighttime restricted feeding in rats. Neuroscience letters, 440(1), 54-58.
273. Verwey, M., Lam, G. Y., & Amir, S. (2009). Circadian rhythms of PERIOD1 expression in the dorsomedial hypothalamic nucleus in the absence of entrained food-anticipatory activity rhythms in rats. European Journal of Neuroscience, 29(11), 2217-2222.
274. Vgontzas, A. N., Bixler, E. O., Tan, T. L., Kantner, D., Martin, L. F., & Kales, A. (1998). Obesity without sleep apnea is associated with daytime sleepiness. Archives of internal medicine, 158(12), 1333-1337.
275. Vgontzas, A. N., Lin, H. M., Papaliaga, M., Calhoun, S., Vela-Bueno, A., Chrousos, G. P., & Bixler, E. O. (2008). Short sleep duration and obesity: the role of emotional stress and sleep disturbances. International journal of obesity, 32(5), 801-809.
276. Vgontzas, A. N., Papanicolaou, D. A., Bixler, E. O., Kales, A., Tyson, K., & Chrousos, G. P. (1997). Elevation of plasma cytokines in disorders of excessive daytime sleepiness: role of sleep disturbance and obesity. The Journal of Clinical Endocrinology & Metabolism, 82(5), 1313-1316.
277. Vrang, N., Hansen, M., Larsen, P. J., & Tang-Christensen, M. (2007). Characterization of brainstem preproglucagon projections to the paraventricular and dorsomedial hypothalamic nuclei. Brain research, 1149, 118-126.
278. Wagner, K. M., Roeder, Z., DesRochers, K., Buhler, A. V., Heinricher, M. M., & Cleary, D. R. (2013). The dorsomedial hypothalamus mediates stress-induced hyperalgesia and is the source of the pronociceptive peptide cholecystokinin in the rostral ventromedial medulla. Neuroscience, 238, 29-38.
279. Wakamatsu, H., Yoshinobu, Y., Aida, R., Moriya, T., Akiyama, M., & Shibata, S. (2001). Restricted-feeding-induced anticipatory activity rhythm is associated with a phase-shift of the expression of mPer1 and mPer2 mRNA in the cerebral cortex and hippocampus but not in the suprachiasmatic nucleus of mice. European Journal of Neuroscience, 13(6), 1190-1196.

280. Wan, S., Coleman, F. H., & Travagli, R. A. (2007). Glucagon-like peptide-1 excites pancreas-projecting preganglionic vagal motoneurons. American Journal of Physiology-Gastrointestinal and Liver Physiology, 292(6), G1474-G1482.
281. Wang, Q., & Brubaker, P. (2002). Glucagon-like peptide-1 treatment delays the onset of diabetes in 8 week-old db/db mice. Diabetologia, 45, 1263-1273.
282. Warwick, Z. S., Synowski, S. J., & Bell, K. R. (2002). Dietary fat content affects energy intake and weight gain independent of diet caloric density in rats. Physiology & behavior, 77(1), 85-90.
283. Warwick, Z. S., & Weingarten, H. P. (1995). Determinants of high-fat diet hyperphagia: experimental dissection of orosensory and postingestive effects. American Journal of Physiology-Regulatory, Integrative and Comparative Physiology, 269(1), R30-R37.
284. Wellen, K. E., & Hotamisligil, G. S. (2005). Inflammation, stress, and diabetes. The Journal of clinical investigation, 115(5), 1111-1119.
285. Welsh, D. K., Logothetis, D. E., Meister, M., & Reppert, S. M. (1995). Individual neurons dissociated from rat suprachiasmatic nucleus express independently phased circadian firing rhythms. Neuron, 14(4), 697-706.
286. West, K. E., Jablonski, M. R., Warfield, B., Cecil, K. S., James, M., Ayers, M. A., ... & Brainard, G. C. (2011). Blue light from light-emitting diodes elicits a dose-dependent suppression of melatonin in humans. Journal of applied physiology.
287. Wettergren, A., Schjoldager, B., Mortensen, P. E., Myhre, J., Christiansen, J., & Holst, J. J. (1993). Truncated GLP-1 (proglucagon 78–107-amide) inhibits gastric and pancreatic functions in man. Digestive diseases and sciences, 38(4), 665-673.
288. Wheeler, M. B., Lu, M. I. N. G., Dillon, J. S., Leng, X. H., Chen, C. H. U. A. N., & Boyd 3rd, A. E. (1993). Functional expression of the rat glucagon-like peptide-I receptor, evidence for coupling to both adenylyl cyclase and phospholipase-C. Endocrinology, 133(1), 57-62.
289. WHO. (2000). Obesity: preventing and managing the global epidemic. Report of a WHO Consultation. WHO Technical Report Series 894. World Health Organization, Geneva.
290. WHO. (2022). WHO European regional obesity report 2022. World Health Organization. Regional Office for Europe.
291. Williams, D. L., Baskin, D. G., & Schwartz, M. W. (2006). Leptin regulation of the anorexic response to glucagon-like peptide-1 receptor stimulation. Diabetes, 55(12), 3387-3393.
292. Winzell, M. S., & Ahrén, B. (2004). The high-fat diet–fed mouse: a model for studying mechanisms and treatment of impaired glucose tolerance and type 2 diabetes. Diabetes, 53(suppl_3), S215-S219.
293. Wynne, K., Park, A. J., Small, C. J., Meeran, K., Ghatei, M. A., Frost, G. S., & Bloom, S. R. (2006). Oxyntomodulin increases energy expenditure in addition to decreasing energy intake in overweight and obese humans: a randomised controlled trial. International journal of obesity, 30(12), 1729-1736.

294. Xiao, Q., Gu, F., Caporaso, N., & Matthews, C. E. (2016). Relationship between sleep characteristics and measures of body size and composition in a nationally-representative sample. BMC obesity, 3, 1-8.
295. Yang, L., Scott, K. A., Hyun, J., Tamashiro, K. L., Tray, N., Moran, T. H., & Bi, S. (2009). Role of dorsomedial hypothalamic neuropeptide Y in modulating food intake and energy balance. Journal of Neuroscience, 29(1), 179-190.
296. Yamazaki, S., Numano, R., Abe, M., Hida, A., Takahashi, R. I., Ueda, M., ... & Tei, H. (2000). Resetting central and peripheral circadian oscillators in transgenic rats. Science, 288(5466), 682-685.
297. Yoon, S. J., Kim, H. J., & Doo, M. (2016). Association between perceived stress, alcohol consumption levels and obesity in Koreans. Asia Pacific journal of clinical nutrition, 25(2), 316-325.
298. Zalesin, K. C., Franklin, B. A., Miller, W. M., Peterson, E. D., & McCullough, P. A. (2008). Impact of obesity on cardiovascular disease. Endocrinology and metabolism clinics of North America, 37(3), 663-684.
299. Zaretskaia, M. V., Zaretsky, D. V., Sarkar, S., Shekhar, A., & DiMicco, J. A. (2008). Induction of Fos-immunoreactivity in the rat brain following disinhibition of the dorsomedial hypothalamus. Brain research, 1200, 39-50.
300. Zarrinpar, A., Chaix, A., Yooseph, S., & Panda, S. (2014). Diet and feeding pattern affect the diurnal dynamics of the gut microbiome. Cell metabolism, 20(6), 1006-1017.
301. Zhao, H., & Rusak, B. (2005). Circadian firing-rate rhythms and light responses of rat habenular nucleus neurons in vivo and in vitro. Neuroscience, 132(2), 519-528.
302. Zhao, Z. D., Yang, W. Z., Gao, C., Fu, X., Zhang, W., Zhou, Q., ... & Shen, W. L. (2017). A hypothalamic circuit that controls body temperature. Proceedings of the National Academy of Sciences, 114(8), 2042-2047.
303. Zhang, C., Barkholt, P., Nielsen, J. C., Thorbek, D. D., Rigbolt, K., Vrang, N., ... & Jelsing, J. (2020). The dorsomedial hypothalamus and nucleus of the solitary tract as key regulators in a rat model of chronic obesity. Brain Research, 1727, 146538.
304. Zhang, N., & Bi, S. (2018). Effects of physical exercise on food intake and body weight: role of dorsomedial hypothalamic signaling. Physiology & behavior, 192, 59-63.
305. Zhang, W., Sunanaga, J., Takahashi, Y., Mori, T., Sakurai, T., Kanmura, Y., & Kuwaki, T. (2010). Orexin neurons are indispensable for stress-induced thermogenesis in mice. The Journal of physiology, 588(21), 4117-4129.
306. Zhang, Y., Kerman, I. A., Laque, A., Nguyen, P., Faouzi, M., Louis, G. W., ... & Münzberg, H. (2011). Leptin-receptor-expressing neurons in the dorsomedial hypothalamus and median preoptic area regulate sympathetic brown adipose tissue circuits. Journal of Neuroscience, 31(5), 1873-1884.

Appendices

Publication 1

Authors' statements

Anna Sanetra
Imię i nazwisko
Kandydata
Name and Surname of
Candidate

Kraków, 30.04.2023
Miejscowość i data
Place and date

Oświadczenie / Statement

Ja niżej podpisana jako współautor publikacji pt. *„Electrophysiological complexity in the rat dorsomedial hypothalamus and its susceptibility to daily rhythms and high-fat diet”* oświadczam, że mój wkład w przygotowaniu publikacji polegał na udziale w częściach dotyczących:

I, undersigned as a co-author of the publication entitled *"Electrophysiological complexity in the rat dorsomedial hypothalamus and its susceptibility to daily rhythms and high-fat diet"*, declare that my contribution to the preparation of the publication consisted of participation in the following parts:

- Opracowania koncepcji badań
  Development of research concepts
- Opracowania metodyki badań
  Development of research methodology
- Zbieraniu materiałów
  Data collection
- Wykonaniu oznaczeń
  Measurements
- Analizie i interpretacji wyników
  Analysis and interpretation of results
- Przygotowaniu manuskryptu
  Manuscript preparation
- Przeprowadzenia procesu recenzji
  Manuscript revision

and my individual percentage contribution to the article is 83%

Sandra

.....

Czytelny podpis Kandydata
Legible Candidate signature

Dr Katarzyna Palus-Chramiec
Imię i nazwisko
Współautora
Name and Surname of
Co-Author

Kraków, 30.04.2023
Miejscowość i data
Place and date

Oświadczenie / Statement

Ja niżej podpisana jako współautor publikacji pt. *„Electrophysiological complexity in the rat dorsomedial hypothalamus and its susceptibility to daily rhythms and high-fat diet”* oświadczam, że mój wkład w przygotowaniu publikacji polegał na udziale w częściach dotyczących:

I, undersigned as a co-author of the publication entitled *“Electrophysiological complexity in the rat dorsomedial hypothalamus and its susceptibility to daily rhythms and high-fat diet”*, declare that my contribution to the preparation of the publication consisted of participation in the following parts:

- Opracowania koncepcji badań
  Development of research concepts
- Opracowania metodyki badań
  Development of research methodology
- Nadzorowaniu eksperymentów
  Research supervision
- Redagowaniu manuskryptu
  Manuscript editing

and my individual percentage contribution to the article is 10%

KPalus

.....
Czytelny podpis Współautora
Legible Co-author signature

Dr hab. Łukasz Chrobok
Imię i nazwisko
Współautora
Name and Surname of
Co-Author

Kraków, 30.04.2023
Miejscowość i data
Place and date

Oświadczenie / Statement

Ja niżej podpisany jako współautor publikacji pt. *„Electrophysiological complexity in the rat dorsomedial hypothalamus and its susceptibility to daily rhythms and high-fat diet”* oświadczam, że mój wkład w przygotowaniu publikacji polegał na udziale w częściach dotyczących:

I, undersigned as a co-author of the publication entitled *"Electrophysiological complexity in the rat dorsomedial hypothalamus and its susceptibility to daily rhythms and high-fat diet”*, declare that my contribution to the preparation of the publication consisted of participation in the following parts:

- Opracowania koncepcji badań
  Development of research concepts
- Analizie i interpretacji wyników
  Analysis and interpretation of results
- Redagowaniu manuskryptu
  Manuscript editing

and my individual percentage contribution to the article is 5%

.....
Czytelny podpis Współautora
Legible Co-author signature

Prof. dr hab. Marian H. Lewandowski
Imię i nazwisko Współautora
Name and Surname of Co-Author

Kraków, 30.04.2023
Miejscowość i data
Place and date

Oświadczenie / Statement

Ja niżej podpisany jako współautor publikacji pt. *„Electrophysiological complexity in the rat dorsomedial hypothalamus and its susceptibility to daily rhythms and high-fat diet”* oświadczam, że mój wkład w przygotowaniu publikacji polegał na udziale w częściach dotyczących:

I, undersigned as a co-author of the publication entitled *“Electrophysiological complexity in the rat dorsomedial hypothalamus and its susceptibility to daily rhythms and high-fat diet”*, declare that my contribution to the preparation of the publication consisted of participation in the following parts:

- Opracowania koncepcji badań
  Development of research concepts
- Nadzorowaniu eksperymentów
  Research supervision
- Redagowaniu manuskryptu
  Manuscript editing

and my individual percentage contribution to the article is 2%

Czytelny podpis Współautora
Legible Co-author signature

Publication 2

Authors’ statements

Anna Sanetra
Imię i nazwisko
Kandydata
Name and Surname of
Candidate

Kraków, 30.04.2023
Miejscowość i data
Place and date

Oświadczenie / Statement

Ja niżej podpisana jako współautor publikacji pt. „*High-Fat-Diet-Evoked Disruption of the Rat Dorsomedial Hypothalamic Clock Can Be Prevented by Restricted Nighttime Feeding*" oświadczam, że mój wkład w przygotowaniu publikacji polegał na udziale w częściach dotyczących:

I, undersigned as a co-author of the publication entitled "*High-Fat-Diet-Evoked Disruption of the Rat Dorsomedial Hypothalamic Clock Can Be Prevented by Restricted Nighttime Feeding*", declare that my contribution to the preparation of the publication consisted of participation in the following parts:

- Opracowania koncepcji badań
  Development of research concepts
- Opracowania metodyki badań
  Development of research methodology
- Zbieraniu materiałów
  Data collection
- Wykonaniu oznaczeń
  Measurements
- Nadzorowaniu eksperymentów
  Research supervision
- Analizie i interpretacji wyników
  Analysis and interpretation of results
- Przygotowaniu manuskryptu
  Manuscript preparation
- Przeprowadzenia procesu recenzji
  Manuscript revision

and my individual percentage contribution to the article is 60%

Sandra

.....
Czytelny podpis Kandydata
Legible Candidate

Dr Katarzyna Palus-Chramiec
Imię i nazwisko
Współautora
Name and Surname of
Co-Author

Kraków, 30.04.2023
Miejscowość i data
Place and date

Oświadczenie / Statement

Ja niżej podpisana jako współautor publikacji pt. „*High-Fat-Diet-Evoked Disruption of the Rat Dorsomedial Hypothalamic Clock Can Be Prevented by Restricted Nighttime Feeding*" oświadczam, że mój wkład w przygotowaniu publikacji polegał na udziale w częściach dotyczących:

I, undersigned as a co-author of the publication entitled "*High-Fat-Diet-Evoked Disruption of the Rat Dorsomedial Hypothalamic Clock Can Be Prevented by Restricted Nighttime Feeding*", declare that my contribution to the preparation of the publication consisted of participation in the following parts:

- Opracowania koncepcji badań
  Development of research concepts
- Opracowania metodyki badań
  Development of research methodology
- Zbieraniu materiałów
  Data collection
- Redagowaniu manuskryptu
  Manuscript editing

and my individual percentage contribution to the article is 10%

KPalus

.....
Czytelny podpis Współautora
Legible Co-author signature

Dr hab. Łukasz Chrobok
Imię i nazwisko
Współautora
Name and Surname of
Co-Author

Kraków, 30.04.2023
Miejscowość i data
Place and date

Oświadczenie / Statement

Ja niżej podpisany jako współautor publikacji pt. „*High-Fat-Diet-Evoked Disruption of the Rat Dorsomedial Hypothalamic Clock Can Be Prevented by Restricted Nighttime Feeding*" oświadczam, że mój wkład w przygotowaniu publikacji polegał na udziale w częściach dotyczących:

I, undersigned as a co-author of the publication entitled "*High-Fat-Diet-Evoked Disruption of the Rat Dorsomedial Hypothalamic Clock Can Be Prevented by Restricted Nighttime Feeding*", declare that my contribution to the preparation of the publication consisted of participation in the following parts:

- Opracowania koncepcji badań
  Development of research concepts
- Opracowania metodyki badań
  Development of research methodology
- Zbieraniu materiałów
  Data collection
- Analizie i interpretacji wyników
  Analysis and interpretation of results
- Redagowaniu manuskryptu
  Manuscript editing

and my individual percentage contribution to the article is 10%

.....
Czytelny podpis Współautora
Legible Co-author signature

Dr Jagoda S. Jęczmień-Łazur
Imię i nazwisko
Współautora
Name and Surname of
Co-Author

Kraków, 30.04.2023
Miejscowość i data
Place and date

Oświadczenie / Statement

Ja niżej podpisana jako współautor publikacji pt. „*High-Fat-Diet-Evoked Disruption of the Rat Dorsomedial Hypothalamic Clock Can Be Prevented by Restricted Nighttime Feeding*" oświadczam, że mój wkład w przygotowaniu publikacji polegał na udziale w częściach dotyczących:

I, undersigned as a co-author of the publication entitled "*High-Fat-Diet-Evoked Disruption of the Rat Dorsomedial Hypothalamic Clock Can Be Prevented by Restricted Nighttime Feeding*", declare that my contribution to the preparation of the publication consisted of participation in the following parts:

- Opracowania koncepcji badań
  Development of research concepts
- Opracowania metodyki badań
  Development of research methodology
- Zbieraniu materiałów
  Data collection
- Redagowaniu manuskryptu
  Manuscript editing

and my individual percentage contribution to the article is 5%

Jagoda Jęczmień-Łazur

……
Czytelny podpis Współautora
Legible Co-author signature

Emilia Gawron
Imię i nazwisko
Współautora
Name and Surname of
Co-Author

Kraków, 30.04.2023
Miejscowość i data
Place and date

Oświadczenie / Statement

Ja niżej podpisana jako współautor publikacji pt. „*High-Fat-Diet-Evoked Disruption of the Rat Dorsomedial Hypothalamic Clock Can Be Prevented by Restricted Nighttime Feeding*" oświadczam, że mój wkład w przygotowaniu publikacji polegał na udziale w częściach dotyczących:

I, undersigned as a co-author of the publication entitled "*High-Fat-Diet-Evoked Disruption of the Rat Dorsomedial Hypothalamic Clock Can Be Prevented by Restricted Nighttime Feeding*", declare that my contribution to the preparation of the publication consisted of participation in the following parts:

- Zbieraniu materiałów
  Data collection
- Wykonaniu oznaczeń
  Measurements
- Redagowaniu manuskryptu
  Manuscript editing

and my individual percentage contribution to the article is 5%

Emilia Gawron

.....
Czytelny podpis Współautora
Legible Co-author signature

Jasmin D. Klich
Imię i nazwisko
Współautora
Name and Surname of
Co-Author

Kraków, 30.04.2023
Miejscowość i data
Place and date

Oświadczenie / Statement

Ja niżej podpisana jako współautor publikacji pt. „*High-Fat-Diet-Evoked Disruption of the Rat Dorsomedial Hypothalamic Clock Can Be Prevented by Restricted Nighttime Feeding*" oświadczam, że mój wkład w przygotowaniu publikacji polegał na udziale w częściach dotyczących:

I, undersigned as a co-author of the publication entitled "*High-Fat-Diet-Evoked Disruption of the Rat Dorsomedial Hypothalamic Clock Can Be Prevented by Restricted Nighttime Feeding*", declare that my contribution to the preparation of the publication consisted of participation in the following parts:

- Zbieraniu materiałów
  Data collection
- Redagowaniu manuskryptu
  Manuscript editing

and my individual percentage contribution to the article is 4%

.....
Czytelny podpis Współautora
Legible Co-author signature

Dr Kamil Pradel
Imię i nazwisko
Współautora
Name and Surname of
Co-Author

Kraków, 30.04.2023
Miejscowość i data
Place and date

Oświadczenie / Statement

Ja niżej podpisany jako współautor publikacji pt. *„High-Fat-Diet-Evoked Disruption of the Rat Dorsomedial Hypothalamic Clock Can Be Prevented by Restricted Nighttime Feeding"* oświadczam, że mój wkład w przygotowaniu publikacji polegał na udziale w częściach dotyczących:

I, undersigned as a co-author of the publication entitled "*High-Fat-Diet-Evoked Disruption of the Rat Dorsomedial Hypothalamic Clock Can Be Prevented by Restricted Nighttime Feeding*", declare that my contribution to the preparation of the publication consisted of participation in the following parts:

- Analizie i interpretacji wyników
  Analysis and interpretation of results
- Redagowaniu manuskryptu
  Manuscript editing

and my individual percentage contribution to the article is 4%

Kamil Pradel

Czytelny podpis Współautora
Legible Co-author signature

Prof. dr hab. Marian H. Lewandowski
Imię i nazwisko Współautora
Name and Surname of Co-Author

Kraków, 30.04.2023
Miejscowość i data
Place and date

Oświadczenie / Statement

Ja niżej podpisany jako współautor publikacji pt. „*High-Fat-Diet-Evoked Disruption of the Rat Dorsomedial Hypothalamic Clock Can Be Prevented by Restricted Nighttime Feeding*" oświadczam, że mój wkład w przygotowaniu publikacji polegał na udziale w częściach dotyczących:

I, undersigned as a co-author of the publication entitled "*High-Fat-Diet-Evoked Disruption of the Rat Dorsomedial Hypothalamic Clock Can Be Prevented by Restricted Nighttime Feeding*", declare that my contribution to the preparation of the publication consisted of participation in the following parts:

- Opracowania koncepcji badań
  Development of research concepts
- Nadzorowaniu eksperymentów
  Research supervision
- Redagowaniu manuskryptu
  Manuscript editing

and my individual percentage contribution to the article is 2%

Czytelny podpis Współautora
Legible Co-author signature

Publication 3

Authors’ statements

Anna Sanetra
Imię i nazwisko
Kandydata
Name and Surname of
Candidate

Kraków, 30.04.2023
Miejscowość i data
Place and date

Oświadczenie / Statement

Ja niżej podpisana jako współautor publikacji pt. „*Proglucagon signalling in the rat Dorsomedial Hypothalamus – Physiology and high-fat diet-mediated alterations*" oświadczam, że mój wkład w przygotowaniu publikacji polegał na udziale w częściach dotyczących:

I, undersigned as a co-author of the publication entitled "*Proglucagon signalling in the rat Dorsomedial Hypothalamus – Physiology and high-fat diet-mediated alterations*", declare that my contribution to the preparation of the publication consisted of participation in the following parts:

- Opracowania koncepcji badań
  Development of research concepts
- Opracowania metodyki badań
  Development of research methodology
- Zbieraniu materiałów
  Data collection
- Wykonaniu oznaczeń
  Measurements
- Analizie i interpretacji wyników
  Analysis and interpretation of results
- Przygotowaniu manuskryptu
  Manuscript preparation
- Przeprowadzenia procesu recenzji
  Manuscript revision

and my individual percentage contribution to the article is 65%

.....
Czytelny podpis Kandydata
Legible Candidate signature

Dr Katarzyna Palus-Chramiec
Imię i nazwisko
Współautora
Name and Surname of
Co-Author

Kraków, 30.04.2023
Miejscowość i data
Place and date

Oświadczenie / Statement

Ja niżej podpisana jako współautor publikacji pt. „*Proglucagon signalling in the rat Dorsomedial Hypothalamus – Physiology and high-fat diet-mediated alterations*" oświadczam, że mój wkład w przygotowaniu publikacji polegał na udziale w częściach dotyczących:

I, undersigned as a co-author of the publication entitled "*Proglucagon signalling in the rat Dorsomedial Hypothalamus – Physiology and high-fat diet-mediated alterations*", declare that my contribution to the preparation of the publication consisted of participation in the following parts:

- Opracowania koncepcji badań
  Development of research concepts
- Opracowania metodyki badań
  Development of research methodology
- Zbieraniu materiałów
  Data collection
- Wykonaniu oznaczeń
  Measurements
- Nadzorowaniu eksperymentów
  Research supervision
- Redagowaniu manuskryptu
  Manuscript editing

and my individual percentage contribution to the article is 15%

KPalus

.....
Czytelny podpis Współautora
Legible Co-author signature

Dr hab. Łukasz Chrobok
Imię i nazwisko
Współautora
Name and Surname of
Co-Author

Kraków, 30.04.2023
Miejscowość i data
Place and date

Oświadczenie / Statement

Ja niżej podpisany jako współautor publikacji pt. „*Proglucagon signalling in the rat Dorsomedial Hypothalamus – Physiology and high-fat diet-mediated alterations*" oświadczam, że mój wkład w przygotowaniu publikacji polegał na udziale w częściach dotyczących:

I, undersigned as a co-author of the publication entitled "*Proglucagon signalling in the rat Dorsomedial Hypothalamus – Physiology and high-fat diet-mediated alterations*", declare that my contribution to the preparation of the publication consisted of participation in the following parts:

- Opracowania koncepcji badań
  Development of research concepts
- Opracowania metodyki badań
  Development of research methodology
- Zbieraniu materiałów
  Data collection
- Analizie i interpretacji wyników
  Analysis and interpretation of results
- Redagowaniu manuskryptu
  Manuscript editing

and my individual percentage contribution to the article is 10%

Czytelny podpis Współautora
Legible Co-author signature

Dr Jagoda S. Jęczmień-Łazur
Imię i nazwisko
Współautora
Name and Surname of
Co-Author

Kraków, 30.04.2023
Miejscowość i data
Place and date

Oświadczenie / Statement

Ja niżej podpisana jako współautor publikacji pt. „*Proglucagon signalling in the rat Dorsomedial Hypothalamus – Physiology and high-fat diet-mediated alterations*" oświadczam, że mój wkład w przygotowaniu publikacji polegał na udziale w częściach dotyczących:

I, undersigned as a co-author of the publication entitled "*Proglucagon signalling in the rat Dorsomedial Hypothalamus – Physiology and high-fat diet-mediated alterations*", declare that my contribution to the preparation of the publication consisted of participation in the following parts:

- Opracowania koncepcji badań
  Development of research concepts
- Opracowania metodyki badań
  Development of research methodology
- Zbieraniu materiałów
  Data collection
- Redagowaniu manuskryptu
  Manuscript editing

and my individual percentage contribution to the article is 4%

Jagoda Jęczmień-Łazur

……
Czytelny podpis Współautora
Legible Co-author signature

Jasmin D. Klich
Imię i nazwisko
Współautora
Name and Surname of
Co-Author

Kraków, 30.04.2023
Miejscowość i data
Place and date

Oświadczenie / Statement

Ja niżej podpisana jako współautor publikacji pt. „*Proglucagon signalling in the rat Dorsomedial Hypothalamus – Physiology and high-fat diet-mediated alterations*" oświadczam, że mój wkład w przygotowaniu publikacji polegał na udziale w częściach dotyczących:

I, undersigned as a co-author of the publication entitled "*Proglucagon signalling in the rat Dorsomedial Hypothalamus – Physiology and high-fat diet-mediated alterations*", declare that my contribution to the preparation of the publication consisted of participation in the following parts:

- Zbieraniu materiałów
  Data collection
- Redagowaniu manuskryptu
  Manuscript editing

and my individual percentage contribution to the article is 4%

……
Czytelny podpis Współautora
Legible Co-author signature

Prof. dr hab. Marian H. Lewandowski
Imię i nazwisko
Współautora
Name and Surname of
Co-Author

Kraków, 30.04.2023
Miejscowość i data
Place and date

Oświadczenie / Statement

Ja niżej podpisany jako współautor publikacji pt. „*Proglucagon signalling in the rat Dorsomedial Hypothalamus – Physiology and high-fat diet-mediated alterations*" oświadczam, że mój wkład w przygotowaniu publikacji polegał na udziale w częściach dotyczących:

I, undersigned as a co-author of the publication entitled "*Proglucagon signalling in the rat Dorsomedial Hypothalamus – Physiology and high-fat diet-mediated alterations*", declare that my contribution to the preparation of the publication consisted of participation in the following parts:

- Opracowania koncepcji badań
  Development of research concepts
- Nadzorowaniu eksperymentów
  Research supervision
- Redagowaniu manuskryptu
  Manuscript editing

and my individual percentage contribution to the article is 2%

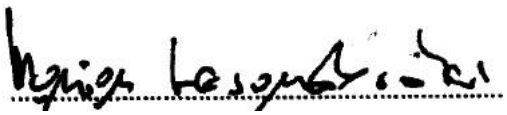

Czytelny podpis Współautora
Legible Co-author signature